# Towards a competitive expression platform

## Strategies to optimize unconventional protein secretion in *Ustilago maydis*

Inaugural Dissertation

for the attainment of the **title of doctor**
in the **Faculty of Mathematics and Natural Sciences**
at the **Heinrich Heine University Düsseldorf**


presented by

**Kai Philip Hußnätter**
from Düsseldorf, Germany

Düsseldorf, June 2021

from the Institute for Microbiology
in the Faculty of Mathematics and Natural Sciences
of the Heinrich Heine University Düsseldorf

Published by the permission of the
Faculty of Mathematics and Natural Sciences at
Heinrich Heine University Düsseldorf

Supervisor: Prof. Dr. Michael Feldbrügge
Institute for Microbiology
Heinrich Heine University Düsseldorf

Co-supervisor: Prof. Dr. Matias Zurbriggen
Institute for Synthetic Biology
Heinrich Heine University Düsseldorf

Date of oral examination: 22.09.2021

The research detailed in this thesis was conducted from January 2017 until June 2021 in Düsseldorf at the Heinrich Heine University Düsseldorf in the Institute for Microbiology under the supervision of Prof. Dr. Michael Feldbrügge.

## Statutory declaration

I hereby declare that this dissertation is the result of my own work, taking into account the “Rules and Principles for Saveguarding and Good Scientific Practice at Heinrich Heine Universität Düsseldorf”. No other person’s work has been used without due acknowledgement. Further I assure that I did not use any other literature than the ones specified and cited.This dissertation has not been submitted in the same or similar form to other institutions. I have not previously failed a doctoral examination procedure.

## Eidesstattliche Erklärung

Ich versichere an Eides Statt, dass die Dissertation von mir selbstständig und ohne unzulässige fremde Hilfe unter Beachtung der „Grundsätze zur Sicherung guter wissenschaftlicher Praxis an der Heinrich-Heine-Universität Düsseldorf“ erstellt worden ist. Keine andere Person wirkte an der Arbeit ohne entsprechende Nennung mit. Darüber hinaus versichere ich, dass keine Literatur außerhalb der genannten und zitierten Quellen genutzt wurde. Die Dissertation wurde in ihrer jetzigen oder ähnlichen Form noch bei keiner anderen Hochschule eingereicht. Ich habe zuvor keine erfolglosen Promotionsversuche unternommen.

Kai P. Hußnätter
Düsseldorf, den 24. Juni 2021

# Abstract

Biotechnological production and secretion of heterologous proteins puts high demands on chassis and production conditions. A broad selection of production hosts is important to fill existing niches. Application of unconventional secretion for export of heterologous proteins in the novel biotechnological production candidate *U. maydis* was established in previous studies. Hitchhiking of the endogenous secretory machinery of chitinase Cts1 via an alternative export route allows secretion of unglycosylated proteins, which can be advantageous for example for distinct pharmaceutical or bacterial targets. In the present study two major strategies were followed to further optimize the system in terms of applicability and yield.

i) Mechanistic insights revealed a connection of unconventional secretion and formation of the secondary septum during cytokinesis, sealing the functional fragmentation zone between mother and daughter cell. Formation of the secondary septum is dependent on the kinase Don3. With its essential role for formation of a functional fragmentation zone, it acts as a gatekeeper for Cts1 secretion. Thus, deletion of *don3* strongly diminishes unconventional secretion. Identification of regulatory components for unconventional secretion allows exploitation towards regulation of this process. To this end, regulation of Don3 was established in the present work on both, transcriptional and post-translational level. While transcriptional regulation is based on a carbon source inducible promoter, post-translational regulation was achieved by an alternative version of Don3, sensitive to an ATP-analogue. Optimization of cultivation and regulation conditions allowed efficient application of either system for protein production. Establishment of an autoinduction process enabled cultivation in batch fermentation with separated protein synthesis and secretion phases. Proof of principle experiments on export of functional nanobodies demonstrated the potential of inducible secretion.

ii) Application of a forward genetic screen revealed the novel secretion factor Jps1 as essential for unconventional secretion Cts1. In the present study, adaptation of this genetic screen for identification of hyper secretion mutations led to isolation of at least four hyper secretion candidates. Important insights for elucidation of the underlying mutation via pooled linkage analysis demonstrated capability and limitations of this system and will direct further optimizations for efficient analysis of hyper secretion mutants and responsible mutations.

In summary, yield and applicability of unconventional secretion of heterologous proteins could be improved towards a more competitive biotechnological expression platform.

# Zusammenfassung

Die biotechnologische Produktion und Sekretion heterologer Proteine stellt hohe Anforderungen an die jeweiligen Expressionssysteme. Eine breite Auswahl an Sekretionssystemen ist daher wichtig, um vorhandene Nischen zu füllen. Die Anwendung der unkonventionellen Sekretion für den Export heterologer Proteine im neuartigen biotechnologischen Produktionswirt *U. maydis* wurde bereits in früheren Studien etabliert. Die Nutzung der endogenen sekretorischen Maschinerie der Chitinase Cts1 über einen alternativen Exportweg, ermöglicht die Sekretion von unglykosylierten Proteinen. Dies kann unter anderem zur Sekretion von pharmazeutisch relevanten oder bakteriellen Proteinen von Vorteil sein. Im Zuge dieser Dissertation wurden zwei Hauptstrategien verfolgt, um das System in Bezug auf Anwendbarkeit und Ausbeute weiter zu optimieren.

i) Einblicke in den Mechanismus der unkonventionellen Sekretion zeigten deren Abhängigkeit von der Bildung des sekundären Septums während der Zytokinese auf. Dieses schließt die funktionelle Fragmentierungszone zwischen Mutter- und Tochterzelle ab. Die Bildung des sekundären Septums ist abhängig von der Kinase Don3, welche dadurch als *Gatekeeper* dieses Mechanismus fungiert. Folglich führt eine Deletion von *don3* zu einer starken Minderung der unkonventionellen Sekretion. Die Identifizierung der regulatorischen Komponenten für die unkonventionelle Sekretion erlaubte die Anwendung zur Regulation dieses Prozesses. Hierzu wurde im Rahmen dieses Projekts die Regulation von Don3 sowohl auf transkriptioneller als auch auf post-translationaler Ebene etabliert. Während die transkriptionelle Regulation auf einem Kohlenstoffquellen-induzierbaren Promotor basiert, wurde die post-translationale Regulation durch eine alternative, ATP-Analog empfindliche, Don3 Version erreicht. Optimierungen der Kultivierung sowie Regulationsbedingungen ermöglichten die effiziente Anwendung beider Systeme zur Proteinproduktion und –sekretion. Die Etablierung eines Autoinduktionsprozesses erlaubte die Kultivierung in *Batch*-Fermentation mit getrennten Phasen der Proteinsynthese sowie Sekretion. Der Prozess der autoinduzierbaren Sekretion wurde mittels Nachweises des Exportes von funktionellen *Nanobodies* verifiziert und zeigte das Potential dieses Systems.

ii) Durch Anwendung eines vorwärts-genetischen Screens wurde der neuartige Sekretionsfaktor Jps1 als essentiell für die unkonventionelle Sekretion von Cts1 identifiziert. Im Rahmen dieser Arbeit führte die Anpassung dieses genetischen Screens zur Identifizierung von Hypersekretionsmutanten. Wichtige Erkenntnisse zur Aufdeckung der zugrundeliegenden Mutationen mittels *pooled linkage analysis* zeigten Möglichkeiten und Grenzen dieser Strategie auf und werden als Grundlage für weitere Optimierungen zur effizienten Analyse von Hypersekretionsmutanten und –mutationen dienen.

Zusammenfassend lässt sich sagen, dass die Ausbeute und Anwendbarkeit der unkonventionellen Sekretion heterologer Proteine maßgeblich verbessert werden konnte. Dies ist ein wichtiger Schritt in Richtung einer wettbewerbsfähigen, biotechnologischen Expressionsplattform.

# Abbreviations

| Abbreviation | Meaning |
|---|---|
| (v/v) | volume per volume |
| (w/v) | weight per volume |
| × g | fold gravitational force |
| °C | degree centigrade |
| 4-MU | 4-methylumbelliferon |
| aa | amino acid |
| ABC | ATP-binding cassette |
| Afu | arabinofuranosidase |
| Amp | ampicillin |
| AMP | anti microbial peptide |
| bE | bEast |
| BoNTA | botulinum toxin A |
| bp | base pair |
| BSA | bovine serum albumin |
| bW | bWest |
| CAR | contractile actomyosin ring |
| CAS9 | CRISPR-associated protein 9 |
| Cbx | carboxin |
| Cdc42 | cell division control protein 42 |
| CGL | Cts1, Gus-Cts1, LacZ-Cts1 reporter |
| CHO | chinese hamster ovary |
| CM | complete medium |
| COP | coat protein complex |
| CRISPR | clustered regularly interspaced short palindromic repeats |
| C-terminal | carboxyterminal |
| DF | downstream flank |
| DNA | desoxyribonucleic acid |
| EDTA | ethylenediaminetetraacetic acid |
| eGfp | enhanced green fluorescent protein |
| ER | endoplasmic reticulum |
| et al. | and other |

| Abbreviation | Meaning |
|---|---|
| EtOH | ethanol |
| Fig. | figure |
| FLP | flippase recombinase |
| g | gram |
| G418 | geneticin |
| gDNA | genomic DNA |
| GEF | guanine exchange factor |
| GH | glycoside hydrolase |
| Glc | glucose |
| GRASP | golgi reassembly stacking proteins |
| Gus | β-glucuronidase |
| h | hour |
| HA | hemagglutinin |
| HCl | hydrochloride |
| HEPES | 4-(2-Hydroxyethyl)piperazine-1-ethanesulfonic acid |
| His | histidin |
| HRP | horseradish peroxidase |
| Hyg | hygromycin |
| IMAC | immobilized metal ion affinity chromatography |
| kb | kilobase |
| kDA | kilo dalton |
| L | liter |
| LacZ | β-galactosidase |
| M | molar (mol/l) |
| mAbs | monoclonal antibodies |
| mb | megabase |
| MeOH | methanol |
| MES | 2-(N-morpholino)ethanesulfonic acid |
| Mfa | mating factor pheromone |
| mg | milligram |
| mL | milliliter |

| Abbreviation | Meaning |
|---|---|
| mM | millimolar |
| mRNA | messenger RNA |
| MUC | 4-methylumbelliferyl β-D-N,N',N"-triacetylchitotrioside |
| MUG | 4-methylumbelliferyl-β-D-glucuronide |
| MVB | multi vesicular body |
| NA-PP1 | 1-(1,1-dimethylethyl)-3-(1-naphthalenyl)-1H-pyrazolo[3,4-d]pyrimidin-4-amine |
| Nat | nourseothricin |
| NB | nanobody |
| NEB | New England Biolabs |
| nosT | nos terminator |
| N-terminal | aminoterminal |
| OD | optical density |
| ONPG | o-nitrophenyl-β-D-galactopyranoside |
| PAGE | polyacrylamide gel electrophoresis |
| PBS | phosphate buffered saline |
| PCR | polymerase chain reaction |
| Pra | pheromone receptor a |
| Prf1 | pheromone response factor 1 |
| PtdInsP | phosphatidyl-inositol-phosphate |
| RAMOS | respiration activity monitoring system |
| RFU | relative fluorescence units |
| RNA | ribonucleic acid |
| RT | room temperature |
| scFv | single-chain variable fragment |
| SDS | sodium dodecyl sulfate |
| Sec | second |
| SHH | streptavidin-histidin-haemagglutinin |
| SNARE | soluble N-ethylmaleimide-sensitive-factor attachment receptor |
| SNP | single nucleotide polymorphism |
| SP | signal peptide |

| Abbreviation | Meaning |
|---|---|
| TBS | tris buffered saline |
| TCA | trichloric acetic acid |
| Tris | tris(hydroxymethyl)amino methane |
| U | unit (enzyme activity) |
| UF | upstream flank |
| UPR | unfolded protein response |
| Usec+ | hyper secretion candidate |
| | |
| UV | ultra violette |
| WT | wild type |
| X-Gal | 5-bromo-4-chloro-3-indolyl-β-D-galactopyranoside |
| X-Gluc | 5-bromo-4-chloro-3-indolyl-β-D-glucuronic acid |
| YL | yeps light |
| | |
| α | anti |
| Δ | deletion |
| µl | microliter |
| µM | micrometer |

# Table of contents

# 1 Introduction

## 1.1 Biotechnological protein production systems

The expected biotechnology market size in 2021 is valued at US$ 1,006.68 billion in 2020. Considering an estimated compound annual growth rate of 15.83%, it will reach US$ 2,438.90 billion in 2028. Health-related applications represent the highest proportion of the biotechnology market with a share of almost 50% (Grand View Research, 2021). Biopharmaceuticals account for around 40% of the global pharmaceutical market (Spadiut et al., 2014). The majority of approved biopharmaceutical products has been produced in one of the three microbial hosts *Escherichia coli, Saccharomyces cerevisiae* or *Pichia pastoris*, or in mammalian cells (Berlec & Strukelj, 2013; Spadiut et al., 2014). Product approvals doubled the typical five-yearly historical approval pace, from January 2015 to July 2018, resulting in 112 product approvals (Walsh, 2018). Important biopharmaceutical products are for example monoclonal antibodies (mAbs), hormones, clotting factors, enzymes and vaccines (Walsh, 2018). Beside the health sector, also other applications like food, agriculture, natural resources or industrial processing play a role in the biotechnology protein market (Grand View Research, 2021). Towards fulfilling the market's demands, different products, and technologies have been rolled out. Genetically modified microbes are used to produce several biotechnologically relevant enzymes such as lipases or proteases for washing agents, enzymes for raw material processing or for synthesis of semi-chemical synthesis (Jaeger & Eggert, 2002; Leisola et al., 2001).

Among different heterologous expression systems, bacterial systems constitute the quickest, simplest and cheapest platforms for protein biosynthesis (Farrokhi et al., 2009). Especially *E. coli* is extensively used since it is thoroughly studied and its physiology is very well understood and can be adapted for biotechnological needs (Berlec & Strukelj, 2013). While most recombinant proteins are expressed in the cytoplasm or directed to the periplasm, only a few mechanisms for efficient secretion of proteins in *E. coli* have been described (Berlec & Strukelj, 2013). For example, exploitation of the Type 1 secretion system is an elegant strategy towards secretion of active, correctly folded protein in sufficient yields (Schwarz, Landsberg, et al., 2012; Schwarz, Lenders, et al., 2012). Application of the endogenous secretion machinery is also performed for gram-positive bacteria. Secretion of heterologous proteins via the Sec and Tat secretion pathway has been demonstrated in species like *Corynebacterium glutamicum* or *Bacillus subtilis* (Cui et al., 2018; Freudl, 2017). Nevertheless, bacterial systems share the common disadvantage of a challenging folding and post-

translational modification of heterologous proteins, which is particularly relevant for eukaryotic proteins. Furthermore, problems of inclusion body formation and proteolytic degradation reduce yields in bacterial expression systems (Baneyx & Mujacic, 2004). Although several approaches tackle these disadvantages, production of functional heterologous proteins in bacterial systems still can be challenging for a number of proteins (Farrokhi et al., 2009; Weickert et al., 1996).

In the case of highly demanding heterologous (eukaryotic) proteins, switching to a eukaryotic expression host can be advantageous. Mammalian cell culture systems are for example prevalent in production of biopharmaceutical therapeutics (Tripathi & Shrivastava, 2019; Walsh, 2018). Especially human cell lines have the advantage of performing native post-translational modifications of proteins (O'Flaherty et al., 2020). The majority of approved heterologous proteins have been produced in Chinese Hamster Ovary (CHO) cells. Understanding of post-translational modification and cultivation in cell suspensions are major reasons for their popularity among the different available expression systems (Berlec & Strukelj, 2013). However, high cultivation costs and risks of viral contaminations complicate upscaling of heterologous protein production in mammalian cell systems (O'Flaherty et al., 2020).

Fungal expression systems share a lot of benefits of mammalian cells and bacterial expression systems. Fast growth in inexpensive media as described for bacterial systems combined with advantages of eukaryotic systems such as proper folding and modifications of proteins are major advantages of fungal expression systems (Berlec & Strukelj, 2013; O'Flaherty et al., 2020). Different filamentous and yeast-like fungal systems are used in biotechnology. Filamentous fungi show a high metabolic versatility and are known to produce several valuable molecules like organic acids, enzymes and antibiotics (El-Enshasy, 2007). Alongside endogenous products, filamentous fungi are also powerful systems for production of heterologous proteins (Punt et al., 2002). Especially the efficient protein secretion capability is a major advantage of filamentous fungi expression systems (Sun & Su, 2019).

*P. pastoris* and *S. cerevisiae* are commonly used yeast expression hosts (Tripathi & Shrivastava, 2019). Especially *S. cerevisiae* is one of the most important biotechnological expression platform organisms because of its easy cultivation and the deep knowledge of its cellular functions (Berlec & Strukelj, 2013; Farrokhi et al., 2009). Understanding of post-translational modifications allowed development and use of different adaptations in protein processing towards increased yield of functional complex proteins (Berlec & Strukelj, 2013; Hamilton et al., 2006; Laukens et al., 2015). Nonetheless, despite further adaptations, fungal expression systems still have some major drawbacks. Post-translational modifications, e.g. glycosylation, still differ from human patterns, which can have severe effects on functionality of the protein (De Pourcq et al., 2010; Gerngross, 2004). Another major problem is the

secretion of endogenous extracellular proteases, limiting the yield of heterologous protein in the supernatant. Although deletion of host proteases can reduce extracellular degradation, fungal organisms require different elaborate deletion strategies (Idiris et al., 2010; Sarkari et al., 2014).

Despite several attempts and strategies to optimize existing systems, development of novel, tailor-made systems meeting specialized criteria is crucial. A manifold repertoire of potential biotechnological expression hosts enables selection of a system precisely fitting to bioproducts' demands.

## 1.2 Eukaryotic protein secretion

### *1.2.1 The classical secretion pathway*

Protein secretion is understood as translocation of proteins from the intracellular to the extracellular space across the plasma membrane. For biotechnological purposes, secretion of proteins can be advantageous since it simplifies downstream processing due to an easy way to separate the desired product in the supernatant from remaining cells. Furthermore, contamination with intracellular proteins is avoided (Flaschel & Friehs, 1993).

Eukaryotic secretion is generally mediated by the conventional secretion pathway, in which proteins are guided to the endomembrane system by their N-terminal signal peptide (Viotti, 2016). The signal peptide located at the N-terminus of the secretory protein is recognized by the signal recognition particle and directed to the endoplasmic reticulum (ER) (Benham, 2012; Siegel & Walter, 1988). Ribosome stalling, docking onto the ER and translation of the protein into the ER lumen takes place. Several ER membrane proteins associate and form a pore for entry of proteins into the ER lumen, with translocation occurring either co- or post-translationally. During the process of translocation, the signal peptide is cleaved off (Johnson & van Waes, 1999). Translation of the nascent polypeptide into the ER presents its entry into the secretory pathway (Lee et al., 2004). The milieu in the ER facilitates protein folding, modification and processing. Its oxidative environment allows disulphide bond formation between free cysteine residues by the protein disulphide isomerase / ER oxireductase system. Chaperons guide newly synthesized proteins into the correct conformation. Furthermore, post-translational modifications like species-specific *N*-glycosylation affecting protein stability and activity take place within the ER lumen (Csala et al., 2012; Lee et al., 2004). Upon correct folding and processing of the protein in the ER lumen, it is forwarded to the Golgi apparatus. Therefore, the ER cargo protein is recruited to the ER membrane and packed into vesicles by budding. Vesicles are COPII (coat protein complex II) coated and guided to the Golgi apparatus (Benham, 2012), where they are recognized by

SNARE (soluble N-ethylmaleimide-sensitive-factor attachment receptor) proteins and fuse with the Golgi membrane (Lee et al., 2004). Additional post-translational modifications take place in the Golgi apparatus, namely *O*-glycosylation and addition of other functional groups, before proteins are sorted for secretion. During this process, they are incorporated in vSNARE-coated vesicles that are guided to the tSNARE-coated plasma membrane where secretion to the extracellular space via exocytosis occurs (Delic et al., 2013; Lee et al., 2004; Potelle et al., 2015). This secretion process is called conventional secretion and is highly conserved in eukaryotes (Ding et al., 2012). However, besides conventional secretion, elucidation of other secretion mechanisms is beginning to emerge.

### *1.2.2 Eukaryotic unconventional secretion mechanisms*

Identification of proteins belonging to the secretome but lacking a signal peptide, raised awareness of the existence of other alternative secretory pathways. Beside absence of a signal peptide, a common feature of all proteins, secreted via these diverse "unconventional" secretion mechanisms is that secretion is not affected by the drug brefeldin A that blocks ER/Golgi dependent secretory mechanisms (Nickel, 2005). Bypassing of ER or Golgi apparatus allows unconventionally secreted proteins to avoid posttranslational modifications that are specific for the endomembrane system or premature interactions with proteins within ER or Golgi (Nickel, 2010). Therefore, unconventional secretion enables secretion of proteins that are sensitive to cellular processes that occur in the ER or Golgi. Furthermore, quick release of proteins allows the cell to respond to cellular stress as exported proteins are often involved in cell survival, immune response and tissue organization (Rabouille, 2017; Rabouille et al., 2012). Mechanisms of unconventional secretion can be categorized according to different parameters. Non-vesicular mechanisms rely on the direct translocation across the plasma membrane, either pore mediated or via membrane transport proteins (Nickel, 2010; Rabouille et al., 2012). Alternatively, protein export can be facilitated via intracellular membrane-bound intermediates, which are directed to the plasma membrane to release unconventionally secreted proteins into the extracellular space. These can be intracellular vesicles like autophagosomes or Golgi-derived vesicles. These routes of unconventional secretion are considered as vesicular pathways (Nickel, 2010). Vesicular and non-vesicular mechanisms can further be categorized in four types where type I & II represent non-vesicular mechanisms while type III and IV constitute vesicular mechanisms. Type I describes pore-mediated translocation across the plasma membrane while type II involves ATP-binding cassette (ABC) transporters in the plasma membrane. Vesicular transport is either mediated by intracellular vesicles such as exosomes or autophagosomes in type III or describes secretion of proteins that contain a signal peptide or transmembrane domain and enter the ER

but bypassing the Golgi apparatus in type IV. Interestingly, Type I to III all are leaderless proteins, while Type IV proteins are the only unconventionally secreted ones, which contain a signal peptide (Figure 1.1) (Rabouille, 2017; Rabouille et al., 2012).

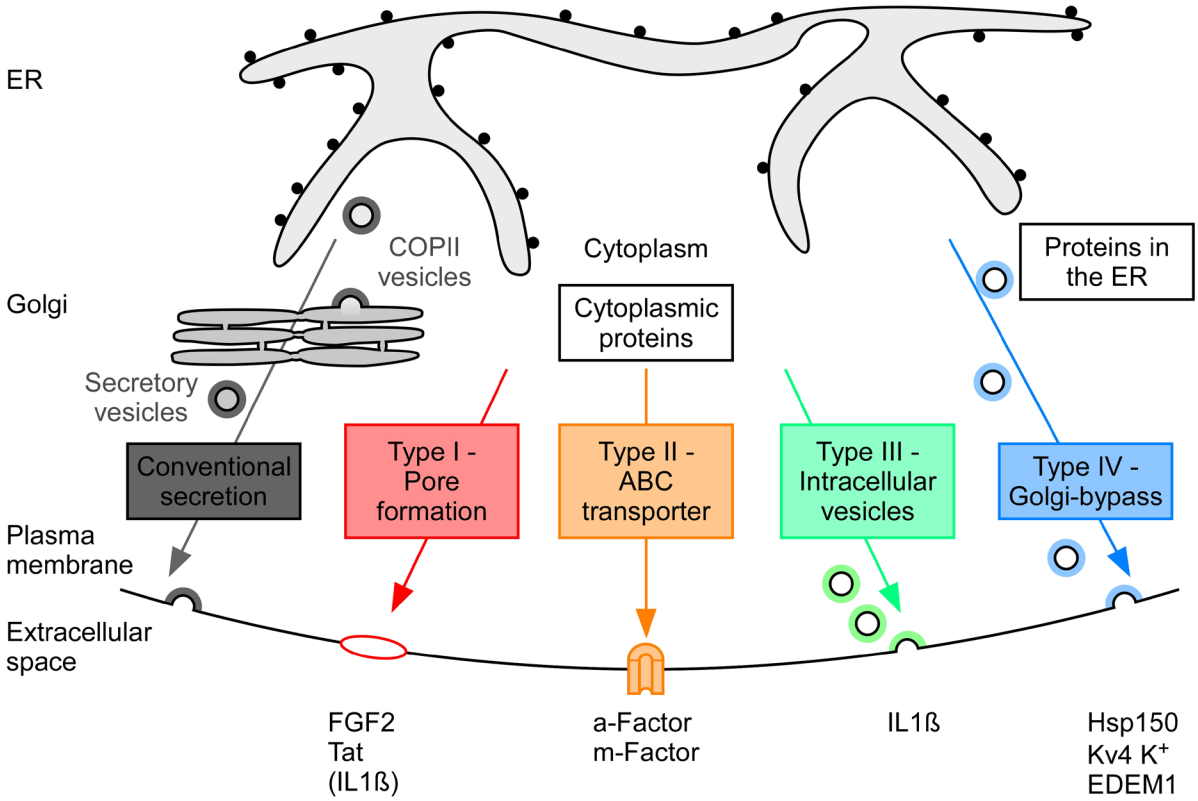


**Figure 1.1. Unconventional secretion mechanisms.** Unconventionally secreted proteins can cross the plasma membrane by non-vesicular mechanisms like pore formation (Type I) or facilitated by ABC transporters (Type II). Vesicular unconventional secretion involves either intracellular vesicles (Type III) or a Golgi-bypass (Type IV). Examples of proteins are listed below the respective mechanism. Classification and visualization according to Rabouille (Rabouille, 2017).

In type I unconventional secretion pathways, pore formation allows cytoplasmic, leaderless proteins to be secreted across the plasma membrane. Pore formation either results in a constitutive secretion or is triggered by inflammation (Rabouille, 2017). One important example of this mechanism is the release of Fibroblast Growth Factor 2 (FGF2). Phosphorylated FGF2 is recruited to the phosphoinositide $PI(4,5)P_2$ at the inner plasma membrane where it oligomerizes, resulting in the formation of a pore in the plasma membrane (Ebert et al., 2010; Steringer et al., 2015). Monomeric FGF2 that passes through the pore is trapped by heparan sulfate proteoglycans at the outside (Nickel & Rabouille, 2009; Zehe et al., 2006). Another example for type I unconventional export of proteins are the HI-viral Tat protein or annexin Anxa2 (Dimou & Nickel, 2018; Rabouille et al., 2012). Type II unconventional secretion is mediated by ABC transporters. *S. cerevisiae* and *Schizosaccharomyces pombe* mating a- and m- factors as well as acylated peptides are secreted via this mechanism (Rabouille, 2017; Rabouille et al., 2012). Type III and type IV

secretion are both dependent on intracellular vesicle structures. Type III secretion describes export via secretory membrane-bound organelles. Beside secretory vesicles, such as exosomes, secretion via autophagosomes and SNARE protein-coated vesicles is described e.g. for *S. cerevisiae* Acb1 (Rabouille, 2017). Another example is the secretion of interleukin 1β (IL1β) via different types of vesicles, like secretory lysosomes, microvesicles and multivesicular bodies. While the exact mechanism is still under investigation, secretion involves exocytosis of IL1β containing vesicles. It was proposed that import of IL1β into vesicles is mediated by stress dependent molecular transporters (Andrei et al., 1999). Interestingly, while inflammatory stress triggers secretion via type I, starvation triggers type III secretion (Rabouille, 2017). Type IV secretion differs from the previously described mechanisms, since proteins carry a signal peptide or transmembrane domain (Rabouille, 2017). Proteins secreted via this mechanism are processed in the ER but reach the plasma membrane directly via alternative routes, e.g. non-COPII vesicles or by bypassing the Golgi. Therefore, type IV secreted proteins are not affected by inhibition of ER Golgi transport using brefeldin A (Grieve & Rabouille, 2011). One example of type IV secretion is heat-shock protein 150 (Hsp150). Secretion of Hsp150 is independent of COPII-coat components as ER exit occurs at specific transitional ER (tER) sites, lacking described COPII-coat components. Also, for the voltage-sensitive potassium channel Kv4 $K^+$ and ER degradation-enhancing mannosidase-like 1 (EDEM1) bypassing of the COPII machinery was described (Grieve & Rabouille, 2011). Circumvention of the Golgi apparatus is mediated by Golgi reassembly stacking proteins (GRASP). Misfolding of transmembrane proteins can trigger ER stress and therefore overwhelming the ER machinery by immature proteins (Jung et al., 2020). ER stress results in activation of a member of the GRASP family, resulting in targeting of specific Golgi-bypass proteins, for example cystic fibrosis transmembrane conductance regulator. Targeted proteins are encapsulated into carriers that are then targeted directly to the plasma membrane (Rabouille, 2017).

## 1.3 The smut fungus *Ustilago maydis*

### *1.3.1 Biology and genetics*

The plant pathogen *Ustilago maydis* is a member of the family Ustilaginaceae in the phylum of basidiomycota. It is the causative agent of smut disease in corn, where infection of *Zea mays* and Teosinte (*Zea mays* subsp. parviglumis) results in formation of galls filled with teliospores (Banuett, 1992; Bölker, 2001). In its biphasic life cycle the smut fungus undergoes a dimorphic switch from haploid yeast like cells in the saprotrophic phase to diploid hyphal cells in a biotrophic phase associated with colonization of plant tissue (Feldbrügge et al.,

2004). In order to pass from the saprotrophic phase to the biotrophic phase and plant infection, two haploid cells need to mate and form a dikaryotic hypha (Feldbrügge et al., 2006). Mating in *U. maydis* is dependent on two loci, the biallelic *a* locus and the multiallelic *b* locus (Banuett & Herskowitz, 1989b; Kronstad & Staben, 1997). The *a* locus, located on chromosome 5, consists of two genes. While the first gene code a precursor for a lipopeptide mating factor pheromone Mfa1/2, the other gene codes for a specific receptor (Pra1/2) for the pheromone from cells of opposite mating (Bölker et al., 1992; Kämper et al., 2020). Compatibility of the *a* locus is a prerequisite for cell recognition, interaction, and fusion (Garcia-Muse et al., 2003). Triggered by a signal cascade, pheromone response factor 1 (Prf1) is expressed which activates transcription of genes of the *b* locus (Hartmann et al., 1996). The *b* locus, located on chromosome 1, encodes the homeodomain transcription factors bEast and bWest (bE, bW) existing in more than 20 alleles. Upon plasmogamy initiated by the Mfa-Pra pheromone receptor system, different subunits of the bE/bW heterodimer interact, regulating genes important for formation of the infectious hyphae (Feldbrügge et al., 2006; Kämper et al., 2020). The life cycle is completed within the host plant, resulting in tumor formation, containing teliospores. After tumor disruption, diploid spores are released and during the process of germination, they undergo meiosis to produce haploid cells (Feldbrügge et al., 2004). Successful mating of two parental strain of different *a* and *b* loci is essential for sexual reproduction and thus to obtain meiotic progeny.

### *1.3.2 U. maydis as a fungal model*

*U. maydis* has been used in molecular biology for more than half a century (Holliday, 1974). Easy cultivation, a completely sequenced and annotated genome and versatile strain engineering methods make *U. maydis* an easily accessible organism (Brachmann, 2001; Holliday, 1974; Kämper et al., 2006; Terfrüchte et al., 2014). Fields of study reach from DNA repair mechanisms and homologous recombination to plant-pathogen interaction and endosome-coupled long distance transport along the microtubule cytoskeleton (Bösch et al., 2016; Holliday, 1974; Olgeiser et al., 2019). Deep insights in basic research laid the foundation for the establishment of various molecular, genetic, and biochemical methods for *U. maydis.* Strain generation via homologous recombination is highly efficient and allows stable genetic manipulations. A versatile Golden Gate toolbox enables fast and easy generation of plasmids for transformation (Terfrüchte et al., 2014).

The annotated genome and described tools open grand possibilities for quick and easy genetic modifications such as deletions, insertions, or gene fusions (Brachmann et al., 2004). A large set of genetic elements like different promoters, reporter genes and selection markers is available for genetic modification (Brachmann et al., 2004; Feldbrügge et al., 2004;

Terfrüchte et al., 2014). A variety of different insertion loci and resistance marker recycling allows for generation of engineered strains, harboring multiple different heterologous elements (Brachmann et al., 2004; Khrunyk et al., 2010; Sarkari et al., 2016; Terfrüchte et al., 2018). Establishment of the CRISPR/Cas9 system in *U. maydis* offers an additional strategy towards strain engineering beside homologous recombination (Mariana Schuster et al., 2016; Zuo et al., 2020).

A deep understanding of cellular processes in conjunction with efficient generation of engineered strains led to a huge variety of different tailored strains optimized for different strategies such as solo-pathogenicity, artificial induction of hyphae or deficiency in extracellular proteases. Furthermore, a broad selection of isolated wild type strains offers different background strains for engineering (Banuett & Herskowitz, 1989b; Becker et al., 2020; Bölker et al., 1995; Brachmann, 2001; Sarkari et al., 2014; Terfrüchte et al., 2018). Importantly, laboratory strain AB33, which harbors genes for hyphal growth under an inducible promoter, does not only allow studies in haploid strains growing hyphal without prior mating, but is also a non-pathogenic strain (Brachmann, 2001). Another important aspect for application of *U. maydis* is the wide variety of different cultivation possibilities. A generation time of two hours, growth in reaction tubes, shaking flasks, fermenters or online measurements in Respiration Activity Monitoring System (RAMOS) devices allow defined cultivation (Terfrüchte et al., 2017; Terfrüchte et al., 2018).

Versatile molecular, genetic and biochemical tools as well as growth in several fermentation conditions with a wide repertoire of growth media makes *U. maydis* a promising candidate also in biotechnological applications (Feldbrügge et al., 2013; Holliday, 1974; Tsukuda et al., 1988; Verduyn et al., 1992). Intrinsic carbohydrate-active enzymes as well as natural valuable products like glycolipids, sugar alcohols, or organic acids harbor great potential for exploitation as a biotechnological cell factory for biomass valorization (Geiser et al., 2016; Wierckx et al., 2021).

### *1.3.3 Unconventional secretion in U. maydis*

In *U. maydi*s, a total of 426 proteins were predicted to carry an N-terminal signal peptide and to be secreted to the supernatant, most of them with unknown function and specific to *U. maydis* (Kämper et al., 2006). Apart from these proteins, mass spectrometry analysis of the apoplastic fluid revealed presence of 65 proteins without a classical secretion signal (Krombach et al., 2018). Previously, also the chitinase Cts1, lacking such N-terminal secretion signal was detected extracellularly, suggesting an unconventional secretion mechanism (Koepke et al., 2011; Stock et al., 2012). It is part of the chitinolytic machinery and harbors a highly conserved glycoside hydrolase (GH) 18 domain (Koepke et al., 2011; Langner et al.,

2015). Interestingly, all other chitinases of the chitinolytic machinery are secreted via signal peptide mediated conventional secretion (Langner et al., 2015).

Unconventional release of Cts1 has been shown to be cytokinesis dependent. In concert with other secreted chitinases, chitinase Cts1 is involved in hydrolyzation of connecting chitin to separate mother and daughter cells (Langner et al., 2015). Separation of mother and daughter cell is initiated by the formation of the primary and secondary septum, which resemble the fragmentation zone (Weinzierl et al., 2002). Primary and secondary septation involve formation of a contractile actomyosin ring (CAR), triggered by Cdc42-Guanine exchange factor (GEF) Don1 and the Ste20-like protein kinase Don3 (Böhmer et al., 2008; Böhmer et al., 2009; Freitag et al., 2011). Don1 and Don3 interact with cell division control protein 42 (Cdc42), initiating a signal cascade (Weinzierl et al., 2002). Deletion of either *don1* or *don3* results in no secondary septation event, cells therefore fail to complete formation of a functional fragmentation zone (Weinzierl et al., 2002). Complementation of *don3* deletion strains via an inducible version rescues the phenotype (Böhmer et al., 2008; Böhmer et al., 2009).

After formation of a functional fragmentation zone separation of mother and daughter cell is dependent on chitinase activity. Cts1 accumulates in the assembled fragmentation zone between mother and daughter cells where it is hypothesized to hydrolyze the remnant chitin cell wall (Langner et al., 2015). Degradation of the fragmentation zone results in release of Cts1 into the supernatant (Reindl et al., 2019). Interestingly, Cts1 also localizes to the fragmentation zone when no secondary septum is formed. During this lock-type secretion, Cts1 stays trapped within an immature fragmentation zone and is therefore not released to the supernatant until the secondary septum is formed, which results in a functional fragmentation zone (Reindl et al., 2019).

Unconventional secretion of Cts1 was verified using the bacterial enzyme β-glucuronidase (Gus) fused to Cts1 as a reporter (Stock et al., 2012). Exploitation of Cts1 as a carrier allows to measure Gus activity in the supernatant. Extracellular Gus activity can be determined quantitatively using the substrate MUG (4-methylumbelliferyl-ß-D-glucuronide) or qualitatively, using the chromogenic substrate X-Gluc (5-bromo-4-chloro-3-indolyl-beta-D-glucuronic acid). Importantly, the presence of a eukaryotic *N*-glycosylation site in the bacterial enzyme is used for verification of the unconventional secretory pathway. While this *N*-glycosylation site is not affected in bacteria, sugar moieties are attached in the endomembrane system of eukaryotes during conventional secretion, leading to its inactivation (Farrell & Beachy, 1990). Since the unconventional secretory route bypasses the endomembrane system and therefore also post-translational modifications such as *N*-glycosylation, Gus remains active when co-exported with Cts1 and can thereby serve as a reporter for unconventional secretion (Figure 1.2) (Feldbrügge et al., 2013; Stock et al., 2012). Importantly,

this also demonstrates that secretion of heterologous proteins fused to Cts1 bypassing the endomembrane system and the cognate modifications is possible (Stock et al., 2012).

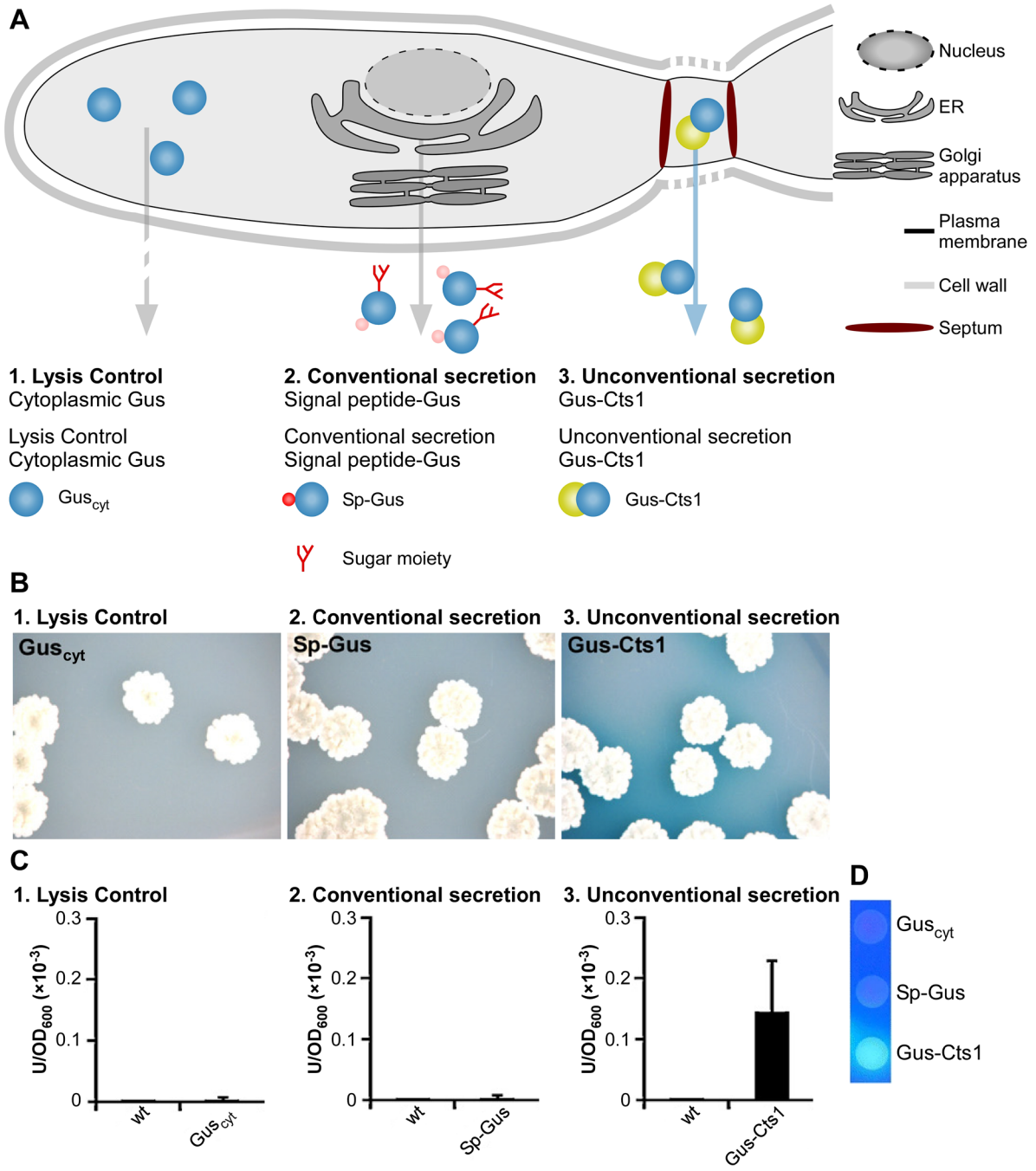


**Figure 1.2. Gus-reporter assay to study unconventional Cts1 secretion. (A)** Schematic model of the different routes and options of Gus localization. Cytoplasmic Gus lacking a secretion signal serves as a lysis control. Gus with an N-terminal signal peptide (that is cleaved off during secretion process) is secreted conventionally, accompanied by attachment of sugar moieties (indicated as pictogram that differs from the actual sugar structure). The secreted enzyme is inactive. Gus fused to Cts1 results in unconventional secretion of the fusion protein and Gus activity is reserved. **(B)** Extracellular Gus activity of strains producing cytoplasmic Gus, Sp-Gus and Gus-Cts1 on CM-X-Gluc plates. Blue color indicates Gus activity by chromogenic conversion of X-Gluc (Stock et al., 2012). **(C)** Extracellular Gus activity of cytoplasmic Gus, Sp-Gus and Gus-Cts1 in quantitative liquid assays using MUG as a substrate (Stock et al., 2012). **(D)** Extracellular Gus activity of strains producing cytoplasmic Gus, Sp-Gus and Gus-Cts1 in qualitative plate assays using MUG as a substrate. Generation of the fluorescent product 4-methylumbelliferone was detected using UV light (Feldbrügge et al., 2013).

### *1.3.4 Biotechnological perspectives of unconventional secretion*

Unconventional secretion of Cts1 is of special interest for biotechnological protein production since fusion of a heterologous protein to Cts1 allows co-export (Stock et al., 2012). Proteins are therefore localized to the fragmentation zone and released to the supernatant upon degradation of remnant chitin and separation of mother and daughter cells (Langner et al., 2015; Reindl et al., 2019). Thus, secretion via this lock-type unconventional secretion mechanism is dependent on endogenous Cts1 secretion (Figure 3).

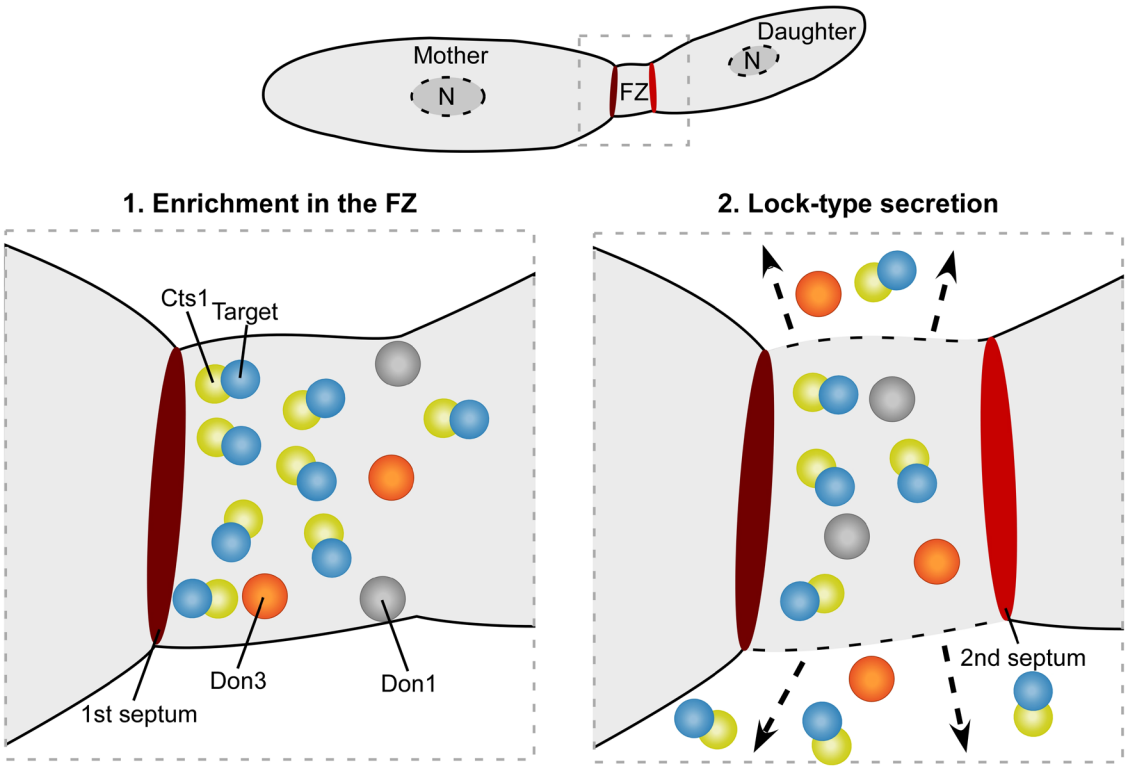


**Figure 1.3. Exploiting lock-type unconventional secretion for export of heterologous proteins.** Heterologous protein, fused to Cts1 is trapped inside the immature fragmentation zone between mother and daughter cell before formation of secondary septum (1, left panel). After initiation of secondary septum formation triggered by Cdc42-GEF Don1 and the Ste20-like protein kinase Don3, functional fragmentation zone is resolved, resulting in release of proteins into the culture supernatant (2, right panel). N, nucleus; FZ, fragmentation zone. Figure adapted from Wierckx and colleagues (Wierckx et al., 2021).

Hitchhiking Cts1 secretion offers the possibility to bypass the endomembrane system avoiding modifications such as *N*-glycosylation. Thus, this mechanism allows to evade major drawbacks eventually restricting the use of glycosylated proteins e.g. decreased stability (Tull et al., 2001), inactivation of (bacterial) enzymes (Stock et al., 2016) or to the elicitation of allergic reactions in pharmaceutical applications (Gerngross, 2004; Walsh & Jefferis, 2006). Furthermore, the Cts1-mediated unconventional secretion enables secretion of proteins up to at least 173 kDa (Stock et al., 2012). Although recent studies demonstrated the potential of unconventional secretion of various biotechnological relevant heterologous targets like carbohydrate-active enzymes for plant biomass degradation (Stoffels et al., 2020), or

biopharmaceutical targets like single-chain antibodies (Sarkari et al., 2014) and nanobodies (Terfrüchte et al., 2017), yields were not yet satisfying.

Post-secretory extracellular degradation of proteins by host proteases proposes the major problem in fungal biotechnological production chassis (Idiris et al., 2010). Indeed, deletion of up to eight endogenous proteases increased stability and yield of secreted proteins (Sarkari et al., 2014; Terfrüchte et al., 2018). However, step-by-step deletion of at least 21 predicted proteases displays a time consuming strategy towards minimization of extracellular proteases activity (Terfrüchte et al., 2018). Therefore, previous studies focused on reduction of protease activity on a larger level: Deletion of the protease Kexin2 (Kex2). In *S. cerevisiae,* Kex2 is known to process other proteases in the Golgi apparatus by cleavage of pro-sequences (Fuller et al., 1988). While deletion of *kex2* indeed decreased the extracellular proteolytic potential markedly, adverse effects, namely cytokinesis defects, formation of aggregates and an overall reduced fitness, diminished the potential of this approach. Another strategy focused on optimizing cultivation conditions to avoid activation of extracellular proteases. Buffered medium to avoid drastic pH shifts also increased stability of unconventionally secreted proteins in ambient pH conditions and by avoidance of pH-dependent activation of extracellular proteases (de Souza et al., 2015; Terfrüchte et al., 2018). These different optimization steps already increased the yields and unconventional secretion of a αBoNTA nanobody. The optimized system resulted in a yield of 140 µg per liter culture supernatant (Terfrüchte et al., 2018).

## 1.4 Aim of the thesis

In recent studies, the biotechnological potential of *U. maydis* for heterologous protein production was demonstrated and optimized on different levels. Improvement of strain generation, optimization of cultivation conditions, evaluation of different targets and understanding of the underlying secretion mechanism were important steps towards establishment of a protein secretion platform (Reindl et al., 2019; Sarkari et al., 2014; Stock et al., 2012; Stoffels et al., 2020; Terfrüchte et al., 2014; Terfrüchte et al., 2017; Terfrüchte et al., 2018). Nevertheless, yields of unconventionally secreted proteins were in a low and in a non-competitive range, needing further improvement to establish an industrially relevant chassis organism.

Two different strategies should be established in the present thesis to increase the overall yield of secreted protein as well as to expand the possible applications of the secretion system.

i) First, an inducible system for regulation of unconventional secretion should be established. Blocking the lock-type secretion mechanism leads to accumulation of Cts1-coupled proteins in the fragmentation zone. This knowledge should be applied to establish a switch that allows trapping secreted proteins in the fragmentation zone until a defined time point in which the proteins are released to the culture supernatant. Uncoupling of biomass formation and secretion comes with the advantage of protection of heterologous proteins in the fragmentation zone upon an external stimulus and secretion of all protein for further processing.

ii) Second, a high-throughput genetic screen should be applied for isolation and identification of hyper secretion mutants. The unconventional secretion capacity of identified mutants should be evaluated and characterized by genome sequencing and pooled linkage analysis.

To this end, the application of elucidated cellular processes for establishment of different tools and strategies should result in major improvements towards a competitive expression platform. Therefore, basic research-driven science lays an important foundation for solving challenges in biotechnological problems.

# Results and key structure of the thesis

In the following sub chapters, approaches of the present work towards optimization of unconventional protein secretion in *Ustilago maydis* are described. The strategies are structured in two main projects: "**Establishment of an inducible secretion system in *Ustilago maydis***" and "**Establishment and adaptation of a forward genetic screen**". Each project consists of a basic research publication and a publication covering applied approaches. Finally, further research perspectives for each project are described.

In a closing chapter, "**8 Final evaluation of biotechnological potential of unconventional secretion in *Ustilago maydis***", the overall achievement of postulated aims is evaluated and further projects for improvement of biotechnological capability of *U. maydis* are discussed.

# Establishment of an inducible secretion system in *Ustilago maydis*

Towards establishment of an inducible system for regulation of unconventional secretion, intrinsic mechanisms of cytokinesis and cell separation were exploited. In the first publication, "**2 The germinal centre kinase Don3 is crucial for unconventional secretion of chitinase Cts1 in *Ustilago maydis***" function of the kinase Don3 in formation of the secondary septum and a functional fragmentation zone was identified as an important perquisite for unconventional secretion of Cts1. Connection of unconventional secretion and cell separation layed an important foundation for different strategies of inducible unconventional secretion. Based on these findings, "**3 Controlling unconventional secretion for production of heterologous proteins in *Ustilago maydis* through transcriptional regulation and chemical inhibition of the kinase Don3**" aimed on establishment of different systems for inducible export of heterologous targets. Don3 induction on transcriptional and post-translational level allowed regulation of cell separation and unconventional secretion. Furthermore, cultivation strategies for different regulatory mechanisms were investigated. To this end, an auto-induction process for time-resolved production and secretion in batch cultivation was established. Further induction mechanisms and perspectives of this system are described in the chapter "**4 Outlook and further perspectives for inducible secretion in *Ustilago maydis*"**

# 2 The germinal centre kinase Don3 is crucial for unconventional secretion of chitinase Cts1 in *Ustilago maydis*

Jörn Aschenbroich [a,b], **Kai P. Hussnaetter** [a,b], Peter Stoffels [a,b], Thorsten Langner [a,1], Sabrina Zander [a,b], Björn Sandrock [c], Michael Bölker [c,d], Michael Feldbrügge [a,b], Kerstin Schipper [a,b,*]

[a] Institute for Microbiology, Cluster of Excellence on Plant Sciences, Heinrich Heine University Düsseldorf, 40204 Düsseldorf, Germany
[b] Bioeconomy Science Center (BioSC), c/o Forschungszentrum Jülich, 52425 Jülich, Germany
[c] Department of Biology, Philipps-University Marburg, 35043 Marburg, Germany
[d] LOEWE Center for Synthetic Microbiology (SYNMIKRO), Hans-Meerwein-Straße 6, 35032 Marburg, Germany
* Corresponding author at: Heinrich Heine University Düsseldorf, Institute for Microbiology, Bldg. 26.12.01.64, 40204 Düsseldorf, Germany. E-mail address: kerstin.schipper@uni-duesseldorf.de (K. Schipper).
[1] Current address: The Sainsbury Lab, Norwich Research Park, Norwich NR4 7UH, United Kingdom.

This review was published in *BBA - Proteins and Proteomics* in December 2019 and is available at doi.org/10.1016/j.bbapap.2018.10.007.

**Relevance of publication**

During cytokinesis, Cts1 accumulates in the fragmentation zone and is released depended on cell cycle and cell separation. Separation of mother and daughter cell requires a functional fragmentation zone, which is enclosed by the primary and secondary septum. The kinase Don3 is essential for formation of the secondary septum and cognate gene deletion mutants show defective cell separation and release of Cts1. This results in formation of cell aggregates with Cts1 trapped in a potentially immature fragmentation zone. Transcriptional complementation of *don3* deletion mutations via an inducible promoter resulted in formation of a functional secondary septum, cell separation and unconventional secretion of Cts1 in inducing conditions. During cultivation, activation of *don3* expression was sufficient to revive Don3 function and therefore unconventional secretion. The novel insights in the unconventional secretion mechanism allow exploitation of involved proteins in synthetic regulatory processes.

## 2.1 Abstract

Unconventional secretion has emerged as an increasingly important cellular process in eukaryotic cells. The underlying translocation mechanisms are diverse and often little understood. We study unconventional secretion of chitinase Cts1 in the corn smut fungus *Ustilago maydis*. This protein participates in the cytokinesis of yeast cells. During budding it localizes to the septated fragmentation zone where it presumably functions in the degradation of remnant chitin to allow separation of mother and daughter cell. However, the mechanistic details of Cts1 export remain unclear.

Here we investigated the mechanism of unconventional Cts1 secretion with a focus on cytokinesis. Cell-cycle inhibition experiments supported the hypothesis that Cts1 export is connected to cytokinesis. To substantiate this finding, we analysed gene deletion mutants impaired in cell separation and discovered that strains defective in secondary septum formation were affected in Cts1 export. The germinal centre kinase Don3 had a particularly strong influence on unconventional secretion. Using a synthetic switch, we unambiguously verified an essential role of Don3 for cytokinesis-dependent Cts1 export via the fragmentation zone. Thus, we gained novel insights into the mechanism of unconventional secretion and discovered the first regulatory component of this process.

## 2.2 Introduction

In recent years unconventional secretion has been uncovered as an important alternative mechanism for protein export in eukaryotic cells. The term “unconventional secretion” collectively describes protein secretion pathways in which the proteins do not possess an N-terminal signal peptide for uptake into the endoplasmic reticulum (ER). Various vesicular and non-vesicular mechanisms have been discovered of which only few examples are understood in detail (Rabouille, 2017; Rabouille et al., 2012). In higher eukaryotes important signalling molecules like interleukin beta (IL-1β), human immunodeficiency virus transactivator protein (HIV Tat) and fibroblast growth factor 2 (FGF2) are subject to unconventional secretion (Brough et al., 2017; Steringer & Nickel, 2018). In the dimorphic corn smut fungus *Ustilago maydis*, chitinase Cts1 is exported by unconventional secretion (Koepke et al., 2011; Stock et al., 2012). This enzyme participates in cell separation of budding cells in the yeast form (Langner et al., 2015).

Cell separation during the yeast-like growth phase is well understood in *U. maydis*. Two septa are formed sequentially during cytokinesis (Freitag et al., 2011; O'Donnell & McLaughlin, 1984; Weinzierl et al., 2002). Initially, a primary septum is initiated at the mother-daughter neck (Weinzierl et al., 2002). Then, a secondary septum delimits the now vacuolated

fragmentation zone and the cells finally separate upon lysis of the connecting cell wall (Langner et al., 2015; Mahlert et al., 2006; Weinzierl et al., 2002). Several mutants with aggregation phenotypes due to cell separation defects are known (Becht et al., 2005; Berndt et al., 2010; Okmen et al., 2018; Sarkari et al., 2014; Wedlich-Soldner et al., 2002) including for example mutants in which the movement of early endosomes is impaired, e.g. by eliminating the motor protein kinesin 3 (Kin3) (Wedlich-Soldner et al., 2002). Similarly, *kexin 2* (*kex2*) deletion mutants, in which processing of different pro-proteins in the Golgi apparatus is abolished, show a cell separation defect (Sarkari et al., 2014). Likely, the cytokinesis defects of such mutants are rather pleiotropic and caused by downstream effects of the respective mutation. Two specific factors regulating secondary septum formation, and thus cytokinesis in the yeast stage, have been described. The first is the guanine nucleotide exchange factor (GEF) Don1. This GEF acts in activating the small GTPase Cdc42, which leads to the initiation of secondary septum formation (Weinzierl et al., 2002). The second is the germinal centre kinase Don3, which triggers septin reassembly that precedes actomyosin ring formation (Böhmer et al., 2009; Freitag et al., 2011). Deletion of either gene results in a cell separation defect and thus, the formation of tree-like cell aggregates (Weinzierl et al., 2002). Due to this defect, yeast colonies of these mutants grown on agar plates are shaped like donuts - hence the name of the proteins (donut proteins) (Weinzierl et al., 2002).

Chitinases are essential in the degradation of the chitin-rich cell wall connecting mother and daughter cell during budding. The chitinolytic machinery of *U. maydis* encompasses three chitinases (Cts1-3) and one N-acetylglucosaminidase, Cts4 (Langner & Gohre, 2016; Langner et al., 2015). Since chitin is part of the structural scaffold of the fungal cell wall (Klis et al., 2006), chitin-remodelling enzymes usually are secreted. In line with this, Cts2-4 carry conventional N-terminal signal peptides for classical secretion via the ER and Golgi apparatus. Interestingly, the GH18 domain chitinase Cts1 lacks this signal. Nevertheless, chitin binding activity as well as Cts1-associated extracellular chitinase activity were experimentally detected using the specific substrate chitotrioside (Koepke et al., 2011; Langner et al., 2015; Terfrüchte et al., 2017). Deletion mutant studies demonstrated that both unconventionally secreted Cts1 and conventionally secreted Cts2 function in cell separation during cytokinesis. Presumably, the two enzymes act together in the degradation of remnant chitin in the fragmentation zone between mother and daughter cell in the non-infectious yeast phase of the fungus (Langner et al., 2015). While single deletion strains are not impaired in cytokinesis, cells lacking Cts1 and Cts2 fail to divide and form aggregates. In line with its biologic function in cell separation, a functional Cts1-Gfp fusion protein (Cts1G) accumulates in the fragmentation zone, probably via translocation from the daughter cell side (Langner et al., 2015). Based on these observations, we addressed the role of cytokinesis in Cts1 export in the present study.

# 2.3 Material and methods

## *2.3.1 Strains, plasmids and culture conditions*

All *U. maydis* strains used or generated in this study are listed in Table 2.1. All strains were obtained by homologous recombination yielding stable genetic backgrounds. For genome insertion at the *ip* locus, integrative plasmids were used (Stock et al., 2012). These plasmids contain an *ip*$^{R}$ allele, promoting carboxin resistance (Broomfield & Hargreaves, 1992; Keon et al., 1991). Integrative plasmids were linearized within the *ip*$^{R}$ allele using the restriction endonucleases SspI or AgeI and then used to transform *U. maydis* protoplasts (Bösch et al., 2016). Stable integration mutants harbouring a single or multiple copies of the plasmid were obtained via homologous recombination (Brachmann et al., 2004; Kämper, 2004). Alternatively, linear constructs were targeted to the *upp1* locus thereby eliminating the encoded protease (Sarkari et al., 2014). For generation of deletion mutants, resistance-cassette containing constructs encased by the respective up- and downstream flanks were excised from the different vectors. The linear DNA parts were used to transform *U. maydis* protoplasts replacing the targeted coding regions by homologous recombination (Bösch et al., 2016). All strains were verified by Southern blot analysis using digoxygenin labelled probes (Merck, Darmstadt, Germany). For *ip* insertions, the probe was obtained with the primer combination oMF502/oMF503 and the template pUMa260 (Loubradou et al., 2001). For *in locus* modifications the flanking regions were used as probes. All oligonucleotides used in this study are shown in Table S2.1.

Assembly of plasmids was performed using standard molecular cloning methods including Golden Gate cloning adapted to fungi (Terfrüchte et al., 2014). Genomic DNA (gDNA) of strain UM521 was used as a template for PCR reactions. Genomic sequences for this strain are stored at the PEDANT database (Web reference: Pedant *U. maydis* genome browser). All plasmids were verified by restriction analysis and sequencing. Deletion plasmids: pUMa2717 harbours the deletion construct for *don3* (UMAG_05543) and was obtained in a Golden Gate reaction with destination vector pUMa1467 (pDest), storage vector pUMa1507 (pStorI_1h) (Terfrüchte et al., 2014) and the upstream and downstream flanking regions amplified by PCR on gDNA using primer combinations oDD637/oDD638 and oDD639/oDD640, respectively. Gus reporter plasmids: All plasmids were inserted in the *ip* locus (Stock et al., 2012). pUMa2335 was generated by inserting a *gus:SHH* fragment into the integrative vector pUMa2113 using NcoI and NotI restriction replacing the *gus:cts1* ORF (Sarkari et al., 2014). For assembly of pUMa2887 the *don1* ORF was amplified using primer combination oMB76/oMB77. The ApaI/AscI hydrolysed PCR product was inserted into pUMa2113 as described above. A similar strategy was used to generate pUMa2888, using primer

combination oMB78/oMB79 to amplify the *don3* ORF. Inducible secretion: All plasmids carry flanking regions for insertion in the *upp1* locus (Sarkari et al., 2014). For generation of pUMa3328 a $P_{otef}$:*gfp*:$T_{nos}$/NatR construct was inserted into a destination vector using restriction enzyme SfiI for insertion in the *upp1* locus (Sarkari et al., 2014). The $P_{otef}$ promoter was then replaced by the $P_{crg}$ promoter obtained from pMF2-1n (Brachmann et al., 2004) by PCR with primers oUPP117/oUPP118 and subsequent digestion with NcoI and SbfI to obtain pUMa3329. pUMa3330 containing inducible *don3:gfp* was synthetized using pUMa3329 as backbone. As insert, a PCR product obtained with oUPP119/oUPP120 to amplify the *don3* ORF using template pUMa2888, was hydrolysed with MfeI. Similarly, pUMa3331 containing the construct for inducible Don3 secretion was obtained using a PCR product generated with oUPP119/oUP136 which was inserted into pUMa2888 using the restriction enzymes MfeI and AscI. Secretion reporter: The integrative plasmid pUMa3306 for constitutive overexpression of arabinofuranosidase (Afu2; UMAG_00837) was generated by Golden Gate cloning using 1 kb flanking regions amplified from gDNA with the oligonucleotides oUP91/oUP92 (upstream flank) and oUP93/oUP94 (downstream flank; Table S2.1). Type IIS restriction enzyme SapI was used for the Golden Gate reaction. For this purpose, pUMa2074 and pUMa2443 served as destination and storage vector, respectively, both harbouring a nourseothricin resistance (NatR)/$P_{oma}$ resistance cassette module (Geiser et al., 2016). To generate the SapI-compatible destination vector pUMa2074 a linker obtained by annealing oRL1181 and oRL1182 was introduced via SacI and XbaI sites into pUMa2062, a pUC57 derivative with a mutagenized SapI restriction site mediating ampicillin resistance. The SapI-compatible storage vector was generated by isolating the NatR/$P_{oma}$ module from pUMa2326 (pStor1_2-5n) (Geiser et al., 2016) using SfiI restriction and combining it with the SfiI hydrolysed backbone of pUMa2242, a pUC57 derivative harbouring a gentamycin resistance gene and a SapI compatible linker region. Detailed plasmid descriptions and maps are provided upon request.

*U. maydis* strains were grown at 28°C with 200 rpm shaking in CM supplemented with 1% (w/v) glucose (CM-glc) (Holliday, 1974) or 1% (w/v) arabinose (CM-ara). Experiments were performed at low optical densities between 0.5 to 1.0 to avoid stationary phase artefacts unless indicated otherwise. For long term incubation, the media were buffered with 0.1M MOPS as mentioned in the protocols below (Terfrüchte et al., 2018).

**Table 2.1.** *U. maydis* strains used in this study.

| Strains | Relevant genotype (resistance) | UMa[1] | Reference | Plasmid transformed (pUMa[1]) | Manipulated locus | Progenitor |
|---|---|---|---|---|---|---|
| AB33 | *a2* $P_{nar}$*bW2bE1* (PhleoR) | 133 | (Brachmann et al., 2001) | | *b* | FB2 |

| | | | | | | |
|---|---|---|---|---|---|---|
| AB33cts1Δ | *a2 $P_{narb}$W2bE1 umag_10419Δ* (PhleoR, HygR) | 387 | (Koepke et al., 2011) | pCts1Δ-HygR (pUMa780) | *umag_10419* (*cts1*) | AB33 |
| AB33Cts1G | *a2 $P_{narb}$W2bE1 umag_10419::egfp* (PhleoR, NatR) | 388 | (Koepke et al., 2011) | pCts1G-NatR (pUMa828) | *umag_10419* (*cts1*) | AB33 |
| AB33don1Δ /Cts1G | *a2 $P_{narb}$W2bE1 umag_10419::egfp umag_10152Δ* (PhleoR, NatR, HygR) | 1838 | This study | pDon1D_Hyg (pUMa2412) (Zander et al., 2016) | *umag_10152* (*don1*) | UMa388 |
| AB33don3Δ /Cts1G | *a2 $P_{narb}$W2bE1 umag_10419::egfp umag_05543Δ* (PhleoR, NatR, HygR) | 1839 | This study | pDon3D_HygR (pUMa2717) | *umag_05543* (*don3*) | UMa388 |
| AB33Gus-Cts1 | *a2 $P_{narb}$W2bE1 $ip^r$ [$P_{oma}$gus:shh:cts1] $ip^s$* (PhleoR, CbxR) | 1289 | (Sarkari et al., 2014) | pRabX1PomaGus-SHH-Cts 1 ubi1 3´UTR (pUMa2113) (Sarkari et al., 2014) | *ip* (*cbx*) | UMa133 |
| AB33don1Δ /Gus-Cts1 | *a2 $P_{narb}$W2bE1 $ip^r$ [$P_{oma}$gus:shh:cts1] $ip^s$ umag_10152Δ* (PhleoR, CbxR, HygR) | 1745 | This study | pDon1D_Hyg (pUMa2412) (Zander et al., 2016) | *umag_10152* (*don1*) | UMa1289 |
| AB33don3Δ /Gus-Cts1 | *a2 $P_{narb}$W2bE1 $ip^r$ [$P_{oma}$gus:shh:cts1] $ip^s$ umag_05543Δ* (PhleoR, CbxR, HygR) | 1742 | This study | pDon3D_HygR (pUMa2717) | *umag_05543* (*don3*) | UMa1289 |
| AB33$Gus_{cyt}$ | *a2 $P_{narb}$W2bE1, $ip^r$ [$P_{oma}$gus:shh] $ip^s$* (PhleoR, CbxR) | 2014 | This study | pRabX1-Poma_Gus-SHH_CbxR (pUMa2335) | *ip* (*cbx*) | UMa133 |
| AB33don1Δ /Gus-Don1 | *a2 $P_{narb}$W2bE1 umag_10152Δ $ip^r$ [$P_{oma}$gus:shh:don1] $ip^s$* (PhleoR, HygR, CbxR) | 1886 | This study | pRabX1-Poma:gus-don1_CbxR (pUMa2887) | *ip* (*cbx*) | UMa1666 |
| AB33Gus-Don1 | *a2 $P_{narb}$W2bE1 $ip^r$ [$P_{oma}$gus:shh:don1] $ip^s$* (PhleoR, CbxR) | 1884 | This study | pRabX1-Poma:gus-don1_CbxR (pUMa2887) | *ip* (*cbx*) | UMa133 |
| AB33don3Δ /Gus-Don3 | *a2 $P_{narb}$W2bE1 umag_05543Δ, $ip^r$ [$P_{oma}$gus:shh:don3] $ip^s$* (PhleoR, HygR, CbxR) | 2029 | This study | pDon3D_HygR (pUMa2717) | *umag_05543* | UMa1885 |
| AB33Gus-Don3 | *a2 $P_{narb}$W2bE1 $ip^r$ [$P_{oma}$gus:shh:don3] $ip^s$* (PhleoR, CbxR) | 1885 | This study | pRabX1-Poma:gus-don3_CbxR (pUMa2888) | *ip* (*cbx*) | UMa133 |
| AB33don1Δ /$Gus_{cyt}$ | *a2 $P_{narb}$W2bE1 umag_10152Δ $ip^r$ [$P_{oma}$gus:shh] $ip^s$* (PhleoR, HygR, CbxR) | 2287 | This study | pRabX1-Poma_Gus-SHH_CbxR (pUMa2335) | *ip* (*cbx*) | UMa1666 |
| AB33don3Δ /$Gus_{cyt}$ | *a2 $P_{narb}$W2bE1 umag_05543Δ $ip^r$ [$P_{oma}$gus:shh] $ip^s$* (PhleoR, HygR, CbxR) | 2288 | This study | pRabX1-Poma_Gus-SHH_CbxR (pUMa2335) | *ip* (*cbx*) | UMa2028 |
| AB33don1Δ | *a2 $P_{narb}$W2bE1 umag_10152Δ* (PhleoR, HygR) | 1666 | (Zander et al., 2016) | pDon1D_Hyg (pUMa2412) (Zander et al., 2016) | *umag_10152* (*don1*) | UMa133 |
| AB33don3Δ | *a2 $P_{narb}$W2bE1 umag_05543Δ* (PhleoR, HygR) | 2028 | This study | pDon3D_HygR (pUMa2717) | *umag_05543* (*don3*) | UMa133 |
| AB33don3Δ /$P_{otef}$Gfp /Gus-Cts1 | *a2 $P_{narb}$W2bE1 umag_05543Δ $ip^r$ [$P_{oma}$gus:shh:cts1] $ip^s$* | 2300 | This study | pDest-upp1Δ_Potef-eGfp-Tnos- | *umag_02178* (*upp1*) | UMa1742 |

| | | | | | | |
|---|---|---|---|---|---|---|
| | *umag_02178Δ::P$_{otef}$:egfp:T$_{nos}$* (PhleoR, CbxR, NatR, HygR) | | | NatR (pUMa3328) | | |
| AB33don3Δ /P$_{crg}$Don3G /Gus-Cts1 | *a2 P$_{nar}$bW2bE1 umag_05543Δ ip$^{r}$ [P$_{oma}$gus:shh:cts1] ip$^{s}$ umag_02178Δ::P$_{crg}$:umag_05543::egfp:T$_{nos}$* (PhleoR, CbxR, NatR, HygR) | 2302 | This study | pDest-upp1Δ_Pcrg-Don3-eGfp-Tnos-NatR (pUMa3330) | *umag_02178* (*upp1*) | UMa1742 |
| AB33don3Δ /P$_{crg}$Don3 /Gus-Cts1 | *a2 P$_{nar}$bW2bE1 umag_05543Δ ip$^{r}$ [P$_{oma}$gus:shh:cts1] ip$^{s}$, umag_02178Δ::P$_{crg}$:umag_05543:T$_{nos}$* (PhleoR, CbxR, NatR, HygR) | 2303 | This study | pDest-upp1Δ_Pcrg-Don3-Tnos-NatR (pUMa3331) | *umag_02178* (*upp1*) | UMa1742 |
| AB33P5Δ /Afu2 | *a2P$_{nar}$bW2bE1 FRT5[um04400 Δ::hyg]FRT5 FRT3[um11908Δ] FRT2[um00064 Δ] FRTwt[um02178Δ] FRT1[um04926Δ] P$_{umag_00387}$:umag_00387Δ:: P$_{oma}$:umag_00387:T$_{nos}$* (PhleoR, HygR, NatR) | 2295 | This study | pDest-Poma_umag00387NatR_ (pUMa3306) | *umag_00837 (afu2)* | UMa1391 (Sarkari et al., 2014) |

[1] Internal strain (UMa) and plasmid (pUMa) collection numbers.

## *2.3.2 Determination of Cts1 activity*

To measure Cts1 activity, liquid assays with intact cells (cell surface activity) were conducted according to published protocols with minor changes (Koepke et al., 2011; Stock et al., 2012). Main cultures were started in CM-glc from a preculture grown over day. Once the fresh cultures had reached an $OD_{600}$ of about 1.0 the suspension was subjected to the MUC assay. The MUC working solution (protect from light, store at 4°C) was prepared from a stock solution (2 mg/ml MUC in DMSO) by diluting it 1:10 with KHM buffer. Black 96-well plates (96 Well, PS, F-Bottom, µCLEAR, black, CELLSTAR, Greiner Bio-One, Frickenhausen, Germany) were used for the assay. 70 µl working solution were mixed with 30 µl of the cell suspension in one well. Activity for each strain was determined in technical triplicates. The plates were sealed with parafilm and incubated in the dark for 1 h at 28°C. The reaction was then stopped by adding 200 µl 1 M $Na_2CO_3$ and relative fluorescence units were determined in a plate reader (Tecan, Männedorf, Switzerland) with a fixed gain of 100 (excitation/emission wavelengths of 360/450 nm). Values for the respective positive control strains were eventually set to 100%. For determination of Cts1 activity in cell extracts, native cell extracts were generated (see Preparation of cell extracts) and adjusted to a total protein concentration of 33,33 µg/ml using PBS buffer. 70 µl working solution were mixed with 30 µl of the cell extracts (containing 1 µg total protein) per well.

### *2.3.3 Quantification of unconventional secretion using the Gus reporter system*

Gus assays were conducted with native cell extracts or cell-free culture supernatants according to slightly modified published protocols (Stock et al., 2012; Stock et al., 2016). Native cell extracts were generated (see Preparation of cell extracts) and adjusted to a total protein concentration of 100 µg/ml using PBS buffer. 10 µl of adjusted native cell extracts were then mixed with 90 µl of Gus-buffer and 100 µl of substrate solution (2 mM MUG, 1/50 volume bovine serum albumin fraction V (BSA) in 1x Gus buffer) in a black 96-well plate. To determine Gus activity in supernatants, 100 µl culture supernatants were mixed with 100 µl of substrate solution. 2x Gus buffer (Stock et al., 2016) was used for the Gus assay. All measurements were conducted in a plate reader (Tecan, Männedorf, Switzerland) for 70 min at 37°C with measurements every 10 min (excitation/emission wavelengths: 365/465 nm). A fixed gain of 60 was used to determine Gus activity in the form of kinetics. 4-MU was used to generate a standard curve. For data evaluation the slope (µmol/min) of the connected data points was determined and eventually set in relation to $OD_{600}$ or µg protein. For relative activities the values for the respective positive control strains were set to 1.

### *2.3.4 Quantification of arabinofuranosidase activity*

For quantification of α-L-arabinofuranosidase activity an overexpression strain of the conventionally secreted arabinofuranosidase Afu2 (UMAG_00837) was generated (see Table 2.1). *p*-nitrophenyl-α-L-arabinofuranoside (pNP-AF; Megazyme, Bray, Ireland) was used as a substrate. The substrate solution was freshly prepared and contained 1.25 mM pNP-AF in 0.1 M NaAc buffer (pH 5.5). For the assay 75 µl culture supernatant was mixed 1:1 with substrate solution in a clear 96 well plate (96 Well, PS, F-Bottom, µCLEAR, clear, CELLSTAR, Bio-One, Frickenhausen, Germany). Product accumulation was determined in a plate reader (Tecan, Männedorf, Switzerland) for 70 min every 10 min with an absorption wavelength of 405 nm at 37 °C. The amount of hydrolysed substrate was determined using *p*-nitrophenole (pNP; Merck, Darmstadt, Germany) in a range of 1 mM to 15.625 nM as a standard.

### *2.3.5 Cell cycle inhibition studies*

For inhibition studies 20 ml main cultures were inoculated in 0.1 M MOPS buffered CM-glc (pH 7) to a starting $OD_{600}$ of 0.08 from an overnight preculture. Sampling started 10 hours post inoculation (p.i.) and was continued every two hours for 18 h. The cell cycle arrest was induced using 3 mg/ml hydroxyurea (HU; f.c.) at 12 h p.i.. Cultures without addition of the reagent served as controls. Prior to sampling the $OD_{600}$ was documented. Then 2 ml aliquots

were harvested by centrifugation (22,000 x g, 5 min, RT). The cell-free supernatant was transferred to a fresh tube and used for Gus and arabinofuranosidase activity assays. Gus-SHH purified from *Escherichia coli* (Stock et al., 2012) was used to exclude potential effects of HU on Gus.

### *2.3.6 Regulated secretion of Cts1 via artificial induction of Don3*

For regulated secretion, *don3* deletion strains harbouring *$P_{crg}$:don3* or *$P_{crg}$:don3-gfp* fusions were used (AB33$P_{crg}$Don3/Gus-Cts1 and AB33$P_{crg}$Don3G/Gus-Cts1; Table 2.1). The *crg* promoter is in its off condition if glucose is used as single C-source and in its on condition if only arabinose is provided. In addition, the strains carry a reporter for unconventional Cts1 secretion expressed from the constitutive $P_{oma}$ promoter (Gus-Cts1) (Hartmann et al., 1999). To assay regulated secretion, precultures were grown in 5 ml YepsLight for 16 to 24 h at 28°C (200 rpm). Main cultures were then inoculated with 400 µl of the precultures in 5 ml CM-glc in the morning and grown over day (28°C, 200 rpm). At night the cultures were again diluted to reach a final $OD_{600}$ of 1 in the next morning using CM-glc or CM-ara. Since cultures grow slower when arabinose is used as C-source the inoculum was increased by 25% for the CM-ara cultures. Cultures are harvested at OD 0.8 to 1.0 in the morning. Therefore, 2 ml culture was centrifuged at 1,500 x g for 5 min and 1 ml of the supernatant was collected in a fresh reaction tube. 100 µl supernatant and 100 µl Gus assay buffer were mixed for a Gus activity assay with the substrate MUG (see Quantification of unconventional secretion using the Gus reporter system). A kinetic was determined for 100 min (5 min intervals) using an excitation wavelength of 365 nm and an emission wavelength of 465 nm (fixed gain: 60). For data evaluation the slope (µmol/min) of the connected data points was determined.

### *2.3.7 Preparation of cell extracts*

The preparation of whole cell protein extracts at denaturing conditions was described earlier (Stock et al., 2012). For native cell extracts the cells were resuspended in PBS buffer after snap freezing. The protein concentration was determined by Bradford assays (Bradford, 1976). For SDS-Page 10 µg whole cell extracts were supplemented with 1x Laemmli buffer and boiled for 10 min. After centrifugation for 5 min at 22,000 x g (RT), the samples were subjected to SDS Page and Western blot analysis.

### *2.3.8 Protein precipitation from culture supernatants*

Secreted proteins were enriched from supernatant samples using trichloracetic acid (TCA) precipitation. Cell free culture supernatant was harvested at an $OD_{600}$ of about 1.0 by centrifugation (4°C, 5 min) and 1 ml supernatant samples were supplemented with 250 µl of

10% (w/v) TCA in reaction tubes. The samples were incubated overnight at 4°C. After washing twice in -20°C acetone the protein pellets were resuspended in 3x Laemmli buffer (Laemmli, 1970) and the pH was neutralized with 1 M NaOH. For SDS-Page analysis the samples were first boiled for 10 min and then centrifuged for 5 min (22,000 x g, RT). The resulting supernatant was subjected to SDS-Page.

### *2.3.9 SDS-Page and Western blot analysis*

Protein samples were analysed by SDS-Page using 10% (w/v) acrylamide gels. Subsequently, proteins were blotted to methanol-activated PVDF membranes using semi-dry blotting. SHH-tagged proteins like Gus-Cts1, Gus-Don1 and Gus-Don3 were detected using a primary anti-HA (1: 3,000; Sigma-Aldrich, St. Louis, USA) antibody. For Cts1G detection a primary anti-GFP (1:1,000) antibody was applied. A primary antibody against actin (1:1,500) was used for loading and lysis controls (MP Biomedicals, Singapore). An anti-mouse IgG-HRP (1:4,000; Promega, Fitchburg, USA) conjugate was used as secondary antibody. HRP activity was detected using the AceGlow Western blotting detection reagent (PeqLab, Erlangen, Germany) and a LAS4000 chemiluminescence imager (GE Healthcare Life Sciences, Freiburg, Germany).

### *2.3.10 Microscopy, image processing and staining procedures*

Microscopic analyses were performed with immobilized budding cells on agarose patches (2% f.c.) using a wide-field microscope setup from Visitron Systems (Munich, Germany), Zeiss (Oberkochen, Germany) Axio Imager M1 equipped with a Spot Pursuit CCD camera (Diagnostic Instruments, Sterling Heights, USA) and the objective lenses Plan Neofluar (40x, NA 1.3), Plan Neofluar (63x, NA 1.25) and Plan Neofluar (100x, NA 1.4). Fluorescent proteins were detected with an HXP metal halide lamp (LEj, Jena, Germany) in combination with filter sets for Gfp (ET470/40BP, ET495LP, ET525/50BP), FM4-64 (ET560/40BP, ET585LP, ET630/75BP; Chroma, Bellow Falls, USA), and DAPI (AT350/50BP, ET400LP, ET460/50BP; Chroma, Bellow Falls, USA). The microscopic system was controlled by the software MetaMorph (Molecular Devices, version 7, Sunnyvale, USA). Image processing including the adjustment of brightness and contrast as well as the determination of fluorescence intensities was performed with MetaMorph. To visualize fungal cell walls and septa 1 ml of cell culture was stained with CW (1 µg/ml f.c.) directly prior to microscopy. Similarly, membranes were stained with FM4-64 (8-24 µM f.c.) and images were taken immediately. A Neubauer counting chamber was used for quantification of secondary septum formation and aggregation. For characterization of cell aggregates, the outermost located cells of the trees were not taken into account to avoid artefacts due to ongoing cell divisions. Alternatively, laser-based

epifluorescence microscopy was performed on a Zeiss Axio Observer.Z1 equipped with a Hamamatsu orca flash 4.0 camera as previously described (Figure 2.1B) (Baumann et al., 2016).

## 2.4 Results

### *2.4.1 Cts1 accumulates at the fragmentation zone during cytokinesis*

In yeast-like cells Cts1 displays a cell cycle-dependent localisation pattern that can be visualized expressing a functional eGfp fusion protein (Cts1G; enhanced Gfp, Clontech; Figure 2.1A; Figure. S2.1) (Koepke et al., 2011; Langner et al., 2015). This very specific localisation suggests that Cts1 may be released via the fragmentation zone. Therefore, we characterized Cts1G localisation in more detail in the background of laboratory strain AB33 (Brachmann et al., 2001). We verified previous results that in non-budding cells the protein was uniformly distributed in the cytoplasm. However, with forming of the daughter cell the protein started to accumulate at the cell boundary. Upon formation of the secondary septum it was then encompassed by the two septa (Figure 2.1A) (Langner et al., 2015). We quantified the fluorescence intensity in non-dividing cells compared to different areas of dividing cells, which had formed the secondary septum (Figure 2.1B). The fluorescence intensity in mother and daughter cells of the two septa stage was similar to single non-dividing cells. By contrast the fluorescence intensity in the fragmentation zone was enhanced about 8-fold compared to the total cytoplasmic fluorescence (Figure 2.1B). Hence, Cts1G strongly accumulates in the fragmentation zone supporting the hypothesis that it is enriched in this area during progression of cytokinesis and subsequently released upon cell separation.

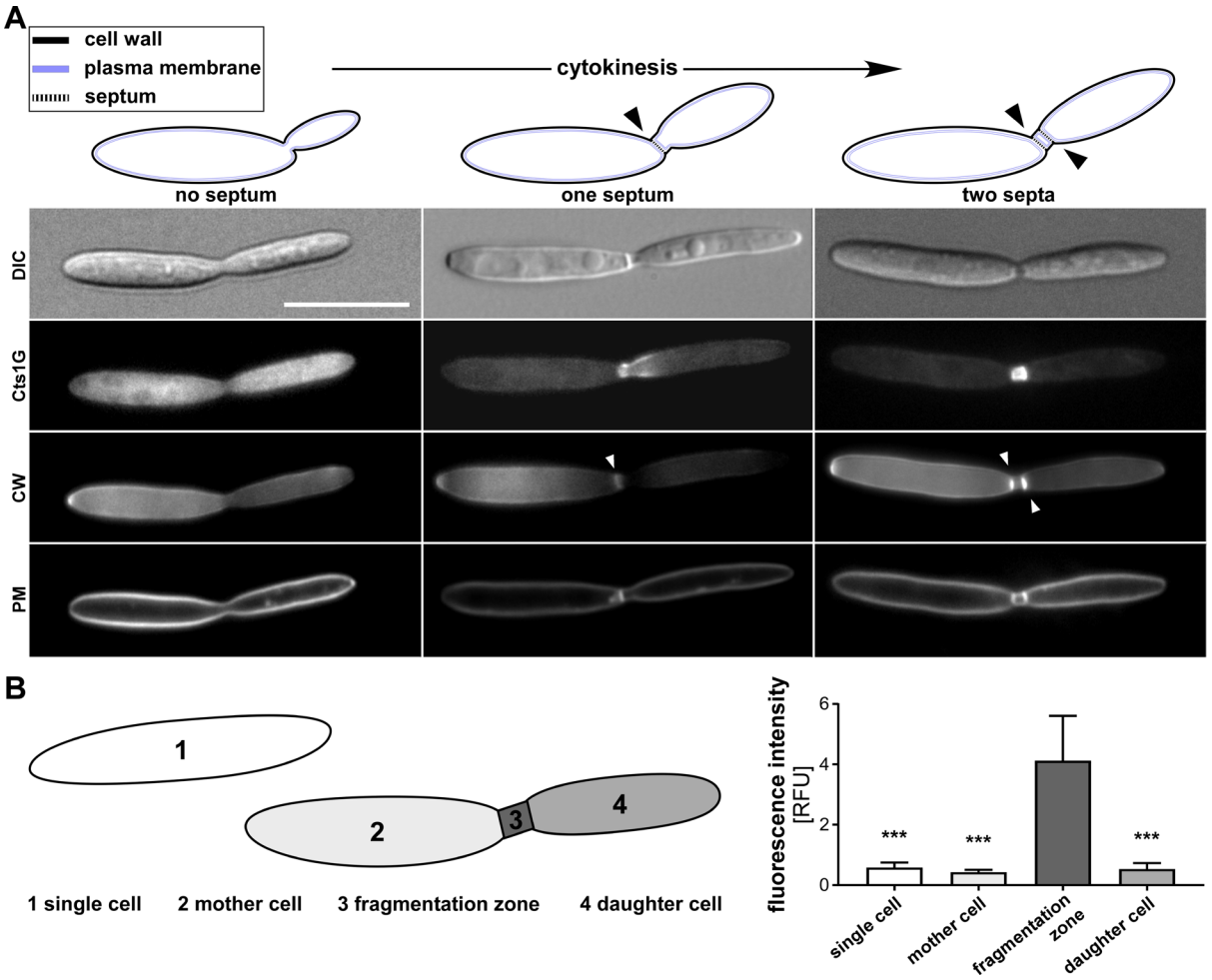


**Figure 2.1. During cell cycle progression Cts1 accumulates in the fragmentation zone. A**, Different stages of the cell cycle in haploid yeast cells of strain AB33 expressing a Cts1-eGfp (Cts1G) fusion protein. During cell cycle progression two septa are sequentially formed, starting with the primary septum at the mother cell side (depicted schematically on top). Micrographs show Cts1G localisation in these different stages (daughter cell formation without septum formation; primary septum only; two septa). For microscopy, representative cells of the distinct stages visualised in the scheme were used. Membranes and cell wall were stained with the lipophilic dye FM4-64 (PM, plasma membrane; early stage, about 0.5 min after addition) and Calcofluor White (CW), respectively. Arrowheads depict septa. DIC, differential interference contrast. Scale bar, 10 µm. **B**, Mean fluorescence intensity (eGfp) over surface area of cells expressing Cts1G determined in different subcellular compartments. Error bars represent standard deviation obtained from multiple pictures of a single culture. 1, single cell (non-budding); 2, mother cell; 3, fragmentation zone; 4, daughter cell. Values for the background control were subtracted for the analysis. At least 31 cells of each stage were analysed. ***, p value < 0.001 (1-way ANOVA, control: fragmentation zone).

## *2.4.2 Unconventional secretion is connected to the cell cycle*

The accumulation of Cts1 in the fragmentation zone suggests that the protein is cell-cycle dependently released via this compartment. Therefore, we used hydroxyurea (HU) to inhibit the cell cycle of yeast-like cells in the S phase (Garcia-Muse et al., 2003). The treatment was performed with two AB33 derivatives: To assay the effect on unconventional secretion we used a strain expressing a Gus-Cts1 fusion protein that is an established reporter for unconventional secretion (Sarkari et al., 2014; Stock et al., 2016). To assay the effect on

conventional secretion we determined the activity of the constitutively expressed intrinsic secreted enzyme arabinofuranosidase Afu2. Growth curves confirmed that the treatment significantly slowed down cell division after a lag phase of about 2 to 4 hours while untreated cells continued to grow exponentially (Figure S2.2). As expected, in the untreated controls both unconventional secretion of Gus-Cts1 and conventional secretion of Afu2 mirrored the slope of the growth curves. This suggests that both proteins were constantly secreted by the cells and accumulated with rising cell densities. Afu2 activity continued to increase after addition of HU, indicating that conventional secretion was only slightly affected by the inhibitor. Afu2 activity in that case rose with a lower slope because the number of secretion-active cells remained steady after cell cycle inhibition (Figure S2.2). By contrast, unconventional secretion was blocked after the addition of HU (Figure 2.2B). This strongly suggests that the release of Cts1 is cell-cycle dependent.

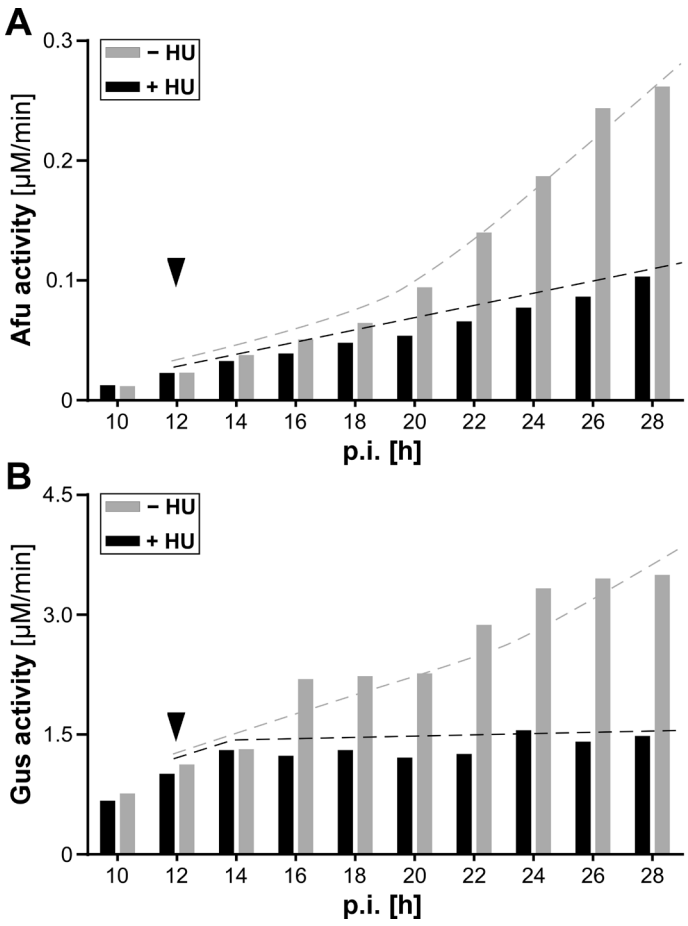


**Figure 2.2. Unconventional but not conventional secretion is cell-cycle dependent. A,** Afu2 activity in AB33P5Δ/Afu2 culture supernatants in the presence or absence of the cell cycle inhibitor HU determined by hydrolysis of the substrate pNP-AF. The time point of HU addition is indicated by an arrowhead. Dashed lines indicate trends. The strain constitutively expresses the intrinsic arabinofuranosidase Afu2, which is secreted via a conventional N-terminal signal peptide. p.i., post inoculation. **B,** Gus activity in cultures of AB33Gus-Cts1 in the presence or absence of the cell cycle inhibitor HU determined by Gus assays using the fluorescent substrate MUG. Dashed lines indicate trends. The strain constitutively expresses the Gus-Cts1 fusion protein which is an established reporter for unconventional secretion. To exclude that the observed effect is due to a direct effect of HU on Gus, we incubated purified Gus control protein produced in *Escherichia coli* (Gus-SHH) (Sarkari et al., 2014) with HU. This did not impair enzyme activity (data not shown). p.i., post inoculation.

## *2.4.3 Don1 and Don3 are important for extracellular chitinase activity*

Since Cts1 export was cell-cycle dependent we tested different mutants impaired in cell separation and deleted the responsible genes in the background of the Cts1G expressing strain. The following mutants were analysed: a mutant lacking Kex2 with a pleiotropic

phenotype including the formation of cell aggregates in the yeast phase (Fuller et al., 1988; Sarkari et al., 2014); a mutant lacking kinesin Kin3 showing impaired endosome movement likely leading to an inefficient assembly of the vacuolated fragmentation zone (Schink & Bölker, 2009; Wedlich-Soldner et al., 2002; Weinzierl et al., 2002); and mutants lacking the septation proteins Don1 or Don3 that directly affect cell separation (Figure 2.3A, upper panel) (Weinzierl et al., 2002). The *don* mutants and the *kin3* deletion strain are known to induce a so-called donut phenotype when colonies are grown on a distinct solid medium (Göhre et al., 2012; Weinzierl et al., 2002). We could confirm the formation of such colonies for our strains and also observed it to some extent in the *kex2* deletion strain (Figure S2.3).

Fluorescence microscopic analysis revealed that in all cases Cts1G still localised in the mother-daughter cell boundary. Even in the absence of a secondary septum (e.g. in the *don1* deletion strain) the protein accumulated at the daughter cell side of the primary septum (Figure 2.3A, Gfp fluorescence). Hence, the translocation of Cts1 to the neck region and its local enrichment in late stages of cytokinesis were not impaired in any of the mutants.

To determine the impact of the different cell separation defects on Cts1 release, we assayed extracellular chitinase activity (Koepke et al., 2011; Langner et al., 2015). A *cts1* deletion strain with diminished chitinase activity on the cell surface was used as a negative control (strain AB33cts1Δ) (Koepke et al., 2011; Langner et al., 2015). Remarkably, *don1* and *don3* deletion strains showed significantly reduced chitinase activities (5.3% and 19.1% remaining activity, respectively) while *kex2* and *kin3* mutants were not impaired (Figure 2.3B). To rule out that the aggregation phenotype of the cells is accompanied by altered growth, which would disturb the measurements, we recorded growth curves and cell dry weight (Figure S2.4). For both *don1* and *don3* mutants the optical densities slightly underrepresented the actual cell numbers during the relevant growth phase. Hence the values obtained in enzyme assays for these strains may be even slightly lower than indicated (Figure 2.3B), further supporting the role of Don1 and Don3 in extracellular Cts1 activity. Moreover, intracellular chitinase activity was enhanced for the two strains (Figure 2.3C) indicating that Cts1 specifically accumulates intracellularly in these strains due to defective unconventional secretion. Western blot analysis of cell extracts revealed that all strains expressed the full length Cts1G fusion protein excluding effects on protein stability as a cause for the observed differences (Figure S2.5A). In line with the enhanced intracellular chitinase activity, Cts1G amounts were slightly increased in cell extracts of *don1* and *don3* deletion strains compared to the other strains. In contrast to intracellular Cts1 the secreted Cts1 fraction can only be detected on the level of free Gfp that remains after proteolytic processing (Figure S2.5B) (Okmen et al., 2018).

In summary, extracellular Cts1 activity is strongly reduced in the *don* mutants suggesting that unconventional secretion of Cts1 is impaired.

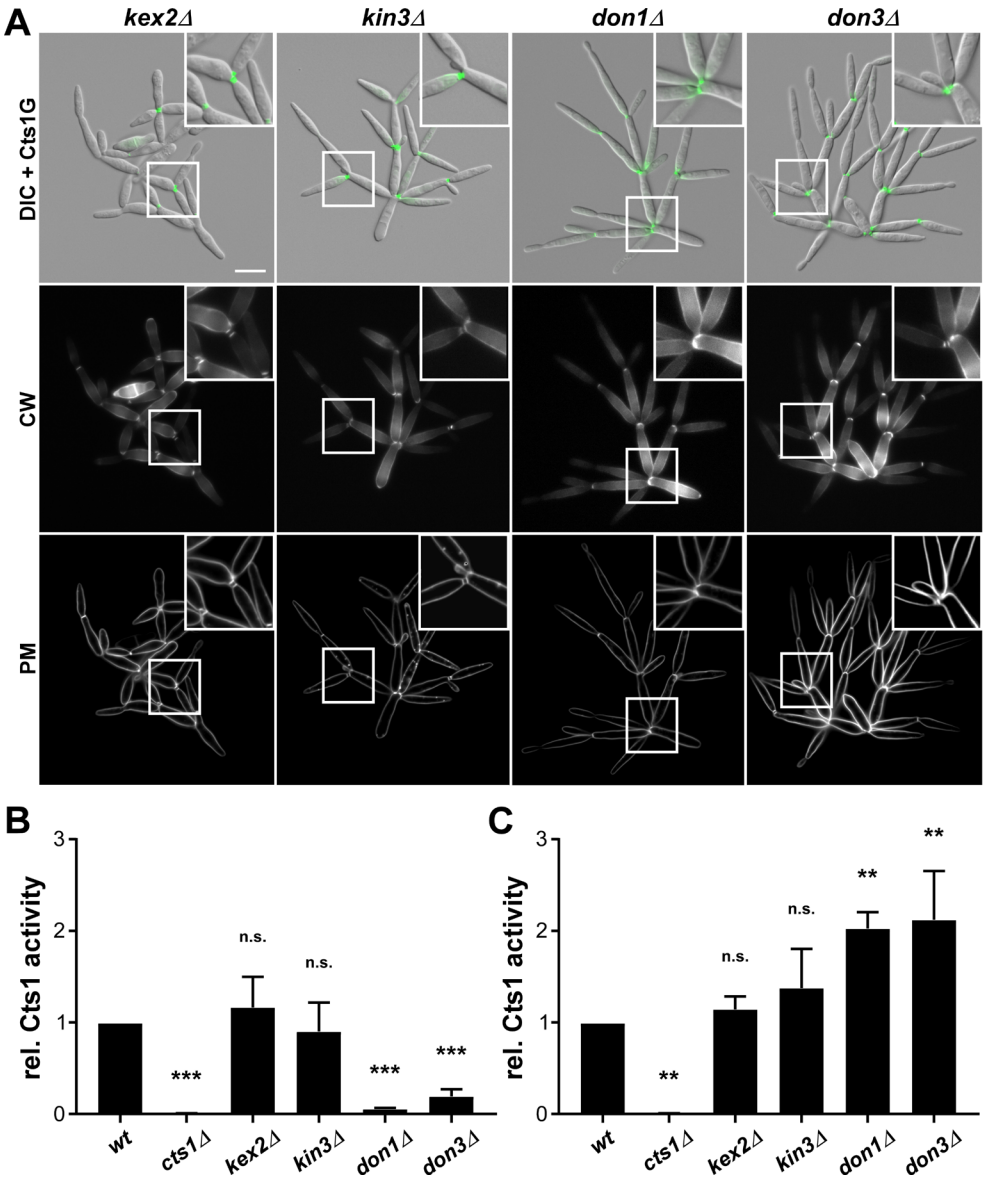


**Figure 2.3 Extracellular Cts1 activity is diminished in *don* mutants. A**, Microscopic analysis of cytokinesis mutants in the yeast stage. Representative cell aggregates are shown for AB33 derivatives lacking the indicated genes. Membranes (PM) and cell wall (CW) were stained with FM4-64 (early stage, about 0.5 min after addition) and Calcofluor White, respectively. DIC, differential interference contrast. CtsG fluorescence is visualised in green in an overlay with the corresponding DIC picture. Inlays show magnified parts of the cell clusters. Scale bar, 10 µm. **B**, Relative chitinase activity on the cell surface of the cytokinesis mutants determined by conversion of the substrate MUC. The experiment was performed in 5 biological replicates. Chitinase activity on the cell surface is representative for Cts1 secretion (Stock et al., 2012). ns, not significant, p value > 0.05; ***, p value < 0.001 (1-way ANOVA, control: wt). **C**, Relative chitinase activity in cell extracts of the cytokinesis mutants determined by conversion of the substrate MUC. The experiment was performed in 3 biological replicates. ns, not significant, p value > 0.05; **, p value 0.001 to 0.01 (1-way ANOVA, control: wt).

## *2.4.4 Specific functions of Don1 and Don3 are required for extracellular Cts1 activity*

To pinpoint potential differences between the mutants an in-depth analysis of the cell aggregation phenotypes was conducted (Figure 2.4A). Expectedly, the control strain

expressing Cts1G grew normal by budding (1 or 2 cells depending on the cell cycle stage) with only about 4% abnormal cell aggregates with 3 to 5 cells. By contrast, the cell separation mutants showed a clearly different behaviour which can be grouped into different severities (Figure 2.4A). The *kex2Δ* mutant exhibited the slightest defect with about 42% of the cells dividing by normal budding (1-2 cells) while the residual cells appear in smaller aggregates of 3-5 (38%) or 6-15 cells (19%). Only a minor fraction of the cells grew in large aggregates of more than 15 cells. The *kin3Δ* strain exhibited less normal growth (about 22%) and the number of aggregates larger than 5 and 15 cells was increased to about 36% and 11%, respectively. The most drastic phenotype could be detected for *don1Δ* mutants with a fraction of 20% growing in cell aggregates of more than 50 cells and only a minor fraction of normally budding cells (less than 6%). Interestingly, in *don3Δ* a mixed picture emerged with many large cell aggregates (7.5%) but also a large fraction of unaffected cells growing normally (39%). These observations indicate that extracellular Cts1 activity does not solely depend on cell separation but probably rather on specific defects in assembly of the fragmentation zone in the *don* mutants.

Since the *don* mutants are known to be defective in secondary septum formation (Weinzierl et al., 2002), we also determined the rate of secondary septum formation in the different cell aggregates. Our quantification confirmed published results in that the *don* mutants exhibited a strongly reduced rate of secondary septum formation of 5.8% for *don1Δ* and 2.5% for *don3Δ* (Figure 2.4B). Unexpectedly, also *kex2* and *kin3* mutants showed a high percentage of absent secondary septa in cell aggregates (31% and 46%, respectively). As efficient Don1 localisation at the fragmentation zone is mediated by endosomal transport involving the Kin3 motor (Schink & Bölker, 2009), this may constitute a secondary effect in the *kin3Δ* strain. Although there still is a strong difference in secondary septum abundance, it is therefore unlikely that the lack of this barrier is the only cause for reduced Cts1 activity in the *don* deletion strains.

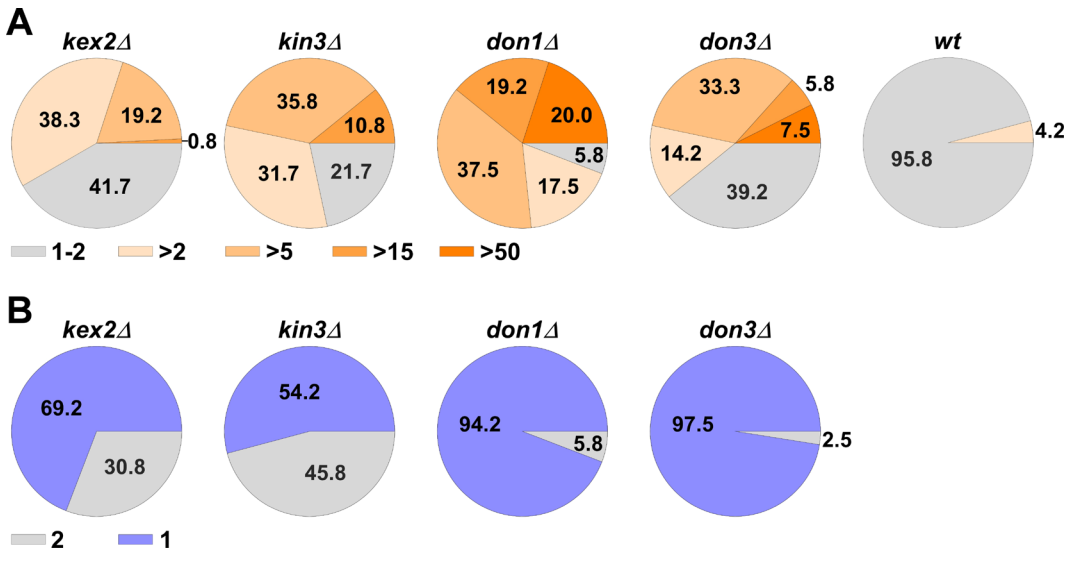

**Figure 2.4. Cell separation mutants show differences in their tree structures. A,** Pie chart indicating the mean number of cells per aggregate (in %) in the different mutants visualized in Figure 2.3A. Categories ranging from 1-2 (normal budding), 3-5, 6-15 and 16-50 and more than 50 connected cells were defined for the analysis. n = 120 cells/aggregates for each strain. **B**, Pie chart depicting the rate of secondary septum formation in cell aggregates of the different mutants (in %). n = 120 cells for each strain.

## *2.4.5 The germinal centre kinase Don3 is exported in low amounts*

The septation proteins Don1 and Don3 accumulate in the fragmentation zone during cytokinesis resembling Cts1 localisation (Langner et al., 2015; Sandrock et al., 2006; Schink & Bölker, 2009). This indicates that the two proteins might also be released into the culture supernatant via the fragmentation zone. To test this, we applied the Gus reporter system to assay unconventional secretion of the two proteins (Stock et al., 2012; Stock et al., 2016). Therefore, we generated strains constitutively expressing protein fusions of Gus-Don1 and Gus-Don3 under the control of the very strong $P_{oma}$ promoter (Hartmann et al., 1999; Sarkari et al., 2014). As a lysis control, strains expressing cytoplasmic Gus at identical strength were included. Western blot analyses revealed that all (fusion) proteins were expressed, with Gus-Don3 showing a higher stability than Gus-Don1 which was partially degraded (Figure S2.6A). PEST sequences in Don1 may be the reason for this observation (Schink & Bölker, 2009). When the reporter constructs encoding Gus-Don1 and Gus-Don3 were alternatively introduced into the respective deletion backgrounds the cell separation phenotype as well as extracellular Cts1 activity levels were rescued in both cases (Figure S2.7) while Gus activity values were comparable to the earlier strains (Figure 2.6A), indicating that the Gus-Don fusion proteins are functional.

Extracellular activity for Gus-Don1 expressing strains did not clearly exceed the levels of the lysis controls. By contrast, a strain expressing Gus-Don3 displayed slight Gus activity in the culture supernatant compared to the background activity of the control strains (Figure 2.5A), suggesting that Don3 is released to the culture supernatant. Consistently, the intracellular activity for Gus-Don3 was very low (Figure 2.5B). However, in general the total extracellular activity of Gus-Don3 was significantly lower (about 22%) than observed for Gus-Cts1. In summary, in contrast to the nucleotide exchange factor Don1, the germinal centre kinase Don3 is likely exported similar to Cts1 but to a much lower extent.

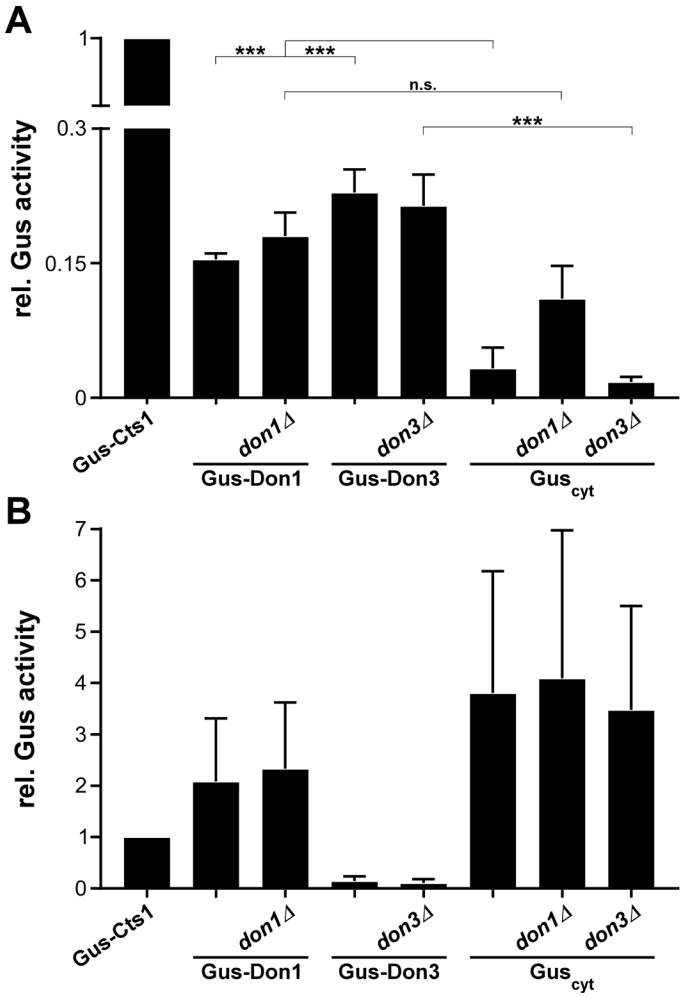


**Figure 2.5. Gus reporter assays suggest Don3 release into the culture medium. A,** Gus reporter assay employed for Don1 and Don3. The diagram depicts relative Gus activities in culture supernatants of different Gus fusion proteins produced in AB33 derivatives. MUG was used as substrate for the assays. AB33Gus-Cts1 served as positive control for unconventional secretion. The assay was performed in three biological replicates. Error bars represent standard deviation. ns, not significant, p value > 0.05; ***, p value < 0.001 (1-way ANOVA). **B,** Gus-assay employed for distinct amounts of cell extracts of similar cultures as shown in A. The assay was performed in three biological replicates. Error bars represent standard deviation.

## *2.4.6 Unconventional Cts1 secretion is diminished in don3 mutants*

Don1 and Don3 were shown to be crucial for extracellular Cts1 activity. To investigate if this parallels with impaired unconventional Cts1 secretion we applied the Gus reporter system (Sarkari et al., 2014; Stock et al., 2012; Stock et al., 2016). To this end, we generated strains expressing Gus-Cts1 in the *don1* and *don3* deletion background. Control strains expressing a cytoplasmic version of Gus ($Gus_{cyt}$) were included to track cell lysis. Western blot analyses of cell extracts confirmed that the strains produced the Gus-fusion protein in comparable amounts while the cytoplasmic controls were present in slightly higher amounts (Figure S2.8A).

Gus activity of *don1* mutants was reduced but only to 56% (Figure 2.6A). This indicates that differences exist between Cts1 secretion and the export of the Gus-Cts1 fusion. The reason for this is currently unclear and will need further investigation.

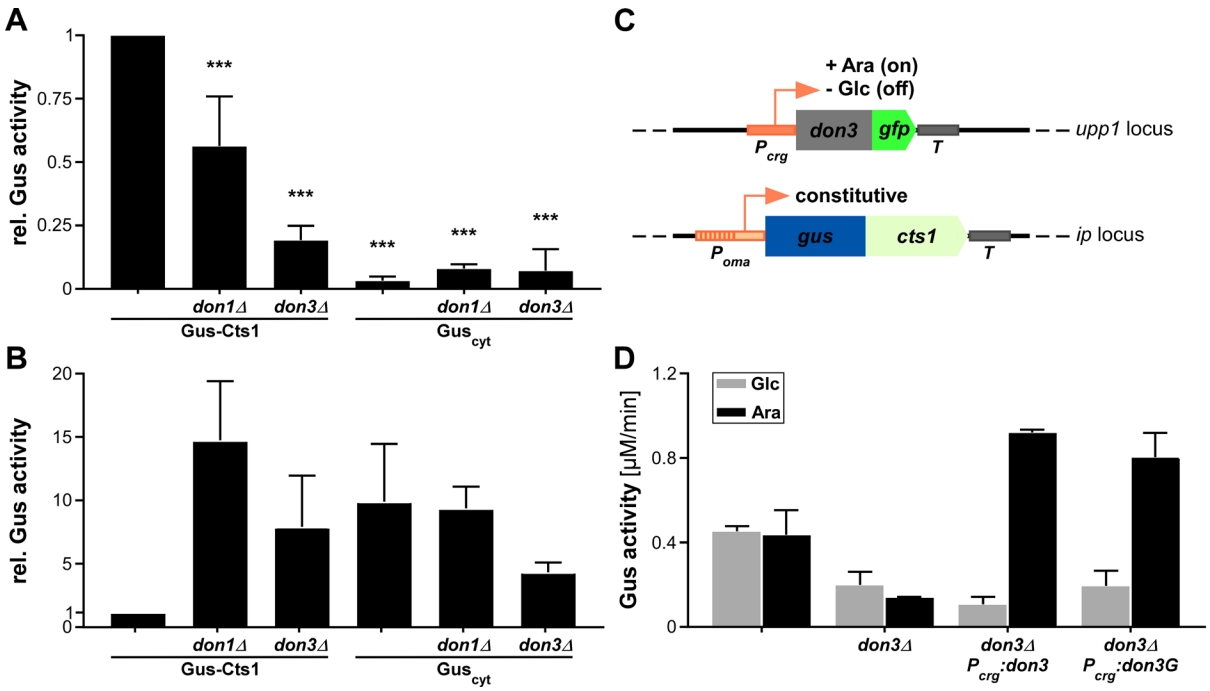


**Figure 2.6. Don3 is of particular importance for efficient Cts1 secretion. A**, Relative Gus activity of different Gus (-fusion) proteins in the culture supernatant assayed with the substrate MUG. All proteins are produced by AB33 derivatives. AB33Gus-Cts1 served as positive control for unconventional secretion while the cytoplasmic version $Gus_{cyt}$ in the background of AB33, AB33don1Δ and AB33don3Δ constitutes a read-out for cell lysis (negative controls). The experiment was performed in 3 biological replicates. Error bars represent standard deviations. ***, p value < 0.001 (1-way ANOVA, control: AB33Gus-Cts1). **B,** Relative Gus activity of different Gus (-fusion) proteins in cell extracts assayed with the substrate MUG. All proteins are produced by AB33 derivatives. AB33Gus-Cts1 served as positive control for unconventional secretion while the cytoplasmic version $Gus_{cyt}$ in the background of AB33, AB33don1Δ and AB33don3Δ constitutes a read-out for cell lysis (negative controls). The experiment was performed in 3 biological replicates. Error bars represent standard deviations. **C,** Rationale of regulated Don3 expression on the genetic level. Strain AB33$P_{crg}$Don3G/Gus-Cts1 contains the inducible promoter leading to *don3G* transcription only if arabinose is present in the medium as single C-source (on condition). In glucose-containing medium the promoter is repressed (off condition) and *don3G* is not transcribed. In addition, the strain carries a reporter fusion (Gus-Cts1) for quantification of unconventional Cts1 secretion. Glc, glucose; Ara, arabinose. **D**, Gus activity in the culture supernatant of strains with regulated *don3* expression. All indicated AB33 derivatives express the Gus-Cts1 fusion protein as a reporter for unconventional secretion. In addition, the indicated modifications were introduced. In the off condition (glucose as single C-source) Cts1 secretion assayed on the level of extracellular Gus activity is very low. By contrast, activity increased strongly under on conditions (arabinose as single C-source). Similar results are obtained in strain AB33$P_{crg}$Don3G/Gus-Cts1 which produces Don3 as a fusion protein with eGfp (Don3G). Glc, glucose; Ara, arabinose. Error bars represent standard deviations.

By contrast, Gus activity of the Don3 mutant was strongly reduced to about 19% (Figure 2.6A). This result is consistent with the extracellular Cts1 activity in the *don3* deletion background which was also about 5-fold reduced (Figure 2.3B). Complementary, Gus activity assays of cell extracts suggest that the protein accumulated intracellularly in both *don* mutants (Figure 2.6B). To confirm this observation, we used a regulatable version of Don3. Previous work has shown that synthetic induction of *don3* via inducible promoters is sufficient to switch between budding growth and aggregation (Böhmer et al., 2008). Therefore, two reporter strains which expressed the Gus-Cts1 reporter protein via a strong constitutive promoter were

generated (Figure 2.6C). In these strains *don3* or *don3G* expression can be regulated via the carbon source dependent promoter $P_{crg}$ (Bottin et al., 1996). In the presence of arabinose the $P_{crg}$ promoter is active and *don3* is expressed while in the presence of glucose the promoter is repressed and *don3* expression is diminished. AB33 and AB33don3Δ expressing eGfp via the constitutive $P_{otef}$ promoter in addition to the Gus-Don3 fusion protein were used for comparison. To test the influence of Don3 on Cts1 secretion all strains were cultivated in both CM-glc and CM-ara. After about 16 h culture Gus activity assays with culture supernatants were conducted as a read-out for Cts1 release (Figure 2.6D). Both control strains showed the expected behaviour displaying constant Gus activities in the two media. Importantly, strains with inducible Don3 or Don3G grown in CM-ara showed 8.5- and 4-fold elevated Gus activity, respectively, compared to the cultivation in CM-glc confirming the assumption that the presence of Don3 is sufficient to induce Cts1 secretion.

To further resolve the process induction of the strain expressing Don3G was followed in a time course experiment for a total of 8 h after induction (Figure S2.9). Microscopic inspection confirmed that Don3G fluorescence was absent at the onset of induction (0 h) and later on, limited to the cells grown in arabinose (“on” state; 8 h) while in cells grown in CM-glc only background fluorescence was detectable (Figure S2.9A). Don3G protein was clearly present at fragmentation zones after induction, and secondary septa as well as delimiting membranes at the daughter cell side were mostly developed. In addition, cells were detached to a great extent and were no longer found in large aggregates at this stage. Gus activity assays confirmed that Gus-Cts1 is already released early on (from about 2 h post induction; Figure S2.9B), showing that *don3* expression is necessary and sufficient to permit unconventional Cts1 secretion.

## 2.5 Discussion

In this study we investigated the mechanism of unconventional Cts1 secretion. We uncovered a clear link to the cell cycle and identified the first regulatory component of this unconventional secretion pathway.

### *2.5.1 Cts1 accumulates in the fragmentation zone and is released cell-cycle dependently*

Over the past years diverse unconventional secretion pathways have been described. However, only a few cases such as the self-sustained translocation of FGF2 in mammalian cells are understood in detail (Dimou & Nickel, 2018). In this example, the interaction with phosphoinositol(4,5)bisphosphate headgroups in the cytoplasmic membrane triggers the

oligomerization of the protein. This leads to membrane insertion and pore formation through which monomers are released with the help of heparan sulfates at the cell surface (Steringer et al., 2017). In the yeasts *Saccharomyces cerevisiae* and *Pichia pastoris*, the sporulation factor Acyl-CoA-binding protein 1 (Acb1) is likely exported upon nutrient starvation via an autophagosomal intermediate (Bruns et al., 2011; Malhotra, 2013). Interestingly, this protein and the mechanistic details of its export are conserved in the amoeba *Dictyostelium discoideum* (Anjard & Loomis, 2005; Kinseth et al., 2007). *U. maydis* secretes small amounts of the peroxisomal sterol carrier protein 2 (Scp1) during hyphal growth. This protein functions as an effector during infection of the host plant maize. Peroxisomal targeting of Scp1 is essential for its virulence function, suggesting that peroxisomes are involved in its secretion (Krombach et al., 2018).

Here we provide strong evidence that unconventional secretion of Cts1 occurs differently, namely via the fragmentation zone of dividing yeast-like cells. To our knowledge this compartment has not yet been considered as actor for the unconventional export of proteins. The fragmentation zone is sealed off from the two cells not only by cell wall material (septa) but also by the cytoplasmic membrane (Figure 2.1A, lower panel), suggesting that the mechanism of relocation from the cytoplasm to the fragmentation zone is the process in which translocation across the membrane occurs. Alternatively, the protein might accumulate in the fragmentation zone before membrane closure and then being sealed off during constriction of the actomycosin ring.

Other enzymes specifically required for the formation of the fragmentation zone could be further substrates of this pathway. Candidates would for example be glucanases (Cabib, 2004; M. Schuster et al., 2016). These cell-wall remodelling enzymes are thought to function together with chitinases in the reorganization of the cell wall during budding (Cabib, 2004; Kuranda & Robbins, 1991). Interestingly, the genome of *U. maydis* encodes a glucanase which lacks a prediction for an N-terminal signal peptide. By contrast, membrane-bound chitin and glycan synthases might be transported to this compartment via secretory vesicles (Renicke et al., 2013; M. Schuster et al., 2016).

Apart from cell wall-modifying enzymes other proteins that play a role during fragmentation zone formation could be released. This is supported by the fact that in case of Don3 we could show with our Gus reporter system that the protein is likely exported into the culture's supernatant, albeit in much lower amounts compared with Cts1. It is conceivable that a kinase could exert additional extracellular functions in the culture supernatant or at the cell wall. Indeed, the conventional secretion of kinases with extracellular functions has recently been demonstrated in mammalian cells (Bordoli et al., 2014; Tagliabracci et al., 2012). By contrast the GEF Don1 was not clearly exported. This enzyme is membrane associated and

relies on the presence of the cognate small GTPase Cdc42 (Hlubek et al., 2008; Mahlert et al., 2006). It is therefore possible that in this case secretion would be futile for the cell.

While our experiments clearly indicate a connection between the fragmentation zone and unconventional Cts1 secretion, the mechanistic details of this process remain largely unclear. An important question is how Cts1 is recruited to the fragmentation zone. Interestingly, the GEF Don1 contains a FYVE domain that mediates attachment to moving endosomes by phosphatidylinositol-3-phosphate (PI3P) binding. These endosomes bidirectionally shuttle throughout the fungal cell (Schink & Bölker, 2009). In the hyphal form, such Rab5a-positive endosomes serve as multi-purpose carriers for extensive long transport of organelles like peroxisomes but also mRNA and ribosomes (Niessing et al., 2018). In the yeast form, prior to cell separation they accumulate in the fragmentation zone explaining the observed localization of Don1 (Schink & Bölker, 2009). However, due to the instability of the protein its localisation could only be resolved after deletion of PEST sequences (Schink & Bölker, 2009). Although Don3 and Cdc42 also localise to the fragmentation zone, their transfer mechanism is yet unknown. Using truncation studies, a distinct motif (T-motif) could be identified that is necessary and sufficient for Don3 targeting to this cellular compartment (Sandrock et al., 2006). For Cts1, a connection to moving endosomes in yeast cells could not be confirmed microscopically, even after removal of a potential PEST sequence in the N-terminal part of the protein (Figure S2.1A), suggesting that its translocation to the fragmentation zone is ruled by a different mechanism.

In essence, cell-cycle dependent accumulation of Cts1 to the fragmentation zone appears to be an important prerequisite for its unconventional export. It is conceivable that a similar strategy of unconventional secretion might be conserved in other yeasts like *Saccharomyces cerevisiae*, because it also harbours a chitinase lacking a signal peptide (Cts2p) (Langner et al., 2015). However, since not all components identified in *U. maydis* are present in this model and the process of septation differs strongly in the two organisms the mechanistic details may vary.

### *2.5.2 Unconventional Cts1 secretion depends on the germinal centre kinase Don3*

We used different cell separation mutants to study the link between cytokinesis and extracellular Cts1 activity. Remarkably, Cts1 activity was drastically reduced for the *don1* and *don3* mutant. Based on the Gus reporter system and the inducible version of *don3* we could demonstrate that Don3 is essential for efficient Cts1 secretion. This germinal centre kinase exhibits important functions during cytokinesis. Each septation event involves a carefully timed choreography of septin dynamics (collar to ring transition), actomyosin ring formation for

membrane invagination and cell wall deposition. Actin polymerisation and the F-BAR domain protein Cdc15 are essential for membrane constriction within the contractile actomyosin ring (Böhmer et al., 2009). Don3 regulates the septin collar to ring transition during formation of the secondary septum (Böhmer et al., 2009). Interestingly, an additional role of Don3 and its interaction partner Dip1 in a SIN/MEN-related signalling network, which regulates nuclear envelope breakdown (NEBD) during mitosis, has been proposed (Sandrock et al., 2006). Here, we found a novel link between Don3 and unconventional secretion. Possibly, assembly of a functional fragmentation zone for which Don3 activity is required is the key to making the cell competent for unconventional secretion. This process could be connected to membrane biology, for example to the actomyosin ring formation necessary for membrane constriction or the vacuolation of the fragmentation zone. To uncover this link phosphorylation targets of Don3 should be detected, e.g. by phosphoproteomics (Sandrock et al., 2006; Xue & Tao, 2013). In the future, the formation of the fragmentation zone needs also to be analysed in more detail.

## 2.6 Conclusion

In this study we demonstrated that unconventional Cts1 secretion is cell-cycle dependent and especially requires the septation factor Don3 for efficient export. While our results strongly support the hypothesis that Cts1 is released after translocation to the fragmentation zone, further work will be required for better insights into the mechanistic details of Cts1 translocation into this area during cytokinesis. Genetic screens were very helpful in uncovering the conventional secretion pathway (Mellman & Emr, 2013; Novick et al., 1980). In the future similar strategies could also reveal novel actors needed for unconventional Cts1 secretion. Although specific mechanisms may be implicated in the translocation in *U. maydis*, the overall strategy of exporting proteins during cell division may be conserved in other yeast-like growing fungi.

***Keywords***
Cell cycle, chitinase, cytokinesis, germinal centre kinase, unconventional secretion, *Ustilago maydis*

***Author contributions***
J.A., **K.H.**, P.S., T.L. and S.Z. designed and performed the experiments. K.S., M.B., B.S. and M.F. directed the study. K.S. wrote the manuscript with input of all co-authors.

***Acknowledgements***
We thank V. Göhre, L. Plücker, C. Haag and all lab members for valuable discussion as well as B. Axler for excellent technical support of the project. We are grateful to José Pérez Martin for valuable advice on cell cycle inhibition, to M. Reindl for providing strain UMa2014, to J. Stock for generating pUMa2335 and to K. Müntjes for providing the SapI-compatible Golden Gate cloning vectors. M.F. was supported by CEPLAS DFG-EXC 1028. M.B. was supported by SFB 987 "Microbial Diversity in Environmental Signal Response“. The work was funded in part by the SFB1208 Membrane Dynamics and Identity (TP A09).

## 2.7 Supplementary data

**Table S2.1.** DNA oligonucleotides used in this study.

| Designation | Nucleotide sequence (5´ – 3´) |
|---|---|
| oDD101 | GGTCTCCGGCCATGCTCGCAAGTCATGTGCTATC |
| oDD102 | GGTCTCGCTGCAATATTGGATGCGAGCTGTTGTCG |
| oDD107 | GGTCTCGCCTGCAATATTGGACATGAGTGACATGCAGC |
| oDD108 | GGTCTCCAGGCCCCGAGCCGGTTGAACGCTAAG |
| oDD637 | GGTCTCGCCTGCAATATTGCTCGCTGCATCCACGG |
| oDD638 | GGTCTCCAGGCCGATGGGTGGTGAGGCCCAGAGAAAGC |
| oDD639 | GGTCTCCGGCCACTAAGCATCTCCCTACATTCG |
| oDD640 | GGTCTCGCTGCAATATTGCTGACTTTGGTCTGTCGAGGG |
| oMB76 | TTGGCGCGCCATGGCTTCCGCCTCCAGG |
| oMB77 | CGGGCCCCTATTTGGAAGTGCTTTCG |
| oMB78 | TTGGCGCGCCATGCCCAACCTACCACTACC |
| oMB79 | CGGGCCCTCAGTAGCCCATCCATCG |
| oMB436 | CGGGCCCCTATGGTACCCACACGGGC |
| oMB437 | CGTAAGCATCATTGCGCACTTTGTGGTCAGG |
| oMB448 | CCTGACCACAAAGTGCGCAATGATGCTTACG |
| oMF502 | ACGACGTTGTAAAACGACGGCCAG |
| oMF503 | TTCACACAGGAAACAGCTATGACC |
| oRL1181 | GTGAGAAGAGCCATATGGCTCTTCAGTC |
| oRL1182 | CTAGGACTGAAGAGCCATATGGCTCTTCTCACAGCT |
| oUPP117 | CATGCCTGCAGGGGCCGCTACCTGGCTTATCG |
| oUPP118 | GATCCCATGGCAATTGCCTCAGGCCTATTATGGTATC |
| oUPP119 | GATCCAATTGATGCCCAACCTACCACTACC |
| oUPP120 | GATCCAATTGAGGCGCGCCAGTAGCCCATCCATCGCGTACG |
| oUP91 | AGAGGCTCTTCCGTGCAATATTAGGCCAGGCTCGAACAGATCGTC |
| oUP92 | AGAGGCTCTTCCGGCCTCGTGTTTGATCGTGAAGACAATGCC |
| oUP93 | AGAGGCTCTTCCCCTATGAAGTCTCTCAGCTTGTCTTGGG |
| oUP94 | AGAGGCTCTTCCGACAATATTGGATGTAGGGACCAAGCTCC |
| oUP136 | GATCGGCGCGCCTCAGTAGCCCATCCATCGCG |

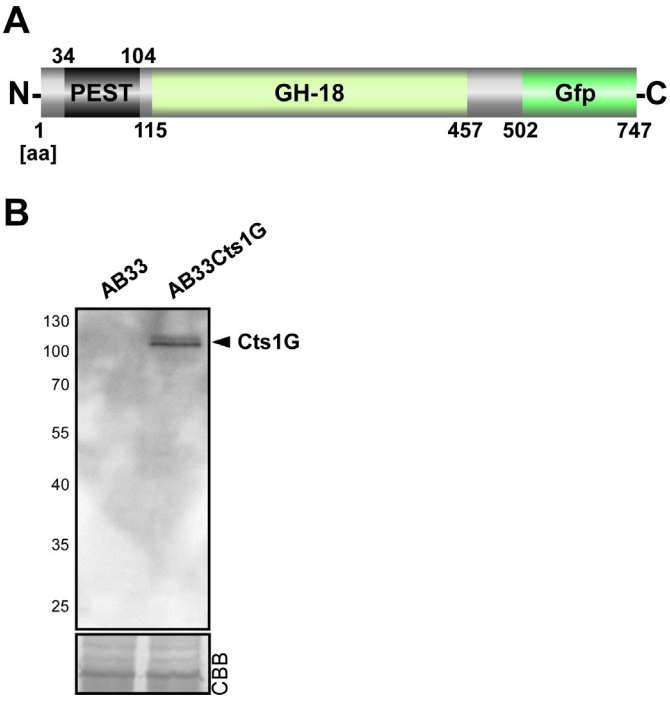


**Figure S2.1. Cts1G is expressed as a full-length fusion protein. A,** Schematic showing the protein structure with the enzymatic GH18 domain and a predicted PEST sequence. eGfp has been fused to the C-terminus. aa, amino acids. **B,** Western blot analysis of 10 µg cell extracts of AB33 and its derivative expressing Cts1G using anti-Gfp antibodies. Arrowhead depicts the Cts1G full-length fusion protein band which is known to run above the calculated size of about 82 kDa (Stock et al., 2012). CBB, Coomassie Brilliant Blue staining of the membrane.

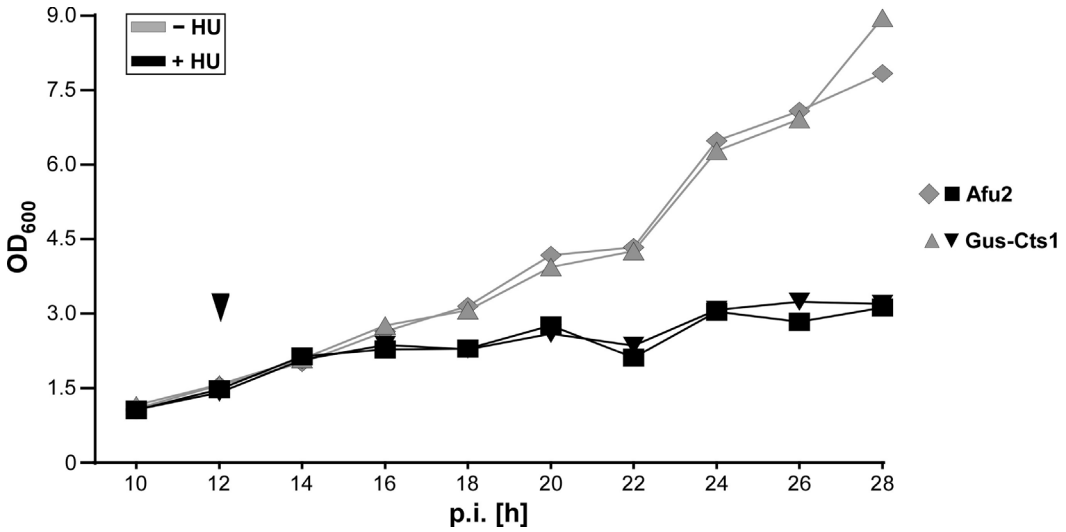


**Figure S2.2. Cell division stagnates after treatment with hydroxyurea.** Growth curves were recorded by determining the optical densities at 600 nm ($OD_{600}$) for the two reporter strains AB33Gus-Cts1 (unconventional secretion) and AB33P5Δ/Afu2 (conventional secretion). To inhibit the cell cycle cultures were inoculated with an $OD_{600}$ of 0.08 and treated with 3 mg/ml HU (f.c.) after 12 h (arrowhead, black curves). Untreated cultures were used as controls (grey curves). Sampling was performed starting at 10 h post inoculation (p.i.) every two hours. The inhibitory effect could be determined after a lag phase of about 3 hours.

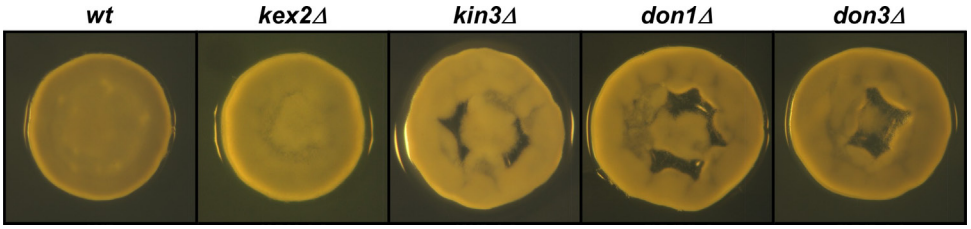


**Figure S2.3. Donut colony formation of cell separation mutants.** Comparative analysis of donut colony formation on YepsLight plates (Tsukuda et al., 1988). Liquid cultures of indicated mutants were spotted on YepsLight plates and incubated for 3 days at 28°C. Photographs show single colonies.

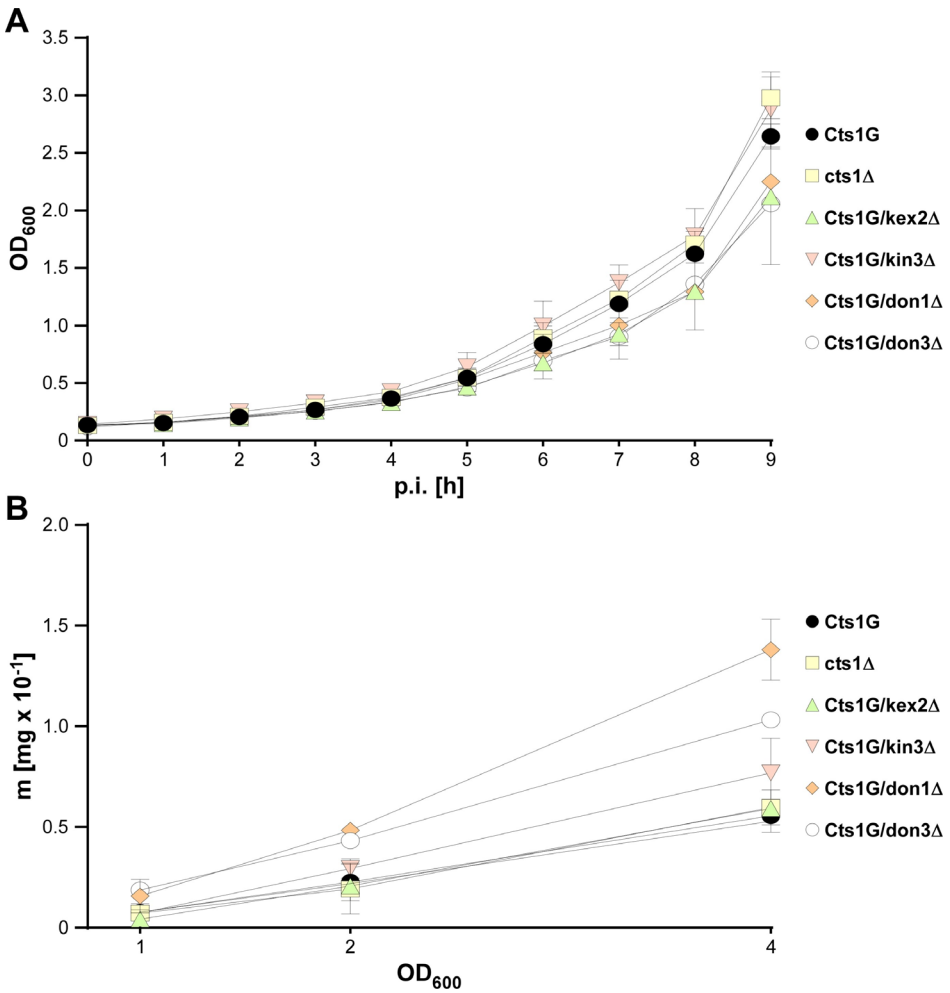


**Figure S2.4. Growth of cytokinesis mutants in the yeast stage.** Comparative determination of cell growth by optical density at 600 nm and cell dry weight. The experiments were performed in biological triplicates. **A,** Growth curves determined by $OD_{600}$ measurements of indicated AB33Cts1G derivatives and AB33cts1Δ. Strains lacking *don1*, *don3* and *kin3* grew slightly slower than the progenitor AB33Cts1G and the *kex2* mutant. **B,** Since optical density values of cell aggregates might be inaccurate, $OD_{600}$ measurements were verified with parallel dry weight determination. The graph shows a comparison of optical density and cell dry weight for three different adjusted optical densities ($OD_{600}$ of 1, 2 and 4). The results suggest that for most strains the $OD_{600}$ correlates well with the dry mass of the cells. However, $OD_{600}$ values of AB33don1Δ/Cts1G and AB33don3Δ/Cts1G increasingly underestimate the actual cell mass with rising optical densities. This is also true for AB33kin3Δ/Cts1G to a lower extent at optical densities above 1.0. Cts1 activity assays were conducted at $OD_{600}$ of 1.0, meaning that values obtained in enzyme assays for strains AB33don1Δ/Cts1G and AB33don3Δ/Cts1G may be even slightly lower than indicated (Figure 2.3B), further supporting the role of Don1 and Don3 for unconventional Cts1 secretion.

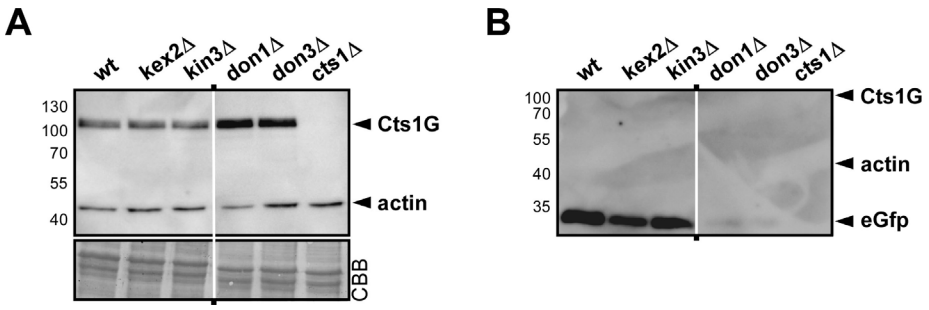


**Figure S2.5. Western blot analysis of Cts1G in different AB33 derivatives. A**, Western blot confirming the expression of Cts1 in the different strain backgrounds (AB33Cts1G derivatives carrying different deletions). AB33cts1Δ lacking Cts1 was used as negative control. Cell extracts (10 µg) were used for the blot. Cts1G was detected with anti-Gfp antibodies while antibodies against actin were used as loading control. The lanes shown were part of a single blot which was reassembled for better clarity. wt, AB33Cts1G. CBB, Coomassie Brilliant Blue staining of the membrane. **B**, Western blot analysis of culture supernatants of indicated AB33 derivatives. AB33cts1Δ lacking Cts1 was used as negative control. Cts1G was detected with anti-Gfp antibodies. Anti-actin antibodies served as lysis controls. The lanes shown are part of a single blot which was reassembled for better clarity. wt, AB33Cts1G.

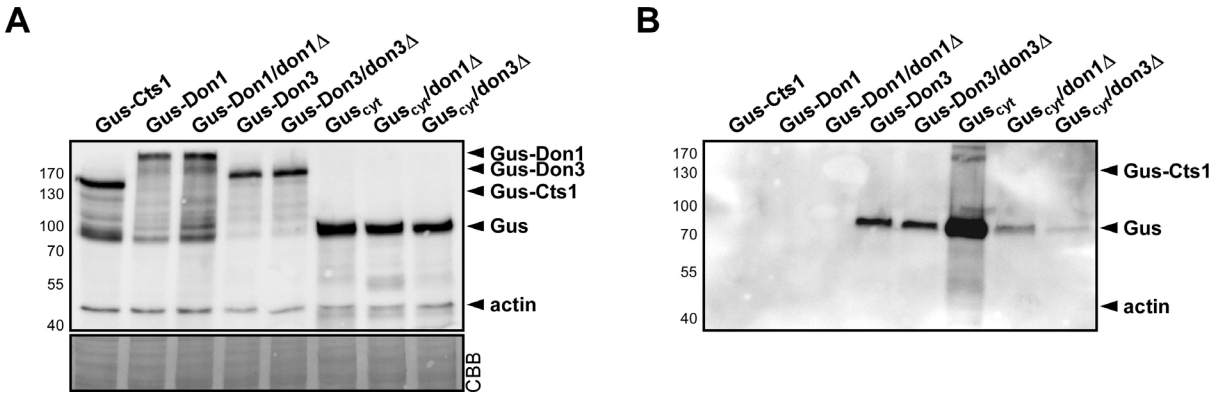


**Figure S2.6. Western blot analysis of strains expressing Gus-Don1 and Gus-Don3 fusions. A,** Western blots of cell extracts (10 µg each) using antibodies directed against the HA-tag in the SHH-fusion proteins and against actin (loading control) were performed to check the integrity of the produced proteins. CBB, Coomassie Brilliant Blue staining of the membrane. **B,** Similar Western blots of TCA-precipitated culture supernatants were used to detect secretion and/or protein leakage from the cells. Anti-actin antibodies served as lysis control. Gus signals were obtained in culture supernatants of Gus-Don3 expressing strains and of strains showing high levels of intracellular Gus activity. We assume that in the latter case misfolded or aggregated protein that accumulates intracellularly due to the strong overproduction may be released via an unknown mechanism to relieve cell stress. This assumption fits with the lack of extracellular activity in these strains. Interestingly, similar observations have recently been made in mammalian cells and designated a misfolding-associated protein secretion (MAPS) pathway which involves endosomes (Lee et al., 2016). For Gus-Don1 the extracellular detection of the protein might be difficult due to the presence of the PEST sequences and/or its association with membranes (Schink & Bölker, 2009). Also Gus-Cts1 is difficult to detect in AB33 due to proteolytic processing (Okmen et al., 2018; Sarkari et al., 2014; Stock et al., 2012). For Gus-Don3 degradation bands corresponding to the size of Gus are present, which fits the observed elevated Gus activity in the culture supernatant (Figure 2.5B).

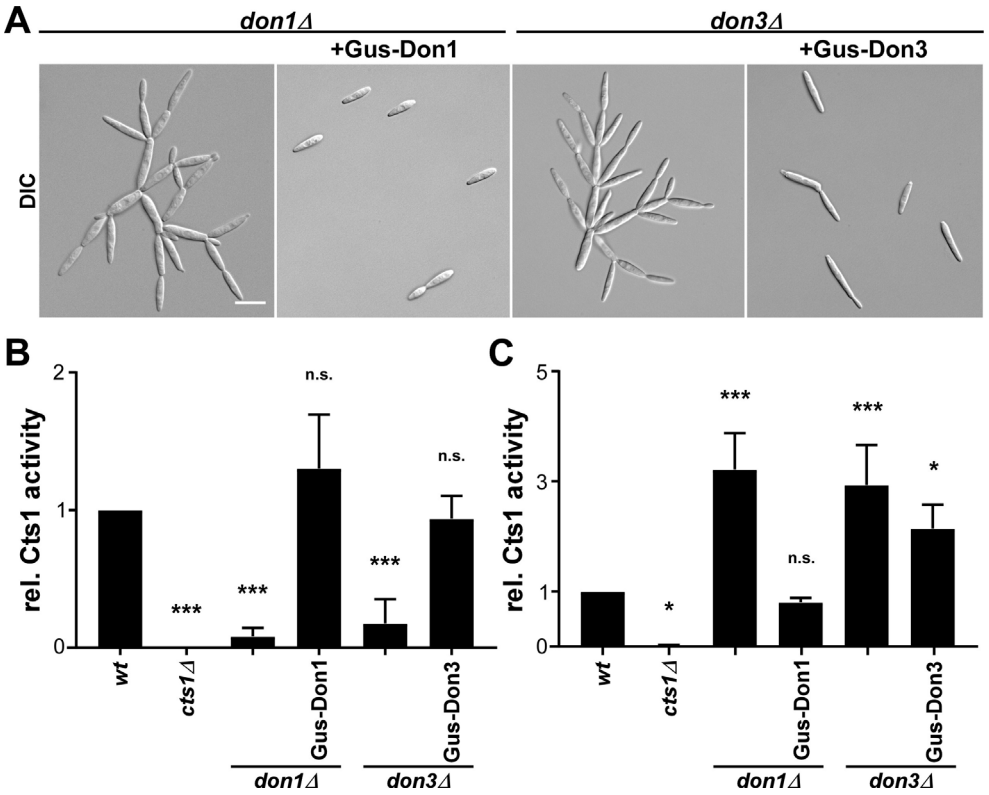


**Figure S2.7. Gus-Don1 and Gus-Don3 protein fusions complement extracellular Cts1 activity in the respective *don* deletion strains. A**, Microscopic analysis of AB33 derivatives producing Don1 and Don3 protein fusions with the reporter for unconventional secretion, Gus. Yeast-like growth indicates functional cell separation and thus complemenation. DIC, differential interference contrast. **B**, Relative Cts1 activities in culture supernatants assayed with the substrate MUC in the indicated AB33 derivatives. Chitinase activity in AB33 (wt) and AB33cts1Δ served as positive and negative control, respectively. The assay was performed in three biological replicates. Error bars represent standard deviation. n.s., not significant, p value > 0.05; ***, p value < 0.001 (1-way ANOVA, control: wt). **C**, Relative Cts1 activities in cell extracts (1 µg each) assayed with the substrate MUC in the indicated AB33 derivatives. Chitinase activity in AB33 (wt) and AB33cts1Δ served as positive and negative control, respectively. The assay was performed in three biological replicates. Error bars represent standard deviation. n.s., not significant, p value > 0.05; *, p value 0.01 to 0.05; ***, p value < 0.001 (1-way ANOVA, control: wt).

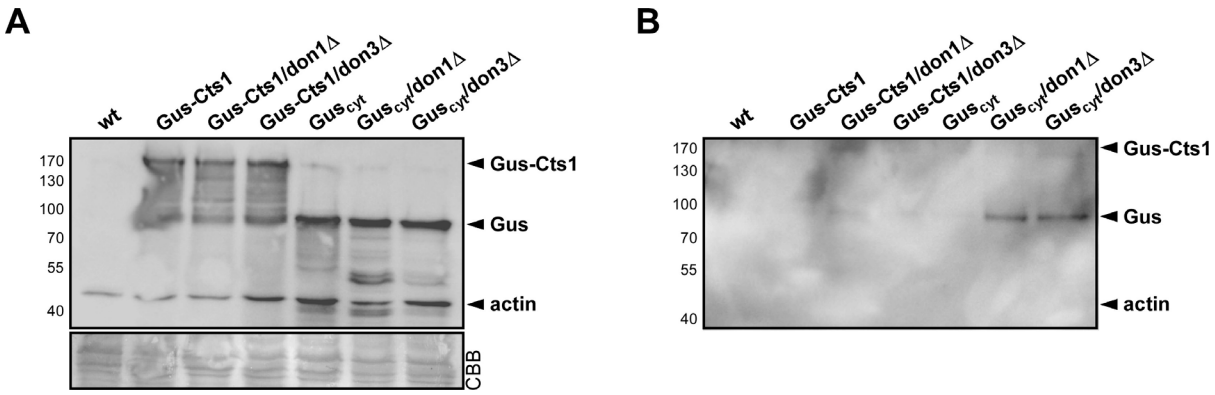


**Figure S2.8. Western blot analysis of different AB33 derivatives expressing Gus-Cts1. A**, Integrity of the fusion proteins was tested by Western blot analysis using cell extracts (10 µg protein each). The blot was probed with antibodies directed against the HA-tag in the SHH tagged Gus (-fusion) proteins and actin (loading control). wt, AB33. CBB, Coomassie Brilliant Blue staining of the membrane. **B,** Western blot analysis of the culture supernatant of indicated AB33 derivatives. The blots were probed with antibodies directed against the HA-tag in the SHH tagged Gus (-fusion) proteins. Unexpectedly, although no enzyme activity could be determined, the Gus protein could be detected in small amounts in the culture supernatants of the lysis controls. By contrast no signals were obtained with anti-actin antibodies which also served as lysis control. Also, in this case we assume that the cell eliminates disfunctional protein because the released amounts are not reflected by extracellular Gus activity (Lee et al., 2016). Gus-fusions to Cts1 could not be detected in culture supernatants although at least for Gus-Cts1 high Gus activity can be determined extracellularly. This observation is likely due to the fact that intact protein is processed by extracellular proteases and hence, very unstable as observed in previous studies (see Figure 2.3E) (Okmen et al., 2018; Sarkari et al., 2014; Terfrüchte et al., 2018). wt, AB33.

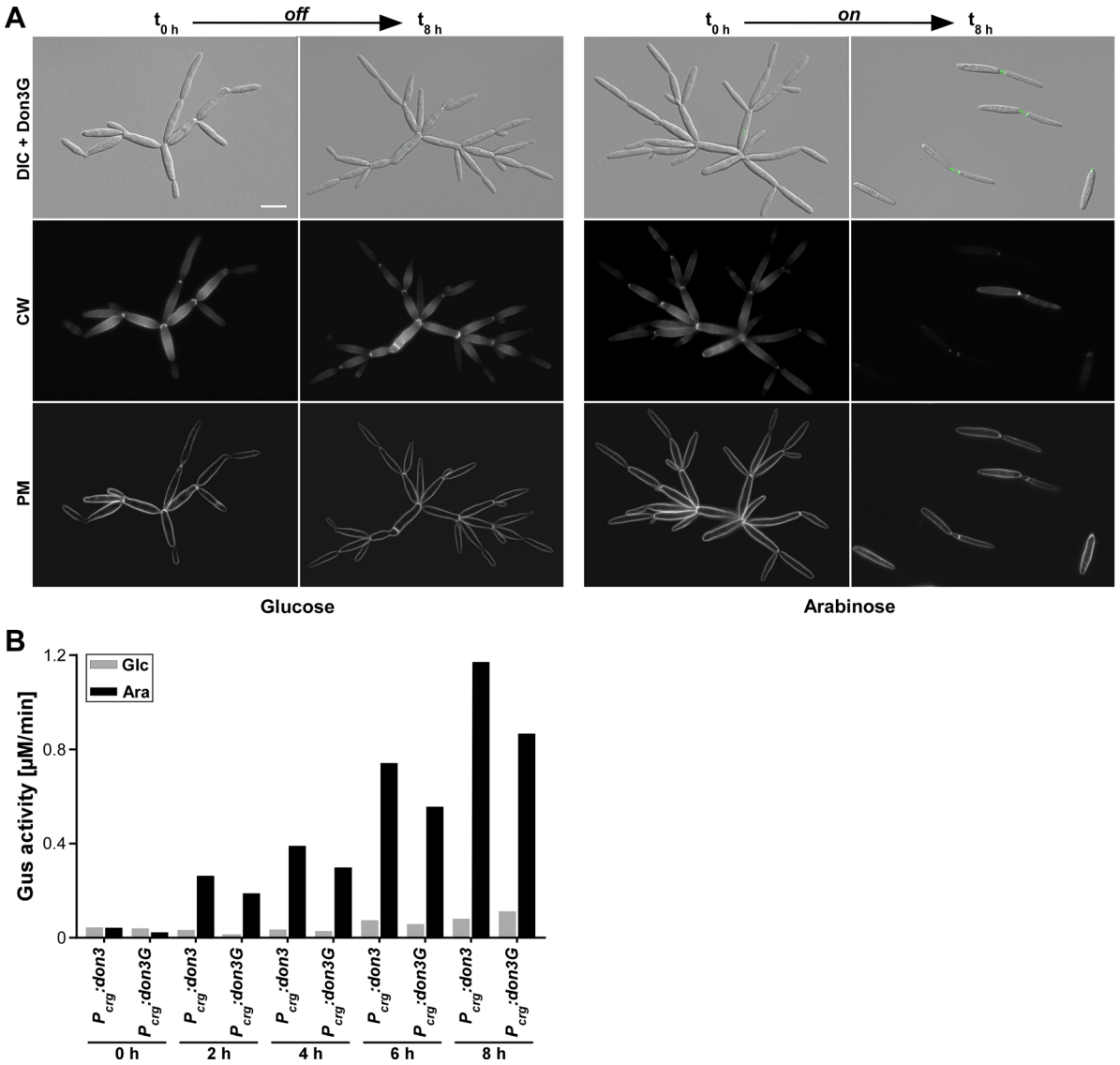


**Figure S2.9. Time-resolved release of Cts1 after *don3* induction. A,** Microscopic visualization of a Don3G induction time course. $t_0$, culture was grown in glucose (off condition). $t_8$, culture was shifted from glucose (Glc) to arabinose (Ara) for 8 h. DIC, differential interference contrast; green, eGfp fluorescence of Don3G; CW, cell wall stained with Calcofluor White; PM, plasma membrane stained with FM4-64. Scale bar, 10 µm. **B,** Relative Gus activity in the culture supernatant of strains with regulated *don3* or *don3G* expression. Cultures of indicated strains were pre-grown in non-induced conditions (glucose as single C-source). After washing, the cultures were split and either grown on glucose (off) or arabinose (on).

# 3 Controlling unconventional secretion for production of heterologous proteins in *Ustilago maydis* through transcriptional regulation and chemical inhibition of the kinase Don3

**Kai P. Hussnaetter**[1], Magnus Philipp[1], Kira Müntjes[1], Michael Feldbrügge[1] and Kerstin Schipper[1,*]

[1] Institute for Microbiology, Heinrich Heine University Düsseldorf, Universitätsstraße 1, 40225 Düsseldorf, Germany
* Correspondence: Kerstin.schipper@hhu.de; Tel.: +49-211-811-0451

This review was published in *Journal of Fungi (Special Issue Smut Fungi*) in March 2021 and is available at doi.org/10.3390/jof7030179.

**Relevance of publication**

Previous studies demonstrated the general possibility of inducing unconventional secretion via regulation of Don3. Unconventional secretion of Cts1 is dependent on formation of a functional fragmentation zone between mother and daughter cell by initiation of a secondary septum insertion by Don3. Deletion of *don3* results in mutants defective in cell separation and diminished release of Cts1 from the fragmentation zone. Complementation under inducing conditions rescued the phenotype, resulting in Cts1 secretion upon the external stimulus. Induction of secretion allows fine-tuned release of unconventionally secreted protein. The results support a model of lock type secretion where trapped Cts1 accumulates in the immature fragmentation zone from where it is released.

In this follow up project, different regulatory systems for induction were established and characterized. Transcriptional regulation via complementation of *don3* mutants with a carbon source dependent promoter allowed for induction of unconventional secretion. Establishment of an autoinduction medium enabled batch fermentation of strains, uncoupling heterologous protein production and cell growth from unconventional secretion without the need for medium shifts. The applicability and efficiency of this strategy was demonstrated by autoinduced unconventional secretion of anti-Gfp nanobodies.

Furthermore, an alternative, ATP-analogue sensitive Don3 version was used for post-translational regulation. The alternative Don3 version is fully functional in the absence of the inhibitor, while it becomes inactive after its addition. Importantly, biosynthesis of Don3 is not affected, whereby removal of the inhibitor resulted in a fast activation of unconventional

secretion upon removal of inhibitor. The two different regulatable systems established in this work allow for a well-adjusted selection of induction and cultivation conditions.

## 3.1 Abstract

Heterologous protein production is a highly demanded biotechnological process. Secretion of the product to the culture broth is advantageous because it drastically reduces downstream processing costs. We exploit unconventional secretion for heterologous protein expression in the fungal model microorganism *Ustilago maydis*. Proteins of interest are fused to carrier chitinase Cts1 for export via the fragmentation zone of dividing yeast cells in a lock-type mechanism. The kinase Don3 is essential for functional assembly of the fragmentation zone and hence, for release of Cts1-fusion proteins. Here, we are first to develop regulatory systems for unconventional protein secretion using Don3 as a gatekeeper to control when export occurs. This enables uncoupling the accumulation of biomass and protein synthesis of a product of choice from its export. Regulation was successfully established at two different levels using transcriptional and post-translational induction strategies. As a proof-of-principle, we applied autoinduction based on transcriptional *don3* regulation for the production and secretion of functional anti-Gfp nanobodies. The presented developments comprise tailored solutions for differentially prized products and thus constitute another important step towards a competitive protein production platform.

## 3.2 Introduction

Recombinant proteins are ubiquitous biological products with versatile industrial, academic, and medical applications (Mattanovich et al., 2012; Tripathi & Shrivastava, 2019). Well-established hosts for protein production include, e.g., bacteria such as *Escherichia coli* (Gopal & Kumar, 2013), yeasts such as *Saccharomyces cerevisiae* or *Pichia pastoris* (Baghban et al., 2019; Mattanovich et al., 2012) or mammalian and insect tissue cultures (Contreras-Gomez et al., 2014; O'Flaherty et al., 2020). Importantly, the nature of a protein largely influences the choice of a particular expression system, and not every protein is adequately expressed in the standard platform of choice (Saccardo et al., 2016). Thus, there is not a universal protein expression system and the demand for alternative production hosts is increasing. In general, secretory systems are advantageous because the protein product is exported into the medium allowing for economic and straightforward downstream processing workflows (Balasundaram et al., 2009). Due to their extraordinary secretion capacities and inexpensive cultivation, fungal expression hosts are promising candidates for novel platforms and already the preferred hosts for the production of proteases and other hydrolytic enzymes (Wang et al., 2020; Ward, 2012). However, the synthesis of heterologous proteins still imposes major challenges in fungal expression hosts (Nevalainen & Peterson, 2014). One reason is the occurrence of atypical post-translational modifications during conventional secretion via

the endomembrane system (Iturriaga et al., 1989). Furthermore, secreted fungal proteases are often destructive to the exported products (Idiris et al., 2010; Ward, 2012). Hence, it is important to further develop tailor-made strategies to provide a broad repertoire of potent fungal host organisms and enable the economic production of all relevant requested proteins in their functional form.

In the past years, we have established heterologous protein production based on unconventional chitinase secretion in the fungal model microorganism *Ustilago maydis* (Feldbrügge et al., 2013; Sarkari et al., 2016; Stock et al., 2012; Terfrüchte et al., 2018). The phenomenon of unconventional secretion has been described for an increasing number of eukaryotic proteins (Dimou & Nickel, 2018; Rabouille, 2017). Well-characterized examples include mammalian fibroblast growth factor 2 which is released via self-sustained translocation (Steringer et al., 2017; Steringer & Nickel, 2018) and acyl-CoA binding protein Acb1 exported via specialized compartments of unconventional secretion (CUPS) (Cruz-Garcia et al., 2018). However, in most other cases detailed mechanistic insights are still lacking. Furthermore, biotechnological applications for these systems have been proposed (Nickel, 2010) but have not been described to date.

In our system, chitinase Cts1 is used as a carrier for export of proteins of interest. The main advantage of this unique system is that proteins do not have to pass the endomembrane system as they would during conventional secretion. This circumvents post-translational modifications such as *N*-glycosylation and other drawbacks such as size limitations of the endomembrane system. Since non-natural *N*-glycosylation of proteins can be destructive to their activity (Iturriaga et al., 1989; Tull et al., 2001) unconventional secretion is a good choice for sensitive proteins such as those originating from bacteria (Stoffels et al., 2020). Bacterial β-glucuronidase (Gus) for example cannot be secreted in an active form via the conventional pathway (Iturriaga et al., 1989). By contrast, Cts1-mediated unconventional secretion results in active protein in the culture supernatant. As a versatile reporter, Gus is therefore also perfectly suited to detect and quantify unconventional secretion (Stock et al., 2012; Stock et al., 2016). The applicability of the expression system has been shown by successful production of several functional proteins such as single-chain variable fragments (scFvs), nanobodies, or different bacterial enzymes such as Gus, β-galactosidase (LacZ), or polygalacturonases (Sarkari et al., 2014; Stock et al., 2012; Stoffels et al., 2020; Terfrüchte et al., 2017).

Recently, we obtained the first insights into the cellular mechanism of unconventional secretion (Aschenbroich et al., 2019; Reindl et al., 2019; Reindl et al., 2020). During cytokinesis of yeast cells, a primary septum is formed at the mother cell side, followed by a secondary septum at the daughter cell side, delimiting a so-called fragmentation zone (Figure 3.1A) (Weinzierl et al., 2002). Upon formation of the daughter cell, Cts1 is targeted to this zone

and likely functions in degradation of the remnant cell wall to separate mother and daughter (Figure 3.1B). Here, it acts in concert with a second, conventionally secreted chitinase, Cts2 (Langner et al., 2015). Genetic screening identified the potential anchoring factor Jps1, a yet undescribed protein that exhibits an identical localization as Cts1 and is crucial for its export (Figure 3.1C) (Reindl et al., 2020). In addition, the presence of two proteins required for secondary septum formation, guanine nucleotide exchange factor (GEF) Don1 and germinal center kinase Don3 (Figure 3.1D), is essential for Cts1 secretion. Loss of either protein involved in septum formation results in the formation of cell aggregates and a strongly diminished extracellular chitinase activity (Aschenbroich et al., 2019). This suggested a lock-type mechanism for Cts1 secretion (Reindl et al., 2019). Interestingly, Don3 itself was also found to be released similar to Cts1 (Aschenbroich et al., 2019).

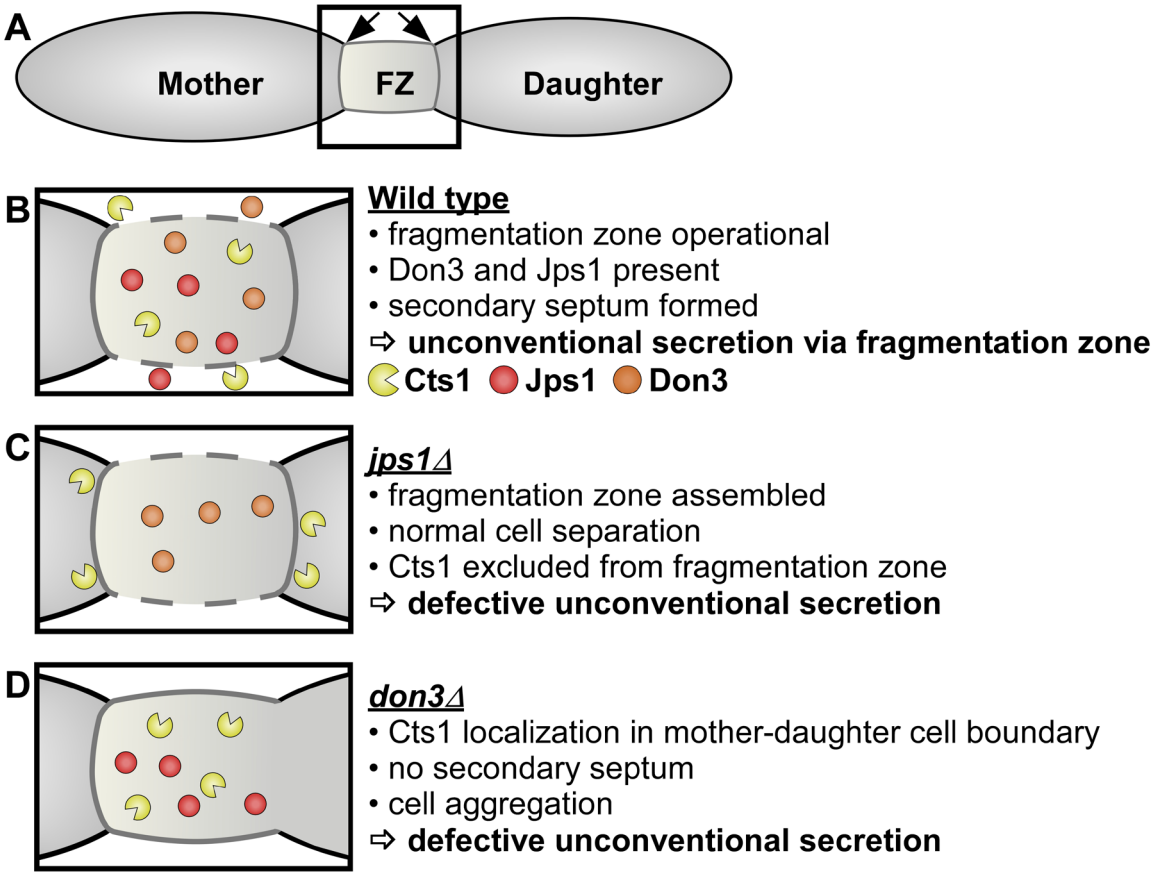


**Figure 3.1. Current schematic model of lock-type secretion and implications for heterologous protein export in *U. maydis*.** (**A**) Unconventional secretion of chitinase Cts1 occurs during cytokinesis of yeast cells. Prior to budding, a primary septum is assembled at the mother cell side, followed by a secondary septum at the daughter cell side. The two septa delimit a so-called fragmentation zone (FZ), a small compartment filled with different proteins and membrane vesicles (not shown). Position of septa is indicated by arrows. (**B**) In the wild-type situation, Cts1 accumulates in the fragmentation zone and participates in cell separation. Recent research identified the potential anchoring factor Jps1 and the septation factors Don1 (not shown) and Don3, which are essential for Cts1 secretion. (**C**) In the absence of Jps1, Cts1 is excluded from the fragmentation zone and unconventional secretion is abolished. Nevertheless, cell separation occurs normally. (**D**) In the absence of Don3, the secondary septum is not assembled, and cell separation is hampered, leading to the formation of cell aggregates. Cts1 still accumulates at the mother-daughter cell boundary but its unconventional secretion is abolished. Modified from published figure: Arrangement was adapted.

Here, we established for the first-time regulatory mechanisms for protein production by unconventional secretion, which are based on our recent insights into the export pathway. Efficient regulation was achieved by two basic strategies: i) transcriptional and ii) post-translational induction of the previously identified unconventional secretion factor Don3. This led to new regulatory options including an autoinduction process, which can be applied depending on the need of the product of interest.

# 3.3 Material and methods

## *3.3.1 Molecular biology methods*

All plasmids (pUMa vectors) generated in this study were obtained using standard molecular biology methods established for *U. maydis* including Golden Gate cloning (Brachmann et al., 2004; Kämper, 2004; Terfrüchte et al., 2014). Genomic DNA of *U. maydis* strain UM521 was used as template for PCR reactions. The genomic sequence for this strain is stored at the EnsemblFungi database (Web reference: EnsemblFungi *U. maydis* genome browser). All plasmids were verified by restriction analysis and sequencing. Oligonucleotides applied for cloning are listed in Table 3.1. The generation of pUMa3329_Δupp1_$P_{crg}$-eGfp-Tnos-natR, pUMa2113_pRabX1-$P_{oma}$_gus-SHH-cts1, pUMa2240_Ip_$P_{oma}$-his-anti-Gfpllama-ha-Cts1-CbxR and pUMa2775_um03776D_hyg had been previously described (Aschenbroich et al., 2019; Reindl et al., 2020; Stock et al., 2012; Terfrüchte et al., 2017) but often used in differing strain backgrounds in the present study (for references see Table 3.2). For generation of pUMa4234_Δupp1_$P_{crg}$-jps1-eGfp-Tnos-natR and pUMa4235_Δupp1_$P_{crg}$-jps1-Tnos-natR, *jps1-gfp* or *jps1* were amplified and inserted into an *upp1* insertion vector. Therefore, pUMa3330 (Aschenbroich et al., 2019) was digested using MfeI and AscI, serving as cloning backbone. A PCR product obtained with primer combination oUM910/oUM912 for *jps1-gfp* or oUM910/oUM911 for *jps1* using pUMa3095 (Reindl et al., 2020) as a template, was inserted into the digested backbone. For generation of pUMa4308_Δupp1_$P_{crg}$-don3(M157A)-Tnos-natR and pUMa4313_Δupp1_$P_{crg}$-don3(M157A)-eGfp-Tnos-natR site-directed mutagenesis using primer pair oAB23/oAB24 was performed on plasmids pUMa3331 or pUMa3330 (Aschenbroich et al., 2019), respectively, resulting in exchange of a single base pair (Web reference: Agilent). For generation of pUMa3293_pPjps1—jps1-eGfp_CbxR, *jps1* promoter was amplified using primer combination oUP65/oUP66, *jps1* was amplified using primer combination oMB190/oMB520, *eGfp* was amplified using primer combination MB521/oMB522. PCR products were digested using BamHI, EcoRI, NotI, NdeI and inserted in the digested backbone pUMa2113 (Sarkari et al., 2014). Detailed cloning strategies and vector maps will be provided upon request.

**Table 3.1.** DNA oligonucleotides used in this study.

| Designation | Nucleotide Sequence (5′–3′) |
|---|---|
| oUM910 | GATCCAATTGATGCCAGGCATCTCCAAGAAGCC |
| oUM911 | GATCGGCGCGCCTTAGGATTCCGCATCGATTGGGG |
| oUM912 | GATCGGCGCGCCTTACTTGTACAGCTCGTCCATGC |
| oAB23 | GCTACAAGCTCTGGATCATTGCTGAGTATCTAGCAGGTGGATCC |
| oAB24 | GGATCCACCTGCTAGATACTCAGCAATGATCCAGAGCTTGTAGC |
| oRL946 | CCGATCCACAAGCTTCGGTGCTTGGATTGG |
| oRL947 | CGGTGTTGCCATGAACACCGATGGCCAGTG |
| oRL948 | GGTACTTGTGCTCGGGGAACACCTCGGCGA |
| oRL949 | GTTTTGTCTCGTTCCGTGCGTCGACGACAGA |
| oMF502 | ACGACGTTGTAAAACGACGGCCAG |
| oMF503 | TTCACACAGGAAACAGCTATGACC |
| oUP65 | GGAATTCCATATGGCGAGCCTTGAGGCTGCGTTCC |
| oUP66 | CGGGATCCGATTTGCAAGTCGTGGGCCTTCG |
| oMB190 | GATTACAGGATCCATGCCAGGCATCTCC |
| oMB520 | CATGAATTCGGATTCCGCATCGATTGGGG |
| oMB521 | TCAGAATTCATGGTGAGCAAGGGCGAGG |
| oMB522 | CATGCGGCCGCCTTACTTGTACAGCTCGTCC |

## *3.3.2 Strain generation*

*U. maydis* strains used in this study were obtained by homologous recombination yielding genetically stable strains (Table 3.2) (Bösch et al., 2016). All strains were derived from strain AB33. In this laboratory strain, the *b* mating type locus has been manipulated by insertion of compatible *b* genes controlled by a nitrogen-inducible promoter. This allows for a switch between yeast and filamentous growth by use of different nitrogen sources in the cultivation medium (Brachmann et al., 2001). Genomic integrations were positioned either at the *ip* or the *upp1* locus, two established loci for genomic integrations. The *ip* locus encodes an iron-sulfur protein of the respiratory chain. Exchanging a single amino acid in this enzyme renders the cells resistant against the antibiotic carboxin (Keon et al., 1991). Plasmids carrying the $ip^R$ gene mediating carboxin resistance were used and integrated in the native $ip^S$ locus of carboxin sensitive strains (Stock et al., 2012). For transformation, these integrative plasmids were digested within the $ip^R$ region using the restriction endonuclease SspI, resulting in a linear DNA fragment. For insertions at the *upp1* locus (*umag_02178*) (Sarkari et al., 2014), plasmids harbored a nourseothricin resistance cassette and the integration sequence, flanked by homologous regions for the respective insertion locus. For transformation, the insertion cassette was excised from the plasmid backbone using SspI or SwaI (Terfrüchte et al., 2014).

For generation of deletion mutants, hygromycin resistance cassette containing constructs flanked by regions homologous to the 5'and 3´ sequences of the genes to be deleted were used. Again, deletion cassettes were excised from plasmid backbones prior to transformation (Terfrüchte et al., 2014). For all genetic manipulations, *U. maydis* protoplasts were transformed with linear DNA fragments for homologous recombination. All strains were verified by Southern blot analysis (Bösch et al., 2016). The *upp1* locus encodes the secreted aspartatic protease Upp1. Along with other genes for secreted proteases *upp1* can be deleted without causing any morphologic phenotype while the proteolytic activity in the culture supernatant is reduced and heterologous proteins are stabilized (Sarkari et al., 2014). For *upp1* insertion, digoxigenin-labelled probes were obtained by PCR using primer combinations oRL946/oRL947 and oRL948/oRL949 on template pUMa1538 (Sarkari et al., 2014). For in locus modifications the flanking regions were amplified as probes. For *ip* insertions, the probe was obtained by PCR using the primer combination oMF502/oMF503 and the template pUMa260 (Loubradou et al., 2001). Primer sequences are listed in Table 3.1.

**Table 3.2.** *U. maydis* strains used in this study. Strains were obtained by homologous recombination using antibiotic resistance cassettes for selection: PhleoR, phleomycin resistance; CbxR, carboxin resistance; HygR, hygromycin resistance; NatR, nourseothricin resistance. Don3*, version of kinase Don3 carrying an amino acid exchange at position 157 (methionine replaced by alanine).

| Strains | Relevant genotype/ resistance | UMa[1] | Plasmids transformed[2]/ resistance | Manipulated locus | Progenitor (UMa[1]) | Reference |
|---|---|---|---|---|---|---|
| AB33 | *a2 P$_{nar}$bW2bE1PhleoR* | 133 | pAB33 | *b* | FB2 [43] | (Brachmann et al., 2001) |
| AB33 Gus-Cts1 | *a2 P$_{nar}$bW2bE1* PhleoR *ip$^{S}$[P$_{oma}$gus:shh:cts1]ip$^{R}$* CbxR | 1289 | pUMa2113/ CbxR | *ip* | 133 | (Sarkari et al., 2014) |
| AB33 don3Δ/ Gus-Cts1 | *a2 P$_{nar}$bW2bE1* PhleoR *ip$^{S}$[P$_{oma}$gus:shh:cts1]ip$^{R}$* CbxR *umag_05543Δ*_HygR | 1742 | pUMa2717/ HygR | *umag_05543*[3] *(don3)* | 1289 | (Aschenbroich et al., 2019) |
| AB33 don3Δ | *a2 P$_{nar}$bW2bE1* PhleoR *umag_05543Δ*_HygR | 2028 | pUMa2717/ HygR | *umag_05543 (don3)* | 133 | (Aschenbroich et al., 2019) |
| AB33 don3Δ/ P$_{otef}$ gfp/ Gus-Cts1 | *a2 P$_{nar}$bW2bE1* PhleoR *ip$^{S}$[P$_{oma}$gus:shh:cts1]ip$^{R}$* CbxR *umag_05543Δ*_HygR *upp1::[P$_{otef}$gfp]* NatR | 2300 | pUMa3328/ NatR | *umag_02178 (upp1)* | 1742 | (Aschenbroich et al., 2019) |
| AB33 don3Δ/ P$_{crg}$ gfp/ Gus-Cts1 | *a2 P$_{nar}$bW2bE1* PhleoR *ip$^{S}$[P$_{oma}$gus:shh:cts1]ip$^{R}$* CbxR *umag_05543Δ*_HygR *upp1::[P$_{crg}$gfp]* NatR | 2301 | pUMa3329/ NatR | *umag_02178 (upp1)* | 1742 | This study |
| AB33 don3Δ/ P$_{crg}$don3-gfp/ Gus-Cts1 | *a2 P$_{nar}$bW2bE1* PhleoR *ip$^{S}$[P$_{oma}$gus:shh:cts1]ip$^{R}$* CbxR *umag_05543Δ*_HygR *upp1::[P$_{crg}$don3:gfp]* NatR | 2302 | pUMa3330/ NatR | *umag_02178 (upp1)* | 1742 | (Aschenbroich et al., 2019) |

| | | | | | | |
|---|---|---|---|---|---|---|
| AB33 don3Δ/ $P_{crg}$don3/ Gus-Cts1 | *a2 $P_{narb}$W2bE1* PhleoR *ip$^{S}$[$P_{oma}$gus:shh:cts1]ip$^{R}$* CbxR *umag_05543Δ*_HygR *upp1::[$P_{crg}$don3]* NatR | 2303 | pUMa3331/ NatR | *umag_02178 (upp1)* | 1742 | (Aschenbroich et al., 2019) |
| AB33 jps1Δ | *a2 $P_{narb}$W2bE1* PhleoR *umag_03776Δ*_HygR | 2092 | pUMa2775/ HygR | *umag_03776 (jps1)* | 133 | (Reindl et al., 2020) |
| AB33 jps1Δ/ Gus-Cts1 | *a2 $P_{narb}$W2bE1* PhleoR *umag_03776Δ*_HygR *ip$^{S}$[$P_{oma}$gus:shh:cts1]ip$^{R}$* CbxR | 2991 | pUMa2113/ CbxR | *ip* | 2092 | This study |
| AB33 jps1Δ/ $P_{crg}$jps1-gfp/ Gus-Cts1 | *a2 $P_{narb}$W2bE1* PhleoR *umag_03776Δ*_HygR *ip$^{S}$[$P_{oma}$gus:shh:cts1]ip$^{R}$* CbxR *upp1::[$P_{crg}$jps1:gfp]* NatR | 3053 | pUMa4234/ NatR | *umag_02178 (upp1)* | 2991 | This study |
| AB33 jps1Δ/ $P_{crg}$jps1/ Gus-Cts1 | *a2 $P_{narb}$W2bE1* PhleoR *umag_03776Δ*_HygR *ip$^{S}$[$P_{oma}$gus:shh:cts1]ip$^{R}$* CbxR *upp1::[$P_{crg}$jps1]* NatR | 3054 | pUMa4235/ NatR | *umag_02178 (upp1)* | 2991 | This study |
| AB33 don3Δ/ $P_{crg}$don3*-gfp/ Gus-Cts1 | *a2 $P_{narb}$W2bE1* PhleoR *ip$^{S}$[$P_{oma}$gus:shh:cts1]ip$^{R}$* CbxR *umag_05543Δ*_HygR *upp1::[$P_{crg}$don3$^{M157A}$:gfp]* NatR | 3069 | pUMa4313/ NatR | *umag_02178 (upp1)* | 1742 | This study |
| AB33 don3Δ/ $P_{crg}$don3*/ Gus-Cts1 | *a2 $P_{narb}$W2bE1* PhleoR *ip$^{S}$[$P_{oma}$gus:shh:cts1]ip$^{R}$* CbxR *umag_05543Δ*_HygR *upp1::[$P_{crg}$don3$^{M157A}$]* NatR | 3070 | pUMa4308/ NatR | *umag_02178 (upp1)* | 1742 | This study |
| AB33 don3Δ/ $P_{crg}$don3* | *a2 $P_{narb}$W2bE1* PhleoR *umag_05543Δ*_HygR *upp1::[$P_{crg}$don3$^{M157A}$]* NatR | 3346 | pUMa3331/ NatR | *umag_02178 (upp1)* | 2028 | This study |
| AB33 don3Δ/ $P_{crg}$don3/ NB-Cts1 | *a2 $P_{narb}$W2bE1* PhleoR *ip$^{S}$[$P_{oma}$his:*anti-*GfpNB:ha:cts1]ip$^{R}$* CbxR *umag_05543Δ*_HygR *upp1::[$P_{crg}$don3$^{M157A}$]* NatR | 3410 | pUMa2240/ CbxR | *ip* | 3346 | This study |
| AB33 jps1Δ $P_{jps1}$jps1-gfp | *a2 $P_{narb}$W2bE1*PhleoR *umag_03776Δ*_HygR *ip$^{S}$[$P_{jps1}$jps1:gfp]ip$^{R}$*CbxR | 2274 | pUMa3293/ CbxR | *ip* | 2092 | This study, supplementary data |

[1] Internal strain collection numbers. Strains are called UMa plus a 4-digit number as identifier. [2] Plasmids generated in our working group are integrated in a plasmid collection and termed pUMa plus a 4-digit number as identifier. [3] Genes of *U. maydis* are indicated with a 5-digit *umag* number referring to the current genome annotation at EnsembleFungi (Web reference: EnsemblFungi *U. maydis* genome browser).

### *3.3.3 Cultivation*

*U. maydis* strains were cultivated at 28 °C in complete medium (CM) supplemented (Holliday, 1974) with 1% (w/v) glucose (CM-glc) or with 1% (w/v) arabinose (CM-ara) if not described differently or in YepsLight (Tsukuda et al., 1988). CM cultures were eventually buffered with 0.1 M MES as mentioned in the respective section. Solid media were supplemented with 2% (w/v) agar. Growth phenotype and Gfp fluorescence in different media was evaluated using the BioLector microbioreactor (m2p-labs, Baesweiler, Germany) (Funke et al., 2010). MTP-R48-B(OH) round plates were inoculated with 1500 µL culture per well and

incubated at 1000 rpm at 28 °C. Backscatter light with a gain of 25 or 20 and Gfp fluorescence (excitation/emission wavelengths: 488/520, gain 80) were used to determine biomass and accumulation of Gfp.

### *3.3.4 Transcriptional and post-translational regulation of Gus-Cts1 secretion*

To assay regulated secretion, precultures were grown in 5 mL YepsLight for 24 h at 28 °C at 200 rpm. 200 µL culture was transferred into 5 mL fresh YepsLight medium and grown for an additional 8 h under identical conditions. After regeneration, cultures were diluted to reach a final $OD_{600}$ of 1.0 after 16 h in CM-glc or CM-ara. Since *U. maydis* proliferates slower in arabinose, inoculation volume for arabinose cultures was increased by 60%. Cultures were harvested at $OD_{600}$ 0.8 to 1.0 by centrifugation of 2 mL culture at 1500 × *g* for 5 min. 1.8 mL supernatants were transferred to fresh reaction tubes and stored at −20 °C until Gus activity determination.

To assay post-translational regulation, cells were incubated in CM-ara or CM-ara containing 1 µM (f.c.) NA-PP1. Since cultures grow slower when arabinose is used as carbon source and NA-PP1 was added to the medium, the inoculum was increased by 130%.

For evaluation of time-dependent secretion using both transcriptional and post-translational regulation, strains were inoculated in CM-glc, CM-ara and CM-ara with NA-PP1 to reach a final $OD_{600}$ of 1.0 after 16 h. Cells were then washed in $H_2O$ and resuspended in CM-ara. Supernatant samples were taken 0, 1, 2, 4, and 8 h post-induction as described above, and Gus activity was determined.

### *3.3.5 Quantification of unconventional secretion using the Gus reporter*

Extracellular Gus activity was determined to quantify unconventional Cts1 secretion using the specific substrate 4-methylumbelliferyl-β-d-glucuronide (MUG, bioWORLD, Dublin, OH, USA). Cell-free culture supernatants were mixed 1:1 with 2× Gus assay buffer (10 mM sodium phosphate buffer pH 7.0, 28 µM β-mercaptoethanol, 0.8 mM EDTA, 0.0042% (*v/v*) lauroyl-sarcosin, 0.004% (*v/v*) Triton X-100, 2 mM MUG, 0.2 mg/mL (w/v) BSA) in black 96-well plates. Relative fluorescence units (RFUs) were determined using a plate reader (Tecan, Männedorf, Switzerland) for 100 min at 28 °C with measurements every 5 min (excitation/emission wavelengths: 365/465 nm, Gain 60). For quantification of conversion of MUG to the fluorescent product 4-methylumbelliferone (MU), a calibration curve was determined using 0, 1, 5, 10, 25, 50, 100, 200 µM MU.

### *3.3.6 SDS PAGE and Western blot analysis*

To verify protein production and secretion in cell extracts and supernatants, respectively, Western blot analysis was used. 50 mL cultures were grown to an $OD_{600}$ of 1.0 and harvested at 1500 × *g* for 5 min in centrifugation tubes. Until further preparation, pellets were stored at −20 °C while supernatants were supplemented with 10% trichloracetic acid (TCA) and incubated on ice. For preparation of cell extracts, cell pellets were resuspended in 1 mL cell extract lysis buffer (100 mM sodium phosphate buffer pH 8.0, 10 mM Tris/HCl pH 8.0, 8 M urea, 1 mM DTT, 1 mM PMSF, 2.5 mM benzamidine, 1 mM pepstatinA, 2× complete protease inhibitor cocktail (Sigma/Aldrich, Billerica, MA, USA)) and agitated with glass beads at 1500 rpm for 10 min at 4 °C. Subsequently, the cell suspension was frozen in liquid nitrogen and crushed in a pebble mill (Retsch, Haan, Germany; 2 min at 30 Hz, 2 times). After centrifugation (6000× *g* for 30 min at 4 °C), the supernatant was separated from cell debris and was transferred to a fresh reaction tube. Protein concentration was determined by Bradford assay (BioRad, Hercules, CA, USA) (Bradford, 1976) and 10 µg total protein was used for SDS-PAGE. For the enrichment of proteins from culture supernatants, TCA supplemented supernatants were kept at 4 °C for at least 6 h and centrifuged at 22,000×*g* for 30 min at 4 °C. The precipitated protein pellets were washed twice with −20 °C acetone and resuspended in 3× Laemmli buffer (neutralized with 120 mM NaOH). Samples were boiled at 95 °C for 10 min and centrifuged for 2 min 22,000× g prior to application for SDS-PAGE. SDS-PAGE was conducted using 10% (w/v) acrylamide gels. Subsequently, proteins were transferred to methanol-activated PVDF membranes using semi-dry Western blotting. SHH-tagged Gus-Cts1 was detected using a primary anti-HA antibody (1:4000, Millipore/Sigma, Billerica, MA, USA). For detection of Gfp-tagged proteins such as Don3-Gfp, Don3*-Gfp or Jps1-Gfp a primary anti-Gfp antibody was used (1:4000, Millipore/Sigma, Billerica, MA, USA). An anti-mouse IgG-horseradish peroxidase (HRP) conjugate (1:4000 Promega, Fitchburg, WI, USA) was used as secondary antibody. HRP activity was detected using the Amersham ™ ECL ™ Prime Western Blotting Detection Reagent (GE Healthcare, Chalfont St Giles, UK) and a LAS4000 chemiluminescence imager (GE Healthcare Life Sciences, Freiburg, Germany).

### *3.3.7 Enzyme-linked immunosorbent assay (ELISA)*

For detection of binding activity of respective anti-GfpNB-Cts1 fusions, protein adsorbing 384-well microtiter plates (Nunc® MaxisorpTM, ThermoFisher Scientific, Waltham, MA, USA) were used. Wells were coated with 1 µg Gfp. Recombinant Gfp was produced in *E. coli* and purified by $Ni^{2+}$-chelate affinity chromatography as described earlier (Terfrüchte et al., 2017). 2 µg BSA dealt as negative control (NEB, Ipswich, MA, USA). Samples were applied in a final volume of 100 µL coating buffer (100 mM Tris-HCL pH 8, 150 mM NaCl, 1 mM EDTA) per well

at room temperature for at least 16 h. Blocking was conducted for at least 4 h at room temperature with 5% (w/v) skimmed milk in coating buffer. Subsequently, 5% skimmed milk in PBS (5% (w/v) skimmed milk, 137 mM NaCl, 2.7 mM KCl, 10 mM $Na_2HPO_4$, 1.8 mM $KH_2PO_4$, pH 7.2) were added to respective volumes or defined protein amounts of anti-GfpNB-Cts1 samples purified from culture supernatants or cell extracts via $Ni^{2+}$-NTA gravity flow and respective controls. 100 µL of sample were added to wells coated with GFP and BSA. The plate was incubated with samples and controls overnight at 4 °C. After 3× PBS-T (PBS supplemented with 0.05% (*v/v*) Tween-20, 100 µL per well) washing, a mouse anti-HA antibody 1:5000 diluted in PBS supplemented with skimmed milk (5% *w/v*) was added (100 µL per well) and incubated for 2 h at room temperature. Then wells were washed again three times with PBS-T (100 µL per well) and incubated with a horse anti-mouse-HRP secondary antibody (50 µL per well) for 1 h at room temperature (1:5000 in PBS supplemented with skimmed milk (5% (w/v)). Subsequently, wells were washed three times with PBS-T and three times with PBS and incubated with Quanta RedTM enhanced chemifluorescent HRP substrate (50:50:1, 50 µL per well, ThermoFisher Scientific, Waltham, MA, USA) at room temperature for 15 min. The reaction was stopped with 10 µL per well Quanta RedTM stop solution and fluorescence readout was performed at 570 nm excitation and 600 nm emission using an Infinite M200 plate reader (Tecan, Männerdorf, Switzerland).

### *3.3.8 Microscopic analyses*

Microscopic analyses were performed with immobilized early-log phase budding cells on agarose patches (3% (w/v)) using a wide-field microscope setup from Visitron Systems (Munich, Germany), Zeiss (Oberkochen, Germany) Axio Imager M1 equipped with a Spot Pursuit CCD camera (Diagnostic Instruments, Sterling Heights, MI, USA) and the objective lenses Plan Neofluar (40×, NA 1.3), Plan Neofluar (63×, NA 1.25) and Plan Neofluar (100×, NA 1.4). Fluorescent proteins were detected with an HXP metal halide lamp (LEj, Jena, Germany) in combination with filter set for Gfp (ET470/40BP, ET495LP, ET525/50BP). The microscopic system was controlled by the software MetaMorph (Molecular Devices, version 7, Sunnyvale, CA, USA). Image processing including rotating and cropping of images, scaling of brightness, contrast, and fluorescence intensities as well as insertion of scaling bars was performed with MetaMorph. Arrangement and visualization of signals by arrowheads was performed with Canvas 12 (ACD Systems, Victoria, BC, CA).

# 3.4 Results

## *3.4.1 Evaluating Jps1 as a regulator for unconventional protein export*

The presence of the potential anchoring factor Jps1 is essential for unconventional Cts1 secretion via the fragmentation zone (Figure 3.1B,C) (Reindl et al., 2020). This mechanistic insight might provide the unique possibility of using Jps1 as a regulator for unconventional protein secretion and thus, to establish a first inducible system. To test transcriptional induction of Cts1 export via *jps1*, we used derivatives of laboratory strain AB33 lacking the native gene copy of *jps1* and complemented them with $P_{crg}$ regulated versions of *jps1* or *jps1-gfp,* a fusion to the gene sequence for the green fluorescence protein, encoding a functional fusion protein (Jps1-Gfp; Figure 3.2A) (Reindl et al., 2020). Activity of the $P_{crg}$ promoter depends on the carbon source: The promoter is switched “off” in the presence of glucose and “on” in the presence of arabinose (Bottin et al., 1996). In addition, the strains carried the established reporter Gus-Cts1 as a read-out for unconventional secretion (Figure 3.2A) (Stock et al., 2012). Microscopic analysis revealed that, as expected, the regulated strains grew yeast-like without any different morphological phenotype both in glucose and in arabinose-containing media. However, in contrast to previous localization studies (Reindl et al., 2020), Jps1-Gfp mainly formed intracellular aggregates (about 80%) during all stages of cytokinesis, with only a minor population of about 3% showing the expected localization in the fragmentation zone in late cytokinesis when transcription was induced by arabinose (Figures 3.2B and S3.1). By contrast, control cultures with native Jps1 regulation showed localization in this area in 24% of all investigated cells, likely corresponding to the fraction of cells in the late stage of cytokinesis (Figure S3.1) (Reindl et al., 2020). This suggests that deregulation of Jps1 via $P_{crg}$ interferes with its very specific, cytokinesis-dependent localization. Analysis of unconventional secretion in these strains using the reporter Gus-Cts1 in “off” and “on” conditions revealed that extracellular Gus activities were higher in arabinose than in glucose-containing media, indicating that transcriptional regulation of *jps1* and *jps1-gfp* was successful. However, the base line was elevated and induction levels ranged below two-fold (Figures 3.2C and S3.2). Of note, extracellular Gus activity of a control strain with unconventionally secreted Gus-Cts1 in the *jps1* deletion background (lacking regulated *jps1*) was 4.3 times higher when grown in glucose than the activity during growth in arabinose (Figures 3.2C and S3.2). This suggests that one reason for the weak induction might be the high background. Additionally, the mislocalization of deregulated Jps1-Gfp likely reduces its function during unconventional secretion suggesting that the lock-type mechanism might not efficiently take place in these conditions. Thus, in the present setup transcriptional regulation via *jps1* is not suitable with respect to biotechnological application for the protein expression platform.

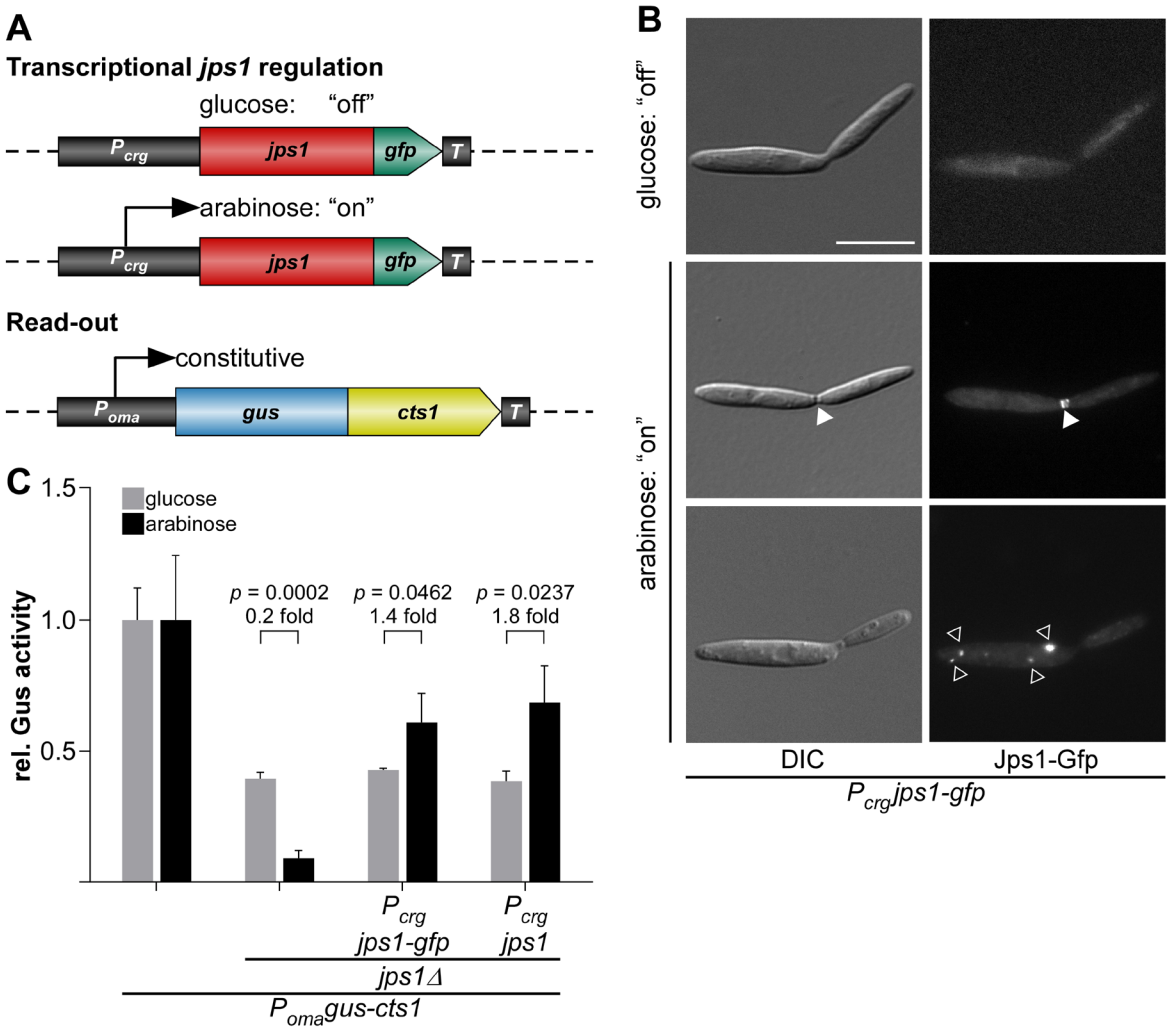


**Figure 3.2. Transcriptional regulation of unconventional secretion via the potential anchoring factor Jps1**. (**A**) Rationale of regulated Jps1 expression on the genetic level. Unconventional secretion factor Jps1 is controlled by the arabinose inducible promoter $P_{crg}$ and constitutively produced Gus-Cts1 is used as a read-out for quantification of unconventional secretion. *T*, transcriptional terminator. (**B**) Micrographs of yeast-like growing cells in the "on" and "off" stage mediated by glucose and arabinose in the medium, respectively. White arrowheads depict the fragmentation zone between mother-daughter cell boundary, open white arrowheads show additional intracellular accumulations of Jps1-Gfp. DIC, differential interference contrast. Scale bar, 10 µm. (**C**) Gus activity in culture supernatants of indicated AB33 Gus-Cts1 derivatives. Enzymatic activity was individually normalized to average values of positive controls secreting Gus-Cts1 constitutively, which were grown in glucose and arabinose-containing cultures. Values for the positive control in the two media do not differ significantly ($p = 0.2022$; Figure S3.2). Strains containing regulated *jps1* or *jps1-gfp* versions show a slight induction of extracellular Gus activity after growth in arabinose-containing medium. Error bars depict standard deviation. The diagram represents results of three biological replicates. Fold change of induced cultures and *p*-values of Student's unpaired *t*-test are shown. Definition of statistical significance: *p*-value < 0.05. Modified from published figure: Arrangement was adapted.

## *3.4.2 Transcriptional regulation of Don3 for unconventional protein export*

Since regulation via Jps1 was not convincing for establishing an efficient inducible protein expression system in the present form, we revisited published results on the transcriptional

regulation of Don3. Studying the Cts1 export mechanism we had observed that induced *don3* expression via the $P_{crg}$ promoter reconstitutes unconventional secretion, confirming the lock-type mechanism via the fragmentation zone. The used AB33 Gus-Cts1 derivatives lack the endogenous *don3* copy and were complemented with *don3* or *don3-gfp* regulated by the $P_{crg}$ promoter (Figure 3.3A) (Aschenbroich et al., 2019). We now reproduced these results focusing on the relevant points for biotechnological application. As observed earlier, the aggregation phenotype was complemented and Don3-Gfp localized to fragmentation zones in arabinose-containing medium (Figure S3.3A) (Aschenbroich et al., 2019; Weinzierl et al., 2002). Deregulated Don3-Gfp solely localized to fragmentation zones of dividing cells (Figure S3.3A) which is identical to published results (Böhmer et al., 2008). Reporter assays revealed induction levels of extracellular Gus activity ranging between five- and seven-fold for Don3-Gfp and Don3, respectively, indicating efficient transcriptional regulation (Figure S3.3B). In Western blot analyses, Don3-Gfp was detected as a full-length protein in cell extracts of cultures grown in arabinose. Culture supernatants revealed the presence of free Gfp, suggesting that the full-length protein is secreted into the extracellular space where Don3 is quickly degraded (Figure 3.3B; Figure S3.3C, D). This is likely caused by secreted proteases, a well-known phenomenon in fungi including *U. maydis* (Aschenbroich et al., 2019; Terfrüchte et al., 2018). The high stability of the remaining Gfp is presumably due to its robust beta-barrel structure (Chiang et al., 2001). A control strain for arabinose induction and cell lysis carrying the gene sequence for cytosolic Gfp under control of $P_{crg}$ was used as a control (AB33 $P_{crg}$gfp) and revealed the presence of cytosolic Gfp in cell extracts but not in culture supernatants of cultures grown in arabinose (Figure 3.3B).

The results confirmed that Don3-mediated regulated secretion efficiently separates cell growth and protein synthesis from secretion. Heterologous proteins are thus kept protected in the cell prior to secretion. For transformation of our findings into a biotechnological process, cycles between cell growth, induction, and protein harvest would be useful. This, for example, reduces the exposure time of the secreted heterologous product in the culture supernatant and thus, potential proteolytic degradation. We tested the robustness of such a strategy by switching between “on” and “off” conditions in cycles over five days while tracking unconventional secretion via the Gus-Cts1 reporter. Indeed, the complete process was reversible and induction levels were comparable throughout the different cycles (Figure 3.3C). This suggests that transcriptional regulation of *don3* is a valuable new tool for heterologous protein production in a cyclic process. In summary, we established a first regulatory strategy for unconventional protein export using a nutrient-dependent promoter.

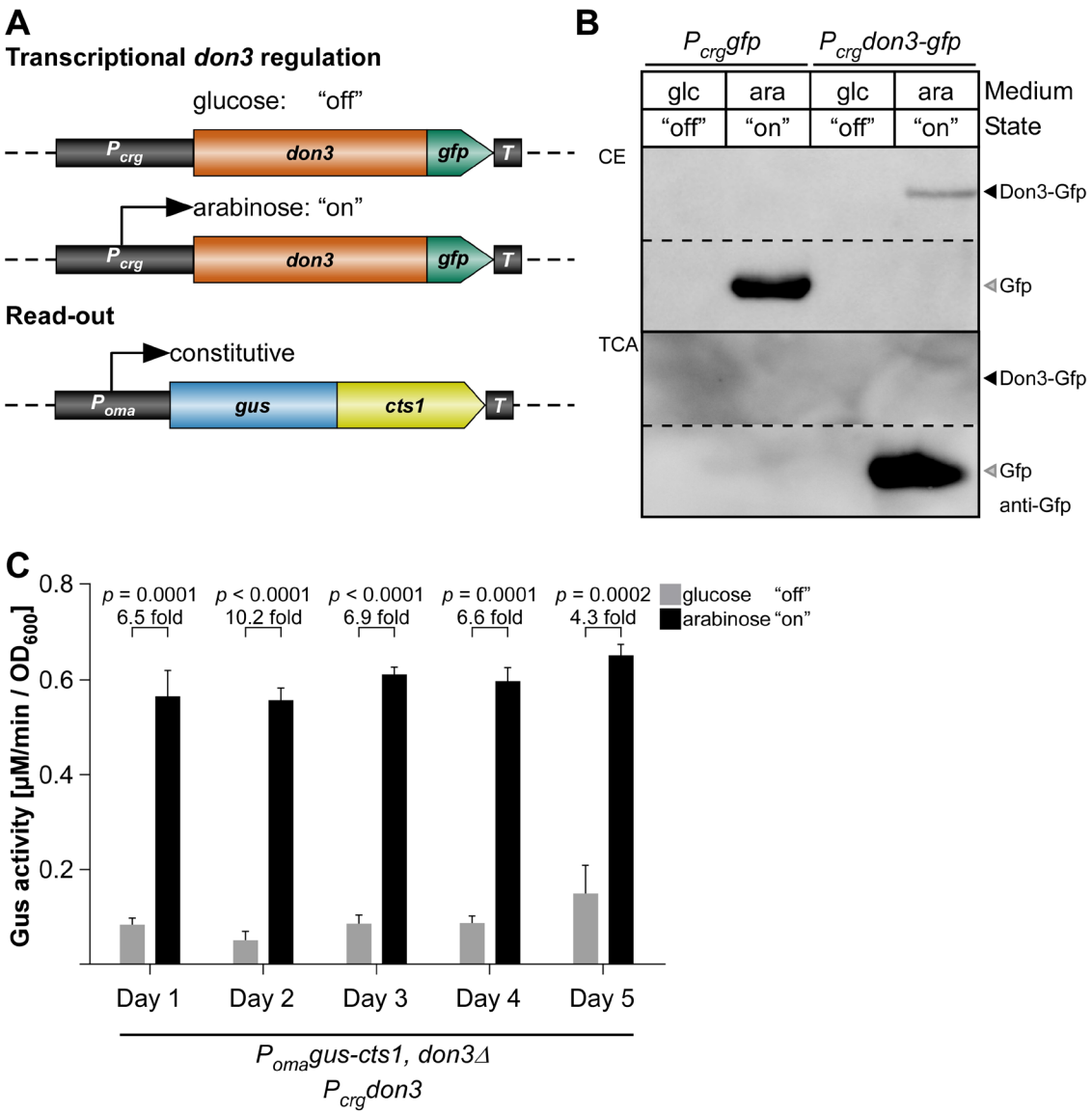


**Figure 3.3. Transcriptional regulation of unconventional secretion via kinase Don3.** (**A**) Exemplary strategy for transcriptional *don3-gfp* regulation of unconventional secretion. Upon supplementation of the medium with glucose, the $P_{crg}$ promoter is inactive, while the addition of arabinose leads to its activation. Constitutive Gus-Cts1 expression is used as a read-out for quantification of unconventional secretion. (**B**) Western blot of cell extracts (CE, upper panel) and TCA precipitated culture supernatants (TCA) depicting Don3-Gfp and cytosolic Gfp (cell lysis control). Primary antibodies against Gfp were used to detect the respective proteins (anti-Gfp). In cell extracts, Don3-Gfp protein is only present upon induction with arabinose. Glc, glucose supplementation; ara, arabinose supplementation. (**C**) Induction of unconventional secretion is reversible upon shift between glucose and arabinose supplementation using strain AB33don3Δ/$P_{crg}$don3/Gus-Cts1. Cultivation of cells in cycles consisting of 16-h growth in CM-glc (supplemented with glucose) and 8 h CM-ara (supplemented with arabinose), allows alternating "on" and "off" states of unconventional secretion. After each cycle, the relative extracellular activity of Gus-Cts1 was determined and cell densities were adjusted for the next cycle. The experiment was conducted over 5 consecutive days. Error bars depict standard deviation. The diagram represents results of four biological replicates. Fold change of induced cultures and *p*-values of Student's unpaired *t*-test are shown. Definition of statistical significance: *p*-value < 0.05.

### *3.4.3 Post-translational regulation of Don3 for unconventional protein export*

Diauxic switches of the carbon source are associated with severe changes in the metabolism of the cell (Chu & Barnes, 2016) and may thus also influence protein production. Therefore, we aimed to test an additional method based on chemical genetics to regulate unconventional secretion without causing a strong metabolic burden to the cell. It is well established that bulky ATP analogs in concert with mutagenized kinase versions can be used to inactivate protein kinases (Bishop et al., 1998). This has also been shown for Don3 using the ATP analogue NA-PP1 (1-(1,1-dimethylethyl)-3-(1-naphthalenyl)-1H-pyrazolo[3 ,4-d]pyrimidin-4-amine) in previous studies (Böhmer et al., 2008; Böhmer et al., 2009). Based on this, we tested, if post-translational regulation of Don3 activity could be used to regulate Cts1-mediated unconventional secretion. Thus, we adapted our regulated system and introduced a respective amino acid exchange in Don3 (M157A) which allows acceptance of the reversible inhibitor (Don3*; Figure 3.4A). When cells were grown under promoter “on” conditions in arabinose with the ATP analog, we observed cell aggregates, suggesting that inhibition of kinase activity was successful, while arabinose cultures lacking the analog grew normal (Figure 3.4B). Accordingly, Don3*-Gfp accumulated at the primary septum of cell aggregates in the presence of the ATP analog (Figure 3.4B), suggesting that the mutation disrupts kinase activity but does not impair biosynthesis and localization of the protein. By contrast, in cells grown without the analog, Don3*-Gfp fluorescence was observed at mother-cell boundaries of budding cells, resembling the natural situation (Figure 3.4B) (Aschenbroich et al., 2019). On the level of unconventional Cts1 secretion, we observed diminished extracellular Gus activity in the presence of the ATP analog and about a five-fold increase in activity in its absence for regulated Don3*-Gfp and seven-fold for regulated Don3* (Figure 3.4C). Western blot analyses confirmed that Don3*-Gfp was present in cell extracts independently from addition of NA-PP1 while free Gfp was only present in culture supernatants grown without the bulky analog. This suggests that Don3*-Gfp is unconventionally secreted only under these conditions (Figure 3.4D; Figure S3.5). These results confirm that post-translational regulation of Don3* is a second possibility to create a regulatory switch, providing the advantage of minimal invasiveness. Thus, we succeeded in establishing a tailor-made strategy to regulated unconventional secretion without drastic metabolic impact for the production host due to adaptation to new media. However, absolute induction levels were slightly lower than for transcriptional regulation (Figure S3.4).

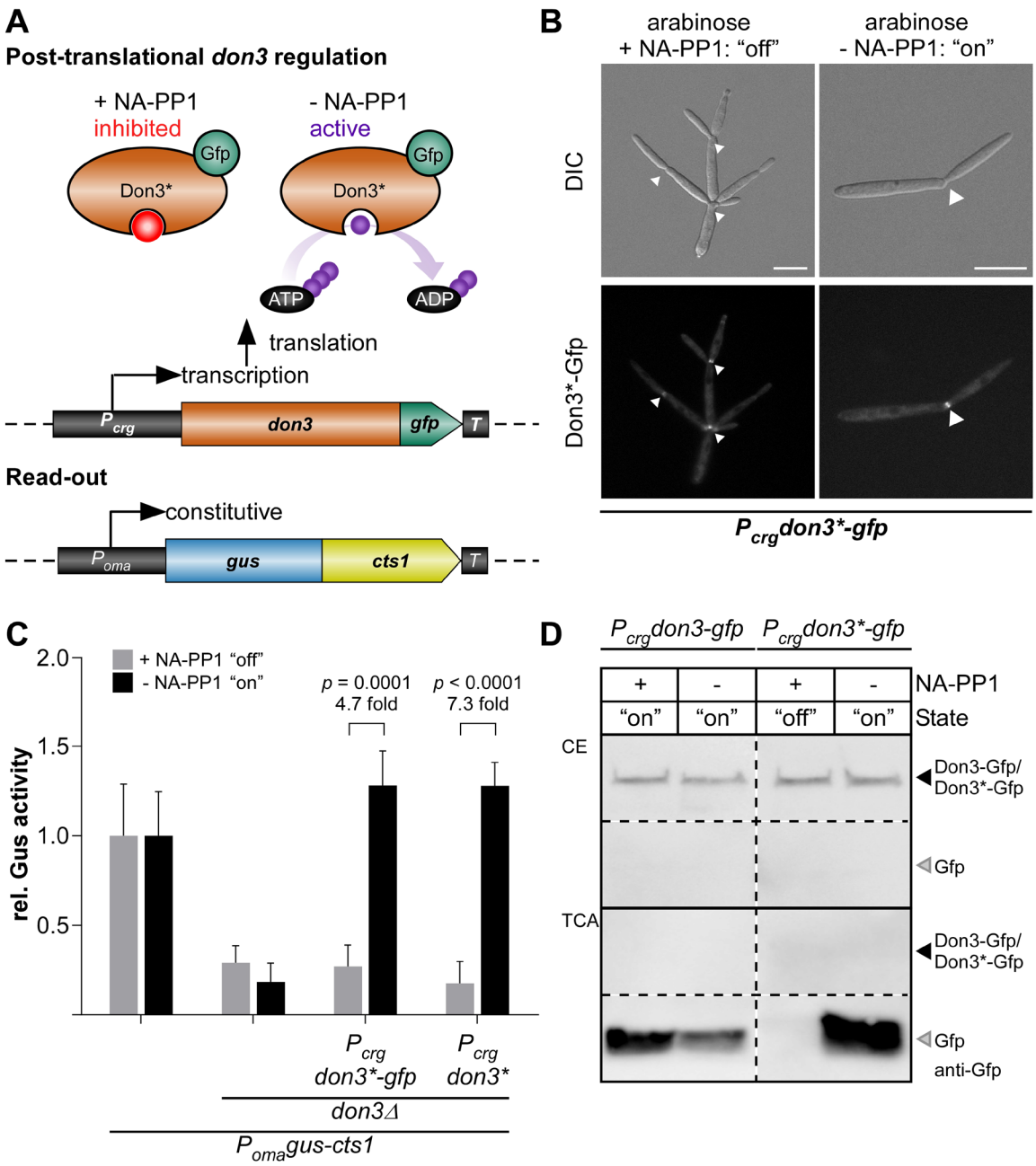


**Figure 3.4. Post-translational regulation of unconventional secretion via inactivation of Don3 kinase activity.** (**A**) Strategy for post-translational regulation of unconventional secretion using the mutagenized Don3 version Don3* in concert with a bulky ATP analog (NA-PP1). (**B**) Micrographs of yeast-like growing cells grown in medium containing arabinose. Cells treated with the bulky ATP analog NA-PP1 are indicated. Arrowheads depict the Gfp signal at the mother-daughter cell boundary. DIC, differential interference contrast. Scale bars, 10 µm. (**C**) Gus activity in culture supernatants of indicated AB33 $P_{oma}$Gus-Cts1 derivatives. Enzymatic activity was individually normalized to average values of positive controls secreting Gus-Cts1 constitutively, which were grown in arabinose-containing cultures. Values of positive controls in the two media do not differ significantly ($p$ = 0.7317; Fig S4). Strains containing regulated *don3** or *don3*-gfp* versions show a strong induction of extracellular Gus activity after growth in arabinose medium without NA-PP1. The diagram represents results of four biological replicates. Error bars depict standard deviation. Fold change of induced cultures and $p$-values of Student's unpaired $t$-test are shown. Definition of statistical significance: $p$-value < 0.05. (**D**) Western blots of cell extracts (CE, upper panel) and TCA precipitated culture supernatants of AB33don3Δ cultures expressing regulated Don3-Gfp and Don3*-Gfp. Primary antibodies against Gfp were used to detect the respective proteins (anti-Gfp). Both fusion proteins are degraded in the supernatant and only free Gfp can be detected. Free Gfp derived from Don3-Gfp was detected in the presence and absence

of NA-PP1. However, no free Gfp derived from Don3*-Gfp was detectable in the presence of NA-PP1, indicating inhibition of unconventional secretion. **Note:** Minor corrections were conducted in this version. In relation to the published Figure 3.4, in subsection D, state of *$P_{crg}$:don3*-gfp* is described as “on” in both cases here.

### *3.4.4 Time-resolved comparison of regulatory switches*

To further elucidate the effects of transcriptional and post-transcriptional Don3 regulation, we directly compared both regulatory methods in a time-resolved manner. Therefore, the strain expressing Don3* was grown in three different media overnight: i) arabinose for constitutive unconventional secretion, ii) glucose for transcriptional inhibition of unconventional secretion, and iii) arabinose and kinase inhibitor NA-PP1 for post-translational inhibition of unconventional secretion (Figure 3.5). Subsequently, cells were washed to remove media components including all previously exported Gus-Cts1 and resuspended in fresh medium containing only arabinose without NA-PP1 for constitutive induction of unconventional secretion. Gus activities were determined after induction at distinct time points for eight hours (Figure 3.5). Cultures pre-grown in glucose showed a high level of induction two hours after medium switch (light blue columns), suggesting that cell aggregates had resolved and accumulated Gus-Cts1 had been secreted at this time point. By contrast, cultures pre-grown with arabinose and the inhibitor for post-translational induction reached similar levels already one hour post-induction (dark blue columns). This is likely due to the fact, that inactive Don3* is produced and localized to the mother-cell boundary in these cells already during the pre-incubation overnight. After removal of the inhibitor, the protein can directly fulfill its function in secondary septum assembly, while after transcriptional inhibition, both the transcript and the resulting translation product first need to be synthesized. The quick response after release of post-translational inhibition is in accordance with earlier studies where kinase inhibition by NA-PP1 was used to address the function of Don3 during septation (Böhmer et al., 2008; Böhmer et al., 2009). By comparison, cultures grown overnight under constitutive induction in arabinose had no intracellular storage of Don3* due to its unconventional secretion during cell separation (Aschenbroich et al., 2019). These cultures thus showed only very weak extracellular Gus activities in the first few hours after induction (white columns). They reached a comparable level to the other cultures only after four hours. After 8 hours, all cultures exhibited extracellular Gus activities, which were not significantly different from each other anymore. The difference in immediate induction levels between the culture preincubated in arabinose lacking NA-PP1 and those preincubated in glucose or arabinose with NA-PP1 might be further boosted by the fact that the latter cells are present in aggregates prior to induction and all these start budding at the same time after induction. These data demonstrate that both regulated systems are advantageous compared to constitutive secretion when cell harvest is conducted within the first few hours after induction.

In summary, regulation was successfully achieved on two different levels, namely exploiting transcriptional and post-translational induction of the gene expression and gene product activity of septation factor Don3, respectively.

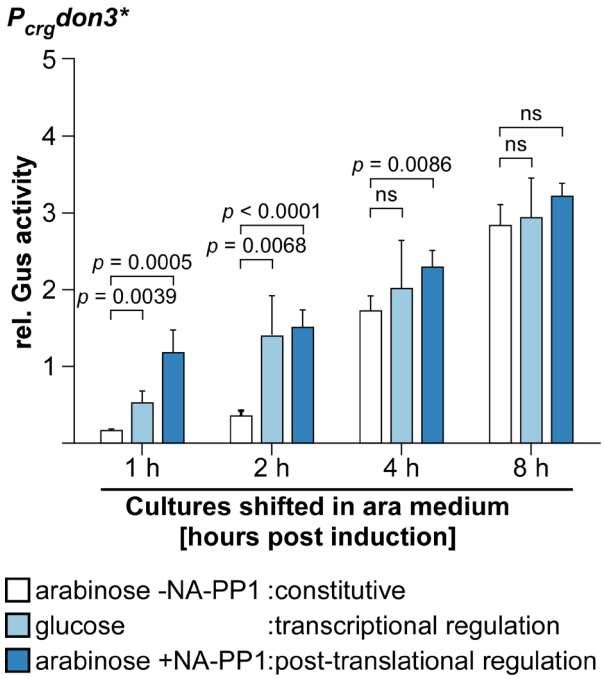


**Figure 3.5. Time-resolved comparison between transcriptional and translational Don3 regulation.** Cells of the Gus-Cts1 reporter strain containing the mutagenized kinase version Don3* (Figure 3.4A) were pre-incubated in medium supplemented with arabinose only (arabinose - NA-PP1, white columns), with glucose only (light blue columns) or with arabinose and the kinase inhibitor NA-PP1 (arabinose + NA-PP1, dark blue columns). After a washing step to remove media components, cells were resuspended in medium containing arabinose and Gus activity was determined for 8 h at distinct time points. Enzymatic activity was normalized to average values of induced overnight culture. The diagram represents results of four biological replicates. Error bars depict standard deviation. *p*-values of Student's unpaired *t*-test between previously normalized culture and induced culture are shown. Definition of statistical significance: *p*-value < 0.05.

## *3.4.5 Establishing an autoinduction process based on transcriptional regulation*

The previously established regulatory tools for Don3 depend on medium switches, which are not easily compatible with biotechnological processes, especially during upscaling in a bioreactor. Hence, we tested if autoinduction can be used to avoid the medium switch but keep the advantage of separated growth/protein synthesis and secretion phase. To establish such a process, we concentrated on transcriptional regulation as anf inexpensive tool. We assayed the activity of the $P_{crg}$ promoter in the presence of different concentrations of glucose and arabinose resembling "off" and "on" state of the system, respectively, using an AB33don3Δ derivative expressing *gfp* under control of the arabinose inducible $P_{crg}$ promoter as a transcriptional reporter (AB33don3Δ/$P_{crg}$gfp). The resulting Gfp protein accumulates in the cytoplasm and can easily be detected by its fluorescence. The strain was cultivated in a

BioLector device with online monitoring of Gfp fluorescence and scattered light as a read-out for fungal biomass in minimal volumes (Figures 3.6 and S3.6A,B) (Funke et al., 2010). Initially, either 1% glucose (56 mM) or 1% arabinose (67 mM) or the two sugars in different ratios were used (0.25:0.75%/0.5:0.5%/0.75:0.25%, adding up to 1% each; Figure S3.6A,B). The Gfp read-out indicated a steadily rising Gfp signal for cultures growing in arabinose as the sole carbon source, while cultures growing in glucose showed only weak background fluorescence. In the presence of different ratios of mixed glucose and arabinose, cultures consumed the preferred carbon-source glucose first and switched to arabinose later, presumably, when the respective amount of glucose was completely metabolized. In general, during cultivation in glucose and arabinose, Gfp fluorescence remained very low during consumption of glucose, followed by an increasing Gfp fluorescence after switching to arabinose (Figure S3.6A,B). The prolonged phase with low fluorescence at a time when biomass is already constantly increasing is a prerequisite for successful autoinduction and indicated that the strategy is successful.

Next, to identify the optimal composition for an autoinduction medium, which is characterized by a prolonged growth phase with minor promoter activity in the beginning and a high plateau of Gfp fluorescence after induction (i.e., after consumption of glucose), we varied the total sugar amounts and the ratios of glucose and arabinose in the medium (Figure 3.6A, B). Again, cultures containing only 1% arabinose or glucose were used as controls (light gray dots, light green lines). For two other cultures, initial biomass formation was initiated with 1% glucose, while induction of the $P_{crg}$ promoter and thus *gfp* expression after glucose consumption was stimulated by either 1% or 2% arabinose. Compared to the arabinose control, these cultures showed a delayed accumulation of Gfp fluorescence indicating successful uncoupling of growth and protein production. The total Gfp fluorescence was more than two-fold higher with elevated total sugar concentrations, which is in line with a higher total biomass (Figure 3.6A,B). However, interestingly, higher initial glucose concentrations of two or three percent did not result in higher biomass formation or Gfp yield (Figure S3.6C,D). A possible explanation is that other factors besides the carbon source in the medium become limiting. The increase of arabinose from 1% to 2% did yield higher biomass but no further increase in Gfp fluorescence (Figure 3.6A,B). Therefore, medium containing 1% glucose and 1% arabinose was selected for further autoinduction experiments (see below). In summary, we established a simple autoinduction protocol that can be applied in a broad variety of biotechnological processes without the need for medium switches.

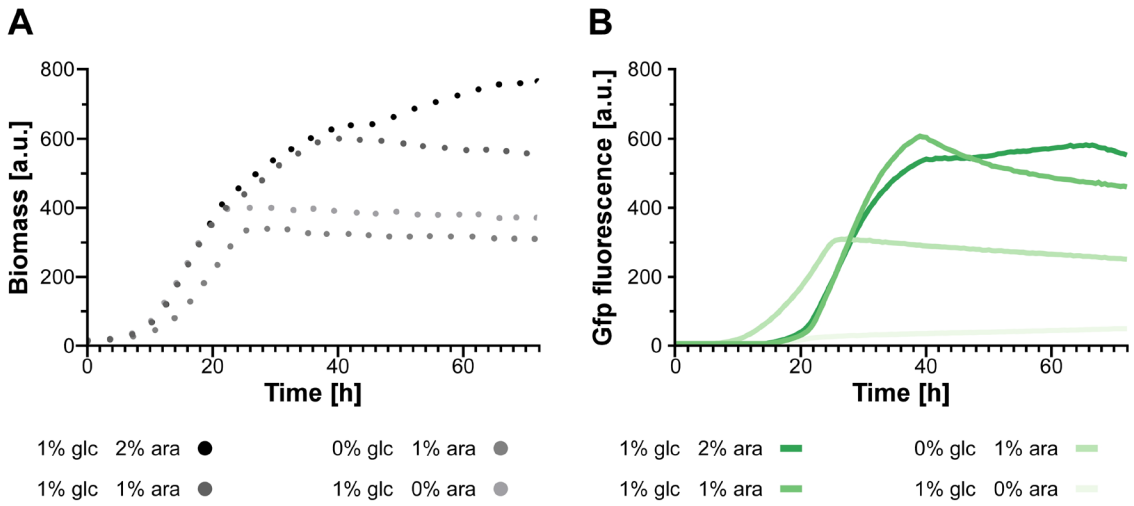


**Figure 3.6. Establishing an autoinduction process based on transcriptional regulation.** (**A**,**B**) Reporter strain AB33don3Δ/$P_{crg}$gfp was cultivated in buffered CM medium supplemented with glucose (glc) and arabinose (ara) in different amounts and ratios as indicated in the diagram. Since in contrast to the experiments before the cultures were incubated for a prolonged time reaching high optical densities, the medium was buffered with 100 mM MES to prevent a drastic pH drop (Terfrüchte et al., 2018). The two parameters fungal biomass (**A**) and Gfp fluorescence (**B**) were recorded online in a BioLector device. Gains: 20 (scattered light); 80 (Gfp).

## *3.4.6 Applying autoinduction for the export of functional nanobodies*

Finally, we applied autoinduction via transcriptional *don3* regulation for the unconventional secretion of heterologous proteins using a nanobody as an example for an established pharmaceutical target protein (Muyldermans, 2013). Therefore, we generated a strain in which a fusion of an anti-Gfp nanobody (Rothbauer et al., 2008) with Cts1 (NB-Cts1) as carrier was expressed by the previously established strategy (AB33don3Δ/$P_{crg}$don3/NB-Cts1; Figure 3.7A). Unconventional secretion of the functional nanobody using Cts1 as a carrier had been established in an earlier study (Terfrüchte et al., 2017). Western blot analysis verified the production and secretion of the fusion protein in arabinose medium (Figure S3.7A,B). Next, we cultivated the strain in buffered autoinduction medium using the most efficient composition (1% glucose, 1% arabinose) in shake flasks and followed synthesis of functional NB-Cts1 fusion protein along the cultivation by BioLector online monitoring (Figure 3.7B) in concert with enzyme-linked immunosorbent assays (ELISA) using the cognate antigen Gfp (Figures 3.7C,D and S7C,D). Gfp binding activity was barely detectable after 8 h of incubation in autoinduction medium in purified culture supernatants (Figure 3.7C) but clearly in cell extracts (Figure 3.7D). After 15 h, ELISA values were strongly enhanced for NB-Cts1 purified from culture supernatants (Figure 3.7B). This corresponded to the time when glucose was presumably depleted from the medium. These results are consistent with the parallel evaluation of an identical culture in the BioLector device. Here, the diauxic switch caused clear adaptations in pH and Dissolved Oxygen Tension (DOT) after approximately 15 h of cultivation

(Figure 3.7B). Thus, an efficient autoinduction process was established on the basis of transcriptional *don3* regulation, allowing for the production of functional heterologous proteins by unconventional secretion. In essence, we successfully applied regulated unconventional secretion for the export of nanobodies.

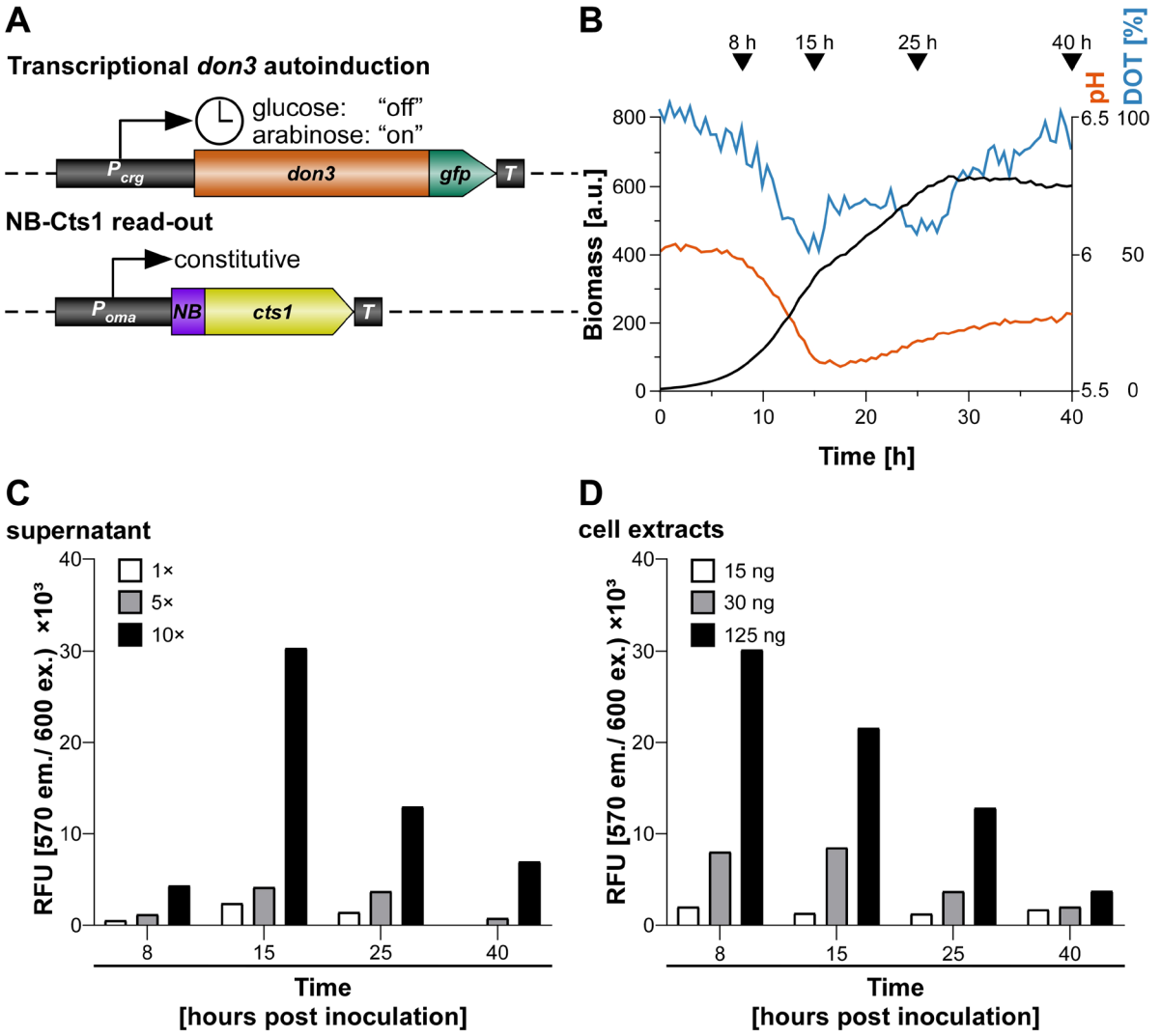


**Figure 3.7. Evaluation of the autoinduction process for unconventional secretion of an anti-Gfp nanobody.** Strain AB33don3Δ/$P_{crg}$don3/NB-Cts1 was inoculated in CM medium supplemented with 1% glucose, 1% arabinose, and buffered with 0.1 M MES. The culture was split into 5 individual flasks for harvest of supernatant proteins, cell extracts and parallel online growth monitoring in BioLector and offline monitoring via photometer. Supernatant was collected at defined time points and unconventionally secreted NB-Cts1 was IMAC purified. Cell extracts were prepared in parallel. For purified supernatant and cell extracts ELISA were performed using purified Gfp as antigen. (**A**) Schematic representation of the genetic setup for transcriptional *don3-gfp* regulation of unconventional secretion in autoinduction medium by activating transcription through arabinose after the consumption of glucose (diauxic switch indicated by clock symbol). NB-Cts1 is constitutively produced but trapped in the cell prior to Don3 synthesis. (**B**) Online monitoring of the cultivation using the BioLector device. Primary ordinate axis shows biomass via backscatter light (gain 20), secondary ordinate axis shows pH, red, and dissolved oxygen tension (DOT), blue. Time points of sampling of parallel grown shake flask cultures are indicated by arrowheads. (**C**) Enzyme-linked immunosorbent assay (ELISA) using NB-Cts1 purified from culture supernatants at indicated time points. 1×, 5× and 10× concentrated purified supernatants, (**D**) ELISA using cell extracts harvested at defined protein amounts containing 15 ng, 30 ng, and 125 ng total protein.

## 3.5 Discussion

In this study, we build on our mechanistic knowledge on Cts1 export to establish the first regulatory systems to control the unconventional secretion of heterologous proteins in *U. maydis*. Systems for regulated or inducible protein production are widespread within the different expression systems. They enable a strict temporal control of the protein production process because growth and protein synthesis can be largely separated (Weinhandl et al., 2014). Although regulated systems are well established for protein production, they are usually based on the direct transcriptional regulation of the promoter of the gene-of-interest (Kluge et al., 2018). Here, we went one step beyond and regulated the mechanism of secretion rather than the gene-of-interest itself. While a deep knowledge of the conventional secretion pathway in eukaryotes exists (Feyder et al., 2015), we are not aware of any regulatory system based on these mechanistic insights that are currently applied for heterologous protein production, at least in fungal systems.

Regulation based on septation factor kinase Don3 was successfully achieved on two different levels, namely exploiting transcriptional and post-translational inhibition of the gene expression and gene product activity, respectively. Don3 is essential for secondary septum formation (Weinzierl et al., 2002) and thus acts as a kind of gate keeper for lock-type unconventional secretion (Aschenbroich et al., 2019; Reindl et al., 2019; Reindl et al., 2020). When Don3 is not present or inactive, the product destined for Cts1-mediated secretion is formed along with the cell growth but trapped within the cell where it is protected from frequently occurring extracellular proteases (Sarkari, 2014; Terfrüchte et al., 2018). Both regulatory levels are powerful tools for biotechnological application: while transcriptional control is inexpensive and useful for cheap products, post-translational control is more expensive due to the need of inhibitor but comes with a faster release of the protein avoiding long exposure of the product to proteases. Thus, the latter method is appropriate for high prize products such as pharmaceutical proteins exemplified by antibody formats such as nanobodies (Ecker et al., 2015). Furthermore, proteins that are prone to proteolytic degradation might benefit from the fast release by post-translational induction.

By contrast, only a weak induction was achieved using transcriptional *jps1* regulation. Controlling Jps1 expression would be very attractive because its absence is not connected to morphological changes as observed for Don3 (Reindl et al., 2020). In the future, the use of alternative inducible promoters might lead to a significant improvement of the system by reducing the background activity during “off” conditions. For example, an orthogonal system such as tetracycline-regulated gene expression could be used (Berens & Hillen, 2003). It avoids metabolic effects that might arise with nutrient-dependent promoters and allows for titration of the expression strength. The system has already been applied in fungi including *U.*

*maydis* (Meyer et al., 2011; Zarnack et al., 2006) but needs careful adaptation to the respective application.

Using the example of transcriptional *don3* control in combination with an autoinduction protocol resulted in a first bioprocess. Optimization of yield and simplification of the experimental procedures by reduction of user intervention after culture inoculation are major advantages associated with autoinduction processes applied in industrial biotechnology. While lactose-derived autoinduction is applied in *E. coli* for the T7lac promoter system for years (Fox & Blommel, 2009; Studier, 2005), glycerol/methanol-based autoinduction of the *AOX1* promoter was recently also described for *P. pastoris* as a fungal model organism (Lee et al., 2017). Here, we add a protocol for autoinduction of unconventional secretion to the list.

In the future, we might further adopt our system and establish sophisticated optogenetic regulation (Hughes, 2018; Zhang & Cui, 2015). Light-dependent transcriptional regulation can for example be achieved using phytochromes (Levskaya et al., 2009; Shimizu-Sato et al., 2002). One elegant example for regulation of protein stability is the use of photosensitive degrons derived from plant proteins, which are already successfully applied in *S. cerevisiae* (Jungbluth et al., 2010; Renicke et al., 2013). The advantage of such systems is that they are non-invasive and allow for a precise temporal control of the induction process (Hughes, 2018; Zhang & Cui, 2015). In summary, we here substantially improved the method portfolio for our unconventional protein secretion system and went a further step ahead towards a novel fungal expression platform.

***Keywords***
autoinduction; chemical genetics; cytokinesis; inducible promoter; nanobody; regulated secretion; unconventional secretion; *Ustilago maydis*

***Author Contributions***
**K.H.** and M.P. designed and performed the experiments. K.S. and M.F. directed the study. **K.H**., M.P. and K.M. evaluated and visualized the data. K.S. wrote the manuscript with assistance of K.M. and input of all co-authors. All authors have read and agreed to the published version of the manuscript.

***Funding***
This project is funded by the CLIB-Competence Center Biotechnology (CKB) funded by the European Regional Development Fund ERDF (34.EFRE-0300096).

***Acknowledgments***
We are thankful to B. Axler for excellent technical support of the project. We gratefully acknowledge support in microscopic analyses by S. Wolf and advice on data evaluation by N. Heßler and L. Geißl. Dr. M Terfrüchte provided recombinant purified Gfp for ELISA assays and Dr. M. Reindl generated a control strain for Jps1 localization studies.

***Abbreviations***
Gfp, green fluorescent protein; Gus, β-glucuronidase; IMAC, immobilized metal ion affinity chromatography; MES, 2-(*N*-morpholino)ethanesulfonic acid; MUG, 4-methylumbelliferyl-β-d-glucuronide; NA-PP1, 1-(1,1-dimethylethyl)-3-(1-naphthalenyl)-1H-pyrazolo[3,4-d]pyrimidin-4-amine.

## 3.6 Supplementary data

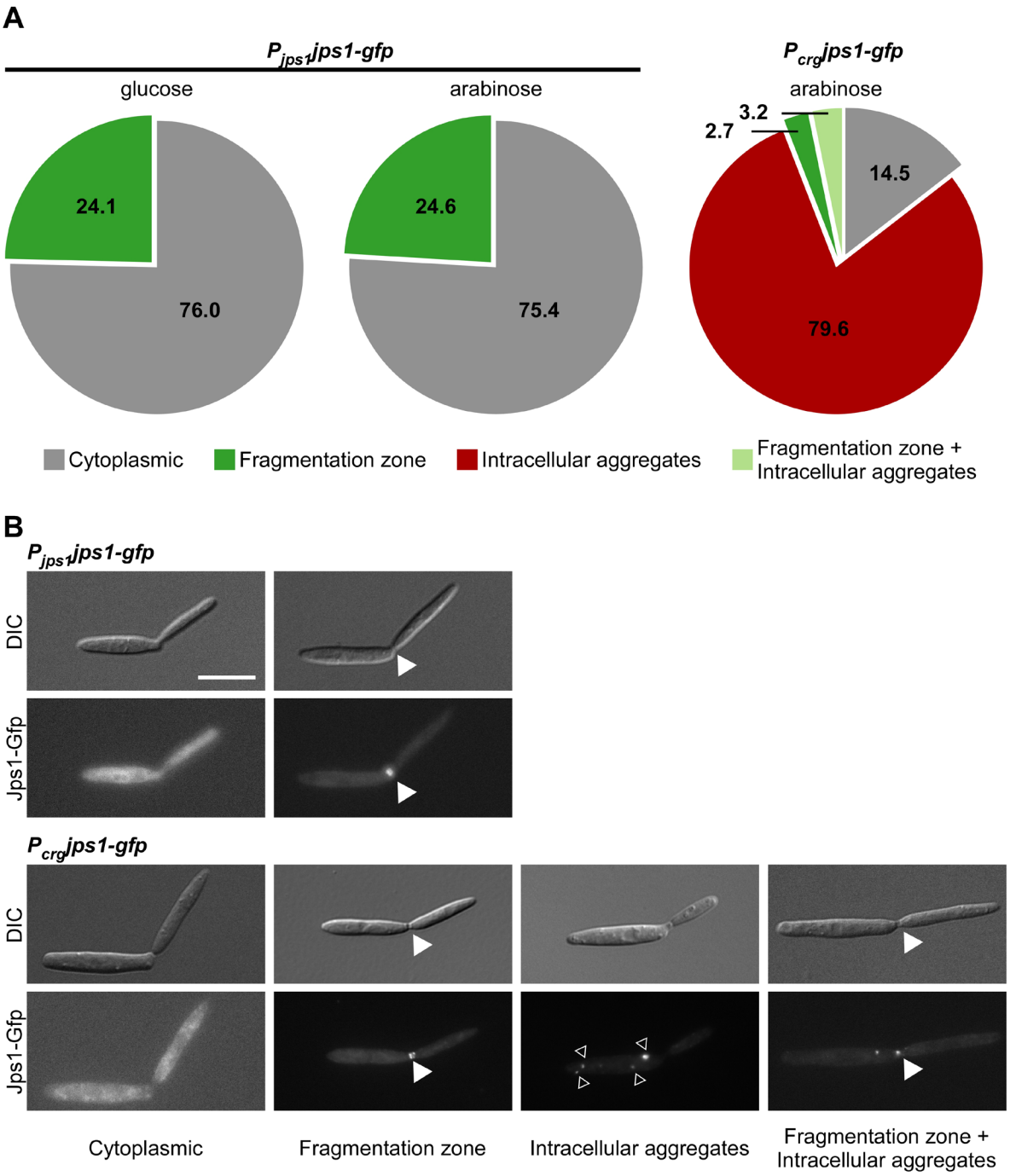


**Figure S3.1. Influence of transcriptional regulation by an arabinose-inducible promoter on Jps1-Gfp localization.** Localization of Jps1-Gfp in the control strain AB33jps1Δ/P$_{jps1}$jps1-gfp (*P$_{jps1}$jps1-gfp*) in which *jps1-gfp* expression is controlled by the native promoter P$_{jps1}$, and the regulable strain AB33jps1Δ/P$_{crg}$jps1-eGfp/Gus-Cts1 in which *jps1-gfp* expression is regulated by arabinose inducible promoter P$_{crg}$. The control strain was grown in both glucose and arabinose to exclude medium effects. The regulable strain was only grown in arabinose for induction of *jps1-gfp* expression. Yeast-like growing cells in all stages of cytokinesis were analyzed. (**A**) Pie charts depict ratios of the different observed localization patterns of Gfp fluorescence: cytoplasmic, fragmentation zone intracellular aggregates, and fragmentation zone + intracellular aggregates. The experiment was conducted in one biological replicate with a total of n=186 cells analyzed (*P$_{crg}$jps1-gfp*, control strains: 130 cells; *P$_{jps1}$:jps1-gfp* after growth in glucose; 79 cells *P$_{jps1}$jps1-gfp* after growth in arabinose). Percentage of cells in

different categories is shown in pie charts. (**B**) Micrographs depicting cells of both strains grown in CM-arabinose. White arrowheads indicate the expected localization of Jps1-Gfp in the fragmentation zone (Reindl et al., 2020), open white arrowheads depict intracellular aggregates. DIC, differential interference contrast; Jps1-Gfp, Gfp signal. Scale bar, 10 µm.

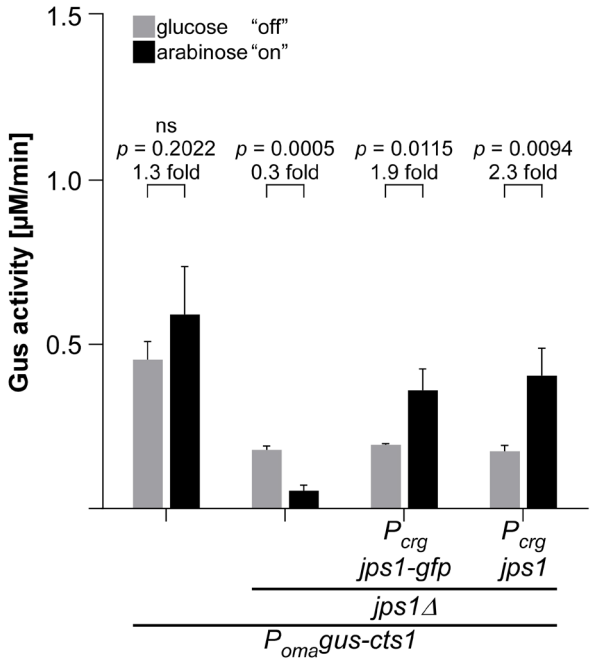


**Figure S3.2. Comparative absolute Gus activity for the assay depicted in Figure 3.2C.** Enzyme activity is shown in µM/min, for Figure 3.2C, average values of control strain AB33 Gus-Cts1 (*P*$_{oma}$*gus-cts1*) were set to 1 and used as reference for other values. No significant difference for the reference strain grown in glucose or arabinose medium was detectable ($p$ = 0.2022). The diagram represents results of three biological replicates. Error bars depict standard deviation. Fold change of cultures and $p$-values of Student's unpaired $t$-test are shown. Definition of statistical significance: $p$-value < 0.05.

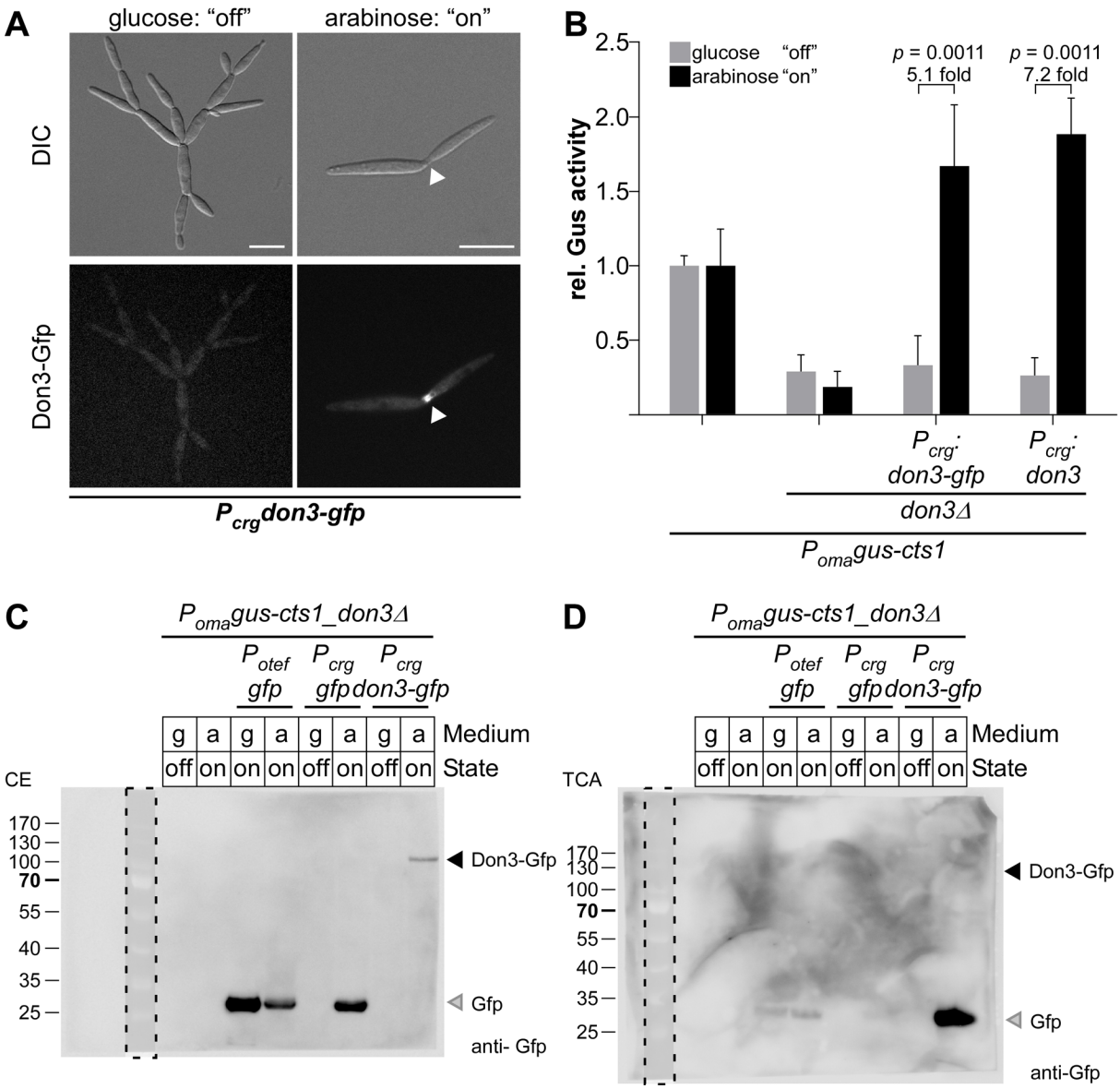


**Figure S3.3**. **Additional data on transcriptional regulation of unconventional secretion via kinase Don3.** (**A**) Micrographs of yeast-like growing cells in the “on” and “off” stage mediated by glucose and arabinose in the medium, respectively. Arrowheads depict the Gfp signal at the mother-daughter cell boundary. DIC, differential interference contrast. Scale bars, 10 µm. (**B**) Gus activity in culture supernatants of indicated AB33 Gus-Cts1 derivatives. Enzymatic activity was individually normalized to average values of positive controls secreting Gus-Cts1 constitutively, which were grown in glucose and arabinose containing cultures. Values of positive controls in the two media do not differ significantly ($p$ = 0.4820; Figure S3.4). Strains containing regulated *don3* or *don3-gfp* versions show a strong induction of extracellular Gus activity after growth in arabinose containing medium. Error bars depict standard deviation. The diagram represents results of four biological replicates. Fold change of induced cultures and $p$-values of Student’s unpaired $t$-test are shown. Definition of statistical significance: $p$-value < 0.05. Complete Western blots of selected signals shown in Figure 3.3D. (**C**) Cell extracts (CE) and (**D**) TCA precipitated supernatants (TCA) of AB33don3Δ/Gus-Cts1 derivatives are shown. Cells were cultivated either in glucose (g) or in arabinose (a) containing medium, resulting in “off” or “on” state of unconventional secretion, respectively. Primary antibodies against Gfp were used to detect the respective proteins (anti-Gfp). Selected strains either express no *gfp* (negative control), *gfp* under the control of a constitutive promoter as positive control ($P_{otef}$*gfp*), *gfp* under the control of an inducible promoter ($P_{crg}$*gfp*), or *don3-gfp* under the control of the inducible *crg* promoter ($P_{crg}$*don3-gfp*), from left to right, respectively. Black arrowhead indicates Don3-Gfp signal (predicted size: 118 kDa), gray arrowheads depict the Gfp signal (predicted size: 27 kDa). Dashed area indicates digitization of protein marker with 70% opacity. **Note:** Minor corrections were conducted in this version. In relation to the published Figure S3.3, $P_{otef}$*:gfp* state is now described as “on” in both media.

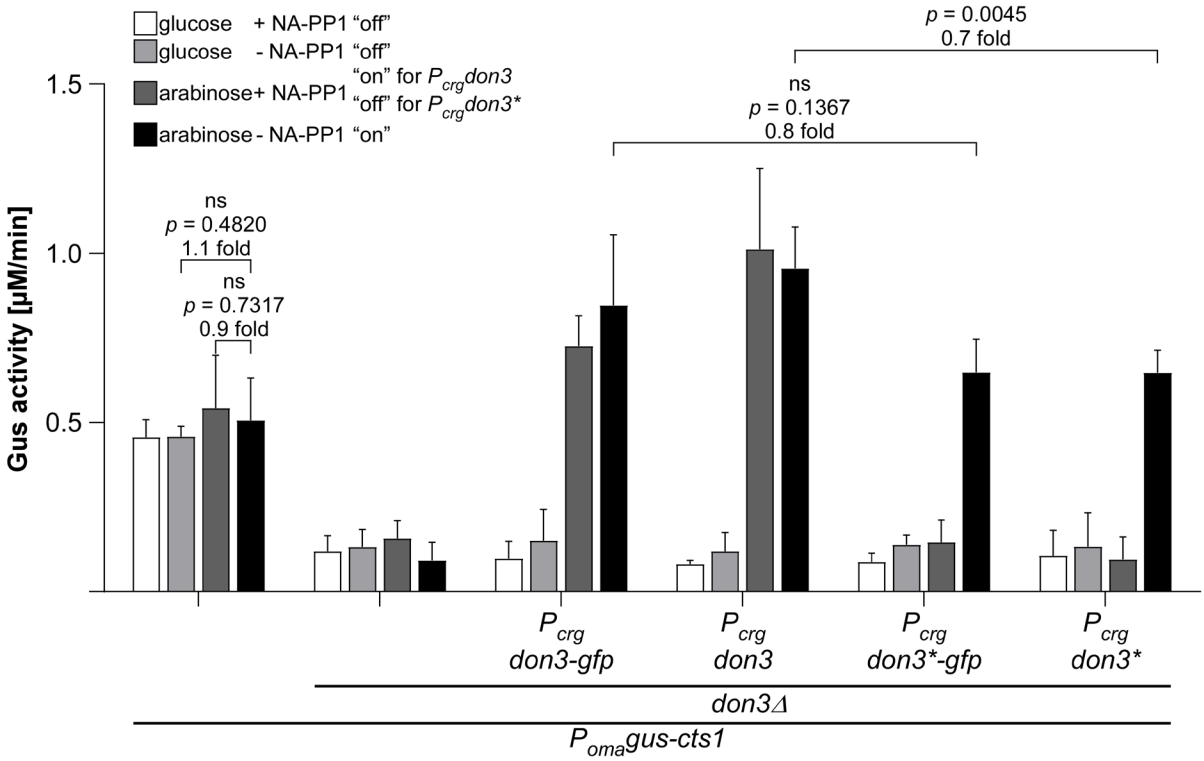


**Figure S3.4. Comparative absolute Gus activity for the assays depicted in Figs. S3B and 4C.** Extracellular Gus activity of all inducible Don3 strains and controls was determined in all four different media. Enzyme activity is shown in µM/min, for Figure 3.3C and 3.4C, average values of control strain AB33 Gus-Cts1 (*$P_{oma}$gus-cts1*) in respective media were set to 1 and used as reference for other values. No significant difference for reference strain grown in glucose or arabinose medium was detectable (P=0.4820, 0.7313). A 0.8-fold, yet not significant change was detected for AB33don3Δ/$P_{crg}$don3-gfp/Gus-Cts1 (*$P_{crg}$don3-gfp*) compared to AB33don3Δ/$P_{crg}$don3*-gfp/Gus-Cts1 (*$P_{crg}$don3*-gfp*), while a significant 0.7 fold change is detectable for AB33don3Δ/$P_{crg}$don3/Gus-Cts1 (*$P_{crg}$don3*) compared to AB33don3Δ/$P_{crg}$don3*/Gus-Cts1 (*$P_{crg}$don3**), suggesting a slightly reduced activity of the post-translational regulated system in comparison to the transcriptional regulated system. The diagram represents results of four biological replicates. Error bars depict standard deviation. Fold change of cultures and *p*-values of Student's unpaired *t*-test are shown. Definition of statistical significance: *p*-value < 0.05.

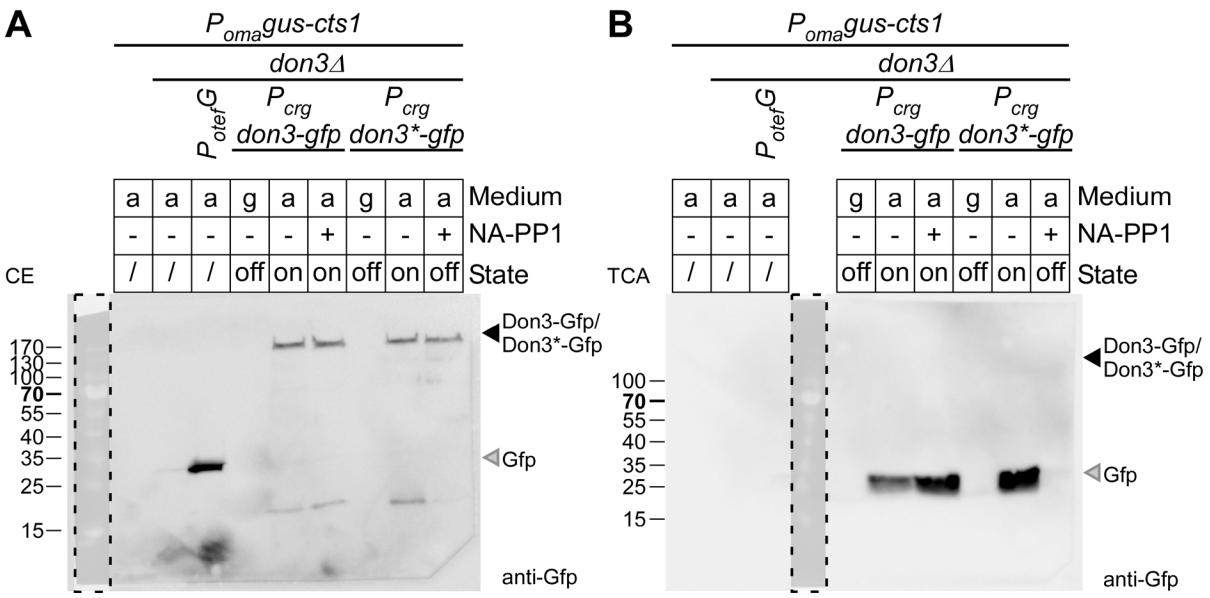


**Figure S3.5. Complete Western blots of selected signals shown in Figure 3.4D.** (**A**) Cell extracts (CE) and (**B**) TCA precipitated supernatants (TCA) of AB33 Gus-Cts1 derivatives are shown. Cells were cultivated in medium containing either glucose (g) or arabinose (a), with (+) or without (-) ATP-analog NA-PP1, resulting in either “on” or “off” state of unconventional secretion. Primary antibodies against Gfp were used to detect the respective proteins (anti-Gfp). Control strains were only cultivated in arabinose medium without NA-PP1 and express either no *gfp* (*$P_{oma}$gus-cts1* and *$P_{oma}$gus-cts1/don3Δ*) or *gfp* constitutively (*$P_{otef}$gfp*). Inducible secretion strains, expressing either *don3-gfp* or *don3*-gfp* cultivated in all three different media are shown on the right. Black arrowheads indicate Don3-Gfp signal (predicted size: 118 kDa), gray arrowheads indicate Gfp signal (predicted size: 27 kDa). Proteins run slightly higher than expected. This phenomenon was observed before (Stock et al., 2012). Dashed area indicates digitization of protein marker with 70% opacity.

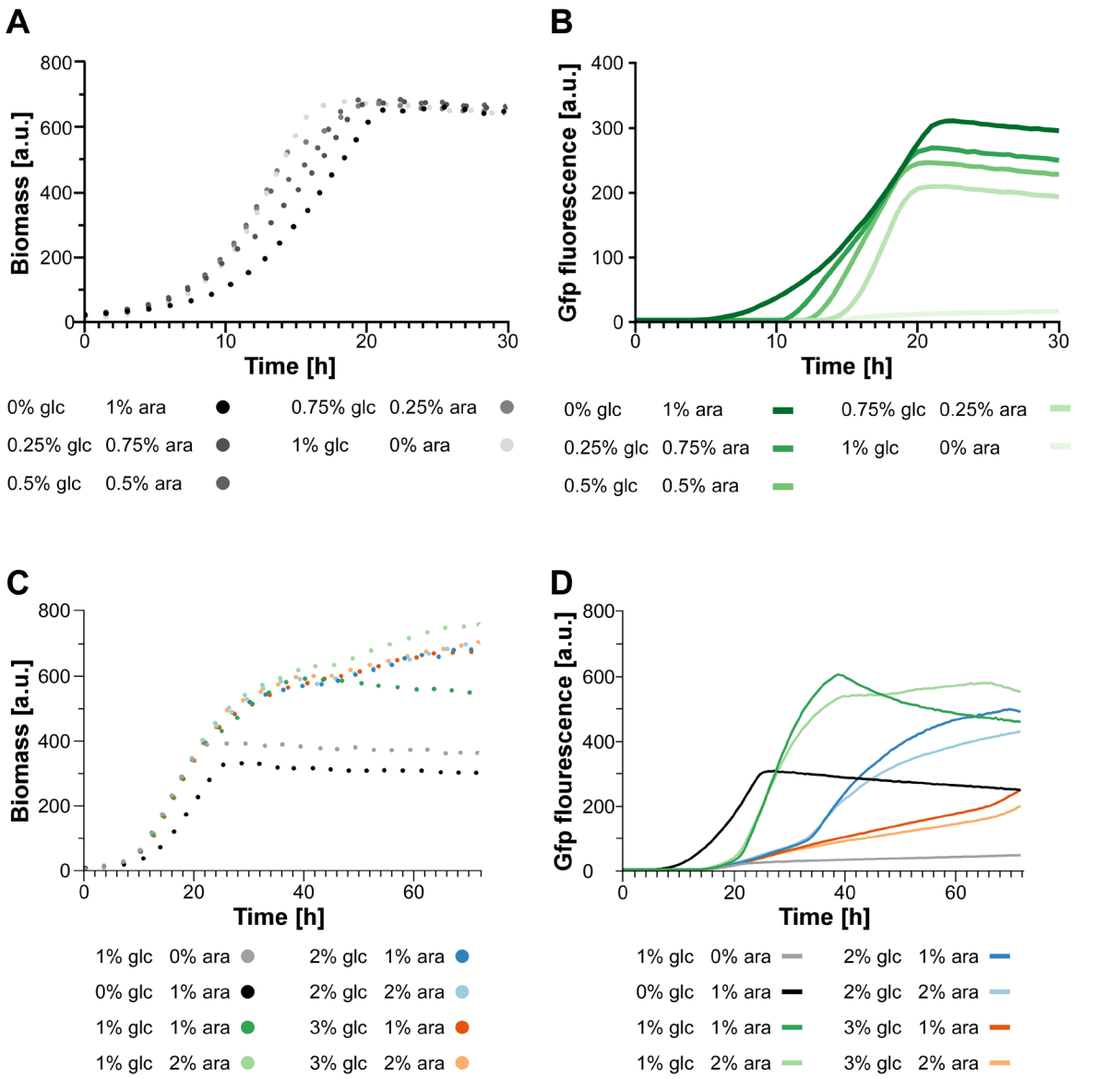


**Figure S3.6. Additional data on establishment of an autoinduction process based on transcriptional regulation via carbon source switch.** Strain AB33don3Δ/$P_{crg}$Gfp/Gus-Cts1 was used as a reporter for $P_{crg}$ activity in buffered CM medium supplemented with different compositions of glucose and arabinose as carbon source. The two parameters fungal biomass and Gfp fluorescence were recorded online in a BioLector device. (**A**,**B**) $P_{crg}$ activity in buffered CM medium supplemented with 1% total sugar in the indicated combinations. (A) Dotted lines represent fungal biomass, gain 25, (**B**) solid lines, Gfp fluorescence, gain 80. (**C**,**D**) Different glucose concentrations (1–3%) for initial growth were followed by either 1% or 2% arabinose for induction of unconventional secretion. (**C**) Dotted lines represent fungal biomass, gain 20, (**D**) solid lines, Gfp fluorescence, gain 80. (glc, glucose; ara, arabinose).

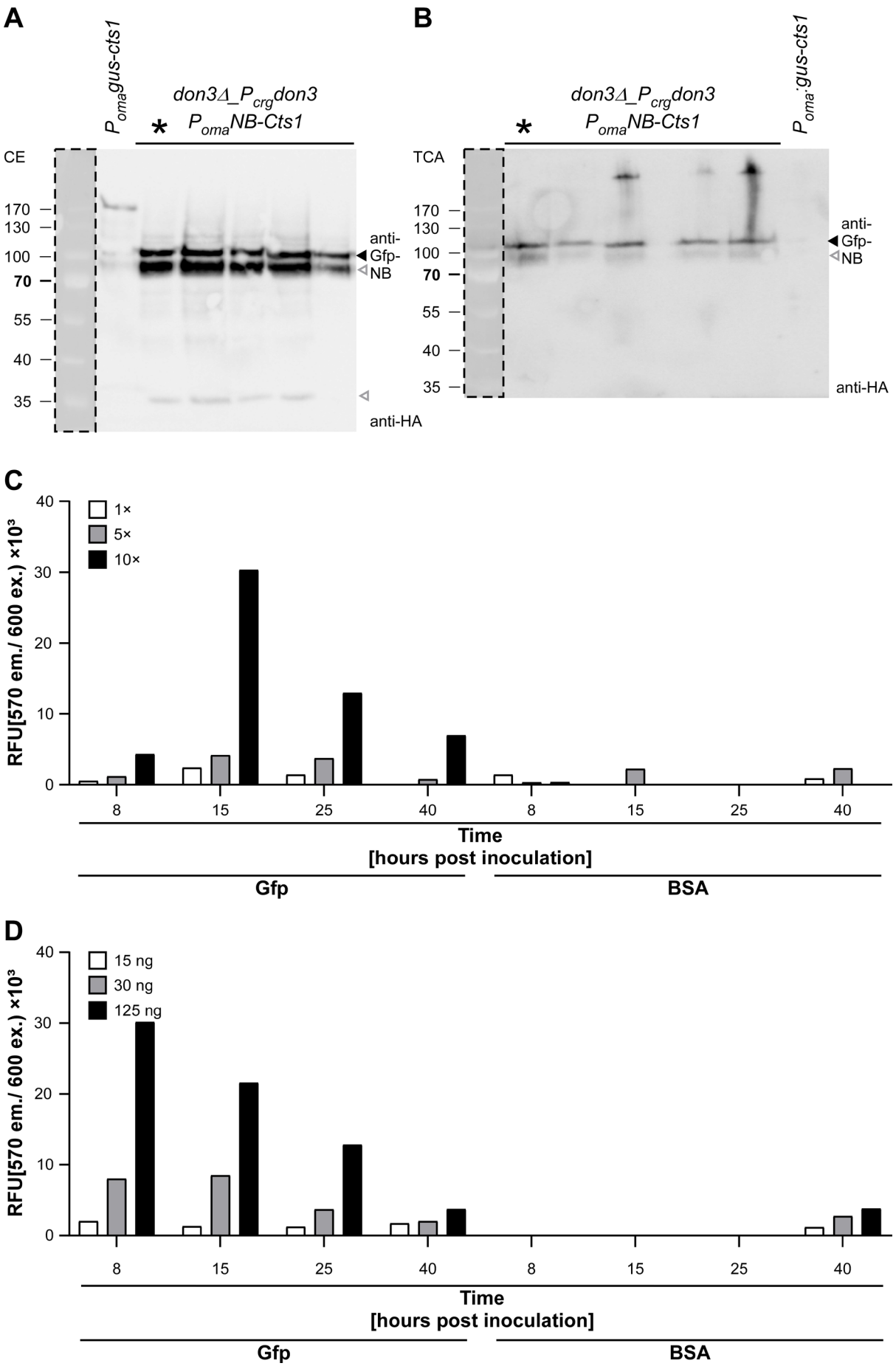
A
$P_{oma}$gus-cts1
don3Δ_$P_{crg}$don3
$P_{oma}$NB-Cts1
*
CE
170
130
100
70
55
40
35
anti-
Gfp-
NB
anti-HA
B
don3Δ_$P_{crg}$don3
$P_{oma}$NB-Cts1
$P_{oma}$:gus-cts1
*
TCA
170
130
100
70
55
40
35
anti-
Gfp-
NB
anti-HA
C
RFU[570 em./ 600 ex.) ×10³
1×
5×
10×
0
10
20
30
40
8
15
25
40
8
15
25
40
Time
[hours post inoculation]
Gfp
BSA
D
RFU[570 em./ 600 ex.) ×10³
15 ng
30 ng
125 ng
0
10
20
30
40
8
15
25
40
8
15
25
40
Time
[hours post inoculation]
Gfp
BSA

**Figure S3.7. Additional data on unconventional secretion of anti-Gfp nanobodies.** (**A**,**B**) Western blot analysis of different anti-Gfp nanobody secreting strains. (**A**) Cell extracts (CE) and (**B**) TCA precipitated supernatants (TCA) of AB33don3Δ/$P_{crg}$don3/NB-Cts1 candidates are shown. Cells were cultivated in medium containing arabinose. Primary antibodies against HA were used to detect the respective proteins (anti-HA). Black arrowheads indicate NB-Cts1 signal (predicted size: 75 kDa), open gray arrowheads indicate known degradation products (Terfrüchte et al., 2017). AB33 Gus-Cts1 was used as a positive control. Proteins run slightly higher than expected. This phenomenon was observed before (Stock et al., 2012). Dashed area indicates digitization of protein marker with 70% opacity. Asterisks indicate selected candidate for further experiments. (**C**,**D**) Complete result of ELISA experiment which is shown in Figure 3.7C and D. Evaluation of autoinduction process using anti-Gfp nanobody fused to Cts1 (NB-Cts1) as read-out. Strain AB33don3Δ/$P_{crg}$don3/NB-Cts1 was cultivated in CM medium supplemented with 1% glucose and 1% arabinose, buffered with 0.1 M MES. The inoculated culture was split into 5 individual flasks for harvest of cell extracts, supernatant and online growth monitoring in a BioLector. Supernatant and cell pellets were collected at defined time points, unconventionally secreted NB-Cts1 was IMAC purified from supernatant and cell extracts were prepared. For purified supernatant and cell extracts ELISA was performed using purified Gfp as antigen and bovine serum albumin (BSA) as a negative control to monitor unspecific retention of NB-Cts1 in wells. (**A**) ELISA of purified supernatants. 1×, 5× and 10× concentrated purified supernatants. (**B**) ELISA of cell extracts containing defined protein amounts of 15 ng, 30 ng and 125 ng whole cell extract.

# 4 Outlook and further perspectives for inducible secretion in *Ustilago maydis*

Secretion of heterologous proteins to the supernatant is favorable in biotechnology since proteins are protected from intracellular proteases and downstream processing is simplified (Flaschel & Friehs, 1993; Heel et al., 2013; Nicaud et al., 1986). However, especially in fungal expression platforms, the presence of extracellular proteases imposes a problem in the production of secretory proteins (Idiris et al., 2010). Inducible systems are promising tools towards rapid and transient release of heterologous proteins for reduced exposure to these proteases. In the framework of protein secretion, such an inducible system has already been described in *E. coli* for a type III system. Here regulation of the operon, coding for proteins formatting the type III secretion flagellar hook basal body, was used for secretion of FlgM. Upon induction of the system, the flagellar hook basal body is assembled and leads to secretion of FlgM. Exploitation of FlgM as a secretion moiety for fusion peptides allows secretion via this mechanism (Heel et al., 2013). In eukaryotic cells, regulation of conventional secretion was achieved through controlled aggregation in the endoplasmic reticulum (ER). Exploitation of a conditional aggregation domain, fused to the protein of interest, results in aggregation of the fusion protein, accumulating in the ER. Secretion is stimulated by addition of a ligand that induces protein disaggregation and cleavage of aggregation domain. Subsequently the free protein is secreted. (Rivera et al., 2000). Importantly, this aggregation-based system was applied *in vivo* and *in vitro* and it is commercialized as iDimerize by Takara (Takara Bio Inc., Kusatsu, Jpn).

In this study, the first successful controlling strategies of unconventional secretion through transcriptional and post-translational inhibition were successfully established in *U. maydis*. Knowledge of unconventional export of Cts1 allows exploitation of the septation factor kinase Don3 on two levels (Figure 4.1). Transcriptional regulation of *don3* as well as post-translational regulation of an alternative Don3 version were applied for complementation of the *don3* deletion phenotype and therefore unconventional secretion of Cts1. While post-translational regulation is favorable for products requiring a fast isolation and processing from culture's supernatant, transcriptional regulation offers versatile application possibilities in batch and fed-batch fermentation including autoinduction.

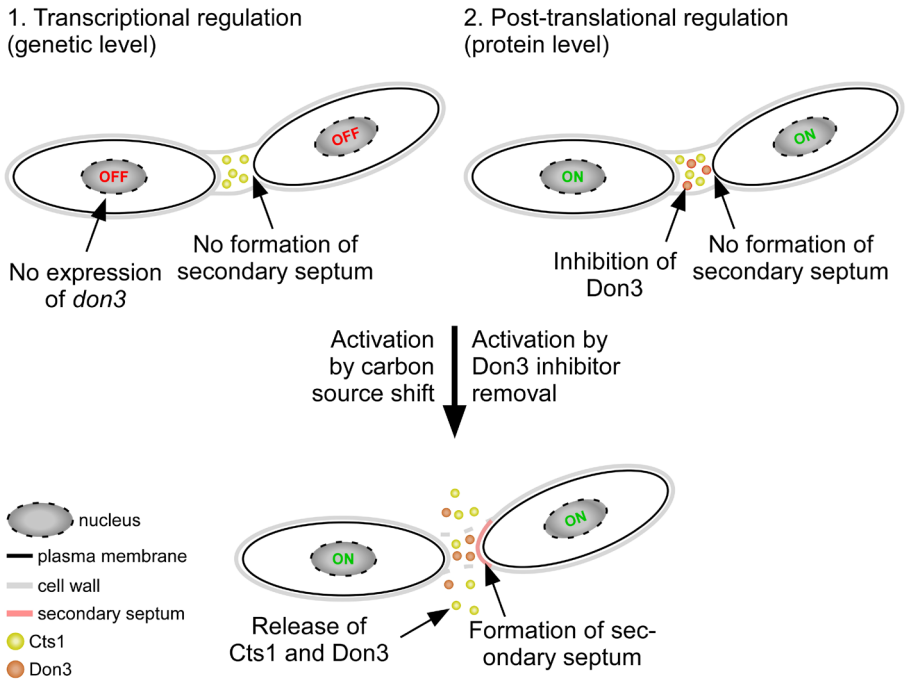


**Figure 4.1. Levels of unconventional secretion regulation via kinase Don3.** Functional Don3 is essential for formation of a secondary septum and therefore formation of a functional fragmentation zone and release of Cts1. **1.** Transcriptional regulation relies on an inducible promoter, controlling expression of *don3*. In the absence of a specific carbon source, the promoter is inactive, therefore no Don3 is present in the cell. Activation is achieved by a carbon source switch, resulting in expression of *don3*. **2.** For post-translational inhibition, a specific ATP analog inhibits Don3. In both cases, formation of a secondary septum and division of mother and daughter cell is prevented and Cts1 stays trapped inside the fragmentation zone. Upon activation, either by carbon source shift, or by removal of inhibitor, the secondary septum is formed and cells divide subsequently. This results in release of Cts1 from the fragmentation zone.

As proof of functionality of the auto-inducible system, successful unconventional secretion of anti-Gfp nanobodies in a regulated process was achieved in this study. Utilization of autoinduction medium allows biomass formation, production and accumulation of heterologous protein and subsequently release of protein in the same cultivation process. However, further characterization is necessary for transfer of the system to larger volumes. While growth and promoter activity via Gfp read-out were monitored in a BioLector microbioreactor, release and purification of nanobodies was conducted in laboratory scale using shaking flasks. Information gained in BioLector microbioreactors is much more comparable to large-scale bioreactors than other laboratory scale fermentation techniques and is therefore highly suited for up-scaling of fermentation processes (Funke et al., 2010). However, the protein yield of unconventional secretion is not yet sufficient for precise read-out of extracellular nanobody activity at different time points in low volumes. Therefore, microbioreactor cultivation was not suitable to monitor nanobody export. Cultivation in shaking flasks could additionally be linked to a Respiration Activity Monitoring System (RAMOS) to determine additional parameter such as oxygen transfer rate (OTR), carbon dioxide transfer rate (CTR) or respiratory quotient (RQ) (Anderlei et al., 2004). This would allow cultivation in

larger volumes, sufficient for nanobody isolation, together with generation of additional information on growth and physiology of cells. Furthermore, read-out generated in RAMOS measurements could be compared to BioLector microbioreactor read-out to gain important insights on reproducibility of the system in different volumes and cultivation devices. To validate data generated in shaking flasks and microbioreactor cultivation, adaption of autoinduction process in a laboratory scale fermenter could give important insights in reproducibility in larger volumes as a perquisite for full manufacturing scale processes (Crater & Lievense, 2018).

Expanding the repertoire of regulated targets can be advantageous especially because deletion of *don3* comes with severe changes in morphology. Adverse effects on yield were described for aggregation of filamentous fungi (Gibbs et al., 2000). Selection of Jps1, as a potential target for regulation was based on the observation that deletion of *jps1* results in drastic decrease of unconventionally secreted protein while cell morphology remained unaltered (Reindl et al., 2020). Unfortunately, localization of Jps1-Gfp under the control of the arabinose inducible $P_{crg}$ promoter was disturbed, leading to the formation of aggregates throughout the cell. Understanding the causes for this mis-localization could help to solve the problem. Co-localization studies of Jps1-Gfp and cellular compartments via established markers or dyes could give insights of the cellular region of accumulation and aggregation (Kilaru et al., 2017). Aggregation of misfolded proteins in so-called aggresomes is described when the intracellular protein degradation machinery is working beyond capacity (Corchero, 2016). Co-Localization of Jps1-Gfp and other proteins, known to accumulate in aggresomes, could reveal a potential organization of misfolded Jps1-Gfp in aggresomes (Johnston et al., 1998). Interestingly, RNA- and DNA-binding abilities for Jps1 were suggested by bioinformatical analysis (PredictProtein, RaptorX) and a preliminary individual-nucleotide resolution UV crosslinking and immunoprecipitation (iCLIP) experiment ((Reindl, 2020); personal communication: N. Stoffel, Institute for Microbiology, HHU Düsseldorf). RNA-binding abilities of Jps1 could thus be involved in formation of processing bodies (P-bodies), cytoplasmic ribonucleoprotein (RNP) aggregates primarily composed of mRNAs and proteins (Luo et al., 2018). P-bodies are involved in post-transcriptional regulation, as they play a role in decay of repressed mRNAs (Luo et al., 2018). Co-localization of P-body markers with Jps1-Gfp could reveal a potential incorporation of Jps1-Gfp in these structures. Localization of Jps1 in aggregates was observed before during heat or starvation stress (personal communication M. Reindl). Here localization looked similar to Khd4 localization, which is also known to accumulate in P-bodies and might be involved in regulation of translation and/or mRNA stability (Feldbrügge et al., 2008). Interestingly Khd4-like localization was only observed for Jps1-Gfp, but not for Cts1-Gfp (personal communication M. Reindl). Therefore, further elucidation of Jps1 localization would be necessary for adaptation as an inducible secretion

regulator. However, interestingly, here this localization was only observed in the inducible Jps1-Gfp version, while constitutively expressed Jps1-Gfp localized in the fragmentation zone, similar to the wild type situation (Reindl, 2020; Reindl et al., 2020). In addition, no effect of different carbon sources was observed for localization of Jps1-Gfp in this study. Correct localization of Jps1-Gfp in the fragmentation zone might be achieved in alternative regulation mechanisms, presumably leading to functional secretion of Cts1.

Since the here established inducible systems require removal of the external stimulus, or exchange of carbon source for induction of unconventional secretion, elaborate medium switches are required for certain approaches. Thus, enlarging the repertoire of different systems by alternative repressors or activators could be advantageous. Such a set of systems, allowing regulation on the levels of DNA, mRNA, or of protein activity is powerful for investigation of induced phenotypes on demand (Faden et al., 2014). One prominent example of a chemically inducible gene expression system is based on the tetracycline repressor protein (TetR) from *E. coli.* Fusion of a viral transactivator and the tetracycline repressor allows gene expression upon binding to the tetracycline operator. Addition of tetracycline or doxycyclin results in a conformational change of TetR leading to prevention of binding to the cognate operator sequence and therefore abolishing gene expression (Gossen & Bujard, 1992). For *U. maydis*, a tetracycline OFF-system was established (Zarnack et al., 2006). Here, a codon-optimized *E. coli* tetracycline repressor protein (TetR) fused to the minimal transactivation domain F of herpes simplex virus protein VP16 resulted in a modified transactivator tTa*. TetR and VP16 domain were separated by a spacer region from phage λ cI protein and the fusion protein was guided to the nucleus via a nuclear localization sequence (NLS) (Zarnack et al., 2006). For the described study, basal, constitutive promoter activity could be reduced by changing the spacer sequences of six tetracycline operator sequence *tetO* binding sites. This construct was fused upstream of the endogenous *mfa1* basal promoter (Zarnack et al., 2006). Therefore, the transactivation domain led to gene expression upon binding of tetracycline regulator to the operator sequence. Gene function was abolished in the presence of tetracycline and doxycycline, demonstrating the efficient generation of a Tet-OFF system (Zarnack et al., 2006).

However, the system did not show reliable results for other investigated targets. Recently an alternative tetracycline system was established. Interestingly, instead of the envisioned Tet-OFF system, a Tet-ON system was obtained (Hüsemann, 2020). In this system, TetR was fused to a short version of the VP16 transactivator, again with a λ cI protein spacer, as transactivator (tTa). Of note, this construct harbored two NLS, one at the C-terminus and one between TetR and the VP16 domain. Furthermore, insertion of restriction enzyme sites resulted in a point mutation at the N-terminus. Thirteen repeats of *tetO* were fused upstream of a $P_{hCMV}$ minimal promoter. Interestingly, *tetO* and the minimal promoter were disrupted by

a 372 nt sequence which likely occurred accidentially during cloning of the construct. Blast search revealed that this sequence is a part of the gene for the fluorescence protein mCerulean (NCBI Genbank accession: MG191280.1, Cloning vector pJPVCS). The sequence alterations inserted during cloning could be an explanation for the reverted function of the Tet-system. Induction with tetracycline in different concentrations led to an 11 to 17 -fold increase of firefly luciferase (FLuc) reporter activity. However, read out of constitutively $P_{otef}$ expressed FLuc was more than 10 - fold higher than the values obtained during tetracycline-regulated gene expression (Hüsemann, 2020). Thus, additional pioneering work to optimize the system for *U. maydis* would be essential.

While chemical regulation on different levels is well established and advantageous for different applications, factors as spatiotemporal resolution or extra costs and toxicity of chemicals can be limiting. Optogenetic regulation would be an elegant and non-invasive alternative way to regulate the system (Müller et al., 2014). For *S. cerevisiae* several optogenetic switches with potential applications in metabolic engineering and biotechnology are established (Figueroa et al., 2021). By contrast, until now, no light regulatable system has been established for *U. maydis*. Recent attempts into this direction addressed establishment of two different blue light-regulated systems to control gene expression (Hüsemann, 2020). The first system is based on a light–oxygen–voltage (LOV)-domain with an epitope tag fused to a PIP-repressor, and a PDZ domain fused to a VP16ff transactivator. A PIP operator sequence (PIR) upstream of a $P_{hCMV}$ minimal promoter controls the heterologous gene of interest. LOV domains are blue-light sensing domains. Upon light induction, a covalent bond between flavin mononucleotide (FMN) and a cysteine residue is formed, resulting in in a conformational change. Therefore, LOV domains can trigger dimerization or rotations of subunits (Müller & Weber, 2013). PIP can bind the PIR sequence and therefore bring the LOV-PIP construct in close proximity of the $P_{hCMV}$ minimal promoter (Fussenegger et al., 2000). Upon blue light induction, conformational change results in presentation of the epitope tag, fused to LOV, which is then recognized by PDZ. Binding of the constructs results in VP16ff transactivator localization at the $P_{hCMV}$ minimal promoter and therefore gene expression of the downstream gene (Hüsemann, 2020).

While the first system is based on conformational change of LOV resulting in presentation of a binding epitope, the second system is based on dimerization of LOV-DNA binding motif (helix-turn-helix (HTH)) (Motta-Mena et al., 2014). To regulate gene expression, a VP16 transactivator (ON-system) or a repressor (OFF-system) is fused to LOV-HTH. In *U. maydis*, upon blue light induction and binding of the LOV-HTH-regulator construct to a respective sequence, VP16 fusions resulted in a slight increase of gene product read out while the repressor constructs resulted in a decrease of gene product read out (Hüsemann, 2020). Of note, the first, PIP-PIR based system shows a very low basal expression and is therefore

interesting for inducible secretion applications, while the LOL-HTH based system showed a strong basal expression (Hüsemann, 2020). With the goal of improvement of this system, different operating sequences could be tested.

Another possibility of optogenic regulation of Don3 activity would be the exploitation of LOV-degron modules. For this technique, exposure of a degradation sequence, fused to LOV, is dependent on blue light. Due to a conformational change, the construct can be recognized by proteolytic enzymes and gets degraded (Renicke et al., 2013). The system has already been successfully established for *S. cerevisiae* (Renicke et al., 2013). For adaptation of this system for light regulation of unconventional secretion, a LOV-degron module, fused to Don3 would need to be constantly degraded during exposure to blue light, resembling the deletion phenotype. Without blue light, stable Don3 then could then support formation of the secondary septum, resulting in cell separation and release of heterologous proteins.

Beside blue light inducible systems, also other wavelengths can be used for control of cellular processes (Zhang & Cui, 2015). For example, red light-induced binding of plant photoreceptors can be applied in a similar strategy as described for the LOV-PIP - PiR system (Shimizu-Sato et al., 2002). For adaptation of a novel system for inducible secretion, a tight control is essential to avoid a basal activity level of Don3. Therefore, selection of an appropriate system strongly depends on a low leakage.

Interestingly, complementation of *don3* under the control of the arabinose inducible $P_{crg}$ promoter results in higher unconventional secretion of the reporter protein than observed in strains harboring *don3* in the endogenous locus under the control of the native promoter $P_{don3}$. Therefore, investigations of influence of expression levels of *don3* on unconventional export could be addressed in the future. Complementation of *don3* deletion via various different promoters could be a fast and straightforward way towards further understanding of the influence of Don3 on unconventional secretion. Importantly, overexpression of kinases, involved in septa formation, can lead to severe phenotypes. For *S. cerevisiae* overexpression of GIN4 kinase was described to induce elongated buds and a G2/M arrest-like phenotype (Akada et al., 1997). Furthermore, stronger *GIN4* overexpression even resembles septin deletion mutant phenotypes (Longtine et al., 1998). Therefore, restrained overexpression has to be considered, especially when influencing an essential cellular process such as cell budding.

In summary, two systems for regulation of unconventional secretion were established. Versatile application of each system allows different cultivation conditions towards an optional release of heterologous proteins. In future, implementation of additional systems should expand the portfolio of different regulation mechanisms. Non-invasive optimization such as optogenetic systems or chemical inducible ON-systems allow even more adaptable strategies for versatile regulated unconventional secretion.

# Establishment and adaptation of a forward genetic screen

To obtain strains with enhanced unconventional secretion for yield improvement, a forward genetic screen was designed and performed. The publication "**5 A novel factor essential for unconventional secretion of chitinase Cts1**" layed the foundation for establishment of the screen. Here, read-out and quantification of different reporter proteins was establishted for generation of an efficient screening strain. Application of the screen revealed unconventional secretion of Cts1 highly dependent on the novel factor Jps1 (jammed in protein secretion screen 1) and thus a new important key player in unconventional secretion. While the first screen focused on isolation of mutant candidates with a diminished unconventional secretion capacity, the second manuscript "**6 Isolation of *Ustilago maydis mutants* with enhanced capacity for unconventional export of heterologous proteins**" adapted the screen for isolation of hyper secretion mutants. Stringent selection parameters were selected towards characterization of different candidates. Finally, pooled linkage analysis was established to gain first insights on bioinformatical identification of underlying mutations.Further improvements of the genetic screen, application of identified mutations and other examples for exploitation of insights obtained by screens are discussed in chapter "**7 Outlook and further perspectives for establishment and adaption of a genetic screen for hyper secretion** candidates"

# 5 A novel factor essential for unconventional secretion of chitinase Cts1

Michèle Reindl [1,2,†], Janpeter Stock [1,2,†], **Kai P. Hussnaetter** [1,2], Aycin Genc [1], Andreas Brachmann [3] and Kerstin Schipper [1,2,*]

[1] Institute for Microbiology, Heinrich Heine University Düsseldorf, Düsseldorf, Germany
[2] Bioeconomy Science Center, Forschungszentrum Jülich, Jülich, Germany
[3] Genetics, Faculty of Biology, Ludwig-Maximilians-Universität München, Planegg-Martinsried, Germany
† These authors have contributed equally to this work
* Correspondence: Kerstin Schipper, kerstin.schipper@uni-duesseldorf.de

This review was published in *Frontiers in Microbiology* in July 2020 and is available at doi.org/10.3389/fmicb.2020.01529.

**Relevance of publication**

Understanding the unconventional secretion mechanism of the chitinase Cts1 is of large interest for application in biotechnological processes. Therefore, for identification of components essential for Cts1 export, a forward genetic screen was established. Mutant candidates, obtained by random UV-mutagenesis were screened based on their unconventional secretion capacity. To this end, the novel unconventional secretion factor Jps1 (jammed in protein secretion screen 1) was identified to be essential for unconventional Cts1 secretion. Localization studies revealed co-localization of Jps1 and Cts1 in the fragmentation zone between mother and daughter cell. While deletion of *jps1* resulted in strongly reduced Cts1 secretion, a *cts1* deletion did not affect Jps1 localization. Preliminary interaction studies pointed towards a weak interaction of Cts1 and Jps1.

Discovery and characterization of components are important steps for elucidation of unconventional secretion mechanism of Cts1. Application of this knowledge for biotechnological approaches can be of great potential. Furthermore, the forward genetic screen resembles a powerful tool for identification of more factors involved in unconventional secretion.

## 5.1 Abstract

Subcellular targeting of proteins is essential to orchestrate cytokinesis in eukaryotic cells. During cell division of *Ustilago maydis*, for example, chitinases must be specifically targeted to the fragmentation zone at the site of cell division to degrade remnant chitin and thus separate mother and daughter cells. Chitinase Cts1 is exported to this location via an unconventional secretion pathway putatively operating in a lock-type manner. The underlying mechanism is largely unexplored. Here, we applied a forward genetic screen based on UV mutagenesis to identify components essential for Cts1 export. The screen revealed a novel factor termed Jps1 lacking known protein domains. Deletion of the corresponding gene confirmed its essential role for Cts1 secretion. Localization studies demonstrated that Jps1 colocalizes with Cts1 in the fragmentation zone of dividing yeast cells. While loss of Jps1 leads to exclusion of Cts1 from the fragmentation zone and strongly reduced unconventional secretion, deletion of the chitinase does not disturb Jps1 localization. Yeast-two hybrid experiments indicate that the two proteins might interact. In essence, we identified a novel component of unconventional secretion that functions in the fragmentation zone to enable export of Cts1. We hypothesize that Jps1 acts as an anchoring factor for Cts1.

## 5.2 Introduction

Protein targeting is required to orchestrate essential cellular functions. Eukaryotic cells particularly rely on this process because of their compartmentalization and the necessity of equipping membrane-enclosed organelles with cognate protein subsets (Sommer & Schleiff, 2014). Protein targeting is mediated mostly by signal sequences. This is exemplified by the N-terminal signal peptide for entry of the endoplasmic reticulum (ER). The endomembrane system was thought to be the only export route for long time. However, recent years challenged this view by the finding that many proteins lacking a signal peptide are secreted by other mechanisms. The term unconventional secretion collectively describes protein export mechanisms that circumvent signal peptide-mediated passage through the canonical endoplasmic reticulum - Golgi pathway (Malhotra, 2013; Rabouille, 2017). Unconventional secretion has been discovered in lower eukaryotes like the fungal model *Saccharomyces cerevisiae* or the amoeba *Dictyostelium discoideum*, but also plays important roles in higher eukaryotes. It is even involved in human disease like in infections with the human immunodeficiency (HIV) or Epstein Barr viruses (Debaisieux et al., 2012; Nowag & Münz, 2015; Rayne et al., 2010). Research revealed that unconventional export mechanisms can be vesicular or non-vesicular(Rabouille et al., 2012), however, molecular details on the different pathways are scarce. The best described examples are self-sustained translocation of

fibroblast growth factor 2 (FGF2) in human cells and the secretion of acyl-binding protein Acb1 via specialized compartments of unconventional secretion (CUPS) in *S. cerevisiae* (Malhotra, 2013; Steringer & Nickel, 2018).

Recently, a novel mechanism of unconventional secretion has been described for chitinase Cts1 in the model microorganism *Ustilago maydis* (Reindl et al., 2019). In its yeast form the fungus grows by budding. In these cells, Cts1 acts in concert with a second chitinase, Cts2, and mediates cell separation during cytokinesis. Elimination of both enzymes results in a cytokinesis defect and the formation of cell aggregates (Langner et al., 2015). Cts2 has a predicted N-terminal signal peptide and is thus thought to be secreted via the conventional secretion route, pointing towards an intricate interplay between both pathways.

In line with its cellular function, Cts1 translocates into the fragmentation zone of budding yeast cells(Aschenbroich et al., 2019; Langner et al., 2015). This unique small compartment arises between mother and daughter cell after consecutive formation of two septa at the cell boundary(Reindl et al., 2019). Recently we demonstrated that Cts1 release depends on cytokinesis by using a cell cycle inhibitor that blocked unconventional but not conventional secretion(Aschenbroich et al., 2019). Furthermore, we showed that the septation proteins Don1 and Don3 are essential for Cts1 release (Aschenbroich et al., 2019). Don1 is a guanosine triphosphate exchange factor (GEF) that is delivered into the fragmentation zone by motile early endosomes, and Don3 is a germinal centre kinase (Böhmer et al., 2009; Weinzierl et al., 2002). Both proteins are required for secondary septum formation and their absence results in an incompletely closed fragmentation zone and thus, a cytokinesis defect similar to the one observed for the *cts1*/*cts2* deletion strain (Langner et al., 2015). Lack of either Don1 or Don3 diminished extracellular Cts1 activity although the protein still localized at the fragmentation zone. Taken together, these observations indicated that the fragmentation zone is its most likely site of secretion, suggesting a lock-type mechanism in which a completely sealed fragmentation zone is essential for export (Aschenbroich et al., 2019; Reindl et al., 2019). To obtain further insights into subcellular targeting and unconventional secretion of Cts1, we here developed and applied a UV mutagenesis screen to identify components of the unconventional secretion pathway.

## 5.3 Material and methods

### *5.3.1 Molecular biology methods*

All plasmids (pUMa vectors, see below and Table 5.1) generated in this study were obtained using standard molecular biology methods established for *U. maydis* including Golden Gate cloning (Bösch et al., 2016; Brachmann et al., 2004; Kämper, 2004; Terfrüchte

et al., 2014). Oligonucleotides applied for sequencing and cloning are listed in Table 5.2. Genomic DNA of strain UM521 (Kämper et al., 2006) was used as template for PCR reactions. All plasmids were verified by restriction analysis and sequencing. Detailed cloning strategies and vector maps will be provided upon request.

Plasmids for stable transformation of *U. maydis*: pUMa2373 (pDest-pep4D_Poma-LacZ-SHH-Cts1_NatR) was obtained in a Golden Gate cloning reaction using two flanking regions obtained by PCR using oligonucleotide combinations oRL1982 x oRL1983 (upstream flank *pep4* locus) and oRL1984 x oRL1985 (downstream flank *pep4* locus), the destination vector pUMa1476 (Terfrüchte et al., 2014) and pUMa2372. Storage vector pUMa2372 contained a $P_{oma}$ controlled non-optimized version of the *lacZ* gene (beta-D-galactosidase, accession NP_414878.1) from *Escherichia coli* Rosetta 2 in translational fusion to the *cts1* gene (*umag_10419*) via an SHH linker (Sarkari et al., 2014) and a nourseothricin-resistance marker cassette (NatR) flanked by BsaI sites. To generate pUMa2335 (pRabX1-Poma_Gus-SHH_cbx), pUMa2113 was hydrolyzed with NcoI and NotI and a Gus-SHH encoding fragment was inserted, replacing the previous insert coding for Gus-SHH-Cts1. Similary, in pUMa2336 (pRabX1-Poma_LacZ-SHH_cbx) the insert in pUMa2113 was replaced via NcoI/NotI restriction/ligation by a fusion gene encoding LacZ-SHH. Both plasmids were integrated in the *ip* locus under the control of the strong, constitutively active *oma* promoter. pUMa2605 was obtained by hydrolysis of p*cts2*Δ_hyg (Langner et al., 2015) with SfiI and replacing the HygR cassette with the G418-resistance cassette (G418R) from pUMa1057 (pMF1g)(Baumann et al., 2012). For assembly of pUMa3012 (pRabX1-Poma_Gus-SHH-Jps1) the *jps1* gene was amplified by PCR using oMB372 x oMB373 yielding a 1844 bp product flanked by AscI and ApaI restriction sites. After hydrolysis with these enzymes the *jps1* gene replaced the *cts1* gene in pUMa2113 (Sarkari et al., 2014). For assembly of pUMa3034 flanking regions were amplified with oDD824 x oDD825 (upstream flank *umag_03776* gene) and oDD819 x oDD820 (3´region of *umag_03776*) and used for SapI mediated Golden Gate cloning including destination vector pUMa2074 and the storage vector pUMa3035. pUMa3035 contained the mCherry gene for translational fusions as well as a HygR cassette. pUMa3111 (pDest-jps1D_G418R) was generated by replacing the HygR cassette in pUMa2775 by a G418R cassette from pUMa1057 using flanking SfiI sites. The progenitor vector pUMa2775 (pDest-jps1D_HygR) was synthetized by SapI mediated Golden Gate cloning with flanking regions obtained by PCR with oDD815 x oDD816 (upstream flank for *umag_03776*) and oDD819 x oDD820 (downstream flank for *umag_03776*), destination vector pUMa2074 and storage vector pUMa2242 harboring a HygR cassette (Aschenbroich et al., 2019). For generation of pUMa3293 (pRabX1-Pjps1_Jps1_eGfp_CbxR) a 1952 bp PCR product obtained with oUP65 x oUP66 (*umag_03776* promoter region) was hydrolyzed with NdeI and BamHI and inserted into a pRabX1 derivative (pUMa3095) upstream of a *jps1*:*gfp* fusion gene (Stock et al., 2012).

pUMa3095 was assembled in a three-fragment ligation of a 1849 bp PCR product of oMB190 x oMB120 (*umag_03776* gene) hydrolyzed with BamHI and EcoRI, a 741 bp PCR product of oMB521 x oMB522 (*gfp* gene) hydrolyzed with EcoRI and NotI and a 6018 bp fragment of vector pUMa2113 (Sarkari et al., 2014) hydrolyzed with BamHI and NotI.

Plasmids for two-hybrid analyses in *S. cerevisae*: All Yeast-two hybrid plasmids were generated on the basis of the Matchmaker III System (Clontech Laboratories Inc., Mountain View, CA, USA). pGAD and pGBKT7 were modified to contain a SfiI site with specific overhangs to exchange the gene of interest. For generation of pUMa2927 (pGAD_Jps1) and pUMa2929 (pGBK_Jps1) a 1869 bp PCR product was obtained with oMB201 and oMB202 (amplifying the *jps1* gene). The PCR product was hydrolyzed with SfiI and inserted into pGAD and pGBK backbones. For generation of pUMa2928 (pGAD_Cts1) and pUMa2930 (pGBK_Cts1), a 1549 bp PCR product was obtained with oMB203 and oMB204 (amplifying the *cts1* gene). The product was hydrolyzed with SfiI and inserted into pGAD and pGBK backbones.

**Table 5.1.** *U. maydis* strains used in this study.

| Strains | Relevant genotype/ resistance | UMa[1] | Plasmids transformed [2]/ resistance | Manipulated locus | Progenitor (UMa[1]) | Reference |
|---|---|---|---|---|---|---|
| FB1[a] | *a1b1* (wild type) | 51 | / | / | Cross of wild type strains UM518 x UM521 | (Banuett & Herskowitz, 1989b) |
| FB2[a] | *a2b2* (wild type) | 52 | / | / | Cross of wild type strains UM518 x UM521 | (Banuett & Herskowitz, 1989b) |
| AB33 | *a2 $P_{nar}$bW2bE1/PhleoR* | 133 | pAB33 (Brachmann et al., 2001) | *B* | UMa52 | (Brachmann et al., 2001) |
| FB6a [a] | *a2b1* | 55 | / | / | Cross of wild type strains UM518 x UM521 | (Banuett & Herskowitz, 1989b) |
| FB6b [a] | *a1b2* | 56 | / | / | Cross of wild type strains UM518 x UM521 | (Banuett & Herskowitz, 1989b) |
| FB2 lacZ-cts1 (screening progenitor) | *a2b2 pep4::[$P_{oma}$:lacZ:shh:cts1]/* NatR | 1501 | pUMa2373 / lacZ-Cts1_NatR | *umag_04926* (*pep4*) (Sarkari et al., 2014) | UMa52 | This study. |
| $FB2^{CGL}$ (screening strain) | *a2b2 upp1:: [$P_{oma}$gus:shh:cts1]*/HygR *pep4::[$P_{oma}$:lacZ:shh:cts1]/* NatR | 1502 | pUMa2374 / *gus-cts1*_HygR | *umag_02178* (*upp1*) (Sarkari et al., 2014) | UMa1501 (Screening progenitor) | This study. |

| | | | | | | |
|---|---|---|---|---|---|---|
| FB1$^{CGL}$ (strain used for back-crossings) | *a1b1 upp1::* *[P$_{oma}$gus:shh:cts1]*HygR *pep4::[P$_{oma}$:lacZ:shh:cts1]* NatR | 1547 | / | / | Derivative of crossing between FB1 and FB2$^{CGL}$ | This study. |
| FB2 Gus$_{cyt}$ | *a2b2 ip$^{S}$[P$_{oma}$gus:shh]ip$^{R}$*CbxR | 1507 | pUMa2335 / *gus*_cbxR | *cbx* | UMa52 | This study. |
| FB2 LacZ$_{cyt}$ | *a2b2 ip$^{S}$[P$_{oma}$lacZ:shh]ip$^{R}$*/CbxR | 1508 | pUMa2336 / *lacZ_cbxR* | *cbx* | 52 (FB2) | This study. |
| FB2$^{CGL}$mut1 | *a2b2 upp1:: [P$_{oma}$gus:shh:cts1]/*HygR *pep4::[P$_{oma}$:lacZ:shh:cts1]/* NatR + UV-induced mutations #24-8 | 1795 | / | UV mutagenized (Fig. 3; Fig. S5). | UMa1502 (screening strain) | This study. |
| FB2$^{CGL}$mut2 | *a2b2 upp1:: [P$_{oma}$gus:shh:cts1]/*HygR *pep4::[P$_{oma}$:lacZ:shh:cts1]/* NatR + UV-induced mutations #4-13 | 1831 | / | UV mutagenized (Fig. 3; Fig. S5). | UMa1502 (screening strain) | This study. |
| FB2$^{CGL}$mut3 | *a2b2 upp1:: [P$_{oma}$gus:shh:cts1]/*HygR *pep4::[P$_{oma}$:lacZ:shh:cts1]/* NatR + UV-induced mutations #3-10 | 1830 | / | UV mutagenized (Fig. 3; Fig. S5). | UMa1502 (screening strain) | This study. |
| AB33 jps1G | *a2 P$_{nar}$bW2bE1/*PhleoR *ip$^{S}$[P$_{jps1}$::umag_03776:gfp] ip$^{R}$*/CbxR | 2299 | pUMa3293 / CbxR | *cbx* | UMa133 | This study. |
| AB33 cts1G | *a2 P$_{nar}$bW2bE1/*PhleoR *umag_10419:gfp/*NatR | 388 | pUMa828 (pCts1G-NatR) (Koepke et al., 2011) | *umag_10419* (*cts1*) | UMa133 | (Koepke et al., 2011) |
| AB33 jps1mC/ Cts1G | *a2 P$_{nar}$bW2bE1/*PhleoR *umag_10419:gfp*/NatR *umag_03776:mcherry*/HygR | 2048 | pUMa3034 / HygR | *umag_03776* (*jps1*) | UMa388 | This study. |
| AB33 jps1Δ | *a2 P$_{nar}$bW2bE1/*PhleoR | 2092 | pUMa2775 / HygR | *umag_03776* (*jps1*) | UMa133 | This study. |
| AB33cts1Δ | *a2 P$_{nar}$bW2bE1/PhleoR umag_10419*Δ/HygR | 387 | pUMa780 (pCts1Δ-HygR) (Koepke et al., 2011) | *umag_10419* (*cts1*) | 133 | (Koepke et al., 2011a) |

[a] FB1, FB2, FB6a and FB6b are used as tester strains for mating and are derived from the same spore obtained after crossing of the wild type strains UM518 and UM521 (Banuett & Herskowitz, 1989a).
Further information in addition to published date:
[1] Internal strain collection numbers. Strains are called UMa plus a 4-digit number as identifier. [2] Plasmids generated in our working group are integrated in a plasmid collection and termed pUMa plus a 4-digit number as identifier.

**Table 5.2.** DNA oligonucleotides used in this study.

| Designation | Nucleotide Sequence (5′–3′) |
|---|---|
| oDD691 | TGACCGTCAACGCATGGC |
| oDD692 | TCGAGAATCGTGGTACCG |
| oDD693 | TTGCAGCCTACAGGCAGG |
| oDD694 | ACGGTGTGGCTGGAGTGG |
| oDD695 | CATCGGTATGCTTGGCTC |
| oDD696 | AGCGTCGAATTGACCGCC |
| oDD697 | GCTGTCAGAGGCGTTTCA |
| oDD698 | CCCAGAACAGCGCGTTCA |
| oDD699 | CGCGCAAACAAGCCAAGA |
| oDD729 | CGTCGTGCAATGCTGCCG |
| oDD730 | TGTCGAGCCTGCCGGTGG |
| oDD731 | AGACTCGGCTGCAGCAGC |
| oDD732 | AAGCTGGACAGGAGTGGG |
| oDD733 | AGATCGTAGCCGCCTTCG |
| oDD734 | TTGCTCCATCGTTGCCCG |
| oDD735 | CGTGAACGTCGCCCCGTA |
| oDD736 | ATGACCAAATCGCCGCCC |
| oDD737 | TGACGCTCCCTGCTCTCC |
| oDD815 | ATAGCTCTTCCGTGCAATATTGTGCTGTGAAGAGTCTCG |
| oDD816 | ATAGCTCTTCCGGCCGATTTGCAAGTCGTGGGC |
| oDD819 | ATAGCTCTTCCCCTCCGCTCCGCATCCCTCGACC |
| oDD820 | ATAGCTCTTCCGACAATATTCATCTACGACGAGATTGGAGG |
| oDD824 | ATAGCTCTTCCGTGCAATATTTGACAACCTCGTCGGG |
| oDD825 | ATAGCTCTTCCCGAGGATTCCGCATCGATTGGG |
| oMB190 | GATTACAGGATCCATGCCAGGCATCTCC |
| oMB201 | GATTACAGGCCATTACGGCCATGCCAGGCATCTCCAAGAAGCC |
| oMB202 | GATTACAGGCCGAGGCGGCCTAGGATTCCGCATCGATTGGGG |
| oMB203 | GATTACAGGCCATTACGGCCATGTTTGGACGTCTTAAGCACAGG |
| oMB204 | GATTACAGGCCGAGGCGGCCTTACTTGAGGCCGTTCTTGACATTGTCCC |
| oMB372 | TTAGGCGCGCCATGCCAGGCATCTCC |
| oMB373 | TTAGGGCCCTTAGGATTCCGCATCGATTGGGG |
| oMB520 | CATGAATTCGGATTCCGCATCGATTGGGG |
| oMB521 | TCAGAATTCATGGTGAGCAAGGGCGAGG |
| oMB522 | CATGCGGCCGCCTTACTTGTACAGCTCGTCC |
| oMF502 | ACGACGTTGTAAAACGACGGCCAG |
| oMF503 | TTCACACAGGAAACAGCTATGACC |
| oRL272 | GACCATGGAGACAACTTCGGTCATCTCCGCG |

| | |
|---|---|
| oRL273 | GCACTAGTATTGATCGTTCCAGAGCACG |
| oRL1124 | AGAGTTTGATCMTGGCTCAG |
| oRL1125 | GACGGGCRGTGWGTRCA |
| oRL1982 | GGTCTCGCCTGCATTTAAATAGGAACGCCGCGTCGGC |
| oRL1983 | GGTCTCCAGGCCTGTCTTGAAGTGAATGTCGG |
| oRL1984 | GGTCTCCGGCCCTGTTGTTCAGTAGCAATGTG |
| oRL1985 | GGTCTCGCTGCATTTAAATCACCCATTCGTGATTCACCAC |
| oUP65 | GGAATTCCATATGGCGAGCCTTGAGGCTGCGTTCC |
| oUP66 | CGGGATCCGATTTGCAAGTCGTGGGCCTTCG |

### *5.3.2 Strains and cultivation conditions*

*U. maydis* strains used in this study were obtained by homologous recombination yielding genetically stable strains (Table 1). For genome insertion at the *ip* locus, integrative plasmids were used (Stock et al., 2012). These plasmids contain an *ip*$^{R}$ allele that mediates carboxin resistance (Keon et al., 1991). Integrative plasmids were linearized within the *ip*$^{R}$ and subsequently used to transform *U. maydis* protoplasts. Mutants harboring a single copy of the plasmid were obtained via homologous recombination (Brachmann et al., 2004; Kämper, 2004). Gene deletion and translational fusions *in locus* were performed with plasmids obtained by either the SfiI- or Golden Gate cloning strategy using plasmids deposited in the Institutes plasmid collection (Brachmann et al., 2004; Terfrüchte et al., 2014)(Web reference: *Ustilago* community). Gene insertion at the *pep4* (*umag_04926*) and *upp1* (*umag_02178*) locus resulted in the deletion of the respective protease-encoding genes and hence, as a positive side-effect for the screen diminished proteolytic activity of the strains (Sarkari et al., 2014). The corresponding plasmids were obtained by Golden Gate cloning (Terfrüchte et al., 2014). All strains generated were verified by Southern blot analysis using digoxygenin labeled probes (Roche). For *ip* insertions, the probe was obtained with the primer combination oMF502/oMF503 and the template pUMa260 (Loubradou et al., 2001). For insertions at the *pep4* or *upp1* locus (Sarkari et al., 2014) and other in-locus manipulations, the two flanking regions (upstream and downstream flanks) were amplified as probes.

*U. maydis* strains were grown at 28 °C in complete medium (CM) supplemented with 1% (w/v) glucose (CM-glc) (Holliday, 1974) or YepsLight (modified from (Tsukuda et al., 1988)). Solid media were supplemented with 2% (w/v) agar agar. CM-glc plates containing 1% (w/v) charcoal (Sigma C-9157) were used for mating assays (Hartmann et al., 1996).

*Saccharomyces cerevisiae* strain AH109 (Clontech Laboratories Inc., Mountain View, CA, USA) was employed for yeast two-hybrid assays. Gene sequences without predicted introns were inserted into the vectors pGAD24 and pGBKT7 generating translational fusions to the Gal4 activation domain (AD) and DNA-binding domain (BD), respectively.

### *5.3.3 Generation of a compatible strain by genetic crossings*

To enable genetic back-crosses with FB2$^{CGL}$ the reporters were also introduced into the compatible strain FB1 by genetic crosses. Therefore, wild type strain FB1 was crossed with screening strain FB2$^{CGL}$ (mating type *a2b2*) using plant infections (see below) to obtain meiotic progeny. These were tested for their ability to mate with FB2. Compatible mating was screened on CM-glc plates containing 1% (w/v) charcoal (Figure S5.1) on which strains harboring different alleles of both mating type loci form fuzzy colonies while strains which do not mate grow in smooth colonies. First, progeny was screened for the presence of the two artificial reporters Gus-Cts1 and LacZ-Cts1. Positive candidates were then tested in mating experiments with tester strains for induction of the fuzzy phenotype in FB2 crosses.

### *5.3.4 Mixing experiments to distinguish intra- and extracellular reporter activities*

To distinguish intra- and extracellular LacZ activity defined cell amounts were mixed on CM-glc/X-Gal plates containing 1% (w/v) glucose and X-Gal (5-bromo-4-chloro-3-indolyl-β-D-galactopyranoside; 20 mg/ml in DMSO, f.c. 60 mg/L in CM-glc). Screening strain FB2$^{CGL}$ and the AB33LacZ$_{cyt}$ control were grown in liquid CM-glc medium until logarithmic phase. Cells were harvested, washed in PBS (1x, pH 7.2) and adjusted to an $OD_{600}$ of 1.0. A $10^{-4}$ serial dilution was prepared in PBS. The diluted suspensions of both strains were mixed in defined ratios and plated in a total volume of 150 µl on CM-glc/X-Gal plates. After incubation for 4 days at 28 °C protected from light, growth and conversion of substrate was photographed. For illumination a Ledgo CN-B150 LED On-Camera Light was used.

### *5.3.5 Gus/LacZ activity plate and membrane assays*

Gus and LacZ activity were tested by indicator plate assays using CM plates containing 1% (w/v) glucose (CM-glc) and the respective chromogenic substrate X-Gluc (5-bromo-4-chloro-3-indolyl-beta-d-glucuronic acid; 0.5 mg/ml in DMSO) or X-Gal (20 mg/ml in DMSO), respectively. Tested strains were grown in CM-glc for 16 hours. After adjusting the cultures to an $OD_{600}$ of 1.0 in sterile PBS, 10 µl suspension were spotted on CM-glc plates and incubated at 28 °C for 2 days. Intracellular Gus and LacZ activity was visualized by placing a nitrocellulose membrane (Amersham ™ Protran TM 0.45 µM NC, GE Healthcare Life Sciences) on top for 24 h at 28 °C. The membrane was then removed and treated with liquid nitrogen for 3 min for cell lysis. Subsequently, it was soaked in X-Gluc buffer (25 µg X-Gluc/ml, solved in DMSO, 5 mM sodium phosphate buffer pH 7.0, 14 µM β-mercaptoethanol, 0.4 mM EDTA, 0.0021% (v/v) lauroyl-sarcosin, 0.002% (v/v) Triton X-100, 0.1 mg/ml (w/v) BSA) or X-

Gal Buffer (1 mg X-Gal/ml, solved in DMSO, 15 mM Sodium phosphate buffer pH 7, 5 mM KCl, 0.5 mM MgSO4, 34 mM β-mercaptoethanol) for Gus and LacZ activity, respectively, and incubated at 37 °C for 18 h.

### *5.3.6 UV mutagenesis*

For UV mutagenesis a 20 ml YepsLight pre-culture of screening strain $FB2^{CGL}$ was inoculated from a fresh plate and incubated overnight (200 rpm, 28 °C). In the morning, the culture was diluted to an $OD_{600}$ of 0.1 in 20 ml (200 rpm, 28 °C). The culture was incubated until it reached an $OD_{600}$ of 0.5. Subsequently it was diluted stepwise to an $OD_{600}$ of 0.00125 (1: 400) in 20 ml YepsLight. 150 µl of the 1:400 dilutions were spread evenly onto CM-glc screening plates containing 10 µg/ml X-Gal. The dried plates were exposed to UV irradiation (30 $mJ/cm^2$) using a Stratalinker device (Stratagene). Plate lids were removed during exposition. Subsequently, plates were incubated for 2 to 3 days at 28 °C until single colonies were grown.

### *5.3.7 Screening for diminished reporter secretion*

Clones that showed reduced or absent LacZ activity (i.e., colorless appearing colonies) after UV mutagenesis on CM-glc screening plates containing X-Gal (see above) were patched on plates containing X-Gluc to additionally assay for extracellular Gus activity. Plates were prepared by spreading 100 µl X-Gluc solution (100 mg/ml stock in DMSO) on CM-glc plates. Plates were incubated for 2 to 3 days on 28 °C. Colorless colonies were patched again on X-Gluc and X-Gal plates simultaneously, this time streaking out larger areas of about 0.5 x 0.5 cm. During the procedure, control strains producing intracellular LacZ or Gus (FB2 $LacZ_{cyt}$ and FB2 $Gus_{cyt}$, respectively), the non-mutagenized screening strain ($FB2^{CGL}$) and the precursor strain lacking any reporters (FB2) were handled in parallel to verify the results (Table 1).

### *5.3.8 Generation of cell extracts and supernatants*

Strains were inoculated in 20 ml CM-glc and incubated at 28 °C overnight. Next morning, the culture was used to inoculate a new culture of 70 ml CM-glc with a starting $OD_{600}$ of 0.05. To detect potential growth defects, growth of the culture was followed by determining the $OD_{600}$ every hour for at least 8 to 10 hours. 2 ml aliquots of supernatants for Gus/LacZ assays and whole cells for Cts1 assays were harvested at $OD_{600}$ of 0.3. Once the culture reached an $OD_{600}$ of 0.7 50 ml were harvested (5 min, 3000 rpm, 4 °C). The supernatant was transferred to a new tube and stored on 4 °C. The cell pellet was used to prepare native cell extracts used for the Cts1, Gus and LacZ assay (modified from (Stock et al., 2016)). To this end the cell pellet was resuspended in 2 ml ice-cold native extraction buffer (1 mM phenylmethylsulfonylfluorid

(PMSF), 2.5 mM benzamidine hydrochloride hydrate, 1 µM pepstatin; 100 µL Roche EDTA-free protease inhibitor cocktail 50×; dissolve in PBS pH 7.4). The suspension was then frozen in pre-chilled metal pots (25 ml, Retsch) using liquid nitrogen. Cells were ruptured at 4 °C using the Retsch mill (10 min, 30 Hz) and then the metal pots were thawed at 4 °C for 1 hour. The cell extracts were transferred to a reaction tube and centrifuge for 30 min (4 °C, 13000 rpm, benchtop centrifuge). Bradford assays were conducted to determine the protein concentrations in the samples (Bradford, 1976).

### *5.3.9 Quantitative determination of Gus and LacZ activity*

Importantly, quantitative Gus, LacZ and Cts1 assays were conducted from a single culture (see below for Cts1 assay). Quantitative Gus and LacZ liquid assays were based on the chromogenic and fluorescent substrates ONPG for the liquid LacZ activity assay (o-nitrophenyl-β-D-galactopyranoside) and MUG for the liquid Gus activity assay (4-methylumbelliferyl-ß-D-glucuronide trihydrate; BioWorld, 30350000-2 (714331), respectively (Stock et al., 2012; Stock et al., 2016). For both the ONPG and the MUG liquid assays (modified from (Stock et al., 2012; Stock et al., 2016)), activity was determined in native cell extracts and in the cell-free culture supernatant of candidate mutants in comparison to control strains (Koepke et al., 2011; Langner et al., 2015; Stock et al., 2012).

The Gus and LacZ assays with cell extracts and cell-free supernatants were conducted according to slightly modified published protocols(Miller, 1959; Stock et al., 2012). To this end, native cell extracts were adjusted to a total protein concentration of 100 µg/ml using PBS buffer. 10 µl of native cell extracts were then mixed in a black 96-well plate (96 Well, PS, F-Bottom, µCLEAR, black, CELLSTAR) with 90 µl of Gus- or Z-buffer and 100 µl of the respective substrate solution (Gus: 2 mM MUG, 1/50 vol. bovine serum albumin fraction V (BSA) in 1x Gus buffer; LacZ: 1 mg/ml ONPG in 2x Z-buffer). For supernatant measurements, 100 µl cell-free supernatants were mixed with 100 µl of the respective substrate solution. 2x Gus buffer (Stock et al., 2012) was used for the Gus assay and 2x Z-buffer (80 mM $Na_2HPO_4$, 120 mM $NaH_2PO_4$*$H_2O$, 20 mM KCl, 2 mM $Mg_SO_4$*$7H_2O$; adjust to pH 7; add 100 mM β-mercaptoethanol freshly) was used for the LacZ assay. The assays were conducted in the Tecan device (Tecan Group Ltd., Männedorf, Switzerland) for 1 h at 37 °C with measurements every 10 min (excitation/emission wavelengths: 365/465 nm for Gus activity; $OD_{420}$ for LacZ activity). A fixed gain of 150 was used for cell extract measurements and fixed values of 60 and 100 for Gus and Cts1 activity assays of culture supernatants, respectively.

For data evaluation the slope during linear activity increase of the kinetic measurements was determined. Values for the screening strain $FB2^{CGL}$ were set to 100% to judge the activities in the mutants.

### *5.3.10 Quantitative determination of Cts1 activity*

The fluorescent substrate MUC was applied for the Cts1 liquid assay (4-methylumbelliferyl β-D-N,N′,N″-triacetylchitotrioside hydrate; M5639 Sigma-Aldrich) (Koepke et al., 2011; Stock et al., 2012). Strain AB33 cts1Δ (UMa387) (Koepke et al., 2011) carrying a *cts1* deletion dealt as negative control for the Cts1 assays. For the MUC assay whole cells were subjected to the assay after washing to detect Cts1 activity at the cell surface. For intracellular activities, cell extracts were used (see above).

The Cts1 activity liquid assay with whole cells or 10 µg of native cell extracts was conducted according to published protocols with minor changes (Koepke et al., 2011; Stock et al., 2012). Once the culture had reached an $OD_{600}$ of 0.3 a 2 ml sample was taken and cells were harvested by centrifugation (3 min, 8000 rpm, bench-top centrifuge). Cells were resuspended in 1 ml KHM buffer (110 mM potassium acetate, 20 mM HEPES, 2 mM $MgCl_2$) (Koepke et al., 2011; Stock et al., 2012), the $OD_{600}$ was documented and the suspension was subjected to the MUC assay. A MUC working solution was prepared form a stock solution (2 mg/ml MUC in DMSO) by diluting it 1:10 with KHM buffer (protect from light, store at 4 °C). Black 96-well plates (96 Well, PS, F-Bottom, µCLEAR, black, CELLSTAR) were used for the assay. 70 µl of working solution were mixed with 30 µl of the cell suspension in one well. Activities for each strain were determined in triplicates. The plates were sealed with parafilm and incubated in the dark for 1 h at 37 °C. The reaction was then stopped by adding 200 µl 1 M $Na_2CO_3$ and relative fluorescence units were determined in a plate reader at excitation and emission wave length of 360/450 nm, respectively, at 37 °C with a fixed gain of 100 (Tecan Reader).

### *5.3.11 Plant infection and genetic back-crosses*

Compatible *U. maydis* strains were subjected to genetic crosses on corn plants. Strain $FB1^{CGL}$ was obtained by genetic crossing of FB1 (mating type *a1b1*) with $FB2^{CGL}$ (mating type *a2b2*). Furthermore, mutagenized strains (derived from the $FB2^{CGL}$ strain background; mating type *a2b2*) which showed strongly reduced Cts1 secretion assayed by all three reporters were subjected to back-crosses with the compatible wild type strain $FB1^{CGL}$ (mating type *a1b1*). For infection of the host plant *Z. mays* (Early Golden Bantam), strains were grown to an $OD_{600}$ of 0.8 in CM-glc, washed three times with $H_2O$, and resuspended to an $OD_{600}$ of 1 in $H_2O$. For infection, compatible strains were then mixed in a 1:1 ratio. The cell suspension was injected into seven day-old maize seedlings. Virulence of strain crosses was quantified using established pathogenicity assays (Kämper et al., 2006). Therefore, 7 days post infection plants were scored for symptom formation according to the following categories: (1) no symptoms, (2) chlorosis, (3) anthocyanin accumulation, (4) small tumors (<1 mm), (5) medium tumors (>1

mm), and heavy tumors associated with bending of stem. For spore collection, mature tumor material was harvested two to three weeks after infection and dried at 37 °C for about 7 days.

### *5.3.12 Spore germination and analysis of progeny*

Spore germination and analysis was conducted according to published protocols (Eichhorn et al., 2006). To germinate spores for progeny analysis after genetic back-crossing of FB1 x $FB2^{CGL}$ or $FB1^{CGL}$ x $FB2^{CGL}$mut1 dried tumor material was homogenized in a mortar, treated with 2 ml of a solution of 3.0% (w/v) copper sulfate for 15 min and washed twice with 1 ml sterile $H_2O$. The spores were then resuspended in 500 µl sterile water. Prior to plating, the spore solutions were supplemented with ampicillin and tetracycline to avoid bacterial contaminations (final concentrations: 600 µg/ml ampicillin; 150 µg/ml tetracycline). Then, 200 µl of 1:1, 1:10 and 1:100 dilutions were spread on CM-glc plates, and incubated for 2 d at 28 °C. Resulting colonies were singled out again on CM-glc plates to guarantee that each colony results from one clone. To identify $FB1^{CGL}$ after crossing of FB1 x $FB2^{CGL}$ progeny was assayed on charcoal plates for their mating types (see below) and on X-Gal and X-Gluc plates for the presence of the two reporters Gus and LacZ. To analyze $FB1^{CGL}$ and $FB2^{CGL}$mut1 again indicator plates containing X-Gal and X-Gluc were used to pre-sort the cells into secretion competent and deficient clones. Candidates were further tested using liquid assays for all three reporters.

### *5.3.13 Mating assay*

For mating assays, cells were grown in CM medium to an $OD_{600}$ of 1.0 and washed once with sterile $H_2O$. Washed cells were adjusted to an $OD_{600}$ of 3 in sterile $H_2O$. Indicated strains were pre-mixed in equal amounts and then co-spotted on CM-glc plates containing 1% (w/v) charcoal. Plates were incubated at 28 °C for 24 h. Tester strains were used as controls (Table 5.2).

### *5.3.14 Genome sequencing and assembly*

Genomic DNA extraction was performed according to published protocols (Bösch et al., 2016), two separate preparations were combined, and the DNA concentration was adjusted to 100 ng/µl using TE-RNase in approximately 500 µl final volume. gDNA quality was verified by PCR reactions using primers specific for the bacterial 16sRNA gene (oRL1124 x oRL1125) and the intrinsic gene *uml2* (*umag_01422*; oRL272 x oRL273). For genome sequencing, DNA libraries were generated using the Nextera XT Kit (Illumina) according to manufacturer's instructions. Sequencing (v3 chemistry) was performed with a MiSeq sequencer (Illumina) at the Genomics Service Unit (LMU Biocenter). Obtained reads were quality trimmed and filtered

with trimmomatic version 0.30 and fasta toolkit version 0.13.2. Sequence assemblies with passed single and paired reads were performed using CLC Genomics Workbench 8.0 (QIAGEN). The genome sequence of UM521 (Web reference: *U. maydis* 521)(Kämper et al., 2006) was used as template for read assembly. Genomic DNA of screening strain FB2$^{CGL}$ was sequenced as reference. This Whole Genome Sequencing (WGS) Shotgun project has been deposited at DDBJ/ENA/GenBank under the accessions JABUOB000000000 and JABUOC000000000 (Web reference: WGS). The versions described in this paper are JABUOB010000000 and JABUOC010000000.

### *5.3.15 Identification of genomic mutations*

For identification of the underlying mutation in progeny of FB1$^{CGL}$ and FB2$^{CGL}$mut1, PCR products were generated from gDNA of progeny clones #3 and #5 which showed no Cts1 activity and no blue halos on X-Gal and X-Gluc indicator plates. To this end, the following primer combinations were used to amplify the indicated genes (Table 5.2): *umag_00493*: oDD691 x oDD729; *umag_06269*: oDD692 x oDD730; *umag_02631*: oDD693 x oDD731; *umag_03776*: oDD694 x oDD732; *umag_04298*: oDD695 x oDD733; *umag_05386*: oDD696 x oDD734; *umag_04385*: oDD697 x oDD735; *umag_04494*: oDD698 x oDD736 and *umag_11876*: oDD699 x oDD737. gDNA was obtained like described (Bösch et al., 2016). Additional sequencing was conducted for *umag_06269* and *umag_03776* using progeny #9, #26, #31 and #39 (not shown). PCR products were sequenced and analyzed for the presence or absence of the mutations identified in genome sequence alignments of FB2$^{CGL}$ and FB2$^{CGL}$mut1.

### *5.3.16 Protein precipitation from culture supernatants*

Secreted proteins were enriched from supernatant samples using trichloric acid (TCA) precipitation. Therefore, culture supernatants were supplemented with 10% (w/v) TCA and incubated overnight on 4 °C. After washing twice in -20 °C acetone the protein pellets were resuspended in minimal amounts of 3x Laemmli-Buffer (Laemmli, 1970) and the pH was eventually neutralized with 1 M NaOH. For SDS-Page analysis the samples were first boiled for 10 min and then centrifuged (22,000 x g, 5 min, room temperature).

### *5.3.17 SDS-Page and Western blot analysis*

Boiled protein samples were separated by SDS-Page using 10% (w/v) acrylamide gels. Subsequently, proteins were blotted to methanol-activated PVDF membranes. The analyzed proteins contained an SHH-tag (Sarkari et al., 2014) and were detected using anti-HA (Sigma-Aldrich, USA) antibodies and anti-mouse IgG-HRP (Promega, USA) conjugates as primary

and secondary antibodies, respectively. HRP activity was detected using AceGlow Western blotting detection reagent (PeqLab, Germany) and a LAS4000 chemiluminescence imager (GE LifeScience, Germany).

### *5.3.18 Yeast-two hybrid assays*

Yeast two-hybrid analysis was carried out using the Clontech MatchMaker III system as described before (Pohlmann et al., 2015). Transformation with plasmids and cultivation were performed using standard techniques (Clontech manual). In addition to negative and positive controls included in the MatchMaker III system, also examples for weakly interacting proteins were included (Pohlmann et al., 2015). Auto-activation was excluded for all tested proteins using controls with control plasmids.

### *5.3.19 Microscopy, image processing and staining procedures*

Microscopic analysis was performed with a wide-field microscope from Visitron Systems (Munich, Germany), Zeiss (Oberkochen, Germany) Axio Imager M1 equipped with a Spot Pursuit CCD camera (Diagnostic Instruments, Sterling Heights, MI) and objective lenses Plan Neofluar (40x, NA 1.3) and Plan Neofluar (63x, NA 1.25). Fluorescence proteins were excited with an HXP metal halide lamp (LEj, Jena, Germany) in combination with filter sets for Gfp (ET470/40BP, ET495LP, ET525/50BP), mCherry (ET560/40BP, ET585LP, ET630/75BP, Chroma, Bellow Falls, VT), and DAPI (HC387/11BP, BS409LP, HC 447/60BP; AHF Analysentechnik, Tübingen, Germany). The system was operated with the software MetaMorph (Molecular Devices, version 7, Sunnyvale, CA). Image processing including adjustments of brightness and contrast was also conducted with this software. To visualize fungal cell walls and septa 1 ml of cell culture was stained with calcofluor white (1 µg/ml) before microscopy.

## 5.4 Results

### *5.4.1 A genetic screen for mutants impaired in Cts1 secretion identifies a novel component*

To identify mutants impaired in Cts1 secretion, a forward genetic screen based on UV mutagenesis was established (Figure 5.1, Figure S5.2; for experimental details see Materials and Methods section). To this end, a screening strain derived from the haploid FB2 wild type strain (mating type *a2b2*) was developed. This allows for co-infections of the host plant maize

with compatible strains of differing *a* and *b* alleles like FB1 (mating type *a1b1*) to obtain meiotic progeny (Banuett & Herskowitz, 1989b).

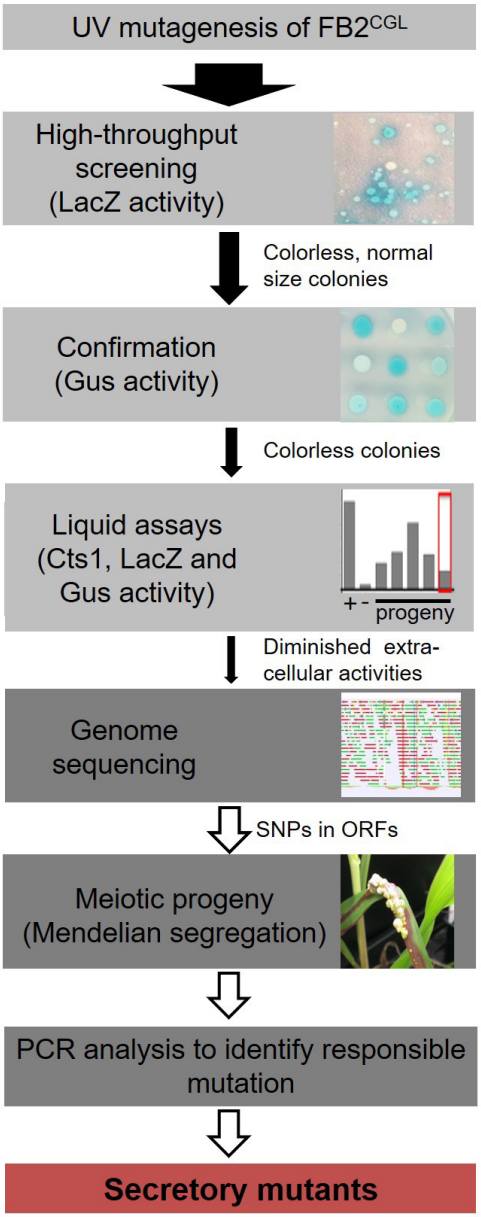


**Figure 5.1. Rationale of the forward genetic screen.** The three reporters LacZ-Cts1, Gus-Cts1 and endogenous Cts1 were used to identify mutants with diminished Cts1 secretion. After UV mutagenesis, a high-throughput screen for absence of LacZ activity of LacZ-Cts1 was conducted on X-Gal containing plates. Next, colonies were patched on X-Gluc containing plates to verify the result with the Gus-Cts1 reporter. Remaining candidates were assayed in quantitative liquid assays for extra- and intracellular LacZ, Gus, and Cts1 activity. Candidates with diminished extracellular activity of all three reporters but unimpaired intracellular activity were collected. After genome sequencing, the mutation responsible for diminished secretion was identified by PCR analysis of different meiotic progeny showing a similar secretion phenotype on loci containing SNPs as identified in the genome comparison with the progenitor strain. For details see Figure S5.2.

To minimize false positive screening hits, three different reporters for Cts1 secretion were employed: the bacterial reporter enzymes β-glucuronidase (Gus; published in (Stock et al., 2012; Stock et al., 2016)) and β-galactosidase (LacZ; newly established for *U. maydis*) as fusion proteins with Cts1 (Gus-Cts1, LacZ-Cts1), and endogenous Cts1 (Koepke et al., 2011). The genetic constructs for Gus-Cts1 and LacZ-Cts1 were stably inserted in the genome at distinct loci resulting in screening strain FB2$^{CGL}$ (Table 5.1) (Figure 5.2A).

Strains harboring cytoplasmic Gus or LacZ were used as lysis controls and to mimic defective Cts1 secretion with intracellular reporter accumulation (control strains FB2 Gus$_{cyt}$ and FB2 LacZ$_{cyt}$). Plate assays with the colorimetric substrates X-Gluc (5-bromo-4-chloro-3-

indolyl-beta-d-glucuronic acid) and X-Gal (5-bromo-4-chloro-3-indolyl-β-D-galactopyranoside) demonstrated that the screening strain developed the expected blue color indicative for extracellular Gus and LacZ activity while the controls showed no color. Artificial cell lysis demonstrated the presence of intracellular reporter activity in the controls confirming the absence of significant cell lysis (Figure 5.2B). Furthermore, quantitative liquid assays with the colorimetric substrate ONPG (o-nitrophenyl-β-D-galactopyranoside) and the fluorogenic substrates MUG and MUC (4-methylumbelliferyl-β-D-glucuronide trihydrate; 4-methylumbelliferyl β-D-N,N′,N″-triacetylchitotrioside hydrate) detecting extracellular LacZ, Gus and Cts1 activity, respectively, revealed strongly enhanced extracellular activities of all reporters in $FB2^{CGL}$ compared to the respective control strains containing cytoplasmic versions or lacking the reporters (Figure 5.2C). Similar activity measurements in cell extracts again confirmed that all reporters were functional (Figure 5.2D). In addition, since we intended to use LacZ activity for high-throughput screening, a mixing experiment to assay its suitability was conducted. Mixing of $FB2^{CGL}$ with FB2 $LacZ_{cyt}$ in different ratios on indicator plates containing X-Gal showed that the ratio of mixing was reflected by the ratio of colonies with a blue halo versus colorless colonies (Figure 5.2E-G). This demonstrated that mutants with defective secretion can be identified vis-a-vis colonies with intact secretion as an important requirement for the screening procedure. Finally, plant infection experiments indicated that pathogenicity of $FB2^{CGL}$ was not impaired, since $FB2^{CGL}$ (*a2b2*) crossed with the compatible mating partner FB1 (*a1b1*) elicited the typical symptoms including tumor formation on maize seedlings (Figure S5.3). Thus, genetic back-crossing experiments are feasible with this strain. In summary, we successfully designed the strain $FB2^{CGL}$ for screening mutants defective in unconventional secretion of Cts1.

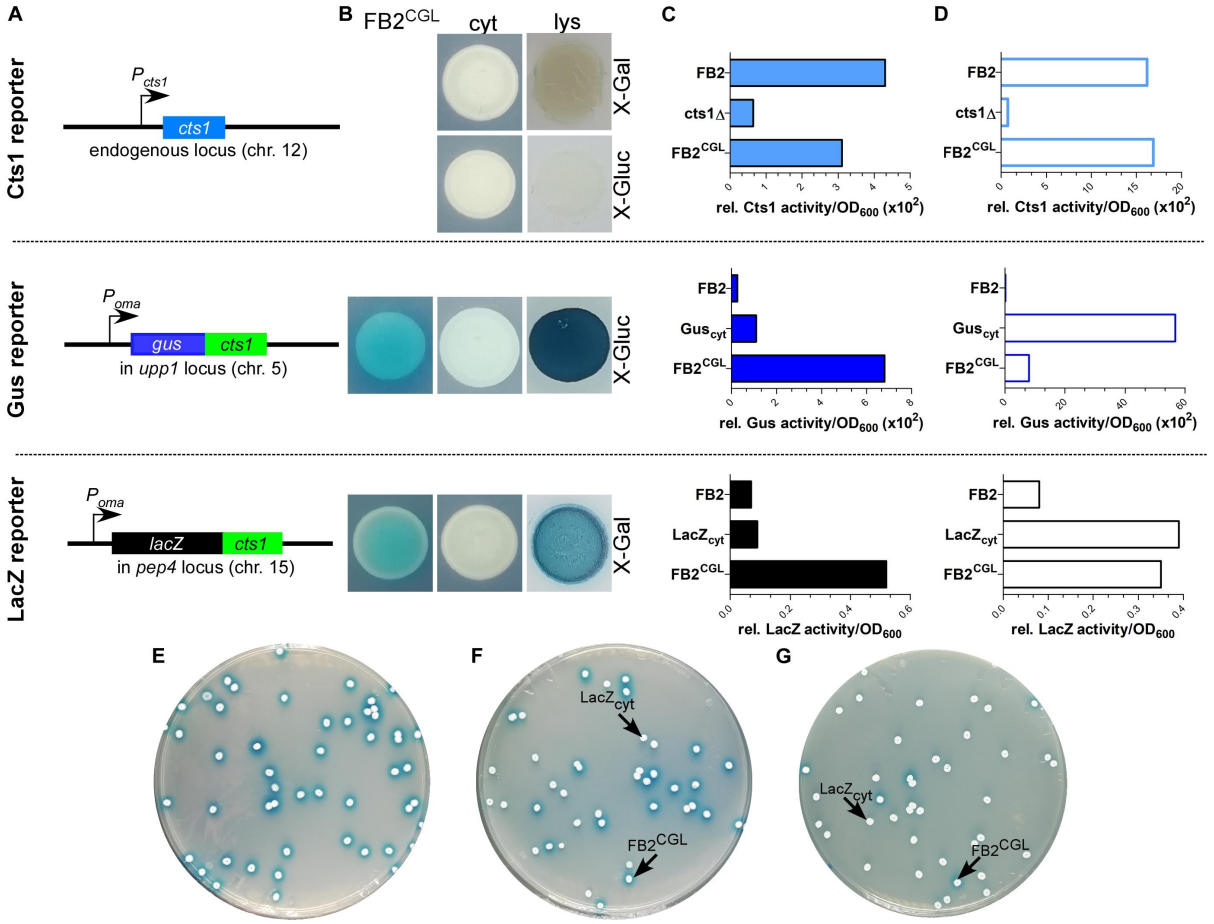


**Figure 5.2. Establishing screening strain FB2$^{CGL}$ harboring three reporters for unconventional secretion. (A)** Scheme of the genetic constructs for the three reporters present in distinct loci of *U. maydis* strain FB2$^{CGL}$. The reporter genes encoding endogenous Cts1 as well as Gus-Cts1 and LacZ-Cts1 are located on three different chromosomes (chr.). While the *cts1* gene on chr. 12 has not been modified and is present in its natural setup controlled by its native promoter active in yeast cells, both *lacZ:cts1* and *gus:cts1* gene fusions were inserted artificially by homologous recombination using described protease loci (Sarkari et al., 2014). Both translational fusion genes are hooked up to the strong synthetic promoter P$_{oma}$ which is constitutively active in yeast cells grown on CM-glc. Insertion of the two reporters results in deletion of the genes *upp1* and *pep4* which both encode harmful extracellular proteases (Sarkari et al., 2014). **(B)** Plate assay to determine the suitability of the used reporters in FB2$^{CGL}$ in comparison to the lysis controls FB2 Gus$_{cyt}$ and FB2 LacZ$_{cyt}$ harboring cytoplasmic reporter enzymes. FB2 was used as negative control containing neither Gus nor LacZ. X-Gluc and X-Gal were applied as colorimetric substrates for Gus and LacZ, respectively. To visualize intracellular reporter activity, cells were lysed using liquid nitrogen. cyt, control strains with intracellular reporter activity or absent reporter activity. lys, cells lysed by treatment with liquid nitrogen. **(C)** Liquid assays using the substrates MUG, ONPG and MUC to determine the suitability of the three reporters Gus-Cts1, LacZ-Cts1 and Cts1, respectively. 10 µg cell extracts of the indicated strains were used to assay intracellular reporter activities. Upper panel: Cts1 activity based on conversion of MUC; middle panel: Gus activity based on conversion of MUG; lower panel: LacZ activity based on conversion of ONPG. Each assay has been performed in one biological replicate. **(D)** Liquid assays using the substrates MUG, ONPG and MUC to determine the suitability of the three reporters Gus, LacZ and Cts1, respectively. Culture supernatants (Gus-Cts1/LacZ-Cts1) or intact cells (Cts1) of indicated strains were tested to determine extracellular reporter activities. Upper panel: Cts1 activity based on conversion of MUC; middle panel: Gus activity based on conversion of MUG; lower panel: LacZ activity based on conversion of ONPG. Each assay has been performed in one biological replicate. **(E-G)** Mixed culture experiments to verify applicability of the LacZ reporter for high-throughput screening on the colorimetric substrate X-Gal. Screening strain FB2$^{CGL}$ and control strain FB2 LacZ$_{cyt}$ were mixed in the indicated rations and plated onto indicator plates containing X-Gal to visualize extracellular LacZ activity (blue color). Photographs were taken after incubation for 1 d. **(E)** 100% FB2$^{CGL;}$ **(F)** 50% FB2$^{CGL}$/50% FB2 LacZ$_{cyt}$; **(G)** 10% FB2$^{CGL}$/90% FB2 LacZ$_{cyt}$.

In order to screen for diminished unconventional Cts1 secretion, strain FB2$^{CGL}$ was subjected to UV irradiation with approximately 1% survival rate (Figure 5.1, Figure S5.2). Mutagenized cells were plated on X-Gal plates to detect extracellular LacZ activity based on the reporter LacZ-Cts1. Approximately 185,000 colonies were screened with a focus on mutants that exhibited normal growth (i.e. normal colony size) but impaired Cts1 secretion. 2,087 candidate mutants showing strongly reduced or absent blue halos were patched on X-Gluc plates employing the Gus marker (Figure 5.1). Of those, 566 that stayed colorless again were retested in qualitative plate assays using both the LacZ and the Gus marker to confirm these results. To this end the mutant candidates were patched each on an X-Gluc and an X-Gal containing plate and the coloration was observed. 112 remaining colorless candidates were assayed for Cts1, Gus and LacZ activity in quantitative liquid assays using the substrates MUC, MUG and ONPG, respectively. The different enzyme activities of the progenitor strain FB2$^{CGL}$ were used as a baseline and set to 100%. Again, mutants showing reduced growth in liquid culture were sorted out to ensure that reduced secretion is not connected to growth problems. Multiple mutants displayed slight reduction in the extracellular activity of the reporters. In addition, three mutants were identified, in which Cts1, LacZ and Gus activity was present intracellularly, but diminished extracellularly (below 20% residual activity in all cases; FB2$^{CGL}$mut1-3; Table 5.1; Figure 5.3A,B). Western blot analysis confirmed equal protein amounts for LacZ-Cts1 and Gus-Cts1 in cell extracts of these mutants (Figure S5.4A). All three mutants showed wildtype growth rates suggesting that reduced secretion is not resulting from growth defects (Figure S5.4B).

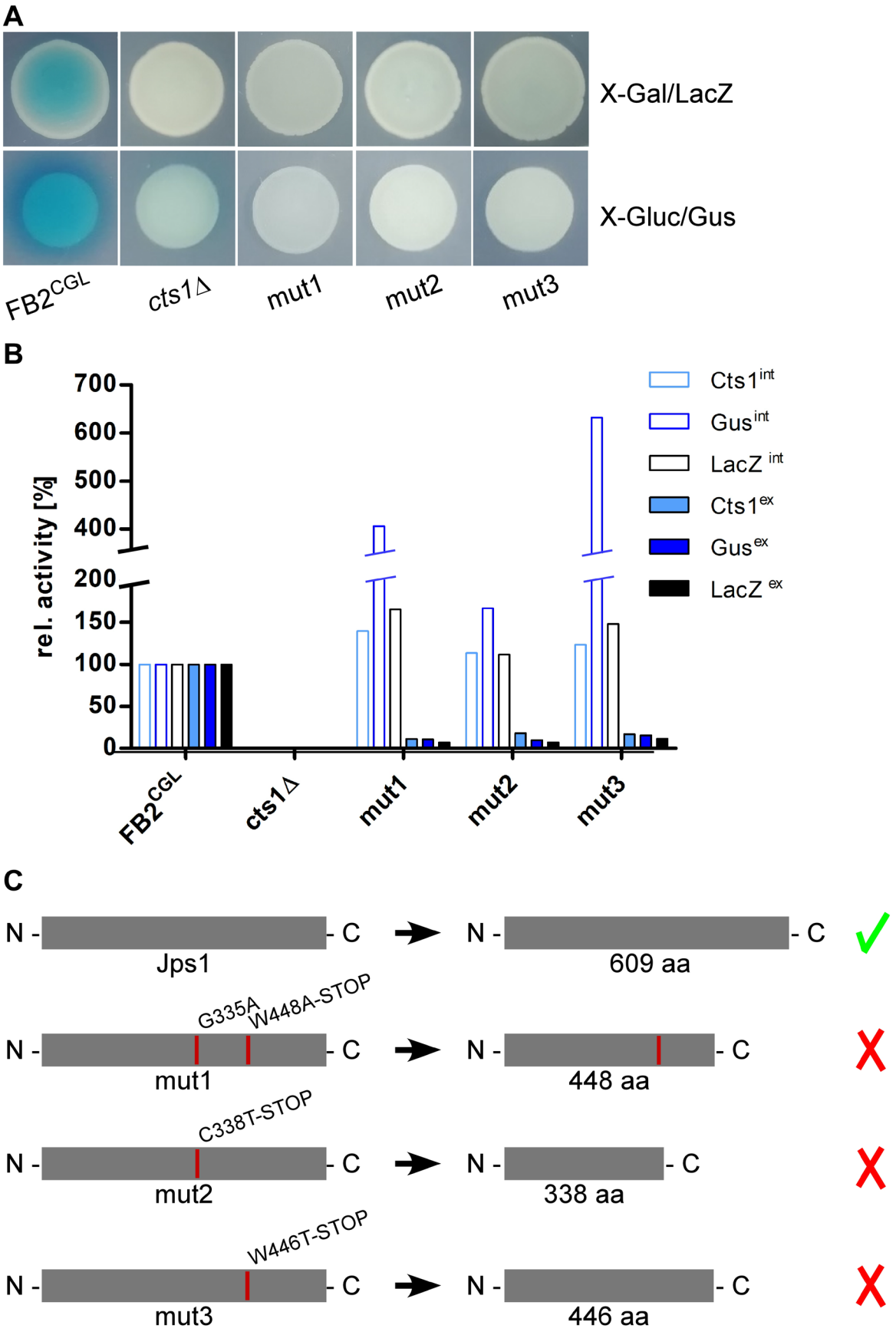


**Figure 5.3. The screen identifies the uncharacterized protein Jps1. (A)** Plate assays of indicated strains for extracellular LacZ activity using X-Gal and extracellular Gus activity using X-Gluc. The

assays are based on secretion of the reporters LacZ-Cts1 and Gus-Cts1 and the respective substrates are only converted, if the fusion protein is secreted. This leads to the formation of blue colonies (and blue halos in case of Gus) resulting from extracellular substrate conversion. Mutants FB2$^{CGL}$mut1, mut2 and mut3 were identified after UV mutagenesis of strain FB2$^{CGL}$ on screening plates (white colonies on both X-Gluc and X-Gal) and show the expected reduced extracellular activities indicating deficiency in Cts1 secretion. **(B)** Quantitative liquid assays detecting intracellular (int, filled columns) and extracellular (ex, open columns) Gus, LacZ and Cts1 reporter activity. Screening strain FB2$^{CGL}$ and a *cts1* deletion mutant (AB33 cts1Δ, 15) were used as positive and negative controls, respectively. Activities obtained for FB2$^{CGL}$ were set to 100% to allow for a direct comparison of all strains. The assay was conducted thrice with similar results and a representative replicate is shown. **(C)** In all three identified mutants, base exchanges in gene *umag_03776*, now termed *jps1*, were identified. At the aa level, mutations result in the introduction of premature stop codons leading to the production of truncated proteins in all three mutants. Mut1 carries an additional aa exchange at position 335. Mutations identified in FB2$^{CGL}$mut1-3 are indicated with red lines in the schematic representation of the protein. The size of native Jps1 is 609 aa. Modified from published figure: Arrangement was adapted.

To identify the responsible mutations whole genome sequencing was conducted for the first of the three identified UV mutants, FB2$^{CGL}$mut1, in comparison to its progenitor FB2$^{CGL}$ using the published sequence of *U. maydis* UM521 as a template for the assembly (Web reference: MycoCosm: *Ustilago maydis* 521). Whole genome sequence (WGS) information was deposited at DDBJ/ENA/GenBank under the accessions JABUOB000000000 and JABUOC000000000 (Web reference: WGS). A total of 32 base-pair substitutions were detected in the comparison of FB2$^{CGL}$ and FB2$^{CGL}$mut1. 9 single nucleotide polymorphisms (SNPs) were located in non-coding regions and were thus unlikely to cause the observed defect in unconventional secretion. The majority of the 23 mutations in coding regions were found to be 5´-C→T or 5´-CC→TT transitions which are expected for UV-induced mutations (Figure S5.5) (Pfeifer et al., 2005). 11 substitutions were irrelevant silent mutations. The remaining 12 SNPs led to 10 aa replacements in 9 encoded proteins and hence constituted the top remaining candidates (Figure S5.5). To locate which of these mutations was responsible for the defective Cts1 secretion, genetic back-crossing experiments were performed using plant infections. FB2$^{CGL}$mut1 was pathogenic in crosses with compatible FB1$^{CGL}$ which carries similar reporter genes but an opposite mating type (Figure S5.1; Figure S5.3; see Materials and Methods). Meiotic progeny was obtained and assayed for extracellular Gus, LacZ and Cts1 activity on indicator plates and by quantitative liquid assays. Based on these results the progeny was grouped into mutants with defective and intact secretion (Figure S5.6). Sequencing of the 9 candidate genes obtained from comparative genome sequencing revealed that all progeny with reduced extracellular reporter activity harbored mutations in gene *umag_03776* (Figure 5.3, Figure S5.6). Strikingly, as detected by PCR with specific primers for this gene and subsequent sequencing also the other two identified UV mutants, FB2$^{CGL}$mut2 and mut3, carried detrimental mutations in *umag_03776*, leading to synthesis of C-terminally truncated proteins (Figure 5.3C). This strongly suggested that this gene is essential for Cts1 secretion. The corresponding gene product was subsequently termed Jps1 (jammed in protein secretion screen 1). While the protein Jps1 has a predicted length of 609

aa, the truncated versions produced in mutants FB2$^{CGL}$mut1, mut2 and mut3 only contained 448, 338 and 446 aa, respectively (Figure 5.3C). In essence, we identified a crucial factor for Cts1 secretion by genetic screening.

### *5.4.2 Jps1 is essential for Cts1 localization and secretion*

Jps1 is annotated as hypothetical protein with unknown function (Web reference: MycoCosm: *Ustilago maydis* 521) and does not contain yet known domains (Web reference: SMART). None of its homologs in other Basidiomycetes has been characterized so far and Ascomycetes like *S. cerevisiae* lack proteins with significant similarities. Thus, to obtain first insights into its function we initially validated the screen by deleting the respective gene in the background of laboratory strain AB33 (Brachmann et al., 2001) using homologous recombination (AB33jps1Δ). Microscopic analysis revealed that budding cells of the deletion strain had a normal morphology comparable to controls like AB33 or the chitinase deletion strain AB33cts1Δ (Figure 5.4A) (Langner et al., 2015). Chitinase assays showed strongly reduced extracellular activity, confirming the essential role of Jps1 for Cts1 secretion (Figure 5.4B). To analyze the localization of Cts1 in a *jpsΔ* background strain AB33 jps1Δ/CtsG expressing a functional Cts1-Gfp (Cts1G) fusion was generated (Figure 5.4C)(Koepke et al., 2011). Microscopic studies revealed that in contrast to its native localization in the fragmentation zone (Figure 5.4D) (Aschenbroich et al., 2019; Langner et al., 2015) the Gfp signal for Cts1G now accumulated intracellularly and at the septa (Figure 5.4E,F). Interestingly, in about 56% of the cases, the signal was detected at the primary septum only, while in the remaining 44% the signal was present at both septa (Figure 5.4G). Cts1G was never observed in the fragmentation zone of the *jps1* deletion strain (Figure 5.4H).

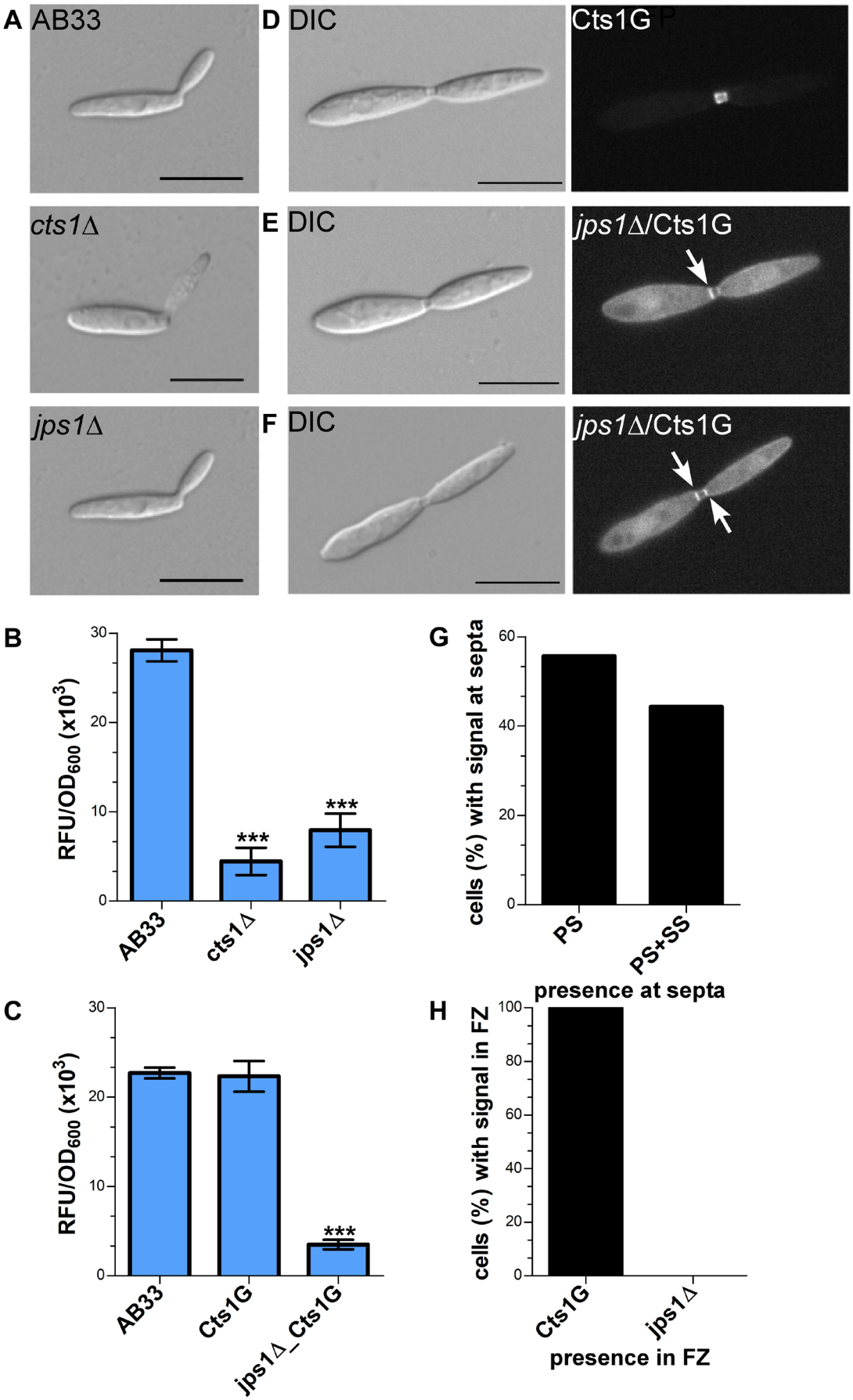
A AB33
D DIC
Cts1G
cts1Δ
E DIC
jps1Δ/Cts1G
jps1Δ
F DIC
jps1Δ/Cts1G
B
RFU/OD600 (x10^3)
AB33
cts1Δ
jps1Δ
***
***
C
RFU/OD600 (x10^3)
AB33
Cts1G
jps1Δ_Cts1G
***
G
cells (%) with signal at septa
PS
PS+SS
presence at septa
H
cells (%) with signal in FZ
Cts1G
jps1Δ
presence in FZ

**Figure 5.4. Jps1 is crucial for unconventional Cts1 secretion. (A)** Micrographs of yeast-like growing cells of indicated strains. The *jps1* deletion strain AB33jps1Δ (jps1Δ) does not show any morphological abnormalities. The *cts1* deletion strain AB33cts1Δ (cts1Δ) and the progenitor laboratory strain AB33 (wt) are shown for comparison. Scale bars, 10 µm. **(B)** *jps1* deletion in the AB33 verifies its essential function in Cts1 secretion. Extracellular Cts1 activity of AB33, AB33jps1Δ and the control AB33cts1Δ is depicted. The assay was conducted in three biological replicates. Error bars indicate standard deviation. ***, p value 0.001; n.s., not significant (two sample t-test). **(C)** Extracellular Cts1 activity of Cts1G expressing strains are comparable to the progenitor strain AB33, suggesting that the protein is functional. The assay was conducted in five biological replicates. Error bars indicate standard deviation. ***, p value 0.001; n.s., not significant (two sample t-test). **(D-F)** Localization of Cts1-Gfp (Cts1G) in AB33 **(D)** and AB33jps1Δ **(D,E)**. While Cts1 accumulates in the fragmentation zone of dividing cells with two septa in AB33 **(D)**, it enriches in the cytoplasm and at the septa in the *jps1* deletion strain. Two different scenarios were observed: Either Cts1 was found only at the primary septum at the mother cell side **(E)** or at both septa **(F)**. White arrows depict septa with Cts1 signal. Scale bars, 10 µm. **(G)** Distribution of Cts1G signal at the primary septum only (PS) and at both septa (PS+SS) of dividing AB33jps1Δ cells with completely assembled fragmentation zones (AB33Cts1G: 900 cells analyzed; AB33jps1Δ/Cts1G: 1370 cells analyzed; three biological replicates). **(H)** Cts1G is restricted from the fragmentation zone. The graph depicts the fraction of cells in exponentially growing cultures of indicated strains with Cts1G accumulation in the fragmentation zone (similar cells analyzed as shown in G). Modified from published figure: Arrangement was adapted.

Next, a strain expressing Jps1 fused to Gfp (Jps1G) was generated to localize the protein (AB33Jps1G). Chitinase assays verified the functionality of the fusion protein (Figure 5.5A). Intriguingly, microscopic analysis revealed that Jps1G accumulated in the fragmentation zone of budding cells, similar to Cts1 (Figure 5.5B). To investigate if Jps1 localization depends on chitinase function, Cts1 was deleted in the background of AB33JpsG (AB33cts1Δ/Jps1G). Interestingly, this did not disturb Jps1 localization. This suggests that Cts1 is dispensable for Jps1 function but not *vice versa*, indicating a unidirectional dependency of Cts1 on Jps1. To further substantiate the apparent co-localization, both proteins were differentially tagged in a single strain, expressing Jps1 fused to mCherry and Cts1 fused to Gfp (AB33Cts1G/Jps1mC). Indeed, both signals completely overlapped in the fragmentation zone in each observed case (Figure 5.5D, E). Since the co-localization studies suggested that the two proteins might interact we conducted yeast two-hybrid assays in which we fused Jps1 with the activation domain (AD) and Cts1 with the binding domain (BD), and *vice versa*. Self-interaction could be detected neither for Jps1 nor for Cts1. A weak interaction between Jps1 and Cts1 could be observed for one of the combinations, namely for BD-Cts1 and AD-Jps1 in serial dilutions on selection plates. We hypothesize that in the other combination (AD-Cts1 and BD-Jps1) the architecture of one of the N-terminal fusions interferes with the interaction of the proteins. Albeit this little inconsistency which needs to be resolved by alternative experimental approaches in the future, the result supports our idea that the two proteins might interact (Figure 5.5F).

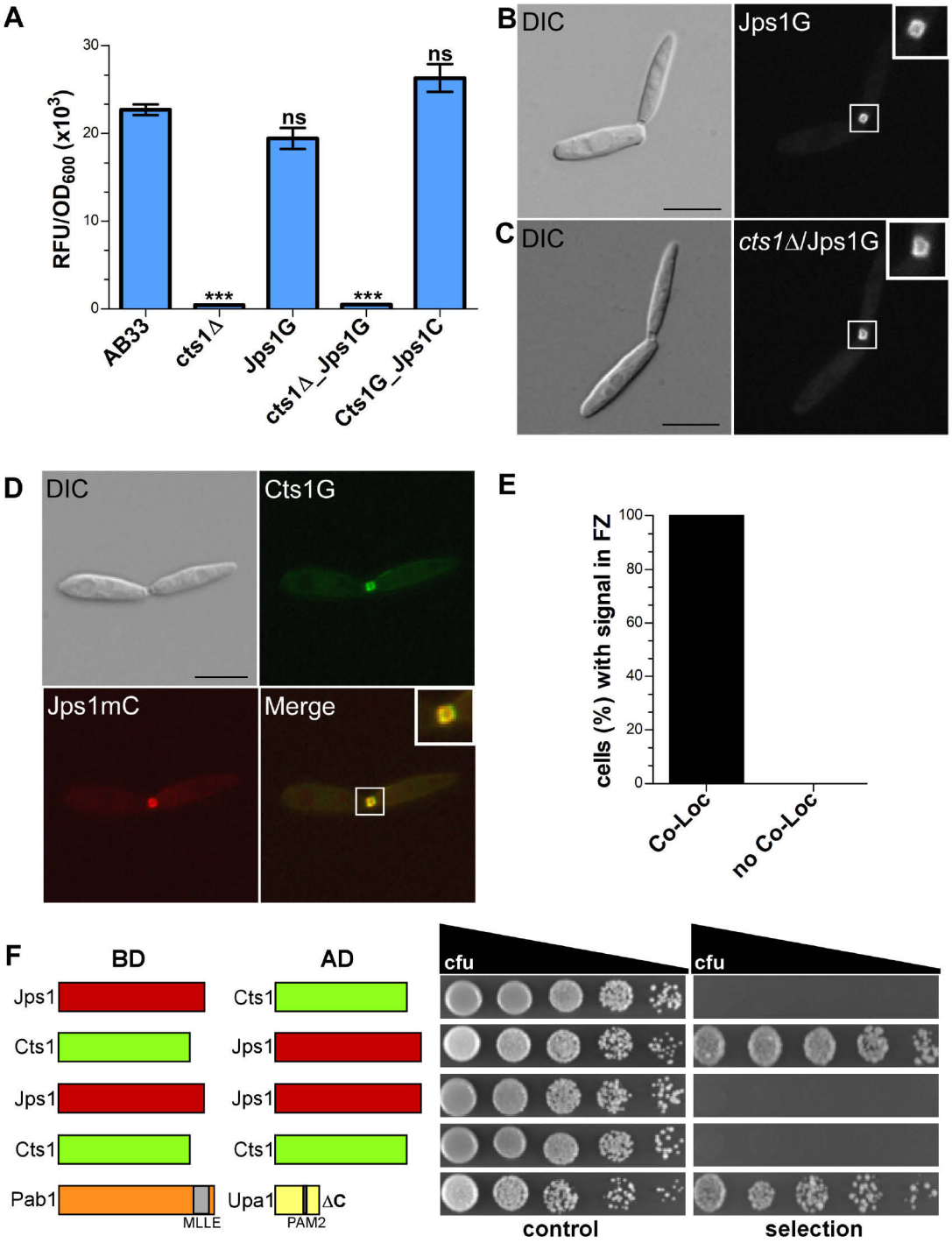


**Figure 5.5. Jps1 co-localizes with Cts1 in the fragmentation zone. (A)** Extracellular Cts1 activity of indicated strains. AB33cts1Δ lacking Cts1 was used as negative control. The Jps1mC fusion protein is functional. The assay was conducted in five biological replicates. Error bars indicate standard deviation. ***, p value 0.001; n.s., not significant (two sample t-test). **(B)** Localization of Jps1G in AB33. The protein accumulates in the fragmentation zone of dividing cells. Scale bar, 10 µm. **(C)** Localization of Jps1G in AB33cts1Δ. Localization of Jps1 in the fragmentation zone is not altered in the absence of Cts1. Scale bar, 10 µm. **(D)** Micrographs of strain AB33Cts1G/Jps1mC indicating co-localization of Cts1G and Jps1mC in the fragmentation zone. **(E)** Quantification of co-localizing signals (Co-Loc) and not co-localizing signals (No Co-Loc) of strain AB33Cts1G/Jps1mC in the fragmentation zones of 970 cells observed. The experiment was conducted in 3 biological replicates with identical outcomes. Not a single cell with differing observations than indicated was detected. **(F)** Yeast-two hybrid assays to analyze protein:protein interactions between Jps1 and Cts1. For the positive control using strains producing Pab1 and Upa1 a weak interaction had been shown before (Pohlmann et al., 2015). BD, binding domain; AD, activation domain.

Thus, our genetic screen identified a novel essential protein for unconventional Cts1 secretion. Co-localization and the putative interaction between Jps1 and Cts1 suggest that Jps1 might act as an anchoring factor for Cts1 that supports its local accumulation in the fragmentation zone.

## 5.5 Discussion

In this study we identified Jps1, a novel factor essential for unconventional export of chitinase Cts1 in budding cells. Jps1 was identified in a forward genetic screen. Such genetic screens are powerful tools to identify important players in unknown pathways (Forsburg, 2001). The prime example is the screen for components of the conventional secretion pathway which has been performed in *S. cerevisiae*. Initially, this temperature-sensitive screen was based on the fact that proteins accumulate in the endomembrane system of cells in which secretion is disturbed. These dense cells can be separated from cells with intact secretion by gradient centrifugation (Novick et al., 1980). The screen was continuously further developed and finally provided a detailed view on the key components of the canonical pathway including all stages of protein export (Mellman & Emr, 2013). Similarly, the here employed screen proved to be very efficient and powerful: in all three obtained mutants, mutations localized to the same gene (*jps1*). On the one hand, this underlines the quality of the screening procedure. On the other hand, this observation may also limit the screen in that other factors may be hard to identify in this screening set up. Alternatively, the repeated identification of the same mutant could be due to the fact that there is only one major factor involved in Cts1 secretion. However, we consider that unlikely. Therefore, in the next step a second copy of Jps1 under its native promoter will be inserted into the genome. This will minimize the risk of identifying the gene again in further screening attempts. Furthermore, we will streamline identification of responsible mutations. Here, we used genetic back-crosses via plant infection in combination with a PCR approach to identify Jps1. For future studies, we will use batch-sequencing of mutants with or without secretion of the reporters (Figure S5.2 steps 10 & 11). Such pooled linkage analysis based on next-generation sequencing is known to have a great statistical power and thus allows an efficient identification of underlying mutations (Birkeland et al., 2010).

In the first screening round we concentrated on mutants that showed a normal growth behavior (i.e. colony sizes similar to untreated cells after UV mutagenesis). Mutants that are impaired in growth are much more complicated to analyze. Discrimination between true secretory defects and reduced secretion due to poor fitness of the cells is very difficult. Hence, it is well conceivable that we missed other important factors, especially because

unconventional Cts1 secretion is tightly connected to cytokinesis (Aschenbroich et al., 2019). This also explains why we did not identify mutants defective in the septation factors Don1 or Don3 which we have shown to be essential for unconventional Cts1 secretion (Aschenbroich et al., 2019). The cognate deletion mutants have a cytokinesis defect and grow in tree-like structures (Weinzierl et al., 2002).

As an alternative application, the screen will be employed to optimize our recently established protein expression platform (Feldbrügge et al., 2013; Sarkari et al., 2016). Here we use Cts1 as a carrier for valuable heterologous proteins. Exploiting the unconventional secretion route brings the advantage that *N*-glycosylation is circumvented and thus, sensitive proteins like bacterial enzymes can be exported in an active state (Sarkari et al., 2014; Stoffels et al., 2020; Terfrüchte et al., 2017). The screen will be adapted to select for mutants with enhanced marker secretion to eliminate existing bottlenecks and thus enhance yields (Terfrüchte et al., 2018). Random mutagenesis screens for hypersecretors were for example key to establish industrial production strains like the cellulase producing filamentous fungus *Trichoderma reesei* strain RutC-30 in which amongst further changes carbon catabolite repression was eliminated (Peterson & Nevalainen, 2012). A restriction enzyme mediated insertion (REMI) screen based on a β-galactosidase reporter has also led to the discovery of a set of mutants showing supersecretion of the reporter in *Pichia pastoris* (Larsen et al., 2013).

Our findings are in line with the proposed lock-type secretion mechanism (Aschenbroich et al., 2019; Reindl et al., 2019). Jps1 supports the subcellular accumulation of Cts1 in the fragmentation zone from where it is likely released (Aschenbroich et al., 2019). While the secretory pathway itself is new, it is conceivable that the molecular details of Cts1 export might be similar to described systems. For example, it could be released via self-sustained translocation through the plasma membrane which has been described for FGF2, but is nowadays discussed also for other proteins like HIV-Tat and interleukin 1beta (Dimou & Nickel, 2018). In the future, biochemical studies will shed light on the molecular pathway of unconventional Cts1 secretion. Interestingly, Jps1 orthologs are restricted to the Basidiomycetes. Hence, lock-type secretion is likely conserved at least in the Ustilaginales like *Sporisorium reilianum*, *Ustilago hordei*, *Pseudozyma aphidis* or *Tilletia walkeri*. This assumption is supported by the finding that Cts1 orthologs lacking predictions for N-terminal signal peptides are also present in these species. Unfortunately, published information about the yeast-like growth of these fungi and potential formation of fragmentation zones is yet scarce. The absence of Jps1 orthologs in *S. cerevisiae* and other Ascomycetes, fits well to the observation that septation in *S. cerevisiae* does not involve formation of a fragmentation zone, suggesting that molecular details of cell division differ between the two organisms (Reindl et al., 2019).

Jps1 is essential for efficient Cts1 localization and secretion while in turn Cts1 is not needed for Jps1 accumulation in the fragmentation zone. This one-sided dependency indicates that Jps1 is an important factor for Cts1 secretion but not *vice versa*. The underlying molecular details and thus the exact role of Jps1 during Cts1 secretion remain to be addressed by detailed biochemical and cell biological studies in the future. It is also not clear how the two proteins reach the fragmentation zone. Moving early endosomes enrich in the fragmentation zone prior to budding and were shown to carry Don1 (Schink & Bölker, 2009; Weinzierl et al., 2002). They are thus prime candidates for transporting proteins into the small compartment. However, we neither observed Cts1 nor Jps1 on these motile organelles (data not shown). While the septation factors Don1 and Don3 seem to play a passive role for Cts1 release by sealing off the fragmentation zone with the secondary septum, Jps1 acts as a third factor which is likely directly involved in the export process. Based on our results, it is conceivable that Jps1 functions as an anchoring factor for Cts1, thus supporting its local accumulation in the fragmentation zone where it likely degrades remnant chitin together with conventionally secreted Cts2 to support cytokinesis (Figure 5.6). In sum, our genetic screen has already proven to be very efficient and an improved version will deal as a basis to identify further key components of unconventional secretion and optimize the connected protein expression platform in the future.

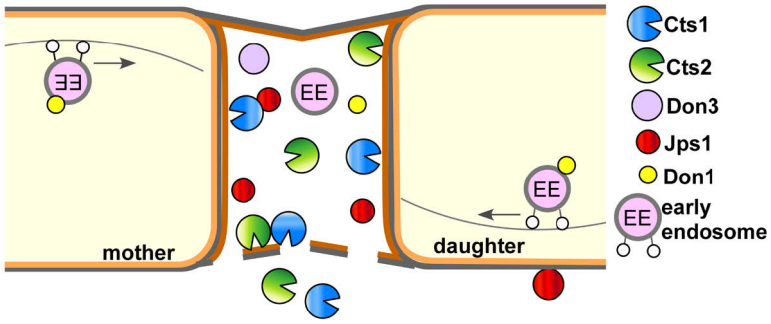


**Figure 5.6. Current model for subcellular targeting and unconventional secretion of Cts1 via anchoring factor Jps1.** Cts1 is targeted to the fragmentation zone via an unconventional secretion mechanism. Motile early endosomes shuttle bidirectionally through the cells and transport the septation factor Don1 which is essential for secondary septum formation. Together with Don3 it localizes to the fragmentation zone formed between mother and daughter cell during cytokinesis. Both Don1 and Don3 are crucial for Cts1 export. The newly identified factor Jps1 also accumulates in the fragmentation zone. We hypothesize that the protein functions in anchoring Cts1 in the small compartment. Here, Cts1 acts in degrading remnant chitin for detaching mother and daughter cell in concert with conventionally secreted Cts2.

***Keywords***
forward genetic screen, β-galactosidase, β-glucuronidase, unconventional secretion, *Ustilago maydis*, UV mutagenesis.

***Author Contributions***
J.S. designed, conducted and evaluated the genetic screen with support of M.R., **K.H.** and A.G., M.R. characterized Jps1 and prepared micrographs, quantifications and enzyme assays. A.B. performed

genome sequencing. K.S. prepared the manuscript with input of all co-authors, directed the project and acquired funding.

***Funding***
This work was funded by the Deutsche Forschungsgemeinschaft (DFG, German Research Foundation) – Projektnummer 267205415 – SFB 1208 (M.F., K.S., M.R.). The scientific activities of the Bioeconomy Science Center were financially supported by the Ministry of Culture and Science within the framework of the NRW Strategieprojekt BioSC (No. 313/323-400-002 13).

***Acknowledgments***
We acknowledge Dr. M. Feldbrügge for continuous support and valuable discussion. We thank B. Axler and U. Meyer for excellent technical support of the project. T.E. Hyland and L. Mielke contributed to the project in the framework of an internship and M. Tulinski and S. Wolf in their Master projects. This manuscript has been released as a pre-print at bioRxiv.

***Data Availability Statement***
This Whole Genome Shotgun project has been deposited at DDBJ/ENA/GenBank under the accessions JABUOB000000000 and JABUOC000000000. The versions described in this paper are JABUOB010000000 and JABUOC010000000.

## 5.6 Supplementary data

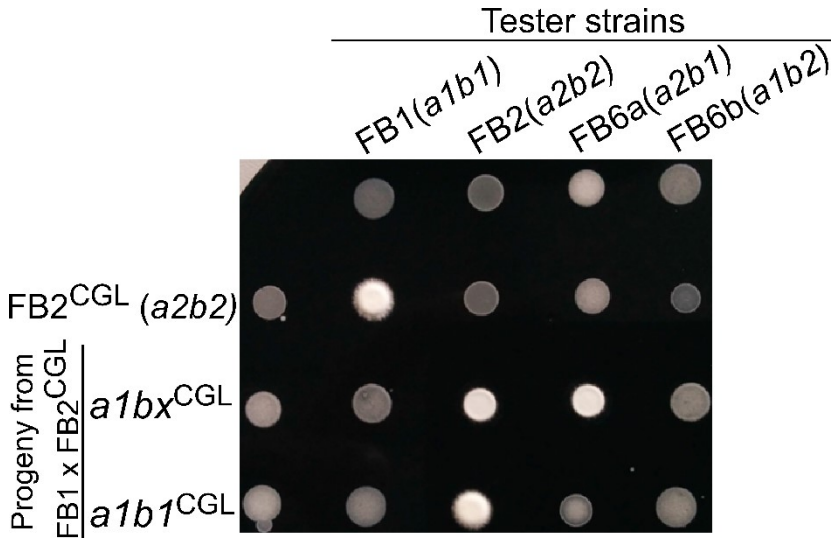


**Figure S5.1. Mating assay to identify FB1$^{CGL}$ with *a1b1* mating type harboring the reporter LacZ-Cts1 and Gus-Cts1 using charcoal plates.** Mating of compatible strains was observed on CM-charcoal plates. Fuzzy colonies indicate mating while smooth colonies show incompatibility. FB1 (mating type *a1b1*), FB2 (mating type *a2b2*), FB6a (mating type *a2b1*) and FB6b (mating type *a1b2*) are tester strains with known genotypes. Progeny carrying the two reporters Gus-Cts1, LacZ-Cts1 was obtained by crossing the screening strain FB2$^{CGL}$ with wild type strain FB1 and tested for mating to identify an *a1b1* clone. One clone of the two displayed clones has an *a1b1* mating type because it shows a fuzzy colony with FB2 but not with FB6a (strain termed FB1$^{CGL}$). This strain was used for genetic back-crosses with mutagenized FB2$^{CGL}$ during the screen.

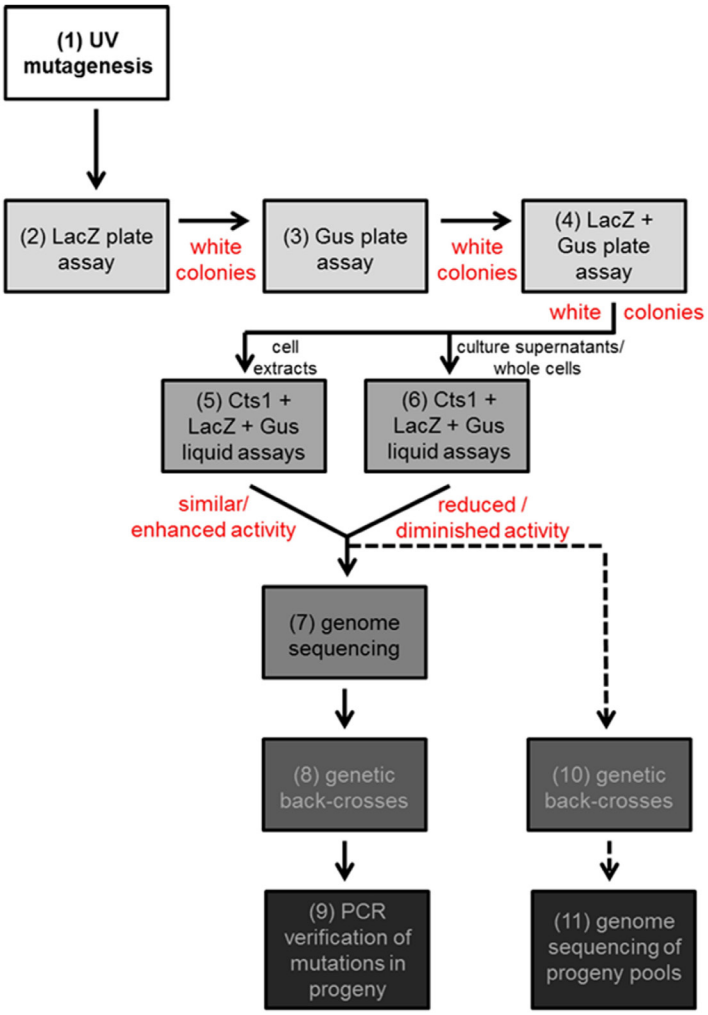


**Figure S5.2. Detailed step-by-step description of the forward genetic screen.** All steps performed to identify factors for unconventional secretion of chitinase Cts1 are indicated in detail. First of all, cells were mutagenized by UV light (1). Next, plate assays were performed (2-4). Initial screening of the mutagenized cells was conducted on X-Gal containing plates (2). White colonies lacking extracellular LacZ activity were then subjected to further plate assays on both X-Gal and X-Gluc (3, 4). Colonies that stayed white on both substrates were analyzed in detail using quantitative liquid assays with substrates for all three unconventional secretion reporters (Cts1, LacZ-Cts1, Gus-Cts1) (5,6). Both intra- (5) and extracellular activities (6) were determined. Genome sequencing and alignment with the progenitor strain $FB2^{CGL}$ revealed multiple mutations (candidate loci) likely resulting from UV treatment (7). Genetic back-crosses with a non-mutagenized FB1 derivative harboring all three reporters ($FB1^{CGL}$) were performed and led to progeny showing defective unconventional secretion while harboring cytoplasmic activity for all three reporters (8). Amplification and sequencing of the candidate loci identified in the alignment identify the responsible mutation (9). In future studies, progeny of the back-crosses could also be pooled according to the absence or presence of unconventional secretion. Genome sequencing of the two pools should also reveal the responsible mutation (10,11).

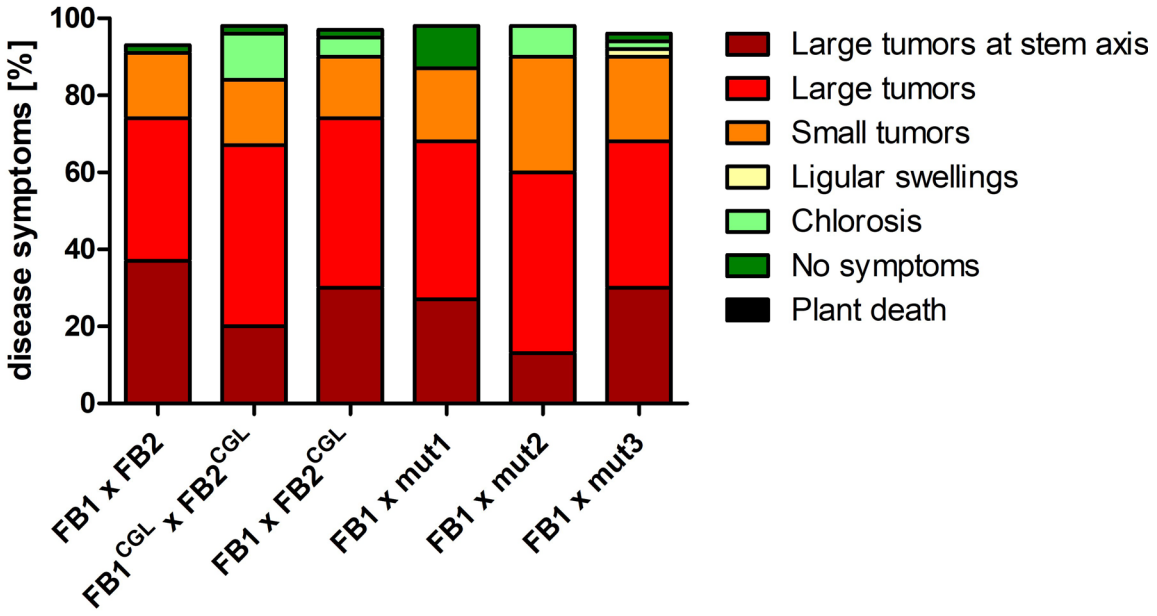


**Figure S5.3. Plant infections with compatible FB1 and FB2 derivatives.** Maize seedlings were inoculated with the indicated compatible strains and disease symptoms scored 7 days post infection. The infection was performed once with 40 plants each. All tested strain combinations were pathogenic and showed symptoms comparable to the wild type cross FB1 (*a1b1*) x FB2 (*a2b2*).

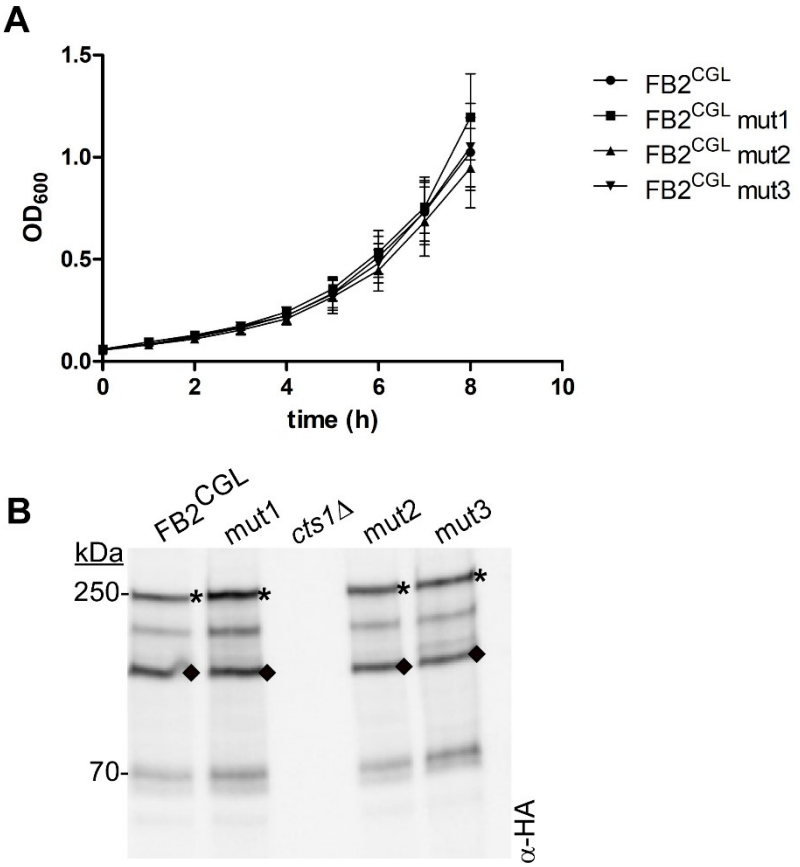


**Figure S5.4. Mutants impaired in Cts1 secretion grow normal and produce similar levels of Gus-Cts1 and LacZ-Cts1 as the screening strain FB2$^{CGL}$. (A)** Growth curves of FB2$^{CGL}$ and the indicated UV mutants. Growth was followed by determining the optical density at 600 nm for eight hours. All strains duplicate with comparable rates. **(B)** Western blot detecting Gus-Cts1 and LacZ-Cts1 levels in FB2$^{CGL}$ and the indicated UV mutants. Antibodies directed against the HA-tag in the SHH linker of the fusion proteins were used for detection. Asterisks and rhombs depict the expected sizes of the fusion proteins LacZ-Cts1 and Gus-Cts1, respectively. A strain lacking the reporters was used as negative control (AB33 *cts1*Δ).

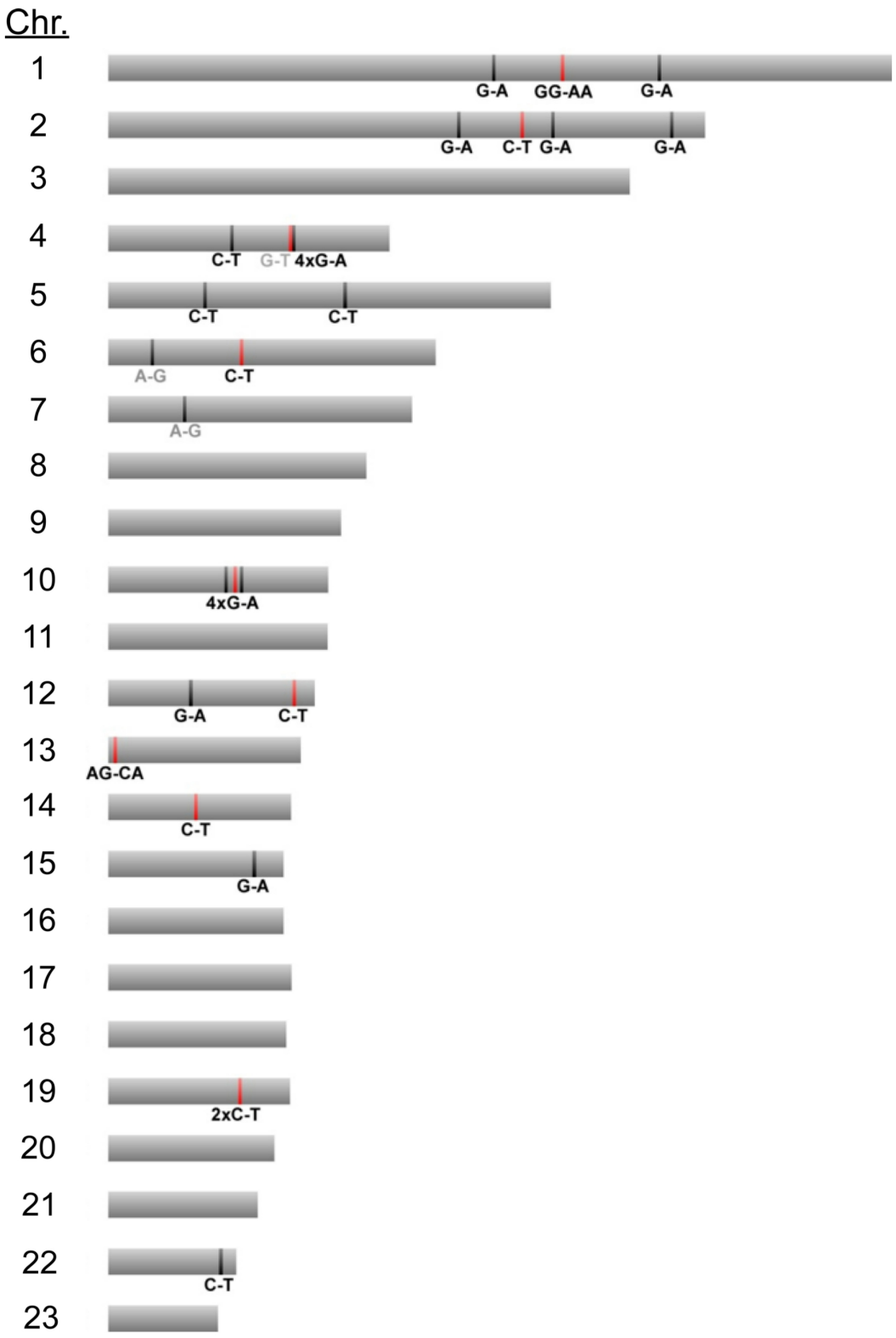


**Figure S5.5. SNPs identified in genome sequence comparisons between screening strain FB2$^{CGL}$ and mutant candidate FB2$^{CGL}$mut1.** The schematic representation shows all 23 chromosomes. Bars depict 32 base changes detected in FB2$^{CGL}$mut1 compared to its progenitor FB2$^{CGL}$. Red bars indicate 12 mutations which go along with amino acid replacements in 9 ORFs and are thus candidates likely responsible for the observed defective secretion. Unexpected base transitions are indicated in grey letters while black letters depict transitions typically observed after UV treatment. Figure dimensions are not to scale.

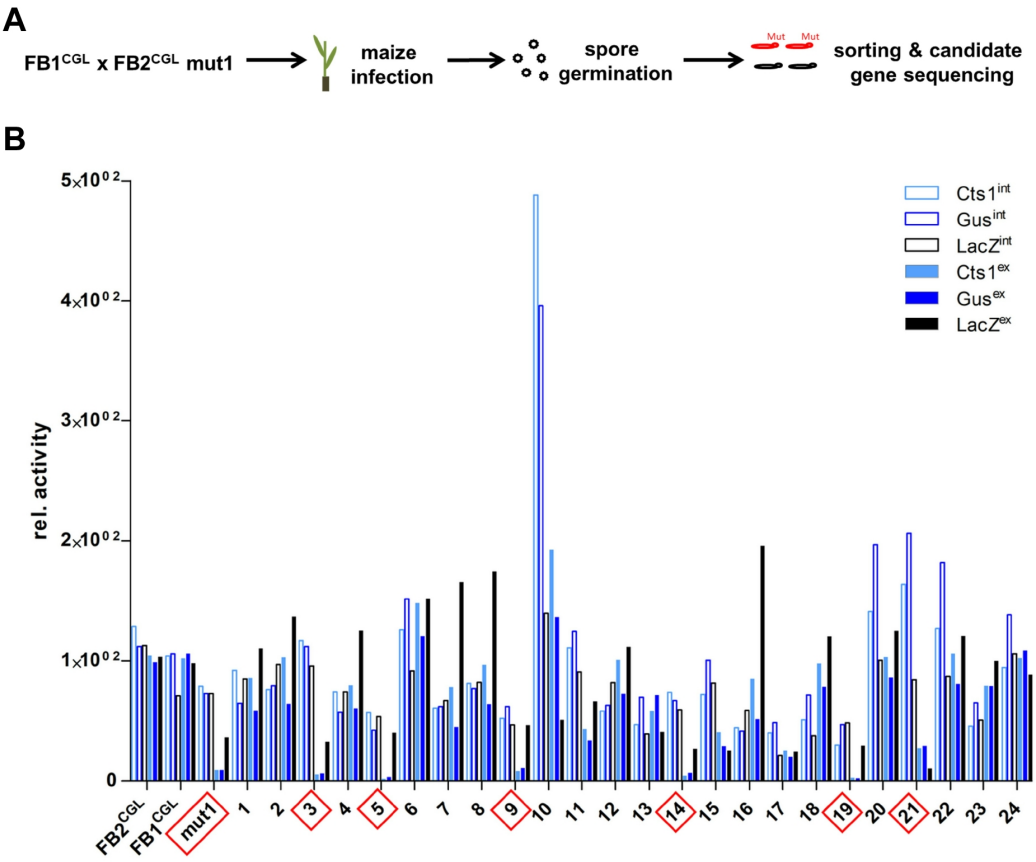


| | Progeny FB1$^{CGL}$ x FB2$^{CGL}$ (# artificially numbered) |
|---|---|
| **Progeny with intact Cts1 secretion** | #1, #2, #4, #6, #7, #8, #10, #11, #12, #13, #15, #16, #17, #18, #20, #22, #24 |
| **Progeny with defective Cts1 secretion** | #3, #5, #9, #14, #19, #21 |

**Figure S5.6. Extracellular Cts1 activity of progeny from the genetic cross of FB1$^{CGL}$ and FB2$^{CGL}$mut1. (A)** Back-crossing strategy to allow for identification of responsible mutations in strain FB2$^{CGL}$mut1. Spores obtained after crossing FB1$^{CGL}$ and FB2$^{CGL}$mut1 were germinated and singled out. Single colonies were sorted into two groups (extracellular reporter activity: yes/no) by assaying extracellular reporter activities on X-Gal and X-Gluc plates and by liquid Cts1 assays with whole cells. **(B)** Liquid Gus, LacZ and Cts1 assays to sort progeny obtained from FB1$^{CGL}$ and FB2$^{CGL}$mut1 crosses. Both extracellular (ex, filled columns) and intracellular (int, open columns) activities were determined. Numbers (#) indicate the different clones obtained from germinated spores. The progenitor strains FB2$^{CGL}$, FB2$^{CGL}$mut1 and FB1$^{CGL}$ were used as references for normal and strongly diminished unconventional secretion. Clones with strongly reduced extracellular activities for all three reporters are listed in C and were used for sequencing. **(C)** Progeny groups obtained after genetic back-crossing based on the results shown in **(B)**. **(D)** Sequencing of diagnostic PCR products was conducted on progeny which did not show extracellular reporter activity using primers that encompass the 12 potential mutations leading to aa exchanges in 9 ORFs. Sequencing revealed mutagenized *umag_03776* to be responsible for the reduction in unconventional secretion. Red: candidate locus mutagenized; green: candidate locus wildtypic.

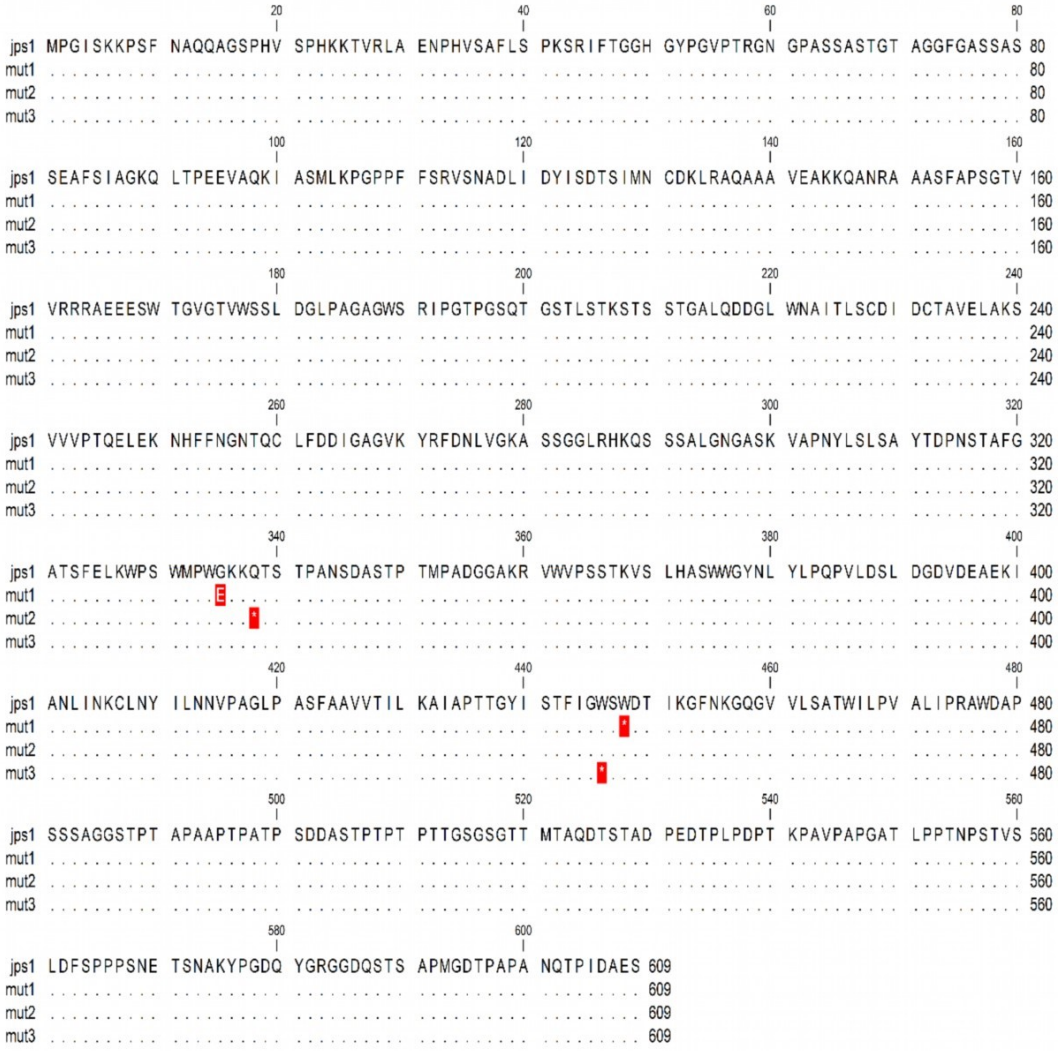


**Figure S5.7. Aa alignment of Jps1 wild type protein and three mutant versions obtained in the UV mutagenesis for candidates with diminished Cts1 secretion.** Red background color indicates aa changes in the mutants in comparison to the native protein (upper line). Asterisks depict stop codons. Mutations result in the production of C-terminally truncated proteins (compare Figure 5.3). Numbers show base pair counts.

# 6 Isolation of *Ustilago maydis* mutants with enhanced capacity for unconventional export of heterologous proteins

**Kai P. Hussnaetter** [1], Magnus Philipp [1], Janpeter Stock [1,#], Tobias Busche [2], Daniel Wibberg, Jörn Kalinoswki [2], Andreas Brachmann [3], Michael Feldbrügge [1], and Kerstin Schipper [1,*]

[1] Institute for Microbiology, Heinrich Heine University Düsseldorf, Düsseldorf, Germany
[2] Centrum für Biotechnologie – CeBiTec, Universität Bielefeld, Bielefeld, Germany
[3] Genetics, Faculty of Biology, Ludwig-Maximilians-Universität München, Planegg-Martinsried, Germany
[#] present address: NUMAFERM GmbH, Merowingerplatz 1a, 40225 Düsseldorf, Germany
* Corresponding author: E-mail: kerstin.schipper@uni-duesseldorf.de (KS)

This manuscript has been prepared for this thesis and has not undergone a peer-review process yet.

**Relevance of publication**

To isolate different mutants with an increased unconventional secretion capacity, a recently established high-throughput forward genetic screen was adapted. To this end, at least four different hyper secretion candidates showed enhanced unconventional secretion of three different reporter proteins. Sequencing of individual candidates revealed variable amounts of mutations and rate of mutations with UV-signature, indicating need for further standardization and optimization of the method. Aiming at further identification of underlying mutations, pooled linkage analysis of meiotic progeny was conducted for one hyper secretion mutant to distinguish relevant mutation from other random mutations. Interestingly, a strong bias to one parental strain was observed, which needs further investigation regarding distribution of genomes upon meiosis. While the exact underlying mutation or reassembly remained hidden, this elaborated first round of the genetic screen provided important insights in bottlenecks in performance and analysis. Further solutions as well as application of isolated hyper secretion mutations should help towards identification of hyper secretion factors.

## 6.1 Abstract

Recombinant proteins have important industrial, pharmaceutic, and academic applications and are thus highly demanded. To efficiently produce each requested protein, novel expression systems beyond established platforms need to be developed. A promising new host is the model fungus *Ustilago maydis*. In the past years, we have established a protein expression system based on unconventional secretion in this organism. To generate a competitive protein production host, different optimization strategies were conducted successfully. However, yields are currently still limiting. Therefore, we adapted a forward genetic screen for the identification of hyper secretor mutants. UV mutagenesis and subsequent screening led to isolation of four hyper secretion candidates in which the unconventional secretion capacity was increased up to four-fold. Meiotic crossings followed by pooled linkage sequence analysis of hyper secretion progeny from one mutant revealed i) a strong sequence bias towards one of the parental strains and ii) presumably a larger region affected by mutagenesis rather than a point mutation responsible for increased secretion. The identification of the relevant sequence modification is pending. In summary, four individual hyper secretion candidates were isolated and characterized. Important insights in potential limitations of the genetic screen and solutions for their elimination were achieved, facilitating future optimization of high-throughput screening and evaluation of hyper secretion candidates.

## 6.2 Introduction

The industrial need for recombinant proteins is tremendous and applications range from high prized medical or diagnostic proteins to bulk products: The product portfolio ranges from monoclonal antibodies to hydrolytic enzymes, catalysts, or proteases and lipases for washing agents (Hermann & Patel, 2007; Jaeger & Eggert, 2002; Leisola et al., 2001; Spadiut et al., 2014; Woodley, 2020). Currently, various protein expression platforms exist and production hosts range from prokaryotic and eukaryotic microbes to insect or mammalian cell culture and cell-free systems (Farrokhi et al., 2009; Gopal & Kumar, 2013; Mattanovich et al., 2012; O'Flaherty et al., 2020; Tripathi & Shrivastava, 2019). However, some proteins are not efficiently produced in the existing expression platforms. Thus, new systems with unique features are continuously developed to occupy prevailing niches (Saccardo et al., 2016).

Secretion of heterologous proteins into the medium notably simplifies downstream processing (Flaschel & Friehs, 1993). Therefore, its application is advantageous especially in biotechnological processes. For secreted proteins of interest, purification is cost-efficient and straightforward as contaminating or unwanted proteins are less abundant in the supernatant and adverse effects of accumulated heterologous protein inside the cell are avoided (El-

Enshasy, 2007; Nicaud et al., 1986). Protein secretion describes in general the process of protein translocation from the intracellular space to the supernatant across the plasma membrane. In eukaryotes, proteins designated for conventional secretion carry an N-terminal signal peptide that facilitates translocation to the endomembrane system (Rabouille, 2017; Viotti, 2016). While secretion of most proteins is mediated via this conventional mechanism, several proteins have been described to bypass the endomembrane route via alternative mechanisms (Nickel, 2005; Nickel & Rabouille, 2009). Described routes are very diverse and can be distinguished in non-vesicular and vesicular pathways (Rabouille et al., 2012). Non-vesicular pathways are defined by direct translocation of proteins across the plasma membrane (Nickel, 2010). This is facilitated either by self-sustained protein translocation or by ABC transporters (Rabouille et al., 2012). Vesicular unconventional secretion pathways involve intracellular vesicular intermediates such as secretory lysosomes, microvesicles or multivesicular bodies (Nickel & Rabouille, 2009; Rabouille et al., 2012). Proteins that enter the endoplasmic reticulum (ER) via a signal peptide but bypass the Golgi apparatus are also included in this group (Rabouille, 2017). Unconventional secretion is largely triggered by cellular stress and exported proteins are often involved in cell survival, immune response and tissue organization (Rabouille, 2017; Rabouille et al., 2012). Alternative secretion routes offer several advantages since they avoid critical post-translational modification steps in the endomembrane system (Nickel, 2010).

To further expand the repertoire of production systems for particular proteins we have established a novel expression system in the model fungus *Ustilago maydis*. This organism uses an unconventional secretion system to export the chitinase Cts1 (Koepke et al., 2011; Stock et al., 2012). *U. maydis* is a fungus, which possess two growth forms, the saprotrophic yeast and an infectious hyphal form causing corn smut disease. In its yeast form, Cts1 secretion is coupled to cytokinesis. Prior to cell division, Cts1 accumulates in a small compartment, the so-called fragmentation zone, connecting mother and daughter cell (Langner et al., 2015; Reindl et al., 2019). Here, Cts1 presumably functions in separating mother and daughter cell by hydrolyzing the connecting cell wall in concert with a second chitinase, Cts2 (Langner et al., 2015). Interestingly, while Cts2 is secreted conventionally, Cts1 lacks an N-terminal signal peptide and therefore bypasses the endomembrane system (Koepke et al., 2011). Exploiting the mechanism of unconventional secretion by using Cts1 as a carrier can be a powerful tool for those heterologous proteins, whose production via the conventional secretion pathway causes major problems. Such problems include post-translational modifications like the attachment of sugar moieties in the process of *N*-glycosylation during the passage of the endomembrane system which can have devastating effects on the produced protein such as decreased stability (Tull et al., 2001), inactivation of enzyme activity (e.g. for bacterial enzymes) (Stock et al., 2016) or elicitation of allergic

reactions in pharmaceutical applications (Walsh & Jefferis, 2006). Furthermore, unconventional secretion allows for export of large proteins of at least 173 kDa (Stock et al., 2012). First milestones showed the potential of this system in *U. maydis*: Successful production and secretion of carbohydrate-active enzymes (Stoffels et al., 2020), single-chain antibodies (Sarkari et al., 2014) and nanobodies (Terfrüchte et al., 2017), or bacterial enzymes like β-galactosidase and β-glucuronidase (Reindl et al., 2020; Stock et al., 2012) was achieved.

Recently, a forward genetic screen based on UV mutagenesis was applied to elucidate components essential for Cts1 secretion by identifying mutants deficient in unconventional secretion. As a read-out, UV mutagenized cells were analyzed for a diminished secretion using extracellular activity of three unconventionally secreted reporter proteins: heterologous β-glucuronidase and β-galactosidase, both fused to unconventionally secreted Cts1 (Gus-Cts1 and LacZ-Cts1, respectively) and endogenous Cts1. Selection of two heterologous reporters in combination with quantification of secretion of endogenous Cts1 has proven efficient to minimize false positive candidates (Reindl et al., 2020). Whole genome sequencing of selected candidates revealed the novel secretion factor Jps1 essential for unconventional secretion of Cts1 (Reindl et al., 2020). The genetic screen offers a great tool for further optimization of the expression system. Here we adapted it for the identification of hyper secretion mutants with enhanced unconventional secretion for biotechnological application in protein export.

## 6.3 Material and methods

### *6.3.1 U. maydis strains*

All *U. maydis* strains used in this study are described in Table 1. Wild type strains were described before (Banuett & Herskowitz, 1989b). Screening strain FB2$^{CGL}$ was established for the previous screen for diminished unconventional secretion (Reindl et al., 2020). Compatible mating strain JS1$^{CGL}$ (*a1b1*) (previously described as FB1$^{CGL}$(Reindl et al., 2020)) for genetic crosses with the screening strain FB2$^{CGL}$ was obtained by crossing the screening strain FB2$^{CGL}$ (mating type *a2b2*) with the wild type strain FB1 (mating type *a1b1*) (Reindl et al., 2020). Generation of hyper secretion candidates was achieved by UV mutagenesis and is described below. Meiotic progeny of hyper secretion candidates were obtained by mating of the respective hyper secretion candidate and JS1$^{CGL}$.

**Table 6.1: *U. maydis* strains used in this study.** Strains were obtained by homologous recombination using antibiotic resistance cassettes for selection: HygR, hygromycin resistance; NatR, nourseothricin resistance.

| Strains | Relevant genotype/ resistance | UMa (1) | Plasmids transformed (2) | Manipulated locus (3) | Progenitor/ (UMa) (1) | Reference |
|---|---|---|---|---|---|---|
| FB1 | *a1b1* | 51 | / | / | (4) | (Banuett & Herskowitz, 1989b) |
| FB2 | *a2b2* | 52 | / | / | (4) | (Banuett & Herskowitz, 1989b) |
| FB6a | *a2b1* | 55 | / | / | (4) | (Banuett & Herskowitz, 1989b) |
| FB6b | *a1b2* | 56 | / | / | (4) | (Banuett & Herskowitz, 1989b) |
| FB2 $^{lacZ\text{-}Cts1}$ (screening strain progenitor) | *a2b2 pep4::[P$_{oma}$:lacZ:shh:cts1] NatR* | 1501 | pUMa2373_lacZ-cts1_NatR | *umag_04926 (pep4)* (Sarkari et al., 2014) | 52 | (Reindl et al., 2020) |
| FB2$^{CGL}$ (screening strain) | *a2b2 upp1:: [P$_{oma}$gus:shh:cts1]HygR pep4::[P$_{oma}$:lacZ:shh:cts1] NatR* | 1502 | pUMa2374/gus-cts1_HygR | *umag_02178 (upp1)* (Sarkari et al., 2014) | 1501 | (Reindl et al., 2020) |
| JS1$^{CGL}$ (compatible mating partner) | *a1b1 upp1:: [P$_{oma}$gus:shh:cts1]HygR pep4::[P$_{oma}$:lacZ:shh:cts1] NatR* | 1547 | / | / | Cross of FB1 x FB2$^{CGL}$ | (Reindl et al., 2020) |
| USec$^{+}$1 (hyper secretion candidate) | *a2b2 upp1:: [P$_{oma}$gus:shh:cts1]HygR pep4::[P$_{oma}$:lacZ:shh:cts1] NatR* UV-mutagenized | 2252 | / | UV mutagenized | UMa1502 (screening strain) | This study |
| USec$^{+}$2 (hyper secretion candidate) | *a2b2 upp1:: [P$_{oma}$gus:shh:cts1]HygR pep4::[P$_{oma}$:lacZ:shh:cts1] NatR* UV-mutagenized | 3330 | / | UV mutagenized | UMa1502 (screening strain) | This study |
| USec$^{+}$3 (hyper secretion candidate) | *a2b2 upp1:: [P$_{oma}$gus:shh:cts1]HygR pep4::[P$_{oma}$:lacZ:shh:cts1] NatR* UV-mutagenized | 3331 | / | UV mutagenized | UMa1502 (screening strain) | This study |
| USec$^{+}$4 (hyper secretion candidate) | *a2b2 upp1:: [P$_{oma}$gus:shh:cts1]HygR pep4::[P$_{oma}$:lacZ:shh:cts1] NatR* UV-mutagenized | 3332 | / | UV mutagenized | UMa1502 (screening strain) | This study |

**(1)** Internal strain collection number: Strains are termed UMa plus a 4-digit number for identification. **(2)** Plasmids are cataloged in a collection and named pUMa plus a 4-digit identifier number. **(3)** Genes in *U. maydis* are termed with a 5-digit *umag* number, referring to the current genome annotation at EnsemblFungi (Web reference: EnsemblFungi *U. maydis* genome browser). **(4)** FB1 (*a1b1*), FB2 (*a2b2*), FB6a (*a2b1*) and FB6b (*a1b2*) were obtained from the same teliospore from mating *U. maydis* wild type isolates U518 (*a2b2*) with *U. maydis* UM521 (*a1b1*) (Banuett & Herskowitz, 1989b).

### 6.3.2 Strain cultivation

*U. maydis* strains were cultured at 28 °C in complete medium (CM) (Holliday, 1974) supplemented with 1% (w/v) glucose or in YepsLight (Tsukuda et al., 1988). Solid media were supplemented with 2% (w/v) agar. Screening plates were supplemented with 1% (w/v) glucose and 60 mg/L 5-bromo-4-chloro-3-indolyl-β-D-galactopyranoside (X-Gal) (CM-glc-X-Gal) or 500 mg/L X-5-bromo-4-chloro-3-indolyl-beta-D-glucuronic acid (X-Gluc) (CM-glc-X-Gluc), respectively.

### 6.3.3 UV-mutagenesis and screening

For UV mutagenesis of the screening strain $FB2^{CGL}$, a 5 mL preculture was used to inoculate a 15 mL main culture with a final $OD_{600}$ of 1.0 after 16 hours. This culture was then diluted to an $OD_{600}$ of 0.1, incubated until it reached an $OD_{600}$ of 0.5 and subsequently diluted to $OD_{600}$ of 0.00125. 150 µl of the dilution were spread on CM-glc-X-Gal plates and the plates (without the plastic lid) were exposed to UV irradiation (30 mJ/$cm^2$) in a UV crosslinker (Stratalinker, Stratagene San Diego, CA, USA). Plates were incubated for 2 to 3 days at 28 °C in the dark until single colonies were grown. Single colonies showing an enhanced intensity of the blue halo were isolated and inoculated in YepsLight. After 16 h at 28 °C, cultures were spotted on CM-glc/X-Gal and CM-glc-X-Gluc plates, as well as stored in 50 % NSY medium (0.8 % (w/v) nutrient broth, 0.1 % (w/v) yeast extract, 0.5 % (w/v) sucrose; 69.6 % (v/v) glycerol) for -80 °C long-term storage.

### 6.3.4 Quantitative reporter activity assay

To assay enzymatic activity of reporter enzymes for unconventional secretion, precultures were grown in 5 mL YepsLight for 16 h at 28 °C at 200 rpm. 200 µl of the culture was transferred in 5 mL fresh YepsLight and grown for additional 8 h under identical conditions. After regeneration, cultures were diluted to reach a final $OD_{600}$ of 1.0 after 16 h in 10 mL CM-glc. Cultures were harvested at $OD_{600}$ 0.8 to 1.0 by centrifugation of 2 ml culture at 1500 × g for 5 min. Supernatants were transferred to fresh reaction tubes and stored at -20 °C until reporter activity determination. Pellets were washed in sterile water and resuspended in KHM buffer (110 mM potassium acetate, 20 mM HEPES, 2 mM $MgCl_2$) at a final $OD_{600}$ of 1.0.

Extracellular activities of unconventionally secreted Gus-Cts1 and LacZ-Cts1 reporter enzymes were determined using the fluorescent substrates 4-methylumbelliferyl β-D galactopyranoside (MUG, bioWORLD, Dublin, OH, USA) for Gus activity and o-nitrophenyl-β-D-galactopyranoside (ONPG, Sigma/Aldrich, Billerica, MA, USA) for the liquid LacZ activity assay, respectively. 100 µl cell free supernatants were mixed with either 100 µl 2× Gus Buffer

(10 mM sodium phosphate buffer pH 7.0, 28 µM β- mercaptoethanol, 0.8 mM EDTA, 0.0042% (v/v) lauroyl-sarcosin, 0.004% (v/v) Triton X-100; add 2 mM MUG and 0.2 mg/ml (w/v) BSA freshly) or 2× Z-Buffer (80 mM Na2HPO4, 120 mM NaH2PO4 × H2O, 20 mM KCl, 2 mM MgSO4 × 7 H2O; adjust to pH 7; add 68 mM β-mercaptoethanol and 3.3 mM ONPG freshly) in black 96-well plates (96 Well, PS, F-Bottom, µCLEAR, black, CELLSTAR) (Reindl et al., 2020; Stock et al., 2012). Relative fluorescence units (RFUs) were determined using a plate reader (Tecan, Männedorf, Switzerland) for 100 min at 28 °C with measurements every 5 minutes (excitation/emission wavelengths: 365/465 nm, Gain 60 for Gus activity; $OD_{420}$ for LacZ activity).

Extracellular activity of unconventionally secreted, endogenous Cts1 on the cell surface was determined using the substrate 4-methylumbelliferyl β-D-N,N',N"-triacetylchitotrioside (MUC, Sigma/Aldrich, Billerica, MA, USA). 30 µl of cells in KHM buffer were mixed with 70 µl KHM buffer supplemented with 0.2 mg/ml MUC in black 96-well plates. Relative fluorescence units (RFUs) were determined using a plate reader for 100 min at 28 °C with measurements every 5 minutes (excitation/emission wavelengths: 360/450 nm, Gain 150).

### *6.3.5 Plant infection*

Meiotic progeny was obtained by genetic crosses of $FB2^{CGL}$ (*a2b2*)-derived hyper secretion candidates with the compatible mating partner $JS1^{CGL}$ (*a1b1*). Compatible mating strain $JS1^{CGL}$ (*a1b1*) is a selected individual, showing activity of all reporters. It was generated by crossing $FB2^{CGL}$ (*a2b2*) and FB1 (*a1b1*) (Reindl et al., 2020). Corn plants were infected in order to obtain in tumor material with teliospores. Therefore, 5 mL YepsLight precultures of all mating partners were used to inoculate 50 mL YepsLight main cultures for a final $OD_{600}$ of 1.0 after 16 hours of incubation. Cells were washed in $H_2O$ and resuspended for an $OD_{600}$ of 3.0. Cell suspensions of compatible mating partners were mixed in a 1:1 ratio. For infection, 250-500 µl mixed cell suspension was injected into 2 to 3 weeks old *Zea mays* (var. Arecibo) seedlings. Plant growth was maintained for 8 more weeks to obtain mature teliospores. For spore collection and isolation, mature tumors, showing black patterns within, were harvested and dried at 37 °C for at least 7 days.

### *6.3.6 Mating in liquid culture*

To observe mating in liquid culture, respective strains were grown in CM-glc for 16 hours, diluted in fresh CM-glc and regenerated until an $OD_{600}$ of 0.5. 2 mL of the cultures were harvested by centrifugation at 1,500 × g for 1 minute. The cell pellets were washed and resuspended in 1 mL $H_2O$. 30 µL of compatible strains were mixed in a Petri dish and incubated for 8 hours at 22 °C.

### 6.3.7 Microscopic analyses

After mating in liquid culture, microscopic analyses were performed for diploid, hyphal cells. Hyphae were immobilized agarose patches (3% (w/v)) and visualized using a wide-field microscope setup from Visitron Systems (Munich, Germany), Zeiss (Oberkochen, Germany) Axio Imager M1 equipped with a Spot Pursuit CCD camera (Diagnostic Instruments, Sterling Heights, MI, USA) and the objective lenses Plan Neofluar (40×, NA 1.3), Plan Neofluar (63×, NA 1.25) and Plan Neofluar (100×, NA 1.4). The microscopic system was controlled by the software MetaMorph (Molecular Devices, version 7, Sunnyvale, CA, USA). Image processing including rotating and cropping of images, scaling of brightness, contrast, and fluorescence intensities as well as insertion of scaling bars was performed with MetaMorph.

### 6.3.8 Spore isolation and germination

Spore germination and isolation was conducted according to published protocols with minor variations (Eichhorn et al., 2006; Reindl et al., 2020). Dried tumor material of infected plants was homogenized in a mortar and resuspended in 2 mL $H_2O$. The suspension was treated with 4 mL 3.0% (w/v) copper sulfate solution for 15 minutes at room temperature. Subsequently, cells were washed twice with 2 mL $H_2O$ and the pellet was solved in 500 µl $H_2O$ supplemented with 600 µg/ml ampicillin and 150 µg/ml tetracycline. 100 µl of 1:1, 1:10 and 1:100 dilutions were spread on CM-glc plates and incubated for 2 to 3 days at 28°C. Single colonies were isolated and extracellular reporter activities as well as mating types were investigated as described.

### 6.3.9 Determination of mating types

CM-glc plates containing 1% (w/v) charcoal (Sigma C-9157) were used for mating assays (Banuett 1989).Two *U. maydis* cultures were mixed and spotted on CM-glc/charcoal plates to investigate hyphae formation. Main cultures were diluted to an $OD_{600}$ of 0.2 regenerated until an $OD_{600}$ of 0.6, mixed in a 1:1 ratio with a mating partner and 5 µl of mixed cells were spotted onto CM-glc/charcoal. After 2-3 days, formation of hyphae was investigated.

### 6.3.10 Isolation of genomic DNA

For isolation of genomic DNA for sequencing, 5 mL dense *U. maydis* culture was harvested by centrifugation at 12,000 × g for 2 minutes. 300 µl glass beads were added and pellet was quick-frozen in liquid nitrogen and stored at -20 °C until preparation. 500 µl 4 °C Phenol/Chloroform/Isoamyl alcohol (ROTI®, Carl Roth, Karlsruhe, Germany) and 500 µl Usti Lysis Buffer (50 mM Tris-HCL, pH 7.5, 50 mM $Na_2$-EDTA, 1 % (w/v) SDS, 4°C) were added

to the pellet and glass beads and reaction tube was agitated at 1500 rpm for 10 minutes. Upon centrifugation at 12,000 × g for 15 minutes, the upper, watery phase was added to 1.5 mL ice-cold ethanol, inverted and centrifuged at 12,000 × g for 5 minutes. This step was repeated twice. The ethanol was removed and pellet was allowed to dry at room temperature for 3 minutes. Pellet was solved in 100 µl 10 mM TrisHCl (pH 8) supplemented with 10 µg/ml RNase A and incubated at 50 °C, agitated at 400 rpm for 10 minutes. Quality was confirmed by Quibit™ measurements (Qubit™, Invitrogen/Thermo Fisher Scientific, Carlsbad, CA, USA).

### *6.3.11 Sequencing and analysis of genomic DNA*

Isolated genomic DNA from *U. maydis* reference strains, UV mutants and selected progeny was used for whole-genome sequencing. For pooled linkage analysis, gDNA of different individuals of meiotic progeny was mixed equimolarly. Illumina DNA library preparation, trimming and mapping of the reads and visualization was performed as described previously (Haupka et al., 2021). The MinION sequencing library was prepared using the Nanopore Rapid DNA Sequencing kit (SQK-RAD04) according to the manufacturer's instructions with changes described before (Wibberg et al., 2020). ReadXplorer 2.2.3 was used for visualization of the processed reads and detection of single nucleotide polymorphism (SNP) of selected strains or pools against respective reference genome. Threshold for mapped reads was set to 90% for individual strains and to 50% for pooled linkage comparison of different pools.

## 6.4 Results

### *6.4.1 Adapting a forward genetic screen to identify hyper secretion candidates*

Here we adapted the previously developed UV mutagenesis screen and applied it towards identification of hyper secretion mutants (Figure 6.1) (Reindl et al., 2020).

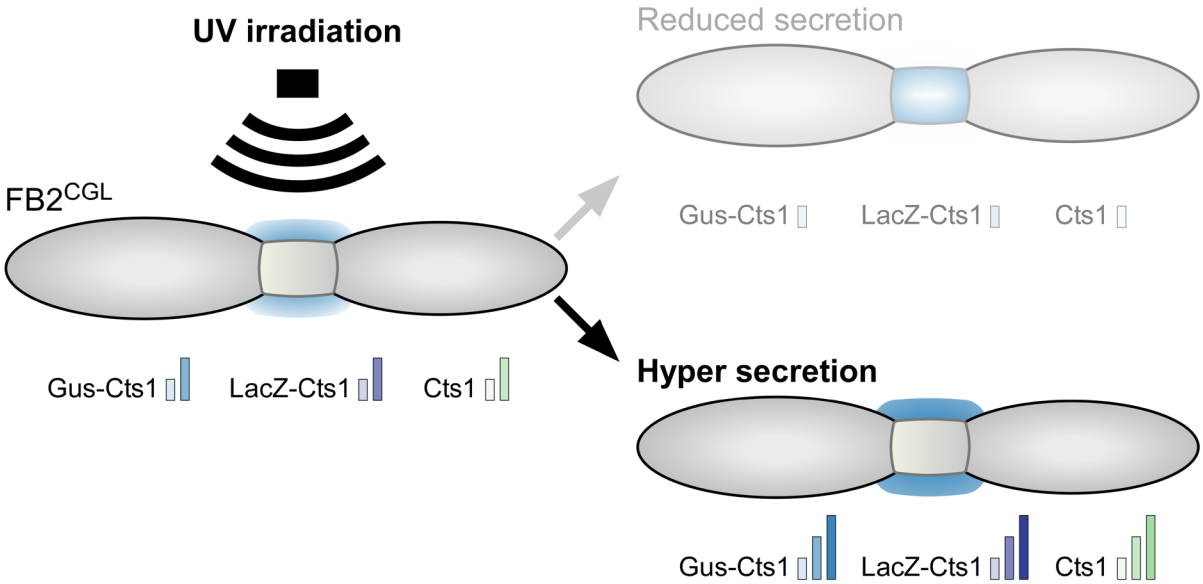


**Figure 6.1. Rationale of genetic screen for mutants with enhanced unconventional secretion.** FB2$^{CGL}$ screening strain (left side), harboring the three reporter proteins for unconventional secretion Gus-Cts1, LacZ-Cts1 and endogenous Cts1, is exposed to UV radiation. Mutagenized cells are subsequently screened for an effect on unconventional secretion of the three reporter proteins using colorimetric and fluorimetric assays. In this study, mutants with enhanced activity of all three reporters are selected for detailed characterization (bottom right scenario).

The forward genetic screen was initially established for identification of mutants deficient in unconventional secretion. It was now adapted to allow identification of hyper secretion mutants (Figure 6.2A). Therefore, the screening strain FB2$^{CGL}$ was used. It harbors the two heterologous reporter enzymes β-glucuronidase (Gus) and β-galactosidase (LacZ) fused to Cts1 for Cts1-mediated unconventional secretion, as well as endogenous Cts1 for direct detection of extracellular chitinase activity (Reindl et al., 2020). Read-out of all three reporters was used to identify mutants with enhanced unconventional secretion after UV-mutagenesis while at the same time diminishing the risk of false positive candidates (Figure 6.1, Figure 6.2A). In a first step, mutants were high-throughput evaluated for extracellular LacZ activity based on conversion of X-Gal in plate assays by the reporter LacZ-Cts1 (Figure 6.2B). Subsequently candidates with apparently enhanced blue coloration were re-grown on X-Gluc plates in order to evaluate the second heterologous reporter, Gus-Cts1, by determining extracellular Gus activity (Figure 6.2C). To this end, approximately 250,000 colonies were qualitatively analyzed on their unconventional secretion capacity in high-throughput. 352 colonies with enhanced extracellular activity of one or both reporters were selected and further evaluated on their LacZ and Gus activity in quantitative liquid assays using the substrates ONPG and 4-MUG, respectively. Analysis in single measurements revealed a diverse distribution of reporter activities among all selected candidates (Figure 6.2D, Figure S6.2, Figure 6.3).

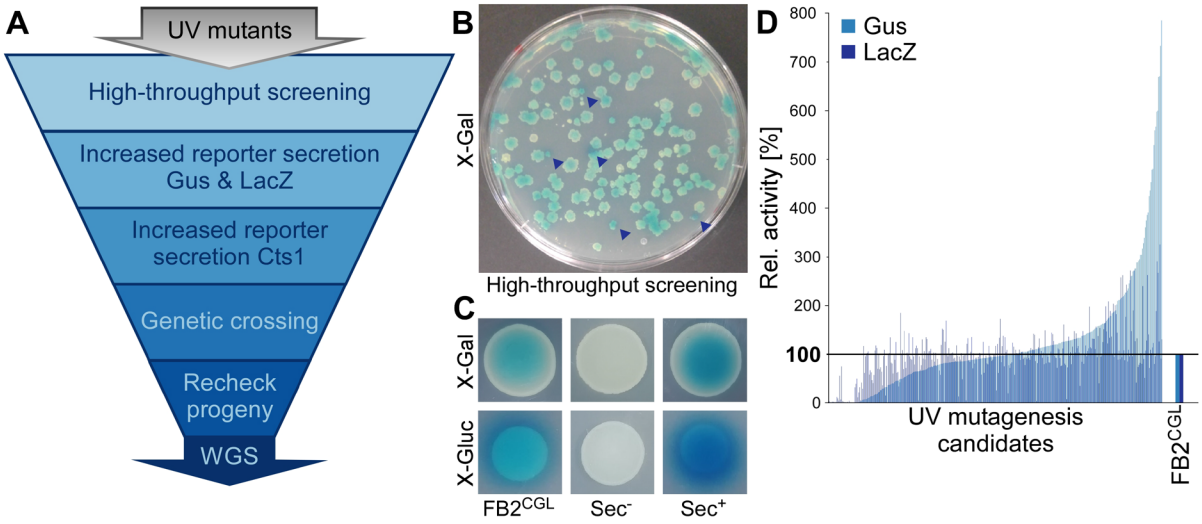


**Figure 6.2. Forward genetic screen for identification of hyper secretion mutants.** (**A**) Procedure of the genetic screen. UV mutants were subjected to high-throughput screening for enhanced extracellular reporter activity. After qualitative evaluation, selected candidates were evaluated with respect to their Gus, LacZ and Cts1 activity in quantitative liquid assays. Confirmed candidates were crossed with a non-mutagenized compatible mating partner and progeny individuals were evaluated, pooled according to their unconventional secretion potential (i.e. wild type and hyper secretion) and prepared for whole genome sequencing. Further information regarding the number of candidates is depicted in Figure S6.1. (**B**) High-throughput selection of hyper secretion mutants. UV-mutagenized FB2$^{CGL}$ cells were incubated on X-Gal containing plates. Colonies showing a blue halo of increased intensity were selected for further analyses (examples marked with blue arrowheads). (**C**) Example of plate assay re-evaluation of hyper secretion candidates. Colonies of the non-mutagenized screening strain FB2$^{CGL}$, a mutant diminished in unconventional secretion (Sec$^-$, FB2$^{CGL}$mut1 (Reindl et al., 2020)) and a mutant showing an increased unconventional secretion (Sec$^+$) obtained in the screen were investigated exemplarily using X-Gal and X-Gluc containing plates. (**D**) Relative Gus and LacZ activity of selected candidates in quantitative, liquid assays. Extracellular activity of reporter enzymes LacZ and Gus of all 352 selected candidates in liquid assays was determined in single measurements and compared to activity levels of progenitor strain FB2$^{CGL}$ (Rel. Gus and LacZ activity = 100%). Candidates were sorted according to their relative Gus activity. Sorting according to LacZ activity is depicted in Figure S6.2.

Out of 352 screened candidates, 158 candidates showed enhanced extracellular Gus activity compared to the non-mutagenized progenitor, and 167 candidates revealed increased extracellular LacZ activity. Importantly, in 92 candidates increased activity was observed for both reporter proteins (Figure 6.3A, B). 45 of the latter 92 candidates show an increased activity of at least 25% for both reporter enzymes. To minimize false positive results, only these candidates were subjected to further analyses of reporter enzyme activities in triplicates. In these experiments, 19 candidates even showed an increased Gus activity above 200% and 21 candidates an increased LacZ activity above 150% (Figure 6.3 C,D). Fourteen candidates met both criteria and were further investigated regarding their endogenous Cts1 activity.

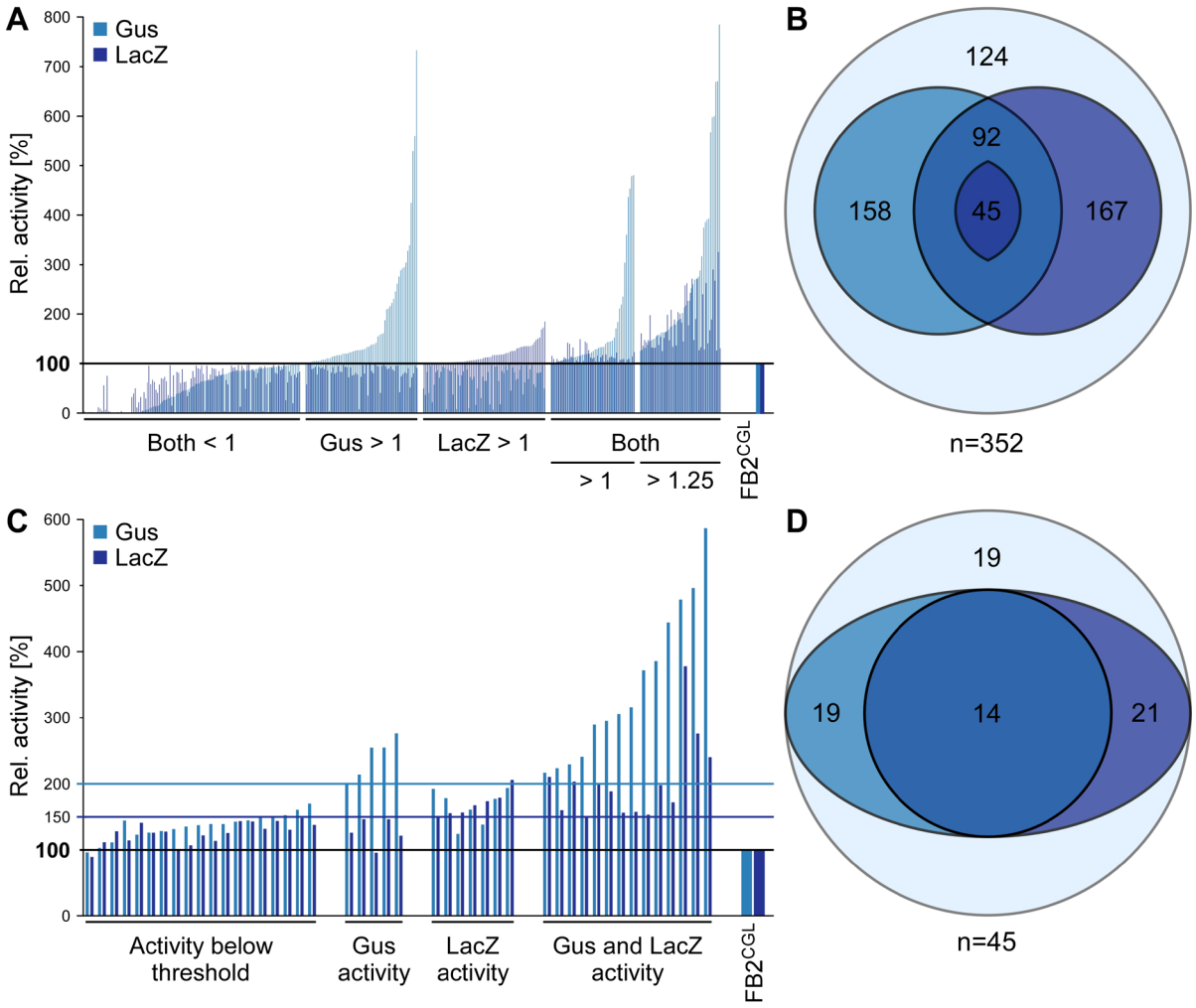


**Figure 6.3. Selection of hyper secretion candidates for further characterization. (A, B)** Single Gus and LacZ activity measurements of all candidates with enhanced blue coloration obtained by high-throughput screening in quantitative liquid assays. **(A)** Relative extracellular Gus and LacZ activity of all investigated candidates depicted in Figure 6.1D. Candidates were sorted into groups using progenitor FB2$^{CGL}$ as a reference (Rel. Gus and LacZ activity = 100%, black line): Activity of both reporters <100% (Σ 124); Gus activity >100%, LacZ activity <100% (Σ 64); LacZ activity >100%, Gus activity <100% (Σ 70), both activities >100% but <125% (Σ 47); both activities >125% (Σ 45). **(B)** Venn diagram of different groups of hyper secretion candidates as depicted in A: 352 total candidates were tested in Gus and LacZ assays. 124 candidates were excluded from further evaluations since Gus and LacZ activity was below FB2$^{CGL}$ reference strain, 158 candidates showed an increased Gus activity, 167 candidates an increased LacZ activity. For 92 candidates, activity of both reporters was increased. 45 candidates were selected for further analysis since their activity increased by 25% in comparison to the non-mutagenized screening strain FB2$^{CGL}$. **(C, D)** Verification of selected hyper secretion candidates in triplicates. **(C)** Relative extracellular Gus and LacZ activity of all investigated candidates depicted in Figure 6.3A and B. For next evaluation threshold was set to 150% LacZ activity (purple line) and 200% Gus activity (blue line). Candidates are sorted into groups: Activity of both reporters below threshold (Σ 19), Gus activity >200% but LacZ activity < 150% (Σ 5), LacZ activity >1.5 but Gus activity < 2 (Σ 7), activity of both heterologous reporters above threshold (Σ 14). Black line indicates FB2$^{CGL}$ relative activity set to 100%, blue line indicates Gus threshold of 200%, purple line indicates LacZ threshold of 150%. **(D)** Venn diagram of different groups of secretion candidates. 45 total candidates were confirmed in Gus and LacZ assays (Figure 6.3B). 19 candidates showed an increased Gus activity above 200%, 21 candidates an increased LacZ activity above 150%. For 14 candidates, activity of both reporters was increased above threshold.

For these fourteen candidates extracellular Cts1 activity was determined to finally visualize the exact impact on endogenous Cts1 secretion. Therefore, conversion of MUC by Cts1 on the surface of whole cells was measured (Figure 6.4A). Two candidates showed ambiguous results and the corresponding data were therefore excluded for improved visualization (data not shown). For six of the candidates measurements revealed that Cts1 activity was diminished or not affected (Figure 6.4A). Four candidates, now named USec$^{+}$1-4, showed a strong increase for all three reporters in a range of 2.5 to 4-fold for Gus, around 2-fold for LacZ and 1.5 to 2-fold for endogenous Cts1. These were therefore selected for further analysis (Figure 6.4B, Figure 6.S3).

In sum, four different candidates showing an unambiguously increased unconventional secretion of all three reporters were obtained after screening of about 250.000 mutagenized cells (Figure 6.4, Figure S6.2). Hence, these strains offer a great potential for application in heterologous protein secretion.

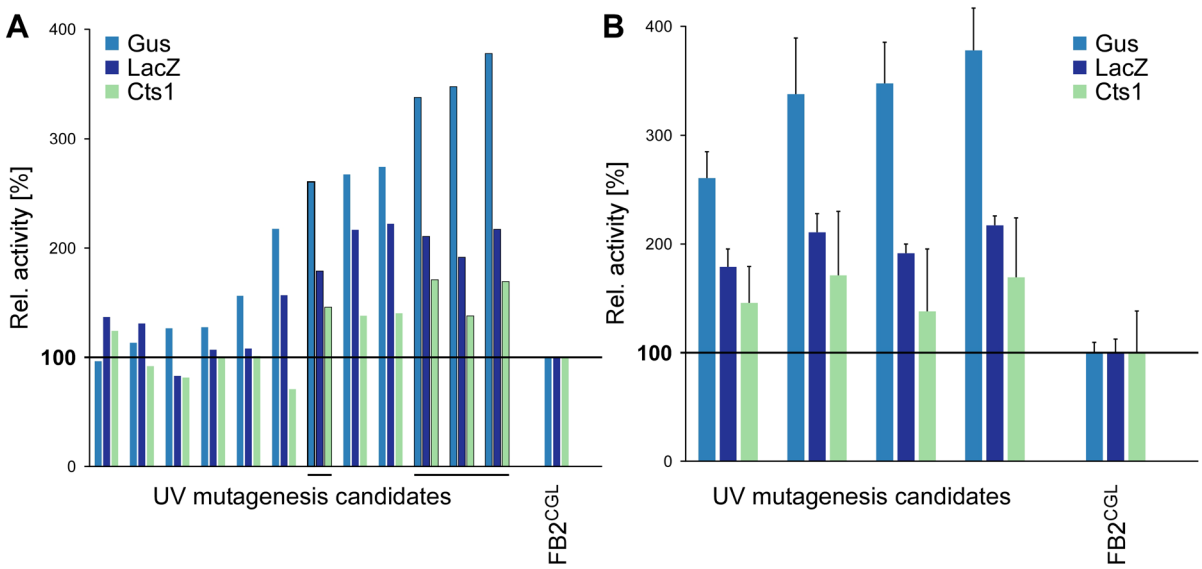


**Figure 6.4. Relative activity of Gus, LacZ and Cts1 for selected candidates in quantitative liquid assays.** Extracellular activity of reporter enzymes LacZ and Gus was determined in supernatants in four replicates, Cts1 activity on the cell surface of whole cells was determined in three replicates. Average activity of FB2$^{CGL}$ was set to 100% and served as standard for all measurements. All candidates were arranged according to their relative Gus activity. **(A)** Extracellular reporter activities of all twelve candidates in comparison to FB2$^{CGL}$ screening strain. Highlights indicate three strongest candidates, selected for further analyses, as well as internal positive control of previous measurements. **(B)** Highlighted candidates from A are shown in detail. Diagrams represent results of four biological replicates. Error bars depict standard deviation. Statistical analysis is described in Figure S6.3.

## *6.4.2 Whole genome sequencing of hyper secretion candidates*

To identify the responsible mutations responsible for hyper secretion of the four selected candidates, whole genome sequencing was conducted. Genome sequences of UV-mutagenized hyper secretors USec$^{+}$1 to Usec$^{+}$4 were compared to their progenitor FB2$^{CGL}$. Interestingly, the amount of single nucleotide polymorphisms (SNP) and 5′-CT or 5′-CCTT UV-

signatures (Brash, 2015; Rastogi et al., 2010) was not consistent among the different candidates. In the previous study, the occurrence of 32 base pair substitutions was described, the majority with UV signatures (Reindl et al., 2020). In the present study, two out of four hyper secretion candidates showed a comparable number of substitution events (USec$^+$3: 28 events; USec$^+$4: 41 events). Nevertheless, occurrence of UV signatures in these candidates between 20 and 40% was drastically lower than described before, with over 70% (Reindl et al., 2020). While the UV-signature was comparable with around 40% of all SNPs among three hyper secretion mutants, USec$^+$3 showed a ratio of only 21% 5′-CT or 5′-CCTT. Despite a comparable ratio of mutations with a UV signature to total mutations in USec$^+$1, USec$^+$2 and USec$^+$4, total numbers of substitution events strongly differ between three for USec$^+$1 to 86 for USec$^+$2 (Table 2). The high variance in the number of SNPs and the proportion of UV-signatures was surprising since the experimental procedure had been kept consistent throughout the experiments in which Usec$^+$1, Usec$^+$3 and Usec$^+$4 were generated. Experiments were conducted over a prolonged time but followed a standardized protocol. Interestingly, USec$^+$2 showed the highest number of total SNPs. During the establishing phase, higher cell count was used in this batch of cultivation while all other parameters of UV mutagenesis including duration and intensity remained unchanged.

**Table 6.2.** Numbers and characteristics of identified base pair substitution mutations in the 4 hyper secretion candidates compared to the published unconventional secretion deficient strain FB2$^{CGL}$mut1.

| | FB2$^{CGL}$mut1 (Reindl et al., 2020) | USec$^+$1 | USec$^+$2 | USec$^+$3 | USec$^+$4 |
|---|---|---|---|---|---|
| No. of SNPs | 32 | 3 | 86 | 28 | 41 |
| UV signatures in SNPs | 29 (72%) | 1 (33%) | 35 (41%) | 6 (21%) | 16 (40%) |
| Amino acid exchanges in coding regions | 12 | 0 | 19 | 5 | 13 |
| UV signatures in SNPs leading to amino acid exchanges | 11 | 0 | 11 | 0 | 7 |

Importantly, due to low coverage during the first round, resequencing of USec$^+$1 increased the number of mutations in comparison to the first sequencing attempt. In total, the two datasets revealed 38 single nucleotide exchanges, which is comparable to the UV-induced mutation rate observed before (Reindl et al., 2020). However, a UV signature proportion of only 42% is still beyond the previously described value (Reindl et al., 2020).

Despite surprising ratio of UV-signature, SNPs were identified for all hyper secretion candidates. Resequencing of USec$^{+}$1 revealed a comparable amount of introduced mutations in comparison to previous analysis. Data of a selected strain can now be used for deeper investigations to identify the underlying mutations.

### *6.4.3 Isolation of meiotic progeny of USec$^{+}$1*

Identification of a beneficial mutation can be a search for a needle in a haystack if the exact localization of the mutated genetic element is unknown. Since in contrast to the earlier approach neither the mutagenized region nor the affected genetic element was known, a pooled linkage analysis was conducted to elucidate the responsible mutation. Genetic linkage by crossing a candidate with a complementary mating partner has the power to rapidly identify the mutation responsible for a phenotype among a lot of other unrelated mutations (Birkeland et al., 2010; Brauer et al., 2006; Ehrenreich et al., 2010).

Therefore, first genetic crossings were conducted. FB2$^{CGL}$ has the mating type *a2b2*. For genetic crossings, strain JS1$^{CGL}$ was used which harbors both heterologous reporters in the compatible mating background *a1b1* (Reindl et al., 2020). Crossings of JS1$^{CGL}$ with UV-mutagenized FB2$^{CGL}$ candidates allows to maintain reporter activity in all progeny and thus enables a straightforward analysis. Genetically compatible strains form white fuzzy colonies on charcoal-containing plates as an effect of hyphae formation after mating (Banuett & Herskowitz, 1989b), a prerequisite for plant infection (Feldbrügge et al., 2004). Efficient mating was observed for all hyper secretion candidates upon crossing with JS1$^{CGL}$ (Figure 6.5A). Infection of *Zea mays* seedlings with JS1$^{CGL}$ crossed with the individual hyper secretion candidates led to formation of tumors on the plants in all cases (Figure. 6.5B, C). Importantly, mating capability of wild type strains, screening strains and hyper secretion candidates was also confirmed microscopically (Figure S6.4). Although infection efficiency was decreased in comparison to a previous plant infection study of the screening strain, scoring revealed a comparable efficiency in all infections for this study. Infection with all hyper secretion candidates led to formation of tumors on *Zea mays* plants (Figure S6.5). This indicates that the mutagenized strains are not affected in mating and pathogenicity when crossed with a JS1$^{CGL}$ partner. Mature tumor material containing viable spores (Figure 6.5D) was harvested and dried. Spores obtained by crossing USec$^{+}$1 with JS1$^{CGL}$ were germinated to obtain haploid progeny for detailed analysis while spore of the other crosses were stored for future analysis.

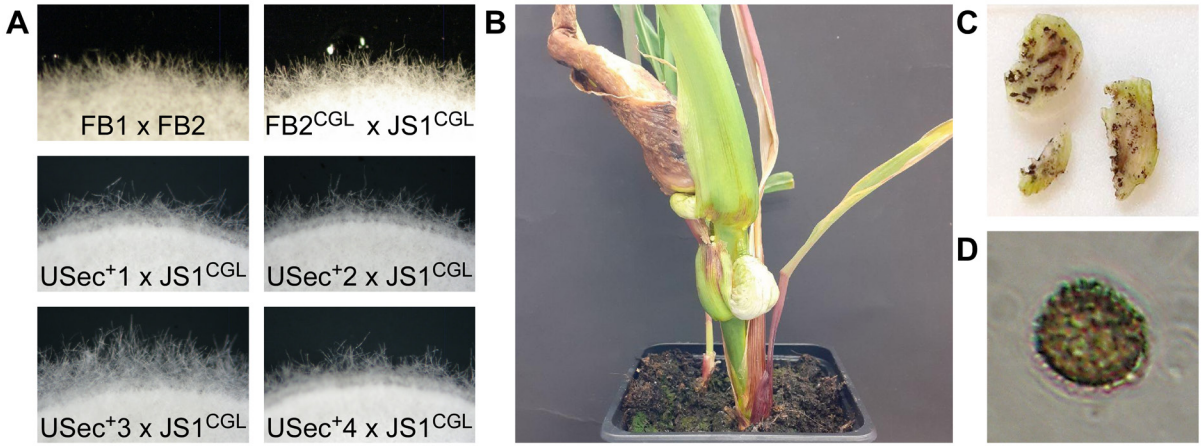


**Figure 6.5. Hyphae formation and genetic crossings of hyper secretion candidates with complementary mating partner JS1$^{CGL}$.** (**A**) Mating assay to confirm mating ability of FB2$^{CGL}$ UV mutagenesis candidates USec$^{+}$1 - USec$^{+}$4 with JS1$^{CGL}$. Mating of FB1 and FB2 served as a wild type control, JS1$^{CGL}$ x FB2$^{CGL}$ mating verified mating ability in reporter strains. Mating of compatible strains was observed on charcoal plates. Fuzzy colonies indicate efficient mating leading to hyphae formation. (**B**) Infection of *Zea mays* plants with JS1$^{CGL}$ x USec$^{+}$1 crossings leads to tumor formation (**C**) containing black teliospores (**D**) with a typical microscopic morphology.

USec$^{+}$1 was selected for pooled linkage analysis. Therefore, isolated individuals of the USec$^{+}$1 x JS1$^{CGL}$ progeny were categorized based on their extracellular reporter activities and mating types. Quantitative Gus and LacZ liquid assays for 24 progeny individuals revealed a distinct distribution (Figure 6.6a): While eight individuals of the progeny showed a lower or similar secretion compared to FB2$^{CGL}$, sixteen individuals exhibited enhanced extracellular activities. Interestingly, extracellular reporter activities of twelve individuals of the progeny even exceeded the parental UV-mutagenized hyper secretion strain USec$^{+}$1. Growth rates of parental strains in comparison to progeny revealed no remarkable differences, suggesting that the mutagenesis did not affect growth behavior of selected strains (Figure S6.6). Influence of growth rate can therefore be excluded as impact for differences in secretion.

For the thirteen progeny candidates showing the highest extracellular activity of unconventionally secreted Gus and LacZ reporters, Cts1 assays were conducted which confirmed the improved unconventional secretion capacity (Figure 6.3B). In sum, meiotic progeny was obtained from the USec$^{+}$1 x JS1$^{CGL}$ crossing of which thirteen hyper secreting individuals as well as three wild type secreting individuals were selected for further analyses.

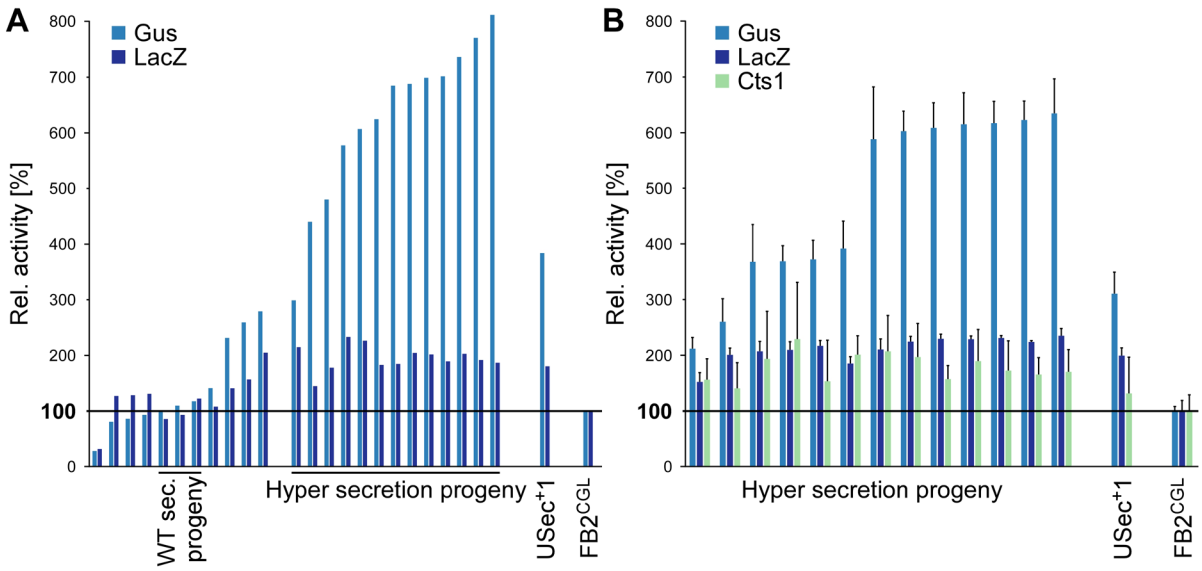


**Figure 6.6. Relative extracellular activity of reporters for unconventional secretion in meiotic progeny. (A)** Extracellular activity of reporter enzymes Gus and LacZ was determined in supernatants in three biological replicates. All candidates were arranged according to their relative Gus activity. Thirteen hyper secretion individuals of the progeny were investigated in detail, depicted in section (B), three candidates showing a wild type-like secretion served as a control in later experiments. Black line indicates the average activity of FB2$^{CGL}$ set to 100%, which served as standard for all measurements. **(B)** Extracellular activity of heterologous reporter enzymes Gus and LacZ and endogenous Cts1 was determined in five biological replicates. In the diagram, the candidates were arranged according to their relative Gus activity. Error bars depict standard deviation. Black line indicates the average enzyme activities of FB2$^{CGL}$ set to 100% and served as standard for all measurements.

## *6.4.4 Determination of mating type distribution*

From Mendelian segregation, an equal distribution of genetic elements of both parental strains is expected among the progeny (Griffiths, 2000). This can easily be tested by analyzing the mating type distribution. Two loci, the *a* and *b* locus which are requisite for mating, exist in *U. maydis*. Mating of meiotic progeny with tester strains of known mating types, FB1 (*a1b1*), FB2 (*a2b2*), FB6a (*a2b1*) and FB6b (*a1b2*), was performed to determine mating types of individual candidates of the progeny (Table 6.2, Figure S6.6). As expected, all FB2$^{CGL}$ derived UV mutants grew fuzzy upon mating with FB1, indicating an *a2b2* mating type (Figure S6.6, Table 6.3). Interestingly, also the majority of the progeny individuals obtained from the USec$^{+}$1 x JS1$^{CGL}$ crossing showed mating type *a2b2*. Only for two out of 13 candidates of hyper secreting progeny an *a2b1* mating type was observed. No individuals formed hyphae after mating with FB2 (*a2b2*) nor FB6a (*a2b1*), indicating that among all tested progeny individuals, not a single *a1* allele was present. For the progeny pool with wild type unconventional secretion levels, both mating type alleles, *a1* and *a2*, were observed. Furthermore, in contrast to an apparently biased mating type, colony morphology was diverse in the individuals with enhanced secretion with one group forming rather mucoid FB1-like colonies and a FB2-like

group with dry colonies. Nevertheless, a strong bias of progeny's mating types towards *a2b2* could be a hint for a defect in the distribution of parental mating types.

**Table 6.3. Mating type and colony morphology in mating assays of hyper secretion strain and individuals of progeny pools.** Wild type strains FB1 and FB2 served as positive controls, screening strain FB2$^{CGL}$ and compatible mating partner JS1$^{CGL}$ served as reference strains. Hyper secretion candidates USec$^{+}$1-4 as well as individuals of the wild type like progeny pool (n=3) and hyper secretion progeny pool (n=13) were crossed with different mating partners (tester strains) and investigated with respect to hyphae formation. Mating assays to determine mating types on charcoal plates are depicted in Figure S6.7.

| Candidate/strain | Mating type | Morphology |
|---|---|---|
| Wild type and parental strains | | |
| FB1 | *a1b2* | FB1 |
| FB2 | *a2b2* | FB2 |
| JS1$^{CGL}$ | *a1b1* | FB1 |
| FB2$^{CGL}$ | *a2b2* | FB2 |
| Hyper secretion candidates | | |
| USec$^{+}$1 | *a2b2* | FB2 |
| USec$^{+}$2 | *a2b2* | FB2 |
| USec$^{+}$3 | *a2b2* | FB2 |
| USec$^{+}$4 | *a2b2* | FB2 |
| WT-like progeny pool | | |
| Neg-1 | Diploid | |
| Neg-12 | *a1b1* | FB2 |
| Neg-19 | *a2b1* | FB1 |
| Hyper secretion progeny pool | | |
| #2 | *a2b2* | FB2 |
| #3 | *a2b1* | FB1 |
| #5 | *a2b2* | FB2 |
| #7 | *a2b2* | FB1 |
| #8 | *a2b2* | FB1 |
| #9 | *a2b2* | FB1 |
| #11 | *a2b2* | FB1 |
| #15 | Indeterminable | FB2 |
| #16 | *a2b1* | FB2 |
| #21 | *a2b2* | FB1 |
| #22 | *a2b2* | FB2 |
| #23 | *a2b2* | FB1 |
| #25 | *a2b2* | FB1 |

### *6.4.5 Pooled linkage analysis of USec⁺1 hyper secretion progeny pool*

Adaptation of pooled linkage analysis and whole-genome sequencing can largely increase output and significance of genetic screens (Birkeland et al., 2010). Towards identification of underlying mutation in a pool of progeny, meiotic mating and sexual recombination is essential. According to Mendelian inheritance, an equal distribution of wild type secretion individuals and hyper secretion individuals would be expected in the progeny (Griffiths, 2000). Therefore, to finally identify the underlying mutation in USec⁺1, genomic DNA of 13 individuals of the progeny showing an increased unconventional secretion (Figure 6.6B) was isolated, pooled and sequenced by MiSeq Illumina™ sequencing and Oxford Nanopore Technologies™ sequencing. A second pool of three progeny individuals with wild type phenotype was sequenced as a control. Assembled genomes of the two pools were compared to reveal the causative mutation. In case of a tight linkage of mutant phenotype and causative genotype, 100% of mutant pool and 0% of wild type pool reads should show the relevant mutation (Birkeland et al., 2010) (Figure 6.7).

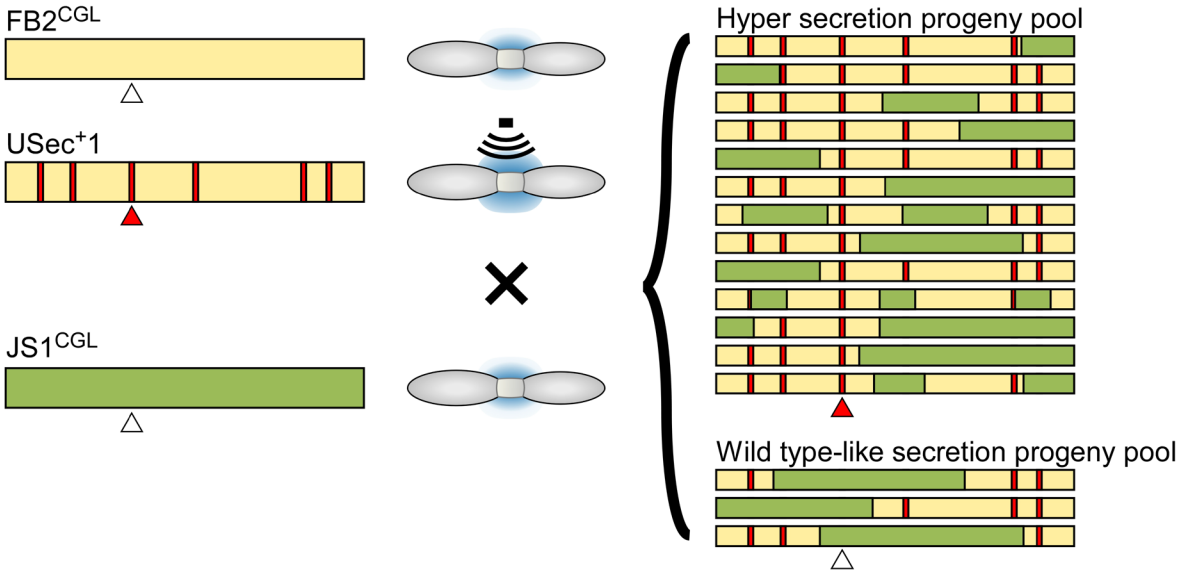


**Figure 6.7. Rationale of sequencing evaluation.** Towards identification of responsible hyper secretion mutation (red triangle) among all UV-induced mutations (red bars), pooled linkage analysis was performed. Hyper secretion candidate USec⁺1 ($FB2^{CGL}$ background, yellow bar) was crossed with compatible mating partner $JS1^{CGL}$, exhibiting a wild type like secretion (green bar). After meiotic crossing and spore germination, haploid progeny now consists of a mix of $FB2^{CGL}$ background genetic sequences (yellow) and $JS1^{CGL}$ sequences (green). Progeny was categorized according to unconventional secretion capacity. While all individuals with an increased unconventional secretion are expected to carry the relevant mutation (red triangle), wild type-like individuals are expected to carry the $JS1^{CGL}$ version of the corresponding region (white triangle). Bars do not represent actual chromosomes and are a schematic rationale of the sequencing principle

In addition, parental genomes were sequenced and compared among each other to get an overview about the number of variances among different parental strains. Comparison of USec⁺1 and $FB2^{CGL}$ to $JS1^{CGL}$ revealed between 4,500 and 5,000 SNPs in all mappings.

Comparable number of SNPs was expected since USec$^{+}$1 was obtained by mutagenesis of FB2$^{CGL}$. While FB2$^{CGL}$ has around 12,500 SNPs in comparison to published and accurately annotated reference genome *U. maydis* strain UM521 (Kämper et al., 2006)(Web reference: *U. maydis* 521), JS1$^{CGL}$ only has around 8,000 SNPs, indicating a higher similarity of JS1$^{CGL}$ to UM521 than FB2$^{CGL}$ to UM521. Numbers of SNPs for all strains are depicted in Table 6.4.

**Table 6.4. Number of SNPs in mappings of different sequencing reads on reference genomes.** Reads of USec$^{+}$1, FB2$^{CGL}$ and JS1$^{CGL}$ were mapped on reference genome of published *U. maydis* wild type isolate UM521 (Kämper et al., 2006) or data from the sequencing conducted for this study.

| Sequencing reads | Reference genome | Number of SNPs |
|---|---|---|
| USec$^{+}$1 | UM521 | 12,835 |
| FB2$^{CGL}$ | UM521 | 12,433 |
| JS1$^{CGL}$ | UM521 | 7,876 |
| USec$^{+}$1 | FB2$^{CGL}$ | 74 |
| FB2$^{CGL}$ | FB2$^{CGL}$ | 6 |
| JS1$^{CGL}$ | FB2$^{CGL}$ | 4,667 |
| USec$^{+}$1 | JS1$^{CGL}$ | 4,928 |
| FB2$^{CGL}$ | JS1$^{CGL}$ | 4,753 |
| JS1$^{CGL}$ | JS1$^{CGL}$ | 18 |

Comparison of hyper secretion progeny pool to parental strain JS1$^{CGL}$ and non-mutagenized screening strain FB2$^{CGL}$ should reveal genetic similarity of progeny as meiotic ancestors of parental strains. Mating type distribution of individuals of the progeny revealed a strong bias towards FB2$^{CGL}$ mating type *a2b2*. Out of 12 individuals of the progeny, all showed an *a2* mating type and all but two individuals showed a *b2* mating type. Since *a* and *b* mating locus are located on different chromosomes, the bias is expected not to be limited to only the mating type. This was confirmed on a genome level by the number of SNPs, depicted in Table 4: more than tenfold more SNPs were observed for the hyper secretion pool against JS1$^{CGL}$ (6,165) than against FB2$^{CGL}$ (498). Interestingly, analysis of an independent reference pool, containing only other hypersecretion candidates USec$^{+}$2-4 without mating showed a similar number of 408 SNPs (data not shown), leading to the assumption, that the genetic background of hypersecretion progeny pool and hypersecretion candidates is very similar. Furthermore, SNPs of wild type secretion progeny pool show smaller differences of 3,758 against FB2$^{CGL}$ and 5,838 against JS1$^{CGL}$. Number of SNPs against UM521 reference genome was comparable among all pools (Table 5). Therefore, the presumed bias of hyper secretion progeny towards FB2$^{CGL}$ was confirmed on a genetic level.

**Table 6.5. Number of SNPs in mappings of different sequencing pool reads on reference genomes.** Reads of USec$^{+}$1 hyper and wild type secretion progeny pool were mapped on reference genome of published *U. maydis* UM521 (Kämper et al., 2006) or FB2$^{CGL}$ and JS1$^{CGL}$ data from the sequencing conducted in this study.

| Sequencing reads | Reference genome | Number of SNPs |
|---|---|---|
| Hyper secretion progeny pool | UM521 | 15,152 |
| Wild type secretion progeny pool | UM521 | 14,278 |
| Hyper secretion progeny pool | FB2$^{CGL}$ | 498 |
| Wild type secretion progeny pool | FB2$^{CGL}$ | 3,758 |
| Hyper secretion progeny pool | JS1$^{CGL}$ | 6,614 |
| Wild type secretion progeny pool | JS1$^{CGL}$ | 5,838 |

Despite obvious mating type and sequence bias of progeny, identified SNPs of different pools were compared in a next step. For this approach, the responsible mutation was expected in every read of the hyper secretion pool and the UV-mutagenized hyper secretion parental strain USec$^{+}$1, but not in wild type secretion pool (Figure 6.7).

Therefore, SNPs in the hyper secretion progeny pool against JS1$^{CGL}$ alignment were identified and compared to SNPs in alignments of the same pool against FB2$^{CGL}$ and of USec$^{+}$1 against FB2$^{CGL}$. Repetitive sequences and low coverage regions can result in multiple hits of mutations to a region in the reference genome. To avoid false positive results, only unique hits of each individual alignment against the respective reference genome were considered for comparison to other alignments. To this end, only one SNP met the criteria. However, deeper insight into the sequence alignment of the hit with unique SNPs in both other alignments, revealed an overall low Blast score, indicating that this hit is not reliable. Strategy and number of identified SNPs are depicted in Figure 6.8. A detailed described can be found in Supplementary information 1. In sum, pooled linkage analysis for SNPs between hyper secretion strain and pool did not reveal the underlying mutation. Therefore, genome comparison needs to be expanded beyond identification of single nucleotide polymorphisms to whole region to further elucidate the underlying mutation events.

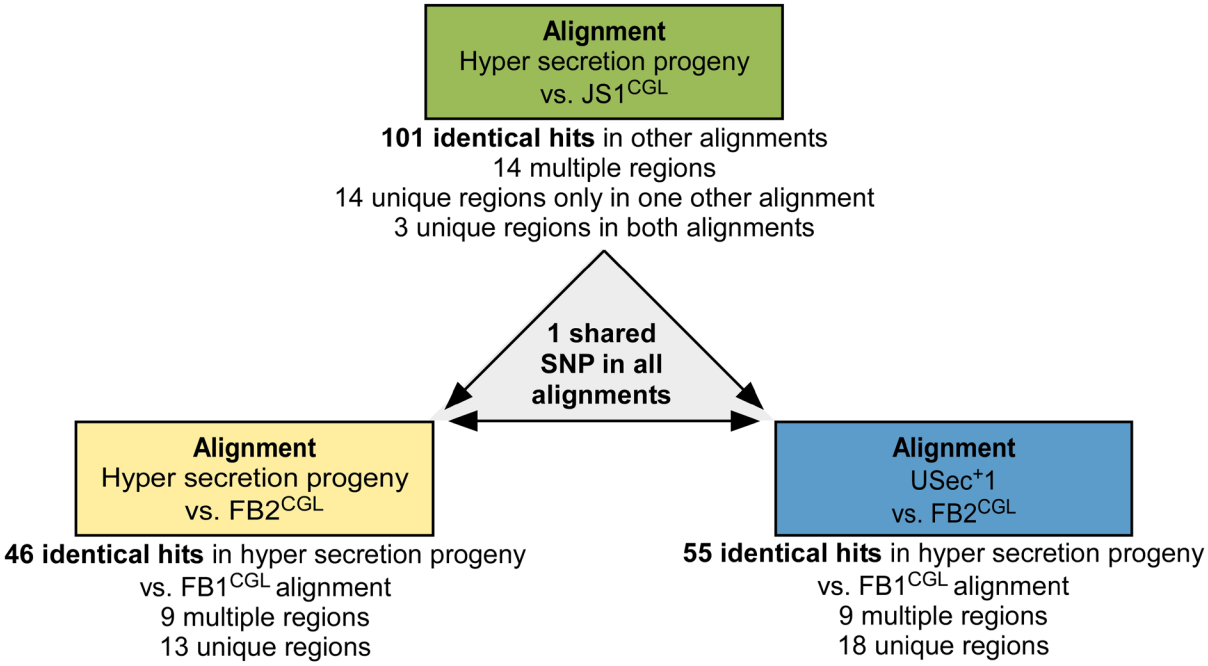


**Figure 6.8. Number of hits of defined criteria determined in pooled linkage analysis.** The alignment of the hyper secretion progeny pool to JS1$^{CGL}$ (green) was compared to the alignment of hyper secretion progeny pool to JS1$^{CGL}$ (yellow) and the alignment of USec$^{+}$1 hyper secretion candidate to FB2$^{CGL}$ (blue). SNPs that were detected in two or all three alignments were considered identical hits. Identical hits were further classified on unique or multiple similarities in other alignments. Unique hits in each individual alignment were compared with different alignments.

## 6.5 Discussion

In this study, we applied a previously established forward genetic UV-mutagenesis screen for identification and isolation of hyper secretion mutants. To this end, of about 250,000 screened mutants, four hyper secretion candidates with up to four-fold increased unconventional secretion capacity were isolated. One candidate was selected for pooled linkage analysis towards identification of underlying mutation.

Forward genetic screens represent a powerful tool to identify genes that are involved in various complex systems and mechanisms (Forsburg, 2001; Page & Grossniklaus, 2002). They have been widely adapted for yeast-like and filamentous fungi and several tools and techniques have been established in the framework of fundamental biology approaches (Casselton & Zolan, 2002; Forsburg, 2001). Strain optimization by mutagenesis is also a well-established technique in biotechnology (Bott & Eggeling, 2017). Several important industrial strains like amino acid producing *Corynebacterium glutamicum* or protein hyper secreting *Trichoderma reesei* were obtained via this technique (Baker, 2009; Bott & Eggeling, 2017). The approach of multiple rounds of mutagenesis is widely used in biotechnology (Baker, 2009; Le Crom et al., 2009; Peterson & Nevalainen, 2012; Schneeberger, 2014). The filamentous ascomycete *T. reesei* is a well-established biotechnological production platform for cellulases

and hemicellulases. The hyper secreting mutant RUT-C30 was obtained after three rounds of random mutagenesis. Applying this technique, hyper secretion comes along with several other mutagenesis events, leading to changes in physiology and structure (Peterson & Nevalainen, 2012). Hence, mutations relevant for the desired hyper secretion phenotype in RUT-C30 remained hidden for several years. Only recently, genome insights obtained by sequencing led to identification and understanding of several mutations (Le Crom et al., 2009; Martinez et al., 2008). Interestingly, beside identified genes encoding proteins involved in secretion, for example endoplasmic reticulum-associated protein degradation (ERAD) pathway key players or proteins involved in protein trafficking, genome sequencing also revealed importance of genes encoding proteins involved in nucleocytoplasmic transport, vacuolar protein trafficking and mRNA turnover for strain improvement (Le Crom et al., 2009; Martinez et al., 2008).

From a strain engineering perspective, it is highly favorable to also identify responsible mutations in hyper secretors to exploit them for export of heterologous proteins. Accumulation of mutations can have adverse effects on fitness and viability (Shibai et al., 2017). As observed in this study, unconventional secretion capacity of progeny even exceeds capacity of the hyper secretion parental strain. Mating with a wild type strain reduced the number of mutations in the individuals of the progeny. Identification of underlying mutations would enable the generation of a tailor-made strain, harboring only defined mutations. This would be a large step towards a competitive production strain. A repertoire of different effective hyper secretion mutations would allow the generation of tailor-made strains in defined backgrounds (Baker, 2009; Schneeberger, 2014). Introduction of relevant mutations into protease-deficient strains would for example be desirable (Sarkari et al., 2014; Terfrüchte et al., 2018). Therefore, detailed understanding of engineered organisms is important for biotechnological applications for strain engineering and improvement.

To identify the underlying hyper secretion mutation in the UV mutagenized screening strain, pooled linkage analysis was conducted. Too little is known about the genetics of unconventional secretion in *U. maydis*, therefore, narrowing down mutation of a specific genetic element was not possible. Comparison of mutations in meiotic progeny and parental strains should constitute an elegant approach to reveal the mutation associated with an increased unconventional secretion capacity. Surprisingly, a strong bias of hyper secretion progeny towards parental FB2$^{CGL}$ screening strain was observed on both mating type and sequence level. Further insights in mating type bias and location of reporter constructs could help to narrow down the underlying mutation to a specific region. While the *a* locus of all hyper secretion progeny was identical to FB2$^{CGL}$ (and therefore also UV-mutagenized USec$^{+}$1) screening strain, little variation was observed for the *b* locus. Interestingly, *a* locus and insertion site of one of the reporter constructs are located on the same chromosome. In the

future, careful bioinformatic investigation could eventually reveal region of the underlying mutation or linkage of unconventional secretion to a certain mating type.

To identify the underlying mutation, its presence in all hypersecretion progeny as well as the hyper secretion parental strain is a prerequisite. However, pooled linkage analysis of SNPs in hyper secretion and wild type secretion pool did not reveal a precise hit meeting these criteria. Therefore, the analysis should be extended towards identification of longer regions that differ between candidates and reference strains. Beside described 5′-CT or 5′-CCTT UV signature, UV radiation also induces double strand breaks, which can be very deleterious due to loss of longer stretches of genetic material (Rastogi et al., 2010). Interestingly, graphical analysis of mapped reads to the reference genome indicated multiple regions without reads in the hyper secretion pool, indicating deletion events (Figure S6.8). Furthermore, also insertion deletion (INDEL) events are described for UV induced mutations (Barsoum et al., 2020). Considering these events could also help elucidate the underlying mutation. However, such analysis is difficult to conduct and could not be achieved in the framework of this study. In future, implementation of pooled linkage analysis in addition for the three remaining candidates should be conducted, hoping that in these cases a precise single hit would guide the way to the responsible genetic variation. Although the analysis for USec$^{+}$1 failed to identify an underlying single nucleotide mutation for hyper secretion, important insights in the potential and limitations of pooled linkage analysis was gained. This knowledge can be applied for further analyses and adaptations.

## 6.6 Conclusion

This study demonstrated the great potential of a forward screening for hyper secretion candidates. High-throughput screening of UV-mutagenized screening strain candidates allowed isolation of at least four hyper secretion candidates. Sequencing analyses identified UV-induced mutations in all candidates. Pooled linkage analysis and meiotic crossing for one candidate revealed a strong bias towards one parental strain. A distinct mutation could not be identified. However, observed deletion events point for chromosome rearrangements as responsible for the hyper secretion phenotype. Deeper sequencing analysis is necessary to elucidate this in detail. Furthermore, repetition of the genetic screen will not only enable generation of additional hyper secretion mutants, a second mutagenesis approach of already mutagenized hyper secretion mutants might also allow for identification of synergistic mutations.

In conclusion, adaptation of the forward genetic screen for isolation of hyper secretion mutants was successful. While identification of underlying mutations is still pending, unconventional secretion of reporters could be increased in different UV-mutagenized candidates. Further

elucidation of underlying mutations will allow for the generation of tailor-made strains, harboring combined beneficial modifications. Increase of unconventional secretion capacity is an important step towards of establishing *U. maydis* as a competitive protein production and secretion platform.

*Keywords*
UV mutagenesis; forward genetic screen; unconventional secretion; *Ustilago maydis*; β-glucuronidase; β-galactosidase; pooled linkage analysis

*Author Contributions*
**K.H.** designed the adapted screen with advice by J.S. and support by M.P. as well as performed all other experiments. T.B., D.W. and A.B. performed bioinformatic analyses. K.S. and M.F. directed the study, J.K. directed the bioinformatical analyses. **K.H.** visualized and evaluated the data and wrote the manuscript with input of K.S.

*Acknowledgments*
We are thankful to B. Axler and U. Meyer for excellent technical support of the project. We gratefully acknowledge support in microscopic analyses by N. Heßler.

*Abbreviations*
aa, amino acid; $^{CGL}$, Cts1, Gus-Cts1, LacZ-Cts1, reporters in screening strains; Gus,β-glucuronidase; LacZ, β-galactosidase; MUC, 4-methylumbelliferyl β-D-N,N',N"-triacetylchitotrioside; MUG, 4-methylumbelliferyl-β-D-glucuronide; ONPG, o-nitrophenyl-β-D-galactopyranoside; SNP, Single nucleotide polymorphism; USec$^{+}$, Hyper secretion candidate obtained in genetic screen; X-Gal, 5-bromo-4-chloro-3-indolyl-β-D-galactopyranoside; X-Gluc, 5-bromo-4-chloro-3-indolyl-β-D-glucuronic acid.

## 6.7 Supplementary material

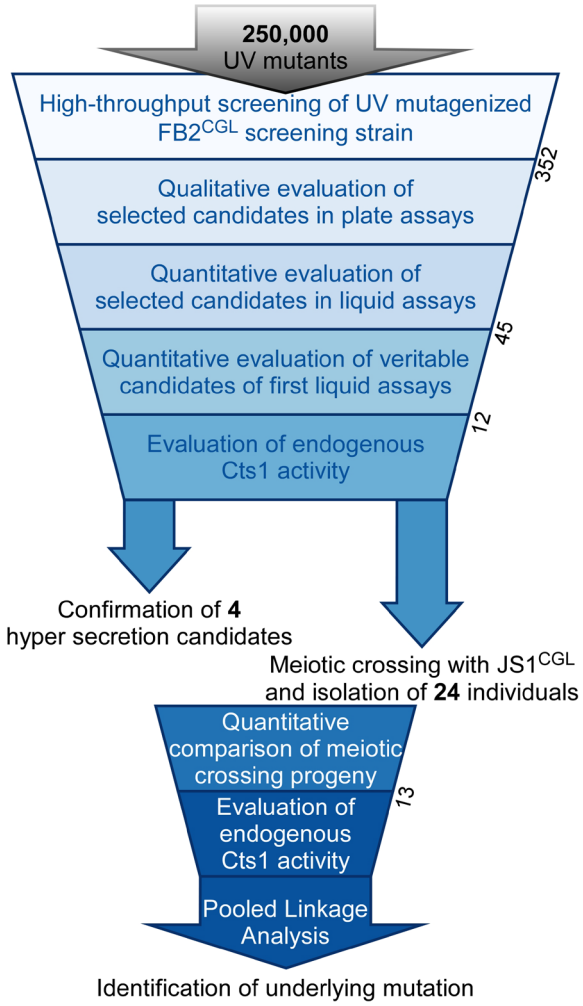


**Figure S6.1. All steps and candidates obtained by the genetic screen.** 250,000 single UV-mutagenized cells were investigated for their qualitative extracellular LacZ activity on CM-X-Gal plates. Of these, 352 candidates with apparently increased coloration were tested on their qualitative Gus activity on CM-X-Gluc plates as well as in quantitative liquid assays for both heterologous reporters. Liquid assays revealed an increased LacZ and Gus of at least 125% for 45 candidates. Verification of these 45 candidates in triplicates revealed 12 candidates with a Gus activity of at least 150% and a LacZ activity of at least 125%. Determination of endogenous Cts1 activity on the cell surface pointed out 4 candidates with a Gus activity considerable higher than FB2$^{CGL}$. To this end, mating with a compatible mating partner and plant infection to produce sexual spores led to 24 meiotic progeny, 16 showing an increased unconventional secretion capacity in comparison to non-mutagenized screening strain. Cts1 assays were conducted for 13 of these candidates, which were subsequently pooled and sequenced for pooled linkage analysis.

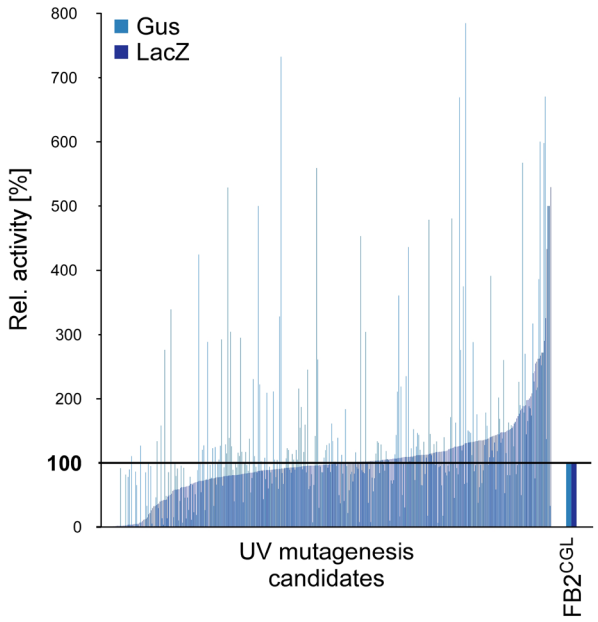


**Figure S6.2. Relative Gus and LacZ activity of selected candidates in liquid assays.** Extracellular activities of reporter enzymes LacZ and Gus, fused to Cts1, of all selected candidates in liquid assays were determined in single measurements and compared to the progenitor strain FB2$^{CGL}$ (Rel. LacZ and Gus activity = 100%, black line). All candidates were sorted according to their relative LacZ activity.

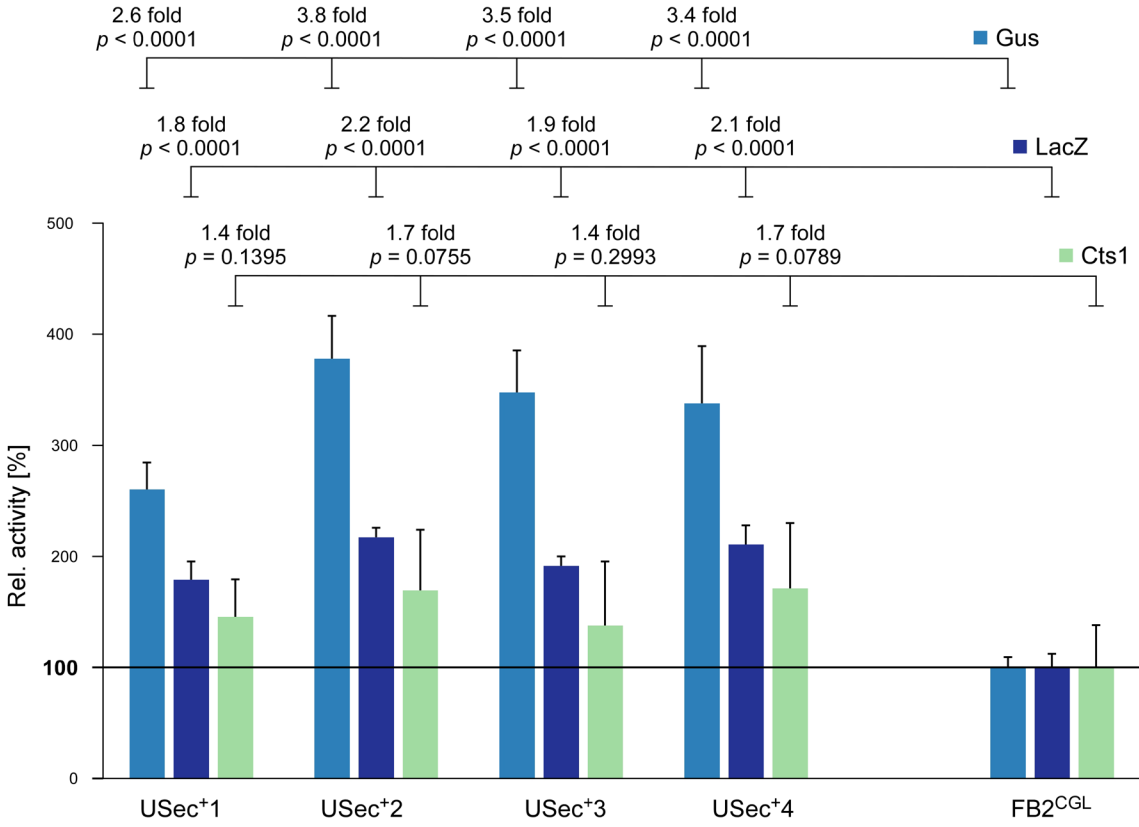


**Figure S6.3. Statistical analysis of Gus, LacZ and Cts1 activities shown in Figure 6.4B.** Extracellular reporter activities of four selected candidates in comparison to FB2$^{CGL}$ screening strain. Error bars depict standard deviation. Fold change of induced cultures and *p*-values of Student's unpaired *t*-test are shown. Black line indicates relative activity of FB2$^{CGL}$, normalized to 100%. Arrangement of candidates differs from Figure 4: In Figure 4 candidates were sorted according their relative Gus activity, here candidates are depicted according their number.

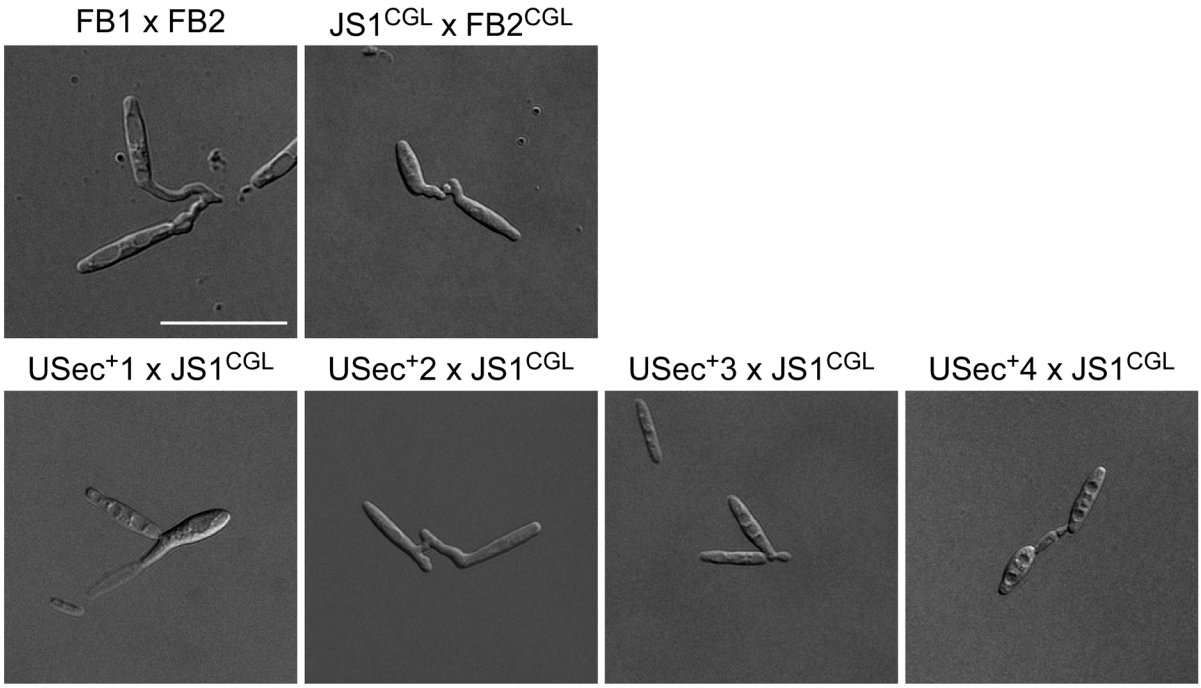


**Figure S6.4. Micrographs of diploid cells after mating.** DIC pictures of diploid cells in mixed culture of compatible mating strains. Wild type (FB1 x FB2) and strains harboring only reporter constructs ($JS1^{CGL}$ x $FB2^{CGL}$) served as positive control (upper panel). UV-mutagenized candidates $USec^{+}1$ – $Usec^{+}4$ were mated with compatible mating partner $JS1^{CGL}$. Scale bar, 20 µm

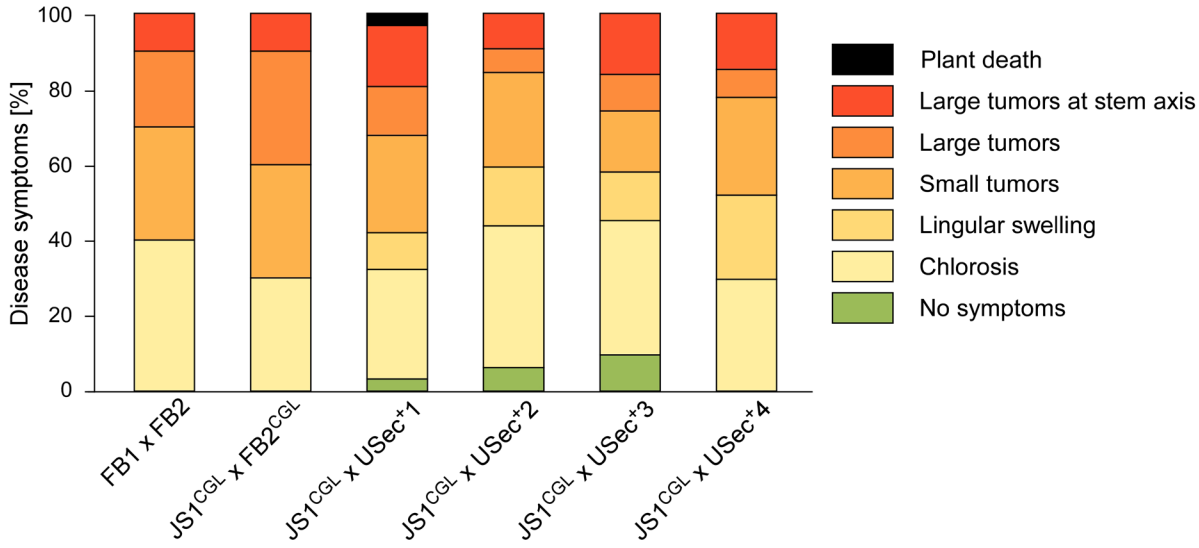


**Figure S6.5. Scoring of disease symptoms by plant infections using compatible FB1 and FB2 derivatives.** *Zea mays* var. *Arecibo* seedlings were infected with the indicated compatible strains. Plant disease symptoms were scored according to respective parameters. Control infections FB1 x FB2 and $JS1^{CGL}$ x $FB2^{CGL}$ were conducted with 10 plants, infections of $USec^{+}$ candidates with $JS1^{CGL}$ were conducted with 30 plants each. All tested compatible strain combinations led to formation of tumors with comparable distribution of symptoms.

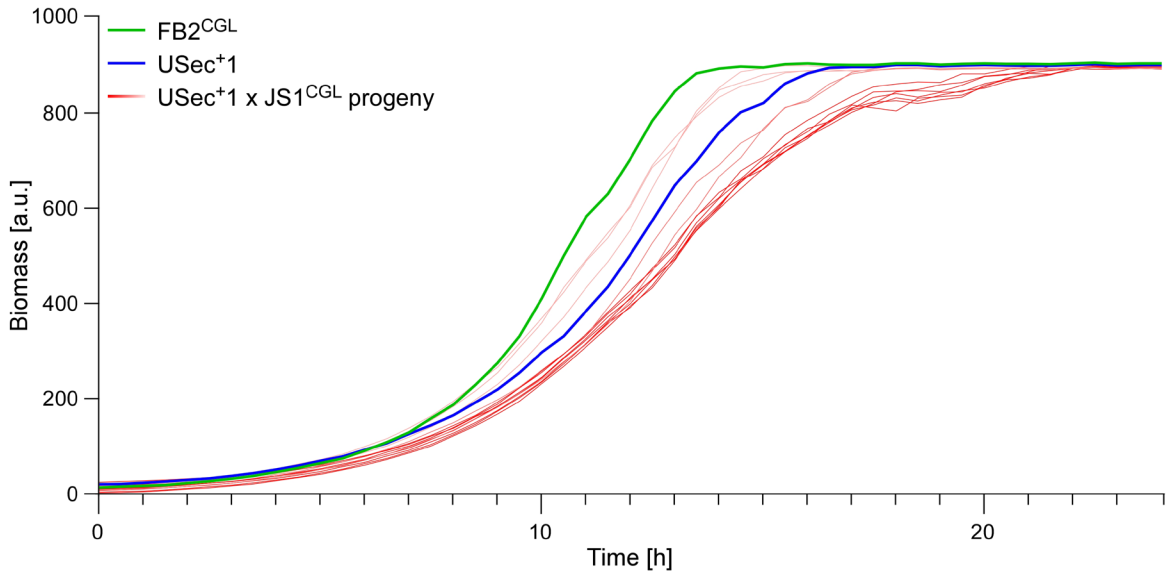


**Figure S6.6. Comparison of growth of FB2$^{CGL}$ screening strain, USec$^{+}$1 hyper secretion candidate and its progeny individuals.** Green line represents non-mutagenized FB2$^{CGL}$ screening strain, blue line mutagenized hyper secretion candidate USec$^{+}$1. A slight reduction of growth rate is observed upon mutagenesis. Growth of progeny individuals, obtained by mating of USec$^{+}$1 with JS1$^{CGL}$, with an increased unconventional secretion (red lines), was compared to FB2$^{CGL}$ and USec$^{+}$1. While growth of some progeny was even higher than for USec$^{+}$1, majority showed an even weaker growth. Fungal biomass was recorded online in a BioLector device (gain 25).

**Figure S6.7. Mating assay to identify mating type of sequenced candidates and progeny.** Mating of compatible strains was determined by investigation of cell morphology on charcoal-containing plates. Fuzzy colonies indicate hyphea formation while smoother colonies indicate similar mating type in one or both loci resulting in yeast-like growth. FB1 (*a1b2*), FB2 (*a2b2*), FB6a (*a2b1*) and FB6b (*a1b2*) served as tester strains with known mating types. Axenic cultures of tester strains were also investigated for cell morphology without mating partners. Red frame indicate hyphae forming colonies. **[Following pages]**

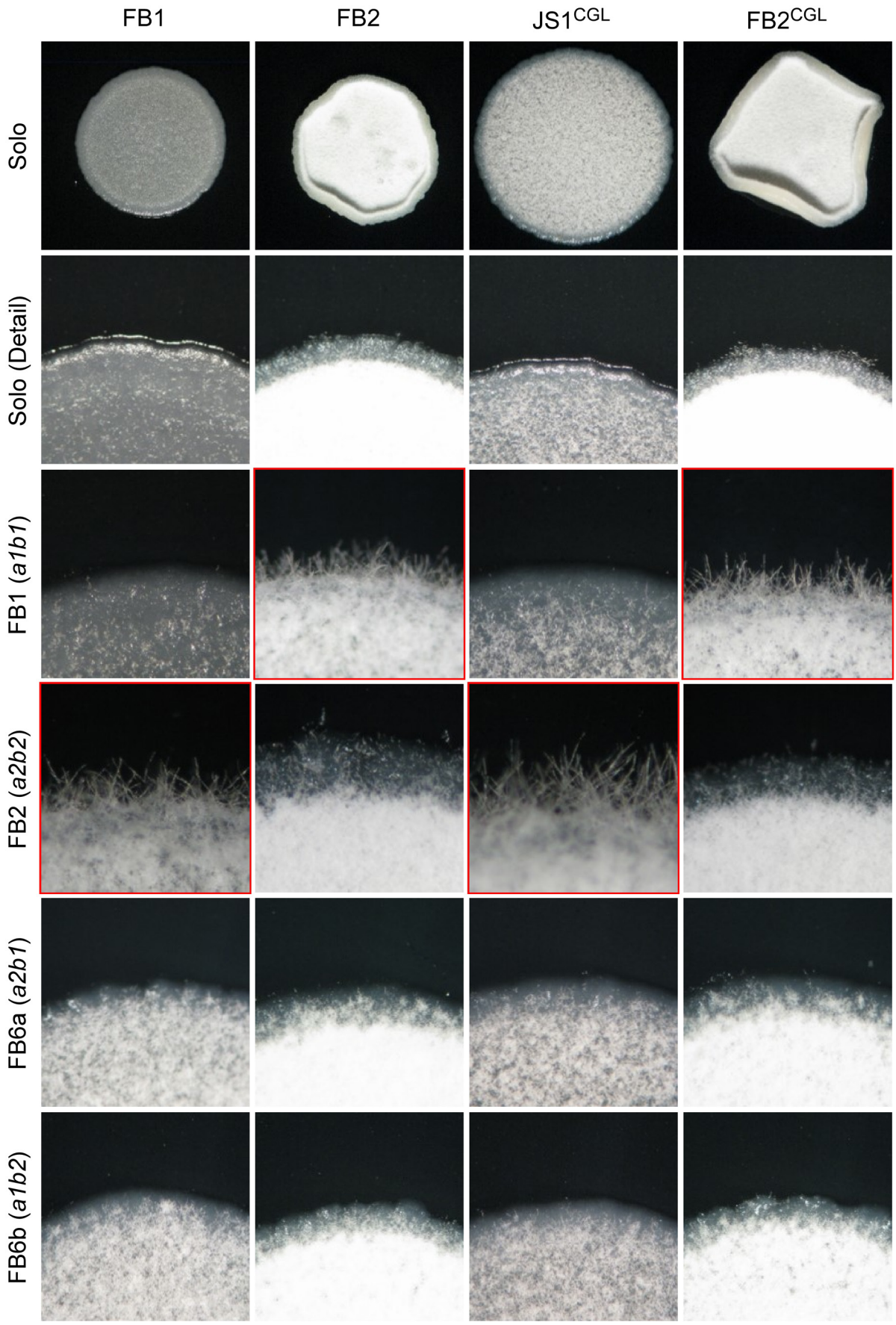
FB1
FB2
JS1CGL
FB2CGL
Solo
Solo (Detail)
FB1 (a1b1)
FB2 (a2b2)
FB6a (a2b1)
FB6b (a1b2)

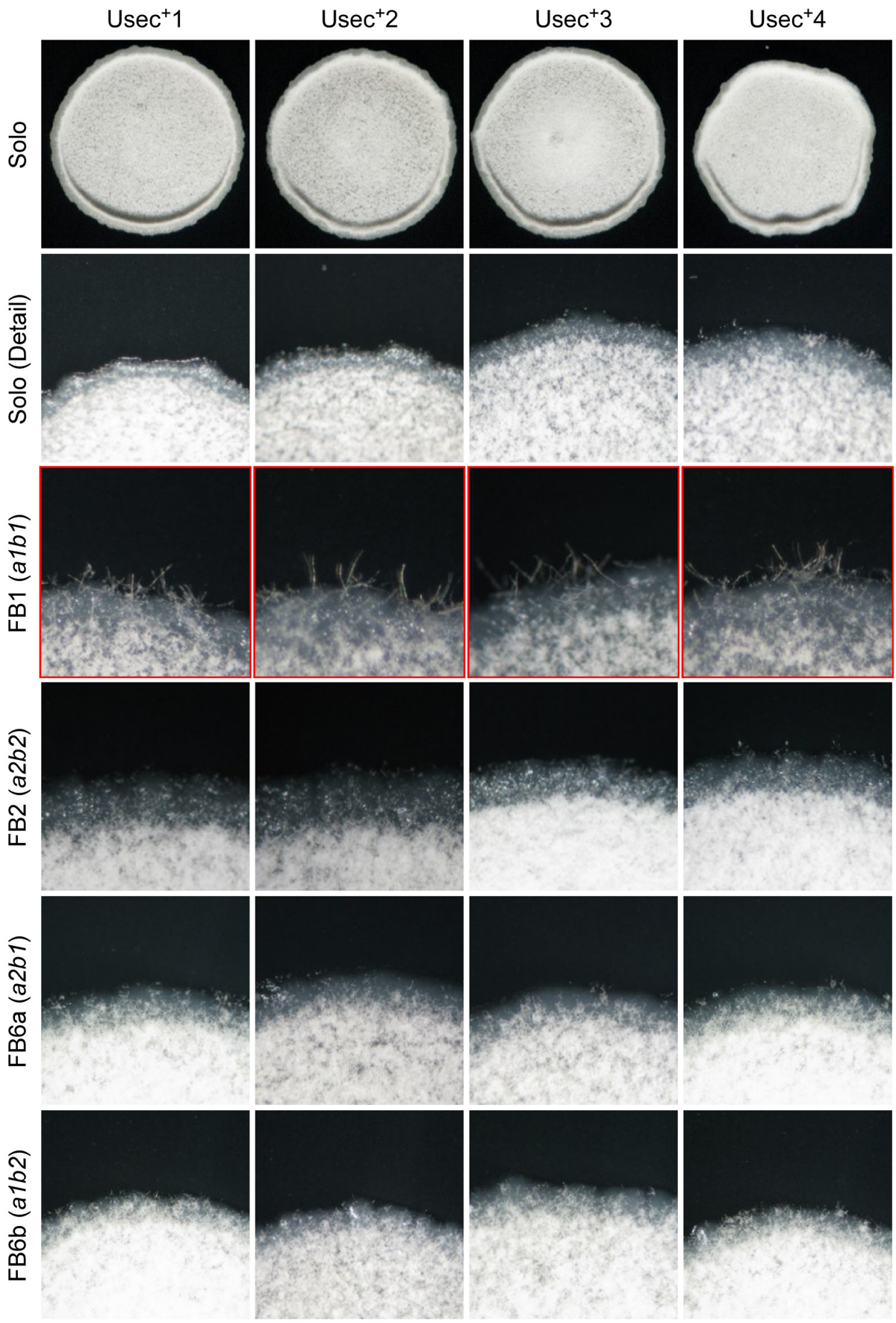
Usec+1
Usec+2
Usec+3
Usec+4
Solo
Solo (Detail)
FB1 (a1b1)
FB2 (a2b2)
FB6a (a2b1)
FB6b (a1b2)

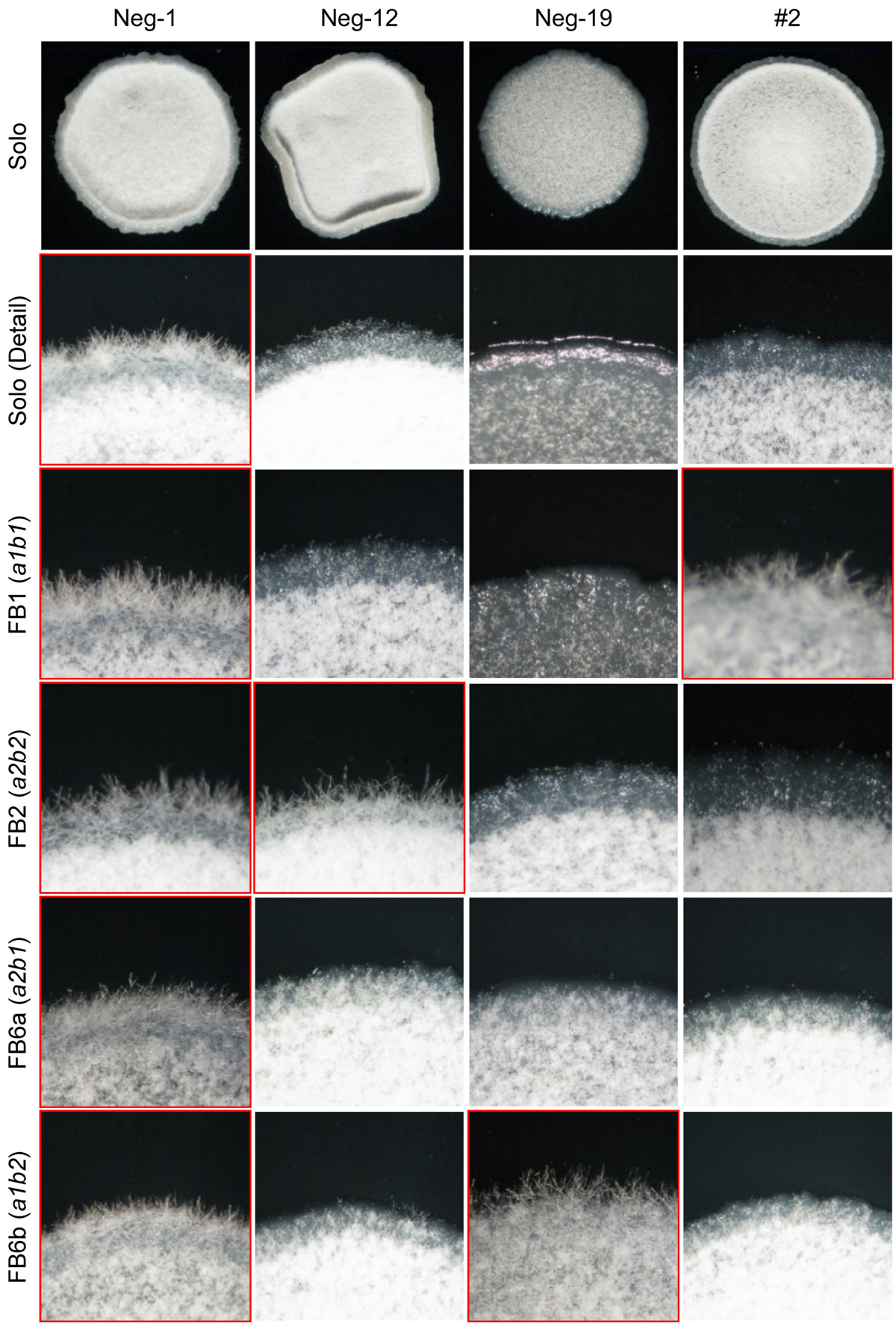
Neg-1
Neg-12
Neg-19
#2
Solo
Solo (Detail)
FB1 (a1b1)
FB2 (a2b2)
FB6a (a2b1)
FB6b (a1b2)

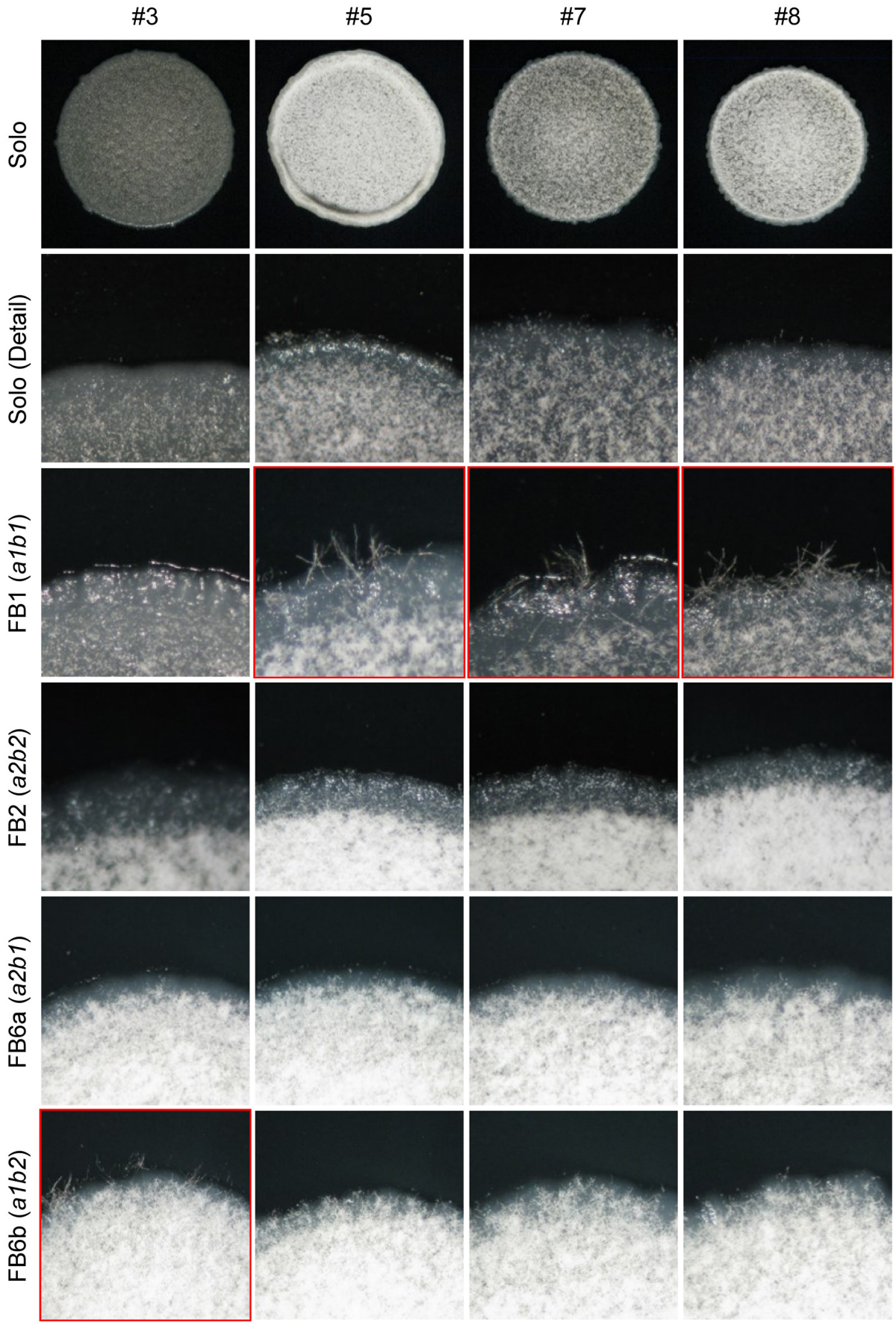
#3
#5
#7
#8
Solo
Solo (Detail)
FB1 (a1b1)
FB2 (a2b2)
FB6a (a2b1)
FB6b (a1b2)

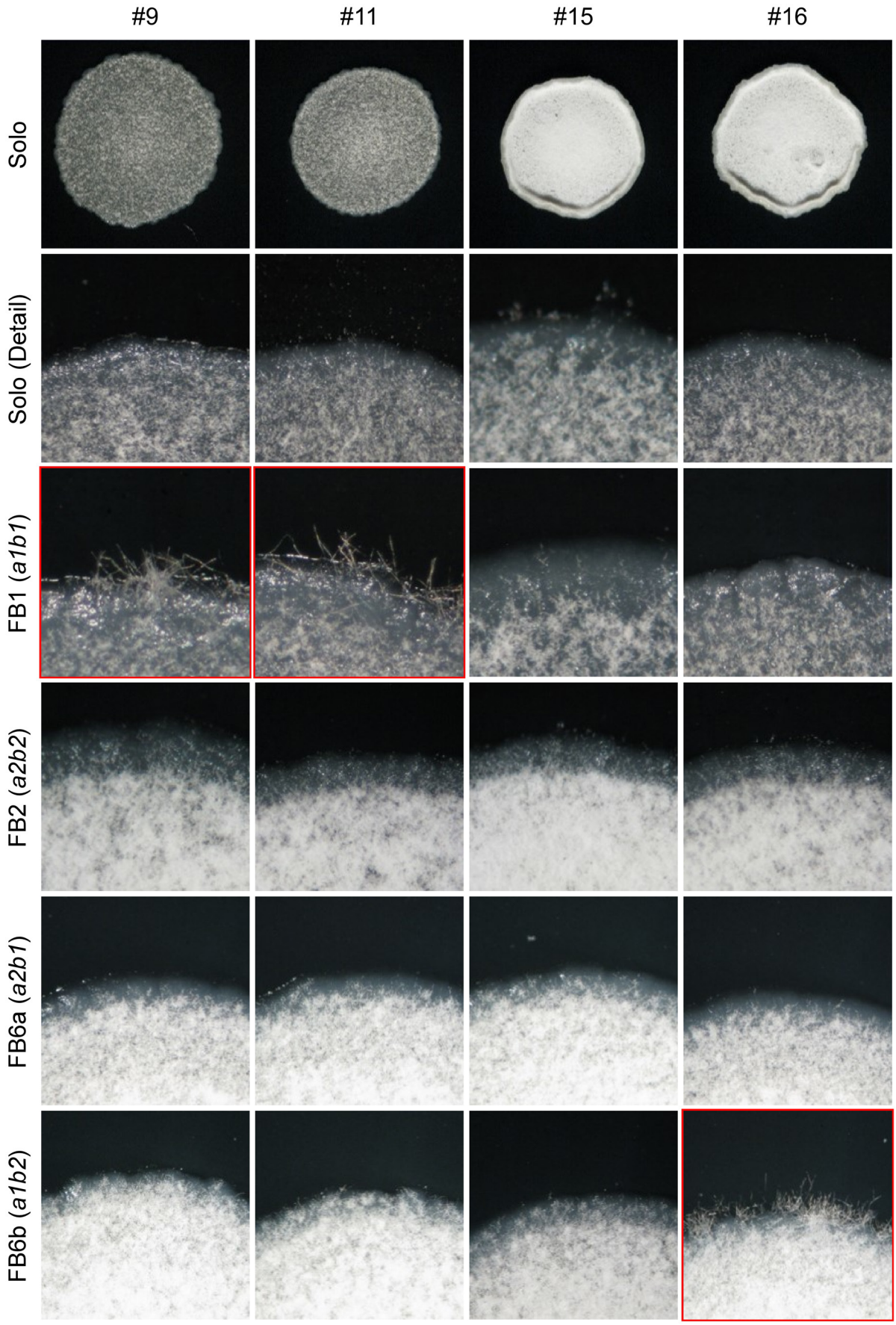
#9
#11
#15
#16
Solo
Solo (Detail)
FB1 (a1b1)
FB2 (a2b2)
FB6a (a2b1)
FB6b (a1b2)

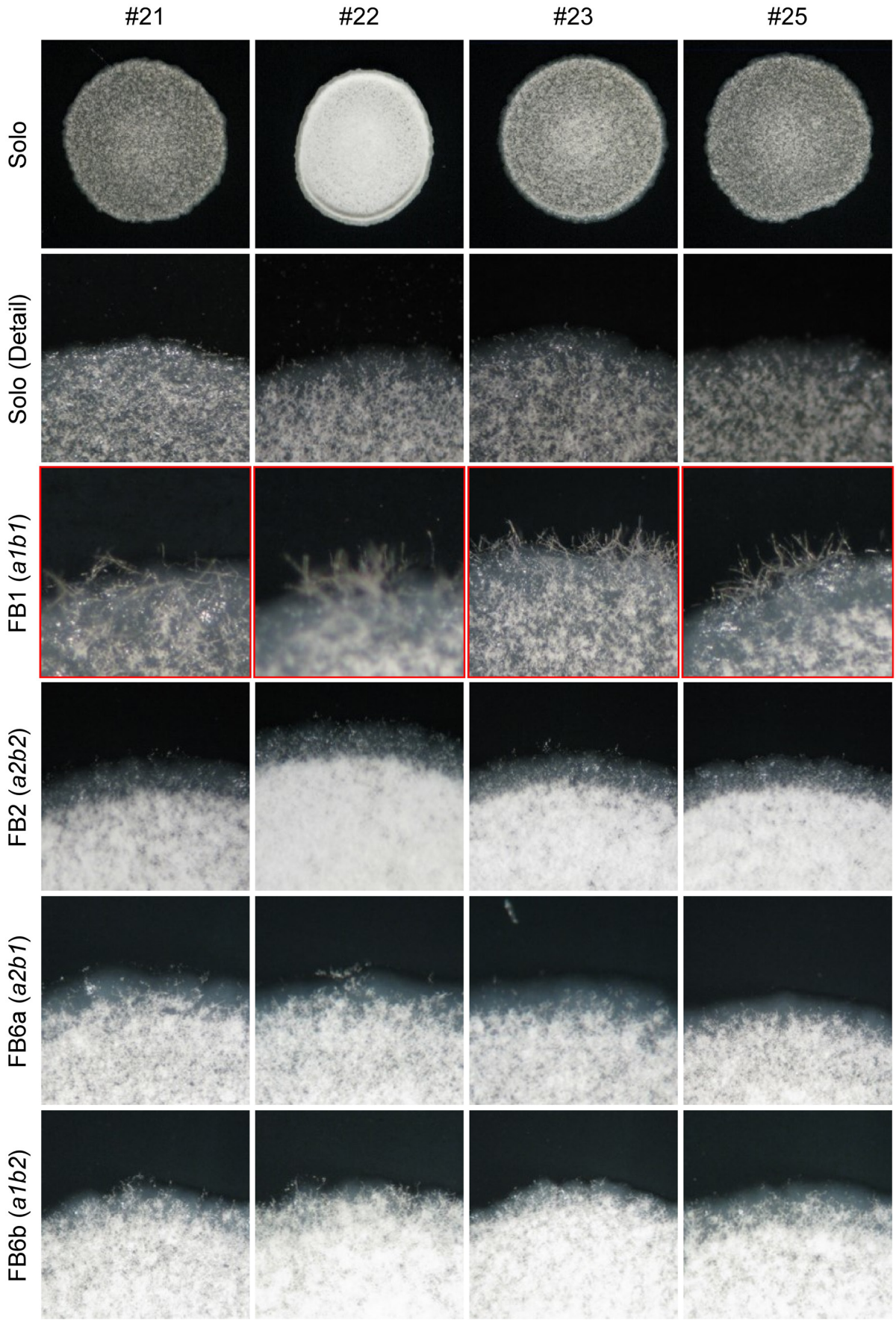
#21
#22
#23
#25
Solo
Solo (Detail)
FB1 (a1b1)
FB2 (a2b2)
FB6a (a2b1)
FB6b (a1b2)

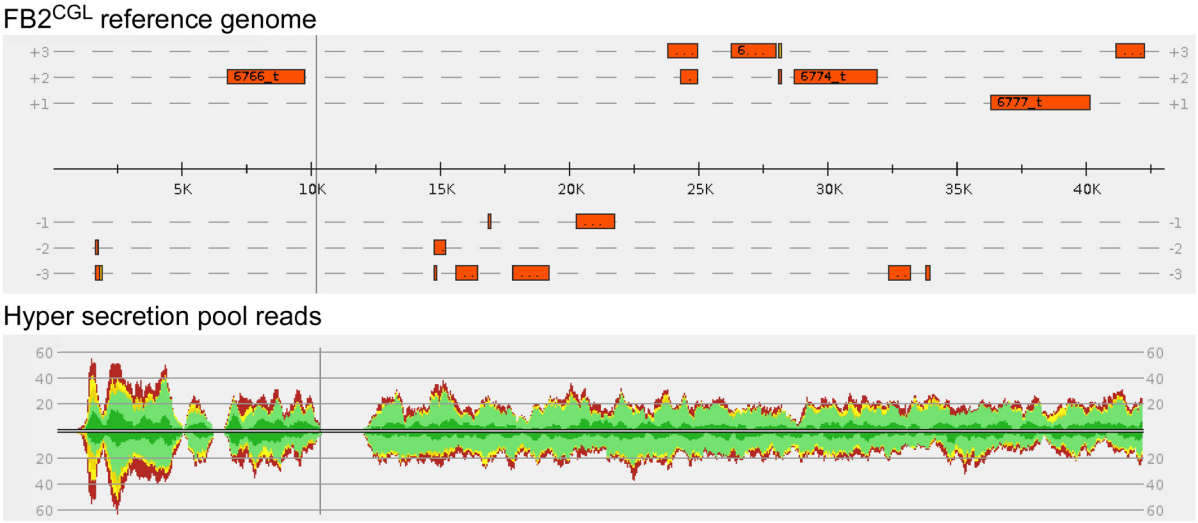


**Figure S6.8. Exemplary alignment of hyper secretion pool reads to FB2$^{CGL}$ reference genome.** Reads of hyper secretion pool (lower panel) were aligned on FB2$^{CGL}$ reference genome (upper panel). Red boxes in FB2$^{CGL}$ scheme represent genes on different reading frames (+3 to -3). Graph on hyper secretion pool panel represents alignment of reads: green: perfect match, yellow: match with minor mistakes, red mainly fitting with mismatches. Scale on the right and left represents the number of reads. No reads in the hyper secretion pool are a hint for sequence deletions. Analysis was conducted with ReadXplorer2.2.3.

### Supplementary Information 1: Description of pooled linkage analysis

A total of 101 hits in the hyper secretion progeny pool against JS1$^{CGL}$ could be aligned to identical mutations in USec$^{+}$1 or the hyper secretion progeny pool against FB2$^{CGL}$. Of these, 46 SNPs of the hyper secretion pool and 55 SNPs of USec$^{+}$1 against FB2$^{CGL}$ were also present in the comparison of the hyper secretion pool against JS1$^{CGL}$. Interestingly, most of the identified SNPs of hyper secretion pool against JS1$^{CGL}$ were not only aligned to one unique SNP in both other alignments, but to multiple hits. After grouping of multiple hits, a total of 14 SNPs identified in the hyper secretion pool against JS1$^{CGL}$ aligned to at least two different regions in the individual alignments. 14 other hits could only aligned to a SNP in one of the other alignments, either USec$^{+}$1 or hyper secretion pool against FB2$^{CGL}$, but not in the other. On the other hand, also for comparison of SNP in USec$^{+}$1 or the hyper secretion pool against FB2$^{CGL}$ to SNP identified in the same pool against JS1$^{CGL}$, multiple hits align to more than one sequence. Out of 55 total hits in the hyper secretion pool, only 18 were unique while the remaining hits can be grouped into nine multiple aligned SNPs. For USec$^{+}$1, 46 total hits were identified, after summarization of multiple aligned SNPs, only 13 remained unique, while other grouped SNPs aligned to 9 different regions in the hyper secretion pool alignment. The alignment hyper secretion pool against JS1$^{CGL}$ revealed only three unique SNPs that could be linked to SNPs in both other alignments. However, of these three hits, only for one the identified SNP was identical between the two other alignments. For the two other hits, the SNP aligned to different regions in the hyper secretion pool and USec$^{+}$1. Nevertheless, this SNP

was also considered a false positive hit afterwards, since an alignment length of only 156 out of 1000 nucleotides with a sequence identity of above 98% was observed which is rather a hint for a repetitive region then for a distinct region in the genome. No comparison of wild type like secretion pool was conducted at this point.

# 7 Outlook and further perspectives for establishment and adaption of a genetic screen for hyper secretion candidates

Adaption of a forward genetic screen for identification of hyper secretion mutants was an important step towards elucidation of the unconventional secretion mechanism and increased unconventional secretion capacity. Genetic screens require careful selection of candidates according to well-defined criteria and a comprehensive quantification for selection of positive candidates (van Rossum et al., 2013). Selection of applicable reporter systems for a screen is another important step to meet the preferred features (van Rossum et al., 2013). Success and applicability of forward genetic screens therefore highly relies on selection of an easy and solid read-out to identify mutants of interest and a defined genetic background of the screening candidates (Page & Grossniklaus, 2002). In our system, application of two heterologous reporters enabled this evaluation in a straightforward manner. Secretion capacity of at least four individual candidates was largely increased for all three reporter proteins in the mutagenized FB2$^{CGL}$ screening strain. Expression of heterologous reporters *gus-cts1* and *lacZ-cts1* was under the control of the strong, constitutive, synthetic $P_{oma}$ promoter [Hartmann *et al.*, 1999]. The use of two copies of this promoter for expression of different genes leads to an overall reduced activity of both heterologous proteins (data not shown), presumably due to metabolic burden or limitation of transcription factor for promoter regulation (Hartmann et al., 1999; Sarkari, 2014). Therefore, removal of both heterologous reporter constructs would be crucial prior to exploitation of hyper secretion screening strains towards application for new heterologous target proteins. This can be achieved on the one hand via an established marker recycling strategy. For *U. maydis*, a marker recycling strategy based on the yeast flippase recombinase (FLP) which recognizes flippase recognition target (FRT) sequences is established. Recombination of FRT sites, up- and downstream of the respective sequence, results in removal of intervening DNA, in this case the heterologous reporter constructs, by excision, leaving one FRT recombination site behind (Khrunyk et al., 2010). However, for this study no selection cassette harboring FRT sites for recycling was used, therefore this could only be applied for future screens. Alternatively, counter selection allows a simple exchange of inserts. Substitution of reporter enzymes with a heterologous target would allow for an exchange of transgenic elements. This event could be verified by selection on the new antibiotic while transformed strains would be sensitive against the antibiotic used for selection of the screen reporter protein (Müntjes et al., 2020).

While utilization of UV-mutagenized strains for after the screen was a well-established technique in early biotechnology, identification and characterization of underlying mutation in isolated mutant strains becomes more and more viable with advanced DNA sequencing techniques (Baker, 2009; Schneeberger, 2014). While classical mutagenesis approaches for generation and isolation of hyper production strains aimed on large-scale mutagenesis followed by selection of favorable strains, nowadays DNA sequencing is applied to understand correlation of genotype and phenotype (Le Crom et al., 2009). Elucidation of responsible mutations for a certain phenotype can be of special interest towards tailor-made biotechnological production chassis (Baker, 2009; Schneeberger, 2014). Using this knowledge, generation of strains by rational design for protein hypersecretion is possible (Baker, 2018).

For *U. maydis* different strains were established for biotechnological production processes. For secretion of heterologous proteins, it is highly recommended to avoid extracellular degradation of proteins by endogenous proteases (Idiris et al., 2010). Deletion of extracellular proteases significantly reduced protease activity in the supernatant, resulting in increased stability of heterologous proteins (Sarkari et al., 2014; Terfrüchte et al., 2018). Introduction of a hyper secretion mutation into a proteases deletion strain can therefore increase yield of secreted proteins in the supernatant. However, it is important to mention that different biotechnological processes require different carefully selected production chassis. While protease deletion strains have been shown to be excellent for production and secretion of heterologous proteins, they are highly outcompeted in terms of production of other products (Geiser et al., 2018).

For identification of underlying hyper secretion mutation, different UV-mutagenized candidates were compared to the FB2$^{CGL}$ screening strain. Interestingly, the number of overall mutations and the amount of UV induced mutations differed among investigated mutant candidates. While for USec$^{+}$1, USec$^{+}$3 and USec$^{+}$4 between 28 and 41 total mutations were identified, around one third with a UV signature, for USec$^{+}$2 the number of identified mutations was doubled, yet at a comparable relative number of mutations with an UV signature was observed. Moreover, the experimental design was in the process of establishment when this candidate was identified, resulting in slightly different conditions. UV mutagenesis was conducted for approximately 1.25 to 2.5 × $10^4$ cells per mL (Bösch et al., 2016). For mutagenesis of USec$^{+}$2, 4 - 8 × $10^6$ cells per mL were used. The more than 300-fold higher cell count could also lead to more cells that survived and thus, a higher total number of mutations. For *U. maydis* ten light-responsive proteins were predicted. Strains with deletion of predicted photolyases were impaired in photoreactivity (Brych et al., 2016). Cultivation in the dark reduced expression of photoreceptor and photolyase genes (Brych et al., 2016). Therefore, also little variations, which are not documented e.g. performing mutagenesis in the

evening following incubation overnight in the dark, can alter outcome. Hence, for standardization of procedure it is recommended to describe the mutagenesis protocol even more carefully. Overall, sample size needs to be enlarged to get statistically significant insights in UV mutagenesis output. For better understanding and optimization of the screen this could be conducted. Nevertheless, experimental set up was sufficient for generation of hyper secretion mutants and deeper investigations on mutagenesis were therefore beyond the scope of this study.

Based on the hypothesis that the responsible mutation is not necessarily located within an open reading frame, its identification turned out to be very complex. Instead of limiting the search to amino acid changes in genes, all mutations were considered. Therefore, an alternative sequencing strategy was followed, based on genetic crossing and pooled linkage analysis of progeny. Determination of mating types of progeny revealed a strong bias towards the parental USec$^{+}$1 mating type *a2b2.* Only two out of thirteen hyper secretion progeny individuals showed an *a2b1* phenotype while no *a1* phenotype was observed. Despite a very small sample size of only two haploid wild type secretion progeny individuals, both *a1* and *a2* are observed. In contrast to determination of mating type, colony morphology revealed an equal distribution of mucoid appearing FB1-like colonies and dry FB2-like colonies. This discrepancy could not be solved yet. Genetic linkage between different genes is a well described phenomena and can therefore be used to narrow down function or position of involved genes (Deed et al., 2017). However, while the *a* locus, containing the *a* specific pheromone gene *mfa1 (um_02382)*, and pheromone receptor, encoded by *pra1 (um_02383)* is located on chromosome 5, *b* locus genes encoding heterodimer transcription factor subunits bEast (*um_12052)* and bWest (*um_00578)* are located on chromosome 1 in close proximity. Hypothesized linkage of one single hyper secretion mutation to *a2b2* mating type can therefore be excluded. Furthermore, albeit the obvious bias, in two hyper secretion individuals of the progeny, *b1* mating type was observed. The fact, that all hyper secretion progeny showed the parental FB2$^{CGL}$/Usec$^{+}$1 *a2* mating type could help narrow down the underlying mutation. Therefore, further insights in linkage of underlying mutation to chromosome 5 located *a* locus might help localize the mutation.

A strong FB2 gene sequence bias in hyper secretion individuals of the progeny was also confirmed on a whole genome level. Based on this observation it appears that for supposed hyper secretion progeny apparently no to very little meiotic events took place. More equal distribution of JS1$^{CGL}$ and USec$^{+}$1 sequences for wild type secretion pool and presence of diploid individuals of the progeny indicates that in general mating, plant infection and formation of teliospores was successful but was not consistent for all isolated individuals. Obvious explanations for these observations do not exist. Survival of haploid USec$^{+}$1 strains is highly unlikely considering prolonged drying of tumor material at 37 °C followed by harvest of

teliospores including steps for removal of single yeast or hyphal cells using copper sulphate. Assuming that nevertheless single haploid cells remained alive during the whole process, the screen needs to be adapted to eliminate risk of false positive hyper secretion "progeny". Incubation and drying of teliospore containing tumors can for example be performed using a vacuum or at even higher temperatures to avoid leftover humidity as an ambient environment for survival of haploid cells (Vijayakrishnapillai et al., 2018; Zahiri et al., 2005). In the end, an elaborated verification of meiotic distribution in the progeny should be performed as quality control prior to sequencing.

Despite the apparent bias in progeny, pooled linkage sequence analysis was performed. Several hits were identical to multiple regions, identified in the other alignments. A reason for identification of one hit for multiple regions, apparently sharing a high similarity, could be repetitive sequences. Repetitive regions make it challenging to identify SNPs in alignments (Treangen & Salzberg, 2011). Interestingly, most hits confer to the end region in contigs. Assuming contigs resemble whole chromosomes, end of contigs would imply telomeric regions, which are known to contain two copies up to many thousand copies of DNA tandem repeats (≥2bp in length) adjacent to each other (Treangen & Salzberg, 2011). However, the high number of contigs of around 70 suggests that several contigs refer to one chromosome (U. maydis contains 23 chromosomes). For this study, ONT sequencing was used for generation of long reads, whose quality was improved using Illumina sequencing. For Illumina sequencing an increasing mismatch rate at the end of the reads is described (Tan et al., 2019). For ONT sequencing the error rate remains consistent throughout sequencing, but the number of reads decreases towards the end (Laver et al., 2015). Lower coverage at the end of contigs, generated by ONT sequencing, therefore raises the challenge to distinguish between a sequencing error and real SNPs, resulting in false positive results. No unique, identical hit for all alignments passed the quality control test. Further narrowing down of mutation to respective regions could allow a deeper insight. Identification of responsible chromosomes or regions, by identification of high accumulation of SNP in a certain area or adaptation of knowledge of mating type assays, could help identify the linkage of hyper secretion capacity and genetic regions. In order to narrow down the mutation to a specific region, mutagenized restriction enzymes sites could be exploited. Amplifying a region, harboring a mutation that deletes a restriction site from hyper secretion progeny pool and reference strains should give insight in combined occurrence of underlying hyper secretion mutation and respective region. While the restriction site is supposed to be intact in JS1$^{CGL}$ and FB2$^{CGL}$, no restriction takes part in USec$^{+}$1. If also in all individuals of the hyper secretion progeny no restriction is observed, the underlying mutation is either in proximity to the deleted restriction site or even exactly this mutation. However, this technique requires the presence of a mutation in a restriction site and is therefore limited (Mahdieh & Rabbani, 2013)

Accumulation of numerous UV-induced mutations also can have an effect on fitness and viability of strains (Shibai et al., 2017). Analysis of unconventional secretion capacity of progeny revealed one third of individuals exceeding the parental hyper secretion activity. Reduction of potentially adverse mutations that might have led to secondary effects could be an explanation for this. Mating USec$^{+}$1, harboring several mutations, with JS1$^{CGL}$ results in progeny with partly the mutation-intercepted USec$^{+}$1 DNA, while the other part originates from the mainly wild type JS1$^{CGL}$ genome. Therefore, mating of a UV-mutagenized strain with a compatible mating partner leads to meiotic progeny with a reduced amount of potential adverse mutations. However, albeit the small differences, growth of parental non-mutagenized FB2$^{CGL}$ screening, USec$^{+}$1 and progeny were still largely comparable. Therefore, potential adverse effects of accumulated mutations likely influenced other cellular processes besides growth rate. However, further insight into underlying beneficial and adverse mutations is necessary to elucidate effects on unconventional secretion capacity. Interestingly, unconventional secretion capacity of several individuals of the progeny was even increased in comparison to parental USec$^{+}$1 strain. This could indicate a potential negative effect on the unconventional export mechanism at a high accumulation of mutations in one strain

Although the responsible mutation for increased secretion remains concealed and needs further investigation, valuable information for subsequent screening rounds was generated during this process. Further optimization of identification of the underlying mutation in progeny pool generation and data evaluation is necessary. Specific steps would for example include adaptations in teliospore germination and harvest to avoid survival of haploid cells (Vijayakrishnapillai et al., 2018; Zahiri et al., 2005), a careful determination and verification of meiotic segregation in progeny, e.g. by mating type assays and understanding of progeny physiology and e.g. by growth or stress investigations. Sequence alignments revealed a high rate of false positive results due to low coverage and repetitive sequences presumably in telomeres (Treangen & Salzberg, 2011). Furthermore, the number of contigs exceeds the number of *U. maydis* chromosomes. Resequencing of reference strains or using published genome data as a scaffold for sequence arrangement could help to close existing gaps, resulting in a more robust reference genome. Mapping of hyper secretion reads to the reference genome revealed deletions of larger sequences, which are also described to potentially be UV-induced (Barsoum et al., 2020). Therefore, ongoing evaluation is considering whole chromosome rearrangements, deletions and insertion.

Beside USec$^{+}$1 and its progeny, USec$^{+}$2, USec$^{+}$3 and USec$^{+}$4 remain untested but also harbor great potential in identification of more hyper secretion mutations. Furthermore, the screen generated several more candidates with an increased unconventional secretion capacity in earlier stages of investigation. These mutants should be analyzed next with the optimized pipeline.

Other valuable methods to identify alternative or complementary mutants with hyper secretion capabilities are selective methods and adaptive laboratory evolution (ALE). *In vivo* selection strategies are based on the maintenance of selection pressure towards the desired criteria (van Rossum et al., 2013). While LacZ used in this study was applied for screening of mutants, it is also described as a tool for selection of hyper secretion candidates by limitation of carbon source (Larsen et al., 2013). Application of this strategy to the screening strain used in this study would allow exploitation of LacZ as a selection marker for growth on lactose on the one hand and as reporter for quantification of hyper secretion on the other hand, combining advantages of both methods in one strain.

Establishment of a selection method for isolation of hyper secretion mutants was shown before (Larsen et al., 2013). Here, a *P. pastoris* strain harboring LacZ fused to a *S. cerevisiae* conventional secretion signal peptide was mutagenized and LacZ secretion was investigated in medium containing lactose as sole carbon source. Candidates that grew on lactose medium due to secretion of LacZ also showed increased secretion of other heterologous proteins (Larsen et al., 2013). While this is an elegant way for *P. pastoris*, adaptation of LacZ as a selection marker in *U. maydis* would need some elaborate preparation. LacZ hydrolyzes lactose to galactose and glucose. While glucose is the preferable carbon source of *U. maydis*, galactose is described to be toxic due to an intermediate of galactose metabolization (Müller, 2019; Schuler et al., 2018). Deletion of hexose transporter gene *hxt1* allows growth on galactose containing medium since Hxt1-mediated galactose uptake is prevented. Interestingly deletion of an enzyme involved in production of the presumably toxic intermediate does not lead to an altered sensitivity in *Δhxt1* cells, suggesting that beside the toxic intermediate other mechanisms also play a role in toxicity (Schuler et al., 2018). Towards generation of a LacZ based unconventional selection strain, deeper insight in galactose toxicity might be necessary. However, avoidance of the toxic intermediate might be sufficient for a distinguishable growth. In addition, function of predicted endogenous secreted β-galactosidases (*umag02204 and umag02356*) has to be analyzed for selection conditions and the respective genes possibly need to be deleted (Mueller et al., 2008). Furthermore, a suitable promoter for expression of *lacZ-cts1* needs to be identified. Strong biosynthesis and secretion of the heterologous reporter that is already sufficient for proliferation on lactose might prevent discrimination between hyper secretion and wild type candidates. In essence, design and establishment of a selection screen in *U. maydis* could be a step forward to identification of numerous alternative or complementary hyper secretion candidates in this organism.

Long-term selection in adaptive laboratory evolution (ALE) would be another strategy towards accumulation of hyper secretion mutations in culture (Dragosits & Mattanovich, 2013; Sandberg et al., 2019). Here enrichment of cytokinesis mutants could be a possible outcome for cell cycle coupled unconventional secretion of Cts1. Long-term selection of strains by

adaptive laboratory evolution (ALE) allows for isolation of optimized microbial production systems without the prerequisite of fully understanding the underlying cellular mechanisms and responsible genetic elements (Dragosits & Mattanovich, 2013; Sandberg et al., 2019). In ALE, cells are cultivated under specific selective conditions, favoring certain physiological aspects. Adaptive changes under selection conditions accumulate in the microbial population and are therefore enriched after a prolonged period of cultivation (Dragosits & Mattanovich, 2013). While ALE studies on substrate utilization, increased tolerance and growth rate optimization are well established, adaption of ALE towards identification of increased secretion can be challenging since the secreted product influences all cells in the culture (Sandberg et al., 2019). Improved secretion upon ALE selection can be a result of other cellular processes, for example changes in a certain pathway results in a higher overall abundance of a compound and therefore also increased secretion, or increased tolerance to secreted compound in the medium also refers to an increased secretion capacity of cells (Holwerda et al., 2020; Pereira et al., 2020). Furthermore, ALE selection on lower temperatures can result in an enhanced membrane permeability due to changes in fatty acid composition. The changes in membrane phenotype and an improved secretion capacity were also observed for fermentation at higher temperature (Song et al., 2018). In the described ALE setups, not the secreted product was the selection parameter, but other cellular processes while enhanced secretion was just a result of adaptation of the cell. For unconventional secretion of Cts1 a dependency to the cell cycle is described (Aschenbroich et al., 2019). Utilization of ALE for identification of cells with an improved growth rate in a defined medium therefore could also result in candidates showing an increased unconventional secretion capacity.

In summary, adaptation of the genetic screen layed the foundation for further studies and improvements in evaluation and performance. Identified bottlenecks and open questions can be addressed towards minor corrections. Furthermore, generation of more candidates, by either another UV mutagenesis round or implementation of discussed improvements, can enlarge the repertoire of different hyper secretion mutations.

# 8 Final evaluation of biotechnological potential of unconventional secretion in *Ustilago maydis*

During the course of this project, major advancements in terms of application strategies and yield of the unconventional secretion system in *Ustilago maydis* were achieved. While previous studies showed successful secretion of high value biopharmaceuticals, low yields proposed a major drawback of this mechanism (Sarkari et al., 2014; Stock et al., 2012; Terfrüchte et al., 2017). Among biopharmaceutical products, antibodies and antibody fragments represent one of the most important groups (Spadiut et al., 2014; Walsh, 2018). Different antibodies and antibody fragments have been established for use in pharmaceutical applications (Joosten et al., 2003) (Figure 8.1). Thus, they represent promising targets for the secretion system which is rather suited for high prized than for bulk products (Terfrüchte et al., 2017).

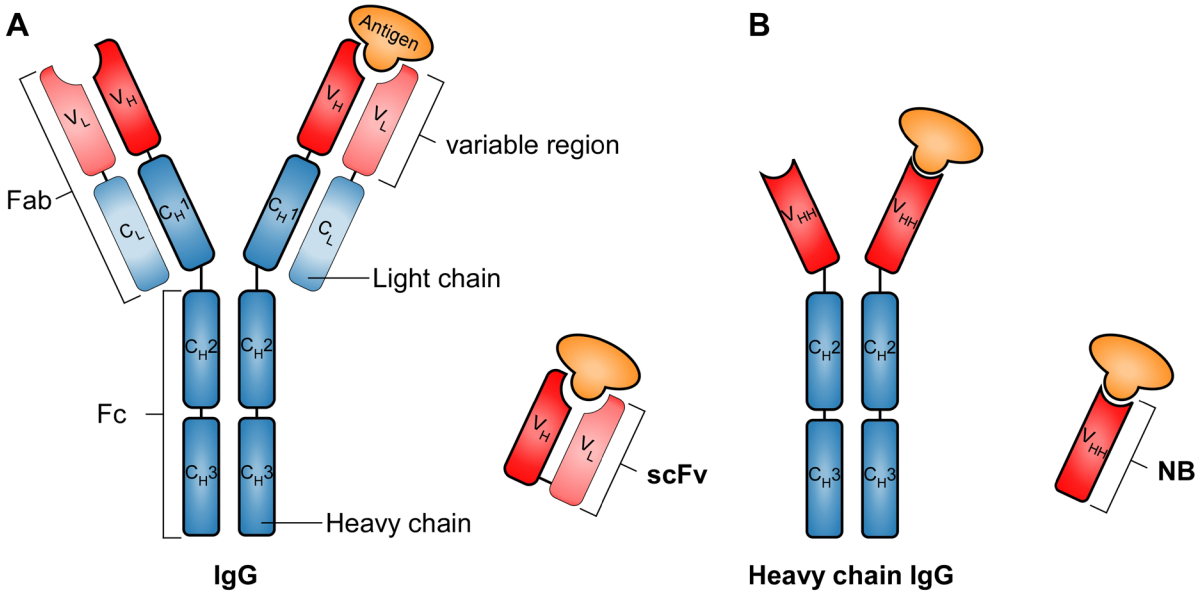


**Figure 8.1. Schematic representation of IgG antibodies and antibody fragments.** Antibodies and antibody fragments are capable of binding an antigen (orange) with unique, variable regions (red). **(A)** Immunoglobulin G (IgG) antibody consists of two identical heavy and light chains. The heavy chains consist three constant heavy chain domains $C_H1$-3 (dark blue) and a variable heavy chain domain $V_H$ (dark red). A constant light chain domain $C_L$ (light blue) and a variable light chain domain $V_L$ (light red) form a light chain. Constant domain $C_H3$ and $C_H2$ of the heavy chains form the non-antigen binding Fc (fragment crystallisable) part. The Fab (fragment antigen binding) region contains constant $C_L$ and $C_H1$ domains and variable, antigen binding $V_H$ and $V_L$ domains of light and heavy chain, respectively. Peptide linked $V_H$ and $V_L$ domains yield in a scFv (single-chain variable fragment) with antigen binding properties. **(B)** Heavy chain IgG antibody of camelidae consists of two identical heavy chains. Each chain is built up of constant domains $C_H3$ and $C_H2$ (blue) and antigen binding $V_{HH}$ domain (red). Isolated $V_{HH}$ can also act induvially, showing high antigen binding properties. The figure is according to (Joosten et al., 2003; Terfrüchte, 2016)

To date the majority of therapeutically approved antibodies is produced in mammalian cell lines. Mammalian post-translational modifications and advanced folding and secretion of proteins reduces concerns of immunogenic reactions of the biopharmaceutical proteins (Frenzel et al., 2013). However, high production costs, difficult handling as well as a long cultivation time and risk of viral contaminations are considerable drawbacks of mammalian production systems. (Frenzel et al., 2013; Kunert & Reinhart, 2016; O'Flaherty et al., 2020). Application of antibody fragments allows antigen-binding properties without need of extensive and specific post-translational modifications and hence these molecules are of rising interest. Therefore, antibody fragments such as single-chain variable fragments (scFv) or nanobodies can be produced in microbial microorganisms, most importantly *E. coli, S. cerevisiae* and *P. pastoris* (Berlec & Strukelj, 2013; Spadiut et al., 2014). Several production systems and expression strategies have been established for various nanobody formats in the described expression hosts. Yields are in a mg per liter range and can vary with the used expression system (Liu & Huang, 2018). Nanobodies produced heterologously in *E. coli* can either be located to the cytoplasm, the periplasm or extracellular space (Sandomenico et al., 2020). Since the cytoplasmic environment has major drawbacks in correct folding of nanobodies and formation of inclusion bodies, secretion is the favorable route (Sandomenico et al., 2020). Nevertheless, different approaches successfully established cytosolic expression and localization of nanobodies, including mimicking the extracellular environment for better folding or exploitation of solubility tags (Liu et al., 2019; Rezaie et al., 2017; Sandomenico et al., 2020). However, the presence of natural oxidizing conditions, folding catalysts and specific chaperones are important advantages for the preferred export of nanobodies into the periplasm (Choi & Lee, 2004; Sandomenico et al., 2020). Diverse signal peptides and routes for translocation, inducible systems and co-expression with chaperons have been established and investigated for enhancing yields in the periplasm (Karyolaimos et al., 2019; Petrus et al., 2019; Sandomenico et al., 2020). Isolation of proteins from the periplasm involves specific strategies such as high pressure, detergents or osmotic shock (Schimek et al., 2020). Further secretion across the outer membrane allows secretion of proteins to the extracellular medium (Sandomenico et al., 2020). Utilization of different signal peptides and upregulation of respective efflux pumps was for example applied for efficient secretion of antigen-binding fragments (Luo et al., 2019).

Using yeasts, heterologously produced proteins can easily be targeted to the extracellular space, which enables easy purification of soluble, functional and correctly folded proteins (Liu & Huang, 2018). Nanobodies can be produced and secreted in *S. cerevisiae* at high levels by fed-batch fermentation (Thomassen et al., 2005). However, accumulation of toxic ethanol and large amounts of endogenous secreted proteins can cause problems in high-density fermentation downstream processing. *P. pastoris* can rapidly grow to high cell densities to

produce nanobodies. In contrast to *S. cerevisiae,* downstream processing is not hindered by ethanol or high amounts of endogenous extracellular proteins (Liu & Huang, 2018). The first heterologous production of nanobodies in *P. pastoris was* described in year 2006 (Rahbarizadeh et al., 2006). In further studies, yield even exceeded *E. coli* periplasmic nanobody expression (Ezzine et al., 2012; Liu & Huang, 2018). Importantly, utilization of conventional secretion pathway also allows export of glycosylated proteins, which can increase toxin- and virus-neutralizing capacity but is also known to decrease antigen binding capacity in other cases (Ezzine et al., 2012; Harmsen et al., 2009; Liu & Huang, 2018). *N*-glycosylation sites are predicted for 10 % of nanobodies, therefore a careful selection of secretory pathway is important (Liu & Huang, 2018). Beside reduced binding efficiency upon *N*-glycosylation, it can confer to a short half-life time or even cause immunogenic reactions when used as biopharmaceuticals in human therapeutics (Gerngross, 2004). The establishment of a eukaryotic expression system that allows secretion of non-glycosylated proteins is therefore of special interest. Several strategies focus for example on deglycosylation of isolated proteins, humanized glycosylation to avoid allergic reactions, codon-optimized non-*N*-glycosylated version of the protein or disruption and modification of an endogenous glycosylation machinery (Arico et al., 2013; Ezzine et al., 2012; Hermanrud et al., 2012; Jacobs et al., 2009). Noteworthy, altered glycosylation patterns or complete absence of glycosylation can also reduce stability of proteins (Karnaukhova et al., 2006; Ward, 2012). Thus, each antibody format needs specific expression hosts and this is further complicated by the detailed requirements of the respective protein.

Unconventional secretion of heterologous proteins mediated by Cts1 in *U. maydis* represents a novel strategy for avoidance of post-translational modifications and has thus the potential to enlarge the repertoire of expression possibilities. Indeed, unconventional export of a functional nanobody directed against botulinum toxin A (BoNTA) fused to Cts1 was achieved in a proof of principle study with yields of 140 µg/L (Terfrüchte et al., 2017). Botulinum neurotoxin nanobodies have high pharmaceutical relevance since they can act as antitoxins by binding to multiple sites decorating the toxin and leading to its neutralization (Mukherjee et al., 2012). Different Botulinum toxin serotypes share a common C-terminus and have a variable N-terminus (Sagane et al., 2012). Co-administration of different BoNTA nanobody antitoxins also showed effectivity against BoNTB, suggesting also effectivity against all other serotypes (Mukherjee et al., 2012). Other studies focused on heterologous production of nanobodies against botulinum toxin E (BoNTE). Purification of nanobodies from *E. coli* periplasm yielded 55 – 57 mg/L in bacterial culture (Bakherad et al., 2013). The final yield for secretion in a eukaryotic system was 16 mg/L in *P. pastoris* fermentation (Baghban et al., 2016). With 140 ng/L, yield of *U. maydis* secreted nanobody is yet more than 100-fold lower

than described for *P. pastoris* system. To become competitive, the system thus needs further improvement in terms of yield and efficiency.

In this study, application of a forward genetic screen allowed isolation of different candidates and progeny individuals with an up to 7-fold increased secretion capacity. This would be a major improvement but still not competitive to other described expression systems. Identification of underlying mutation and combination of various hyper secretion mutations in one tailor-made hyper secretion strain would be a promising strategy to increase yields further.

Another important aspect for improvement of yields is the optimization of cultivation conditions. While highest yield for BoNTA in *U. maydis* was achieved after cultivation for 9 hours, cultivation for secretion of BoNTE in *P. pastoris* was conducted for 4 days (Baghban et al., 2016; Terfrüchte et al., 2017). Prolonged cultivation in *P. pastoris* for 9 days even reached 20 g/L nanobody (Gai et al., 2021). However, high-density fermentation processes pose the problem of degradation of heterologous proteins by host-specific proteases (Idiris et al., 2010; Zhang et al., 2007). While *P. pastoris* is described for relatively low levels of secreted proteases, cell lysis during prolonged incubation results in release of intracellular proteases to the culture medium (Burgard et al., 2020; Sinha et al., 2005). Also for *U. maydis*, adverse effects on yield of heterologous proteins by extracellular proteolytic potential were described (Sarkari et al., 2014; Terfrüchte et al., 2018). While previous studies tackled this problem by deletion of endogenous, extracellular proteases, the present strategy exploited the lock-type secretion mechanism towards protection of heterologous proteins within the fragmentation zone upon induction. Regulation of cell separation via transcriptional or post-translational regulation of Don3 allows control of secretion of heterologous proteins. Therefore, cultivation of *U. maydis* over a prolonged time in high cell density can be achieved without constitutive secretion of Cts1-fused protein of interest and continuous exposure to harmful proteases.

A combinational approach of both strategies would allow cultivation at high cell densities with accumulation of high levels of protected intracellular target protein. Induction of unconventional secretion mechanism by an external stimulus results in rapid release of trapped protein into the extracellular medium for isolation, minimizing the time exposed to extracellular proteases. Together with previous achievements such as optimized cultivation medium, improved construct design and deletion of endogenous, extracellular proteases, the here established novel strategies propose an important addition towards establishment of a competitive expression platform.

Future projects could aim on exploitation of chitin binding properties of Cts1. Previous studies described binding of Cts1 to commercially available chitin magnetic beads (Terfrüchte et al., 2017). Utilization of Cts1 binding capacity as an affinity tag for purification of fusion proteins would be an elegant way for in culture isolation of heterologous proteins. First studies into this direction investigated different native elution strategies (Bauer, 2020)(this work, data

not shown). Additionally, binding efficiency of Cts1 to synthetic *N*-acetylglucosamine oligomers was investigated, giving the potential for generation of an artificial affinity binding system, circumventing cross-interaction with endogenous contaminating proteins (Bauer, 2020). In future, utilization of a Cts1 based purification system could thus simplify downstream processing of heterologous, Cts1-fused proteins.

Furthermore, enlarging the repertoire of unconventionally secreted targets would give important insights on potential and limitations of the system. Importantly, achieved yield is strongly dependent on heterologous protein. Extracellular yield of Gus-Cts1 reporter construct was determined to be threefold higher than detected for anti-BoNTA nanobodies (Terfrüchte, 2016). In addition, neither previously investigated anti-BoNTA nanobody nor anti-Gfp nanobody, used in this study, harbored *N*-glycosylation sites (Gupta & Brunak, 2002)(Web reference: NetNGlyc), although avoidance of post-translational modifications is an important feature of this secretion system. Therefore, application of targets harboring an *N*-glycosylation site whose modification would potentially disrupt protein function would further demonstrate the potential of unconventional secretion. Previous studies demonstrated release of the potential malaria antigen RH5 by this pathway (Terfrüchte, 2016). These parasites do not perform classical *N*-glycosylation and proteins are sensitive to artificial modifications (Crosnier et al., 2013). However, yield and purification were not satisfying and protein function could not be verified (Terfrüchte, 2016). More recent ongoing approaches in this work aimed on export of antimicrobial peptides, harboring predicted *N*-glycosylation sites. While growth of heterologous AMP-producing *E. coli was* diminished, *U. maydis* showed no growth deficits (data not shown). Moreover, beside heterologous production of valuable products, unconventional secretion was also applied for secretion of carbohydrate active enzymes for degradation of plant biomass (Stoffels et al., 2020). Here secretion of bacterial enzymes was facilitated via the unconventional mechanism to avoid potential inactivation of enzymes due to eukaryotic post-translational modification. The presence of conventional and unconventional secretion pathways is therefore an important feature of *U. maydis* towards application as a whole cell factory and valorization of biomass in bioeconomic processes. However, the current yield limitation is also hindering its application to date.

In summary, the here presented improvements further moved *U. maydis* towards a competitive expression platform showed promising potential in biotechnological processes. Extensive application strategies on the one hand and fulfillment of niche demands in biotechnology on the other hand are important properties of this novel and versatile secretion system. Although current yields are beyond other heterologous protein production systems, a broad variety of different strategies offers interesting solutions to existing problems. Within only ten years from discovery of unconventional secretion of Cts1 in basic research to unconventional secretion of pharmaceutical products nowadays, major achievements were

reached and the system strongly advanced. This study aligns in various important previous projects and is an essential building brick towards establishment of a competitive expression platform. Elucidation of further aspects of the unconventional secretion mechanism can be applied for biotechnological processes. Thus, development of different tools and strategies relies on insights in basic research. The promising capability of unconventional secretion of *U. maydis* will be followed up in further studies, towards reaching competitiveness in the future.

# Appendix

## References


Akada, R., Yamamoto, J., & Yamashita, I. (1997). Screening and identification of yeast sequences that cause growth inhibition when overexpressed. *Mol Gen Genet*, *254*(3), 267-274. https://doi.org/10.1007/s004380050415

Anderlei, T., Zang, W., Papaspyrou, M., & Büchs, J. (2004). Online respiration activity measurement (OTR, CTR, RQ) in shake flasks. *Biochem Eng J*, *17*(3), 187-194. https://doi.org/10.1016/S1369-703X(03)00181-5

Andrei, C., Dazzi, C., Lotti, L., Torrisi, M. R., Chimini, G., & Rubartelli, A. (1999). The secretory route of the leaderless protein interleukin 1beta involves exocytosis of endolysosome-related vesicles. *Mol Biol Cell*, *10*(5), 1463-1475. https://doi.org/10.1091/mbc.10.5.1463

Anjard, C., & Loomis, W. F. (2005). Peptide signaling during terminal differentiation of *Dictyostelium*. *Proc Natl Acad Sci U S A*, *102*(21), 7607-7611. https://doi.org/10.1073/pnas.0501820102

Arico, C., Bonnet, C., & Javaud, C. (2013). *N*-glycosylation humanization for production of therapeutic recombinant glycoproteins in *Saccharomyces cerevisiae*. *Methods Mol Biol*, *988*, 45-57. https://doi.org/10.1007/978-1-62703-327-5_4

Aschenbroich, J., Hussnaetter, K. P., Stoffels, P., Langner, T., Zander, S., Sandrock, B., Bölker, M., Feldbrügge, M., & Schipper, K. (2019). The germinal centre kinase Don3 is crucial for unconventional secretion of chitinase Cts1 in *Ustilago maydis*. *Biochim Biophys Acta Proteins Proteom.*, *1867*, 140154. https://doi.org/10.1016/j.bbapap.2018.10.007

Baghban, R., Farajnia, S., Rajabibazl, M., Ghasemi, Y., Mafi, A., Hoseinpoor, R., Rahbarnia, L., & Aria, M. (2019). Yeast expression systems: Overview and recent advances. *Mol Biotechnol*, *61*(5), 365-384. https://doi.org/10.1007/s12033-019-00164-8

Baghban, R., Gargari, S. L., Rajabibazl, M., Nazarian, S., & Bakherad, H. (2016). Camelid-derived heavy-chain nanobody against *Clostridium botulinum* neurotoxin E in *Pichia pastoris*. *Biotechnol Appl Biochem*, *63*(2), 200-205. https://doi.org/10.1002/bab.1226

Baker, S. E. (2009). Selection to sequence: opportunities in fungal genomics. *Environ Microbiol*, *11*(12), 2955-2958. https://doi.org/10.1111/j.1462-2920.2009.02112.x

Baker, S. E. (2018). Protein hyperproduction in fungi by design. *Appl Microbiol Biotechnol*, *102*(20), 8621-8628. https://doi.org/10.1007/s00253-018-9265-1

Bakherad, H., Mousavi Gargari, S. L., Rasooli, I., Rajabibazl, M., Mohammadi, M., Ebrahimizadeh, W., Safaee Ardakani, L., & Zare, H. (2013). In vivo neutralization of botulinum neurotoxins serotype E with heavy-chain camelid antibodies (VHH). *Mol Biotechnol*, *55*(2), 159-167. https://doi.org/10.1007/s12033-013-9669-1

Balasundaram, B., Harrison, S., & Bracewell, D. G. (2009). Advances in product release strategies and impact on bioprocess design. *Trends Biotechnol*, *27*(8), 477-485. https://doi.org/10.1016/j.tibtech.2009.04.004

Baneyx, F., & Mujacic, M. (2004). Recombinant protein folding and misfolding in *Escherichia coli*. *Nat Biotechnol*, *22*(11), 1399-1408. https://doi.org/10.1038/nbt1029

Banuett, F. (1992). *Ustilago maydis*, the delightful blight. *Trends Genet*, *8*(5), 174-180. https://doi.org/10.1016/0168-9525(92)90220-x

Banuett, F., & Herskowitz, I. (1989a). Different *a* alleles of *Ustilago maydis* are necessary for maintenance of filamentous growth but not for meiosis. *Proc. Natl. Acad. Sci. U S A*, *86*(15), 5878-5882. http://www.ncbi.nlm.nih.gov/pubmed/16594058

Banuett, F., & Herskowitz, I. (1989b). Different a alleles of *Ustilago maydis* are necessary for maintenance of filamentous growth but not for meiosis. *Proc Natl Acad Sci U S A*, *86*(15), 5878-5882. https://doi.org/10.1073/pnas.86.15.5878

Barsoum, M., Kusch, S., Frantzeskakis, L., Schaffrath, U., & Panstruga, R. (2020). Ultraviolet mutagenesis coupled with next-generation sequencing as a method for functional interrogation of powdery mildew genomes. *Mol Plant Microbe Interact*, *33*(8), 1008-1021. https://doi.org/10.1094/MPMI-02-20-0035-TA

Bauer, S. (2020). *Monodisperse, sequenzdefinierte N-Acetylglucosaminsulfat-Oligomere und deren Anwendung in der Biologie und Biomedizin* https://docserv.uni-duesseldorf.de/servlets/DerivateServlet/Derivate-58590/2020_BauerS-Dissertation.pdf

Baumann, S., Pohlmann, T., Jungbluth, M., Brachmann, A., & Feldbrügge, M. (2012). Kinesin-3 and dynein mediate microtubule-dependent co-transport of mRNPs and endosomes. *J Cell Sci*, *125*(Pt 11), 2740-2752. https://doi.org/10.1242/jcs.101212

Baumann, S., Zander, S., Weidtkamp-Peters, S., & Feldbrügge, M. (2016). Live cell imaging of septin dynamics in *Ustilago maydis*. *Methods Cell Biol*, *136*, 143-159. https://doi.org/10.1016/bs.mcb.2016.03.021

Becht, P., Vollmeister, E., & Feldbrügge, M. (2005). Role for RNA-binding proteins implicated in pathogenic development of *Ustilago maydis*. *Eukaryot Cell*, *4*(1), 121-133. https://doi.org/10.1128/EC.4.1.121-133.2005

Becker, J., Hosseinpour Tehrani, H., Gauert, M., Mampel, J., Blank, L. M., & Wierckx, N. (2020). An *Ustilago maydis* chassis for itaconic acid production without by-products. *Microb Biotechnol*, *13*(2), 350-362. https://doi.org/10.1111/1751-7915.13525

Benham, A. M. (2012). Protein secretion and the endoplasmic reticulum. *Cold Spring Harb Perspect Biol*, *4*(8), a012872. https://doi.org/10.1101/cshperspect.a012872

Berens, C., & Hillen, W. (2003). Gene regulation by tetracyclines. Constraints of resistance regulation in bacteria shape TetR for application in eukaryotes. *Eur J Biochem*, *270*(15), 3109-3121. https://doi.org/10.1046/j.1432-1033.2003.03694.x

Berlec, A., & Strukelj, B. (2013). Current state and recent advances in biopharmaceutical production in *Escherichia coli,* yeasts and mammalian cells. *J Ind Microbiol Biotechnol*, *40*(3-4), 257-274. https://doi.org/10.1007/s10295-013-1235-0

Berndt, P., Lanver, D., & Kahmann, R. (2010). The AGC Ser/Thr kinase Aga1 is essential for appressorium formation and maintenance of the actin cytoskeleton in the smut fungus *Ustilago maydis*. *Mol Microbiol*, *78*(6), 1484-1499. https://doi.org/10.1111/j.1365-2958.2010.07422.x

Birkeland, S. R., Jin, N., Özdemir, A. C., Lyons, R. H., Jr., Weisman, L. S., & Wilson, T. E. (2010). Discovery of mutations in *Saccharomyces cerevisiae* by pooled linkage analysis and whole-genome sequencing. *Genetics*, *186*(4), 1127-1137. https://doi.org/10.1534/genetics.110.123232

Bishop, A. C., Shah, K., Liu, Y., Witucki, L., Kung, C., & Shokat, K. M. (1998). Design of allele-specific inhibitors to probe protein kinase signaling. *Curr Biol*, *8*(5), 257-266. https://doi.org/10.1016/s0960-9822(98)70198-8

Böhmer, C., Böhmer, M., Bölker, M., & Sandrock, B. (2008). Cdc42 and the Ste20-like kinase Don3 act independently in triggering cytokinesis in *Ustilago maydis*. *J Cell Sci*, *121*(Pt 2), 143-148. https://doi.org/10.1242/jcs.014449

Böhmer, C., Ripp, C., & Bölker, M. (2009). The germinal centre kinase Don3 triggers the dynamic rearrangement of higher-order septin structures during cytokinesis in *Ustilago maydis*. *Mol Microbiol*, *74*(6), 1484-1496. https://doi.org/10.1111/j.1365-2958.2009.06948.x

Bölker, M. (2001). *Ustilago maydis*--a valuable model system for the study of fungal dimorphism and virulence. *Microbiology*, *147*(Pt 6), 1395-1401. https://doi.org/10.1099/00221287-147-6-1395

Bölker, M., Genin, S., Lehmler, C., & Kahmann, R. (1995). Genetic regulation of mating and dimorphism in *Ustilago maydis*. *Can J Bot*, *73*(S1), 320-325. https://doi.org/10.1139/b95-262

Bölker, M., Urban, M., & Kahmann, R. (1992). The a mating type locus of *U. maydis* specifies cell signaling components. *Cell*, *68*(3), 441-450. https://doi.org/10.1016/0092-8674(92)90182-c

Bordoli, M. R., Yum, J., Breitkopf, S. B., Thon, J. N., Italiano, J. E., Jr., Xiao, J., Worby, C., Wong, S. K., Lin, G., Edenius, M., Keller, T. L., Asara, J. M., Dixon, J. E., Yeo, C. Y., & Whitman, M. (2014). A secreted tyrosine kinase acts in the extracellular environment. *Cell*, *158*(5), 1033-1044. https://doi.org/10.1016/j.cell.2014.06.048

Bösch, K., Frantzeskakis, L., Vranes, M., Kämper, J., Schipper, K., & Göhre, V. (2016). Genetic manipulation of the plant pathogen *Ustilago maydis* to study fungal biology and plant microbe interactions. *J Vis Exp*(115). https://doi.org/10.3791/54522

Bott, M., & Eggeling, L. (2017). Novel technologies for optimal strain breeding. *Adv Biochem Eng Biotechnol*, *159*, 227-254. https://doi.org/10.1007/10_2016_33

Bottin, A., Kämper, J., & Kahmann, R. (1996). Isolation of a carbon source-regulated gene from *Ustilago maydis*. *Mol Gen Genet*, *253*(3), 342-352. https://doi.org/10.1007/pl00008601

Brachmann, A. (2001). *Die frühe Infektionsphase von Ustilago maydis: Genregulation durch das bW/bE-Heterodimer* https://edoc.ub.uni-muenchen.de/28/1/Brachmann_Andreas.pdf

Brachmann, A., König, J., Julius, C., & Feldbrügge, M. (2004). A reverse genetic approach for generating gene replacement mutants in *Ustilago maydis*. *Mol Genet Genomics*, *272*(2), 216-226. https://doi.org/10.1007/s00438-004-1047-z

Brachmann, A., Weinzierl, G., Kämper, J., & Kahmann, R. (2001). Identification of genes in the bW/bE regulatory cascade in *Ustilago maydis*. *Mol Microbiol*, *42*(4), 1047-1063. https://doi.org/10.1046/j.1365-2958.2001.02699.x

Bradford, M. M. (1976). A rapid and sensitive method for the quantitation of microgram quantities of protein utilizing the principle of protein-dye binding. *Anal Biochem*, *72*, 248-254. https://doi.org/10.1006/abio.1976.9999

Brash, D. E. (2015). UV signature mutations. *Photochem Photobiol*, *91*(1), 15-26. https://doi.org/10.1111/php.12377

Brauer, M. J., Christianson, C. M., Pai, D. A., & Dunham, M. J. (2006). Mapping novel traits by array-assisted bulk segregant analysis in *Saccharomyces cerevisiae*. *Genetics*, *173*(3), 1813-1816. https://doi.org/10.1534/genetics.106.057927

Broomfield, P. L., & Hargreaves, J. A. (1992). A single amino-acid change in the iron-sulphur protein subunit of succinate dehydrogenase confers resistance to carboxin in *Ustilago maydis*. *Curr Genet*, *22*(2), 117-121. https://doi.org/10.1007/bf00351470

Brough, D., Pelegrin, P., & Nickel, W. (2017). An emerging case for membrane pore formation as a common mechanism for the unconventional secretion of FGF2 and IL-1beta. *J Cell Sci*, *130*(19), 3197-3202. https://doi.org/10.1242/jcs.204206

Bruns, C., McCaffery, J. M., Curwin, A. J., Duran, J. M., & Malhotra, V. (2011). Biogenesis of a novel compartment for autophagosome-mediated unconventional protein secretion. *J Cell Biol*, *195*(6), 979-992. https://doi.org/10.1083/jcb.201106098

Brych, A., Mascarenhas, J., Jaeger, E., Charkiewicz, E., Pokorny, R., Bolker, M., Doehlemann, G., & Batschauer, A. (2016). White collar 1-induced photolyase expression contributes to UV-tolerance of *Ustilago maydis*. *MicrobiologyOpen*, *5*(2), 224-243. https://doi.org/10.1002/mbo3.322

Burgard, J., Grünwald-Gruber, C., Altmann, F., Zanghellini, J., Valli, M., Mattanovich, D., & Gasser, B. (2020). The secretome of *Pichia pastoris* in fed-batch cultivations is largely independent of the carbon source but changes quantitatively over cultivation time. *Microb Biotechnol*, *13*(2), 479-494. https://doi.org/10.1111/1751-7915.13499

Cabib, E. (2004). The septation apparatus, a chitin-requiring machine in budding yeast. *Arch Biochem Biophys*, *426*(2), 201-207. https://doi.org/10.1016/j.abb.2004.02.030

Casselton, L., & Zolan, M. (2002). The art and design of genetic screens: filamentous fungi. *Nat Rev Genet*, *3*(9), 683-697. https://doi.org/10.1038/nrg889

Chiang, C. F., Okou, D. T., Griffin, T. B., Verret, C. R., & Williams, M. N. (2001). Green fluorescent protein rendered susceptible to proteolysis: positions for protease-

sensitive insertions. *Arch Biochem Biophys*, *394*(2), 229-235. https://doi.org/10.1006/abbi.2001.2537
Choi, J. H., & Lee, S. Y. (2004). Secretory and extracellular production of recombinant proteins using *Escherichia coli*. *Appl Microbiol Biotechnol*, *64*(5), 625-635. https://doi.org/10.1007/s00253-004-1559-9
Chu, D., & Barnes, D. J. (2016). The lag-phase during diauxic growth is a trade-off between fast adaptation and high growth rate. *Sci Rep*, *6*, 25191. https://doi.org/10.1038/srep25191
Contreras-Gomez, A., Sanchez-Miron, A., Garcia-Camacho, F., Molina-Grima, E., & Chisti, Y. (2014). Protein production using the baculovirus-insect cell expression system. *Biotechnol Prog*, *30*(1), 1-18. https://doi.org/10.1002/btpr.1842
Corchero, J. L. (2016). Eukaryotic aggresomes: from a model of conformational diseases to an emerging type of immobilized biocatalyzers. *Appl Microbiol Biotechnol*, *100*(2), 559-569. https://doi.org/10.1007/s00253-015-7107-y
Crater, J. S., & Lievense, J. C. (2018). Scale-up of industrial microbial processes. *FEMS Microbiol Lett*, *365*(13). https://doi.org/10.1093/femsle/fny138
Crosnier, C., Wanaguru, M., McDade, B., Osier, F. H., Marsh, K., Rayner, J. C., & Wright, G. J. (2013). A library of functional recombinant cell-surface and secreted *P. falciparum* merozoite proteins. *Mol Cell Proteomics*, *12*(12), 3976-3986. https://doi.org/10.1074/mcp.O113.028357
Cruz-Garcia, D., Malhotra, V., & Curwin, A. J. (2018). Unconventional protein secretion triggered by nutrient starvation. *Semin Cell Dev Biol*, *83*, 22-28. https://doi.org/10.1016/j.semcdb.2018.02.021
Csala, M., Kereszturi, E., Mandl, J., & Bánhegyi, G. (2012). The endoplasmic reticulum as the extracellular space inside the cell: role in protein folding and glycosylation. *Antioxid Redox Signal*, *16*(10), 1100-1108. https://doi.org/10.1089/ars.2011.4227
Cui, W., Han, L., Suo, F., Liu, Z., Zhou, L., & Zhou, Z. (2018). Exploitation of *Bacillus subtilis* as a robust workhorse for production of heterologous proteins and beyond. *World J Microbiol Biotechnol*, *34*(10), 145. https://doi.org/10.1007/s11274-018-2531-7
De Pourcq, K., De Schutter, K., & Callewaert, N. (2010). Engineering of glycosylation in yeast and other fungi: current state and perspectives. *Appl Microbiol Biotechnol*, *87*(5), 1617-1631. https://doi.org/10.1007/s00253-010-2721-1
de Souza, P. M., Bittencourt, M. L., Caprara, C. C., de Freitas, M., de Almeida, R. P., Silveira, D., Fonseca, Y. M., Ferreira Filho, E. X., Pessoa Junior, A., & Magalhães, P. O. (2015). A biotechnology perspective of fungal proteases. *Braz J Microbiol*, *46*(2), 337-346. https://doi.org/10.1590/S1517-838246220140359
Debaisieux, S., Rayne, F., Yezid, H., & Beaumelle, B. (2012). The ins and outs of HIV-1 Tat. *Traffic*, *13*(3), 355-363. https://doi.org/10.1111/j.1600-0854.2011.01286.x
Deed, R. C., Fedrizzi, B., & Gardner, R. C. (2017). *Saccharomyces cerevisiae FLO1* gene demonstrates genetic linkage to increased fermentation rate at low temperatures. *G3 (Bethesda)*, *7*(3), 1039-1048. https://doi.org/10.1534/g3.116.037630
Delic, M., Valli, M., Graf, A. B., Pfeffer, M., Mattanovich, D., & Gasser, B. (2013). The secretory pathway: exploring yeast diversity. *FEMS Microbiol Rev*, *37*(6), 872-914. https://doi.org/10.1111/1574-6976.12020
Dimou, E., & Nickel, W. (2018). Unconventional mechanisms of eukaryotic protein secretion. *Curr Biol*, *28*(8), R406-R410. https://doi.org/10.1016/j.cub.2017.11.074
Ding, Y., Wang, J., Wang, J., Stierhof, Y. D., Robinson, D. G., & Jiang, L. (2012). Unconventional protein secretion. *Trends Plant Sci*, *17*(10), 606-615. https://doi.org/10.1016/j.tplants.2012.06.004
Dragosits, M., & Mattanovich, D. (2013). Adaptive laboratory evolution -- principles and applications for biotechnology. *Microb Cell Fact*, *12*, 64. https://doi.org/10.1186/1475-2859-12-64
Ebert, A. D., Laussmann, M., Wegehingel, S., Kaderali, L., Erfle, H., Reichert, J., Lechner, J., Beer, H. D., Pepperkok, R., & Nickel, W. (2010). Tec-kinase-mediated

phosphorylation of fibroblast growth factor 2 is essential for unconventional secretion. *Traffic*, *11*(6), 813-826. https://doi.org/10.1111/j.1600-0854.2010.01059.x

Ecker, D. M., Jones, S. D., & Levine, H. L. (2015). The therapeutic monoclonal antibody market. *MAbs*, *7*(1), 9-14. https://doi.org/10.4161/19420862.2015.989042

Ehrenreich, I. M., Torabi, N., Jia, Y., Kent, J., Martis, S., Shapiro, J. A., Gresham, D., Caudy, A. A., & Kruglyak, L. (2010). Dissection of genetically complex traits with extremely large pools of yeast segregants. *Nature*, *464*(7291), 1039-1042. https://doi.org/10.1038/nature08923

Eichhorn, H., Lessing, F., Winterberg, B., Schirawski, J., Kämper, J., Müller, P., & Kahmann, R. (2006). A ferroxidation/permeation iron uptake system is required for virulence in *Ustilago maydis*. *Plant Cell*, *18*(11), 3332-3345. https://doi.org/10.1105/tpc.106.043588

El-Enshasy, H. A. (2007). Filamentous fungal cultures–process characteristics, products, and applications. *Bioprocessing for value-added products from renewable resources*, 225-261. https://doi.org/10.1016/B978-044452114-9/50010-4

Ezzine, A., M'Hirsi El Adab, S., Bouhaouala-Zahar, B., Hmila, I., Baciou, L., & Marzouki, M. N. (2012). Efficient expression of the anti-AahI' scorpion toxin nanobody under a new functional form in a *Pichia pastoris* system. *Biotechnol Appl Biochem*, *59*(1), 15-21. https://doi.org/10.1002/bab.67

Faden, F., Mielke, S., Lange, D., & Dissmeyer, N. (2014). Generic tools for conditionally altering protein abundance and phenotypes on demand. *Biol Chem*, *395*(7-8), 737-762. https://doi.org/10.1515/hsz-2014-0160

Farrell, L. B., & Beachy, R. N. (1990). Manipulation of beta-glucuronidase for use as a reporter in vacuolar targeting studies. *Plant Mol Biol*, *15*(6), 821-825. https://doi.org/10.1007/BF00039422

Farrokhi, N., Hrmova, M., Burton, R. A., & Fincher, G. B. (2009). Heterologous and cell free protein expression systems. *Methods Mol Biol*, *513*, 175-198. https://doi.org/10.1007/978-1-59745-427-8_10

Feldbrügge, M., Bölker, M., Steinberg, G., Kämper, J., & Kahmann, R. (2006). Regulatory and structural networks orchestrating mating, dimorphism, cell shape, and pathogenesis in *Ustilago maydis*. In U. Kües & R. Fischer (Eds.), *Growth, Differentiation and Sexuality* (pp. 375-391). Springer Berlin Heidelberg. https://doi.org/10.1007/3-540-28135-5_18

Feldbrügge, M., Kämper, J., Steinberg, G., & Kahmann, R. (2004). Regulation of mating and pathogenic development in *Ustilago maydis*. *Curr Opin Microbiol*, *7*(6), 666-672. https://doi.org/10.1016/j.mib.2004.10.006

Feldbrügge, M., Kellner, R., & Schipper, K. (2013). The biotechnological use and potential of plant pathogenic smut fungi. *Appl Microbiol Biotechnol*, *97*(8), 3253-3265. https://doi.org/10.1007/s00253-013-4777-1

Feldbrügge, M., Zarnack, K., Vollmeister, E., Baumann, S., Koepke, J., König, J., Munsterkotter, M., & Mannhaupt, G. (2008). The posttranscriptional machinery of *Ustilago maydis*. *Fungal Genet Biol*, *45 Suppl 1*, S40-46. https://doi.org/10.1016/j.fgb.2008.03.013

Feyder, S., De Craene, J. O., Bar, S., Bertazzi, D. L., & Friant, S. (2015). Membrane trafficking in the yeast *Saccharomyces cerevisiae* model. *Int J Mol Sci*, *16*(1), 1509-1525. https://doi.org/10.3390/ijms16011509

Figueroa, D., Rojas, V., Romero, A., Larrondo, L. F., & Salinas, F. (2021). The rise and shine of yeast optogenetics. *Yeast*, *38*(2), 131-146. https://doi.org/10.1002/yea.3529

Flaschel, E., & Friehs, K. (1993). Improvement of downstream processing of recombinant proteins by means of genetic engineering methods. *Biotechnol Adv*, *11*(1), 31-77. https://doi.org/10.1016/0734-9750(93)90409-g

Forsburg, S. L. (2001). The art and design of genetic screens: yeast. *Nat Rev Genet*, *2*(9), 659-668. https://doi.org/10.1038/35088500

Fox, B. G., & Blommel, P. G. (2009). Autoinduction of protein expression. *Curr Protoc Protein Sci*, *Chapter 5*, Unit 5 23. https://doi.org/10.1002/0471140864.ps0523s56

Freitag, J., Lanver, D., Böhmer, C., Schink, K. O., Bolker, M., & Sandrock, B. (2011). Septation of infectious hyphae is critical for appressoria formation and virulence in the smut fungus *Ustilago maydis*. *PLoS Pathog*, *7*(5), e1002044. https://doi.org/10.1371/journal.ppat.1002044

Frenzel, A., Hust, M., & Schirrmann, T. (2013). Expression of recombinant antibodies. *Front Immunol*, *4*, 217. https://doi.org/10.3389/fimmu.2013.00217

Freudl, R. (2017). Beyond amino acids: Use of the *Corynebacterium glutamicum* cell factory for the secretion of heterologous proteins. *J Biotechnol*, *258*, 101-109. https://doi.org/10.1016/j.jbiotec.2017.02.023

Fuller, R. S., Sterne, R. E., & Thorner, J. (1988). Enzymes required for yeast prohormone processing. *Annu Rev Physiol*, *50*, 345-362. https://doi.org/10.1146/annurev.ph.50.030188.002021

Funke, M., Buchenauer, A., Schnakenberg, U., Mokwa, W., Diederichs, S., Mertens, A., Müller, C., Kensy, F., & Büchs, J. (2010). Microfluidic biolector-microfluidic bioprocess control in microtiter plates. *Biotechnol Bioeng*, *107*(3), 497-505. https://doi.org/10.1002/bit.22825

Fussenegger, M., Morris, R. P., Fux, C., Rimann, M., von Stockar, B., Thompson, C. J., & Bailey, J. E. (2000). Streptogramin-based gene regulation systems for mammalian cells. *Nat Biotechnol*, *18*(11), 1203-1208. https://doi.org/10.1038/81208

Gai, J., Ma, L., Li, G., Zhu, M., Qiao, P., Li, X., Zhang, H., Zhang, Y., Chen, Y., Ji, W., Zhang, H., Cao, H., Li, X., Gong, R., & Wan, Y. (2021). A potent neutralizing nanobody against SARS-CoV-2 with inhaled delivery potential. *MedComm*, *2*(1), 101-113. https://doi.org/10.1002/mco2.60

Garcia-Muse, T., Steinberg, G., & Perez-Martin, J. (2003). Pheromone-induced G2 arrest in the phytopathogenic fungus *Ustilago maydis*. *Eukaryot Cell*, *2*(3), 494-500. https://doi.org/10.1128/ec.2.3.494-500.2003

Geiser, E., Hosseinpour Tehrani, H., Meyer, S., Blank, L. M., & Wierckx, N. (2018). Evolutionary freedom in the regulation of the conserved itaconate cluster by Ria1 in related Ustilaginaceae. *Fungal Biol Biotechnol*, *5*, 14. https://doi.org/10.1186/s40694-018-0058-1

Geiser, E., Reindl, M., Blank, L. M., Feldbrügge, M., Wierckx, N., & Schipper, K. (2016). Activating intrinsic carbohydrate-active enzymes of the smut gungus *Ustilago maydis* for the degradation of plant cell wall components. *Appl Environ Microbiol*, *82*(17), 5174-5185. https://doi.org/10.1128/AEM.00713-16

Gerngross, T. U. (2004). Advances in the production of human therapeutic proteins in yeasts and filamentous fungi. *Nat Biotechnol*, *22*(11), 1409-1414. https://doi.org/10.1038/nbt1028

Gibbs, P. A., Seviour, R. J., & Schmid, F. (2000). Growth of filamentous fungi in submerged culture: problems and possible solutions. *Crit Rev Biotechnol*, *20*(1), 17-48. https://doi.org/10.1080/07388550091144177

Göhre, V., Vollmeister, E., Bölker, M., & Feldbrügge, M. (2012). Microtubule-dependent membrane dynamics in *Ustilago maydis*: Trafficking and function of Rab5a-positive endosomes. *Commun Integr Biol*, *5*(5), 485-490. https://pubmed.ncbi.nlm.nih.gov/23181166/

Gopal, G. J., & Kumar, A. (2013). Strategies for the production of recombinant protein in *Escherichia coli*. *Protein J*, *32*(6), 419-425. https://doi.org/10.1007/s10930-013-9502-5

Gossen, M., & Bujard, H. (1992). Tight control of gene expression in mammalian cells by tetracycline-responsive promoters. *Proc Natl Acad Sci U S A*, *89*(12), 5547-5551. https://doi.org/10.1073/pnas.89.12.5547

Grand View Research, Inc. (2021). *Biotechnology market size, share & trends: Analysis report by technology (DNA sequencing, nanobiotechnology), by application (health, bioinformatics), by region, and segment forecasts, 2021 - 2028*. https://www.grandviewresearch.com/industry-analysis/biotechnology-market

Grieve, A. G., & Rabouille, C. (2011). Golgi bypass: skirting around the heart of classical secretion. *Cold Spring Harb Perspect Biol*, *3*(4). https://doi.org/10.1101/cshperspect.a005298

Griffiths, A. J. F., Miller, J.H., Suzuki, D.T. (2000). Mendelian genetics in eukaryotic life cycles. In *An Introduction to Genetic Analysis.* W. H. Freeman. https://www.ncbi.nlm.nih.gov/books/NBK21836/

Gupta, R., & Brunak, S. (2002). Prediction of glycosylation across the human proteome and the correlation to protein function. *Pac Symp Biocomput*, 310-322. https://www.ncbi.nlm.nih.gov/pubmed/11928486

Hamilton, S. R., Davidson, R. C., Sethuraman, N., Nett, J. H., Jiang, Y., Rios, S., Bobrowicz, P., Stadheim, T. A., Li, H., Choi, B. K., Hopkins, D., Wischnewski, H., Roser, J., Mitchell, T., Strawbridge, R. R., Hoopes, J., Wildt, S., & Gerngross, T. U. (2006). Humanization of yeast to produce complex terminally sialylated glycoproteins. *Science*, *313*(5792), 1441-1443. https://doi.org/10.1126/science.1130256

Harmsen, M. M., van Solt, C. B., & Fijten, H. P. (2009). Enhancement of toxin- and virus-neutralizing capacity of single-domain antibody fragments by *N*-glycosylation. *Appl Microbiol Biotechnol*, *84*(6), 1087-1094. https://doi.org/10.1007/s00253-009-2029-1

Hartmann, H. A., Kahmann, R., & Bölker, M. (1996). The pheromone response factor coordinates filamentous growth and pathogenicity in *Ustilago maydis*. *EMBO J*, *15*(7), 1632-1641. https://www.ncbi.nlm.nih.gov/pubmed/8612587

Hartmann, H. A., Krüger, J., Lottspeich, F., & Kahmann, R. (1999). Environmental signals controlling sexual development of the corn Smut fungus *Ustilago maydis* through the transcriptional regulator Prf1. *Plant Cell*, *11*(7), 1293-1306. https://doi.org/10.1105/tpc.11.7.1293

Haupka, C., Brito, L. F., Busche, T., Wibberg, D., & Wendisch, V. F. (2021). Genomic and transcriptomic investigation of the physiological response of the methylotroph *Bacillus methanolicus* to 5-aminovalerate. *Front Microbiol*, *12*, 829. https://doi.org/10.3389/fmicb.2021.664598

Heel, T., Vogel, G. F., Lammirato, A., Schneider, R., & Auer, B. (2013). FlgM as a secretion moiety for the development of an inducible type III secretion system. *PLoS One*, *8*(3), e59034. https://doi.org/10.1371/journal.pone.0059034

Hermann, B. G., & Patel, M. (2007). Today's and tomorrow's bio-based bulk chemicals from white biotechnology: a techno-economic analysis. *Appl Biochem Biotechnol*, *136*(3), 361-388. https://doi.org/10.1007/s12010-007-9031-9

Hermanrud, C. E., Pathiraja, V., Matar, A., Duran-Struuck, R., Crepeau, R. L., Srinivasan, S., Sachs, D. H., Huang, C. A., & Wang, Z. (2012). Expression and purification of non-*N*-glycosylated porcine interleukin 3 in yeast *Pichia pastoris*. *Protein Expr Purif*, *82*(1), 70-74. https://doi.org/10.1016/j.pep.2011.11.011

Hlubek, A., Schink, K. O., Mahlert, M., Sandrock, B., & Bolker, M. (2008). Selective activation by the guanine nucleotide exchange factor Don1 is a main determinant of Cdc42 signalling specificity in *Ustilago maydis*. *Mol Microbiol*, *68*(3), 615-623. https://doi.org/10.1111/j.1365-2958.2008.06177.x

Holliday, R. (1974). *Ustilago maydis*. In *Handbook of Genetics* (Vol. 1, pp. 575-595). Plenum Press. https://doi.org/10.1007/978-1-4899-1710-2_31

Holwerda, E. K., Olson, D. G., Ruppertsberger, N. M., Stevenson, D. M., Murphy, S. J. L., Maloney, M. I., Lanahan, A. A., Amador-Noguez, D., & Lynd, L. R. (2020). Metabolic and evolutionary responses of *Clostridium thermocellum* to genetic interventions aimed at improving ethanol production. *Biotechnol Biofuels*, *13*, 40. https://doi.org/10.1186/s13068-020-01680-5

Hughes, R. M. (2018). A compendium of chemical and genetic approaches to light-regulated gene transcription. *Crit Rev Biochem Mol Biol*, *53*(5), 453-474. https://doi.org/10.1080/10409238.2018.1487382

Hüsemann, L. C. (2020). *Development and implementation of (opto-) genetic tools in different eukaryotic organisms and application of synthetic biology approaches for studying plant signaling pathways*

Hussnaetter, K. P. (2016). *Studying the role of the novel factor Jps1 during unconventional secretion of the chitinase Cts1*

Idiris, A., Tohda, H., Kumagai, H., & Takegawa, K. (2010). Engineering of protein secretion in yeast: strategies and impact on protein production. *Appl Microbiol Biotechnol*, *86*(2), 403-417. https://doi.org/10.1007/s00253-010-2447-0

Iturriaga, G., Jefferson, R. A., & Bevan, M. W. (1989). Endoplasmic reticulum targeting and glycosylation of hybrid proteins in transgenic tobacco. *Plant Cell*, *1*(3), 381-390. https://doi.org/10.1105/tpc.1.3.381

Jacobs, P. P., Geysens, S., Vervecken, W., Contreras, R., & Callewaert, N. (2009). Engineering complex-type *N*-glycosylation in *Pichia pastoris* using GlycoSwitch technology. *Nat Protoc*, *4*(1), 58-70. https://doi.org/10.1038/nprot.2008.213

Jaeger, K. E., & Eggert, T. (2002). Lipases for biotechnology. *Curr Opin Biotechnol*, *13*(4), 390-397. https://doi.org/10.1016/s0958-1669(02)00341-5

Johnson, A. E., & van Waes, M. A. (1999). The translocon: a dynamic gateway at the ER membrane. *Annu Rev Cell Dev Biol*, *15*, 799-842. https://doi.org/10.1146/annurev.cellbio.15.1.799

Johnston, J. A., Ward, C. L., & Kopito, R. R. (1998). Aggresomes: a cellular response to misfolded proteins. *J Cell Biol*, *143*(7), 1883-1898. https://doi.org/10.1083/jcb.143.7.1883

Joosten, V., Lokman, C., Van Den Hondel, C. A., & Punt, P. J. (2003). The production of antibody fragments and antibody fusion proteins by yeasts and filamentous fungi. *Microb Cell Fact*, *2*(1), 1. https://doi.org/10.1186/1475-2859-2-1

Jung, S. Y., Kim, S. S., & Yeo, S. G. (2020). Impact of endoplasmic teticulum stress in otorhinolaryngologic diseases. *Int J Mol Sci*, *21*(11). https://doi.org/10.3390/ijms21114121

Jungbluth, M., Renicke, C., & Taxis, C. (2010). Targeted protein depletion in *Saccharomyces cerevisiae* by activation of a bidirectional degron. *BMC Syst Biol*, *4*, 176. https://doi.org/10.1186/1752-0509-4-176

Kämper, J. (2004). A PCR-based system for highly efficient generation of gene replacement mutants in *Ustilago maydis*. *Mol Genet Genomics*, *271*(1), 103-110. https://doi.org/10.1007/s00438-003-0962-8

Kämper, J., Friedrich, M. W., & Kahmann, R. (2020). Creating novel specificities in a fungal nonself recognition system by single step homologous recombination events. *New Phytol*, *228*(3), 1001-1010. https://doi.org/10.1111/nph.16755

Kämper, J., Kahmann, R., Bölker, M., Ma, L. J., Brefort, T., Saville, B. J., Banuett, F., Kronstad, J. W., Gold, S. E., Müller, O., Perlin, M. H., Wosten, H. A., de Vries, R., Ruiz-Herrera, J., Reynaga-Pena, C. G., Snetselaar, K., McCann, M., Perez-Martin, J., Feldbrügge, M., Basse, C. W., Steinberg, G., Ibeas, J. I., Holloman, W., Guzman, P., Farman, M., Stajich, J. E., Sentandreu, R., Gonzalez-Prieto, J. M., Kennell, J. C., Molina, L., Schirawski, J., Mendoza-Mendoza, A., Greilinger, D., Munch, K., Rossel, N., Scherer, M., Vranes, M., Ladendorf, O., Vincon, V., Fuchs, U., Sandrock, B., Meng, S., Ho, E. C., Cahill, M. J., Boyce, K. J., Klose, J., Klosterman, S. J., Deelstra, H. J., Ortiz-Castellanos, L., Li, W., Sanchez-Alonso, P., Schreier, P. H., Hauser-Hahn, I., Vaupel, M., Koopmann, E., Friedrich, G., Voss, H., Schluter, T., Margolis, J., Platt, D., Swimmer, C., Gnirke, A., Chen, F., Vysotskaia, V., Mannhaupt, G., Guldener, U., Munsterkotter, M., Haase, D., Oesterheld, M., Mewes, H. W., Mauceli, E. W., DeCaprio, D., Wade, C. M., Butler, J., Young, S., Jaffe, D. B., Calvo, S., Nusbaum, C., Galagan, J., & Birren, B. W. (2006). Insights from the genome of the biotrophic fungal plant pathogen *Ustilago maydis*. *Nature*, *444*(7115), 97-101. https://doi.org/10.1038/nature05248

Karnaukhova, E., Ophir, Y., & Golding, B. (2006). Recombinant human alpha-1 proteinase inhibitor: towards therapeutic use. *Amino Acids*, *30*(4), 317-332. https://doi.org/10.1007/s00726-005-0324-4

Karyolaimos, A., Ampah-Korsah, H., Hillenaar, T., Mestre Borras, A., Dolata, K. M., Sievers, S., Riedel, K., Daniels, R., & de Gier, J. W. (2019). Enhancing recombinant protein

yields in the *E. coli* periplasm by combining signal peptide and production rate screening. *Front Microbiol*, *10*, 1511. https://doi.org/10.3389/fmicb.2019.01511

Keon, J. P., White, G. A., & Hargreaves, J. A. (1991). Isolation, characterization and sequence of a gene conferring resistance to the systemic fungicide carboxin from the maize smut pathogen, *Ustilago maydis*. *Curr Genet*, *19*(6), 475-481. https://doi.org/10.1007/bf00312739

Khrunyk, Y., Münch, K., Schipper, K., Lupas, A. N., & Kahmann, R. (2010). The use of FLP-mediated recombination for the functional analysis of an effector gene family in the biotrophic smut fungus *Ustilago maydis*. *New Phytol*, *187*(4), 957-968. https://doi.org/10.1111/j.1469-8137.2010.03413.x

Kilaru, S., Schuster, M., Ma, W., & Steinberg, G. (2017). Fluorescent markers of various organelles in the wheat pathogen *Zymoseptoria tritici*. *Fungal Genet Biol*, *105*, 16-27. https://doi.org/10.1016/j.fgb.2017.05.001

Kinseth, M. A., Anjard, C., Fuller, D., Guizzunti, G., Loomis, W. F., & Malhotra, V. (2007). The Golgi-associated protein GRASP is required for unconventional protein secretion during development. *Cell*, *130*(3), 524-534. https://doi.org/10.1016/j.cell.2007.06.029

Klis, F. M., Boorsma, A., & De Groot, P. W. (2006). Cell wall construction in *Saccharomyces cerevisiae*. *Yeast*, *23*(3), 185-202. https://doi.org/10.1002/yea.1349

Kluge, J., Terfehr, D., & Kück, U. (2018). Inducible promoters and functional genomic approaches for the genetic engineering of filamentous fungi. *Appl Microbiol Biotechnol*, *102*(15), 6357-6372. https://doi.org/10.1007/s00253-018-9115-1

Koepke, J., Kaffarnik, F., Haag, C., Zarnack, K., Luscombe, N. M., König, J., Ule, J., Kellner, R., Begerow, D., & Feldbrügge, M. (2011b). The RNA-binding protein Rrm4 is essential for efficient secretion of endochitinase Cts1. *Mol Cell Proteomics*, *10*(12), M111 011213. https://doi.org/10.1074/mcp.M111.011213

Krombach, S., Reissmann, S., Kreibich, S., Bochen, F., & Kahmann, R. (2018). Virulence function of the *Ustilago maydis* sterol carrier protein 2. *New Phytol*. https://doi.org/10.1111/nph.15268

Kronstad, J. W., & Staben, C. (1997). Mating type in filamentous fungi. *Annu Rev Genet*, *31*, 245-276. https://doi.org/10.1146/annurev.genet.31.1.245

Kunert, R., & Reinhart, D. (2016). Advances in recombinant antibody manufacturing. *Appl Microbiol Biotechnol*, *100*(8), 3451-3461. https://doi.org/10.1007/s00253-016-7388-9

Kuranda, M. J., & Robbins, P. W. (1991). Chitinase is required for cell separation during growth of *Saccharomyces cerevisiae*. *J Biol Chem*, *266*(29), 19758-19767. https://www.ncbi.nlm.nih.gov/pubmed/1918080

Laemmli, U. K. (1970). Cleavage of structural proteins during the assembly of the head of bacteriophage T4. *Nature*, *227*(5259), 680-685. https://doi.org/10.1038/227680a0

Langner, T., & Gohre, V. (2016). Fungal chitinases: function, regulation, and potential roles in plant/pathogen interactions. *Curr Genet*, *62*(2), 243-254. https://doi.org/10.1007/s00294-015-0530-x

Langner, T., Özturk, M., Hartmann, S., Cord-Landwehr, S., Moerschbacher, B., Walton, J. D., & Göhre, V. (2015). Chitinases are essential for cell separation in *Ustilago maydis*. *Eukaryot Cell*, *14*(9), 846-857. https://doi.org/10.1128/EC.00022-15

Larsen, S., Weaver, J., de Sa Campos, K., Bulahan, R., Nguyen, J., Grove, H., Huang, A., Low, L., Tran, N., Gomez, S., Yau, J., Ilustrisimo, T., Kawilarang, J., Lau, J., Tranphung, M., Chen, I., Tran, C., Fox, M., Lin-Cereghino, J., & Lin-Cereghino, G. P. (2013). Mutant strains of *Pichia pastoris* with enhanced secretion of recombinant proteins. *Biotechnol Lett*, *35*(11), 1925-1935. https://doi.org/10.1007/s10529-013-1290-7

Laukens, B., De Wachter, C., & Callewaert, N. (2015). Engineering the *Pichia pastoris N*-Glycosylation Pathway Using the GlycoSwitch Technology. *Methods Mol Biol*, *1321*, 103-122. https://doi.org/10.1007/978-1-4939-2760-9_8

Laver, T., Harrison, J., O'Neill, P. A., Moore, K., Farbos, A., Paszkiewicz, K., & Studholme, D. J. (2015). Assessing the performance of the Oxford Nanopore Technologies MinION. *Biomol Detect Quantif*, *3*, 1-8. https://doi.org/10.1016/j.bdq.2015.02.001

Le Crom, S., Schackwitz, W., Pennacchio, L., Magnuson, J. K., Culley, D. E., Collett, J. R., Martin, J., Druzhinina, I. S., Mathis, H., Monot, F., Seiboth, B., Cherry, B., Rey, M., Berka, R., Kubicek, C. P., Baker, S. E., & Margeot, A. (2009). Tracking the roots of cellulase hyperproduction by the fungus *Trichoderma reesei* using massively parallel DNA sequencing. *Proc Natl Acad Sci U S A*, *106*(38), 16151-16156. https://doi.org/10.1073/pnas.0905848106

Lee, J. G., Takahama, S., Zhang, G., Tomarev, S. I., & Ye, Y. (2016). Unconventional secretion of misfolded proteins promotes adaptation to proteasome dysfunction in mammalian cells. *Nat Cell Biol*, *18*(7), 765-776. https://doi.org/10.1038/ncb3372

Lee, J. Y., Chen, H., Liu, A. L., Alba, B. M., & Lim, A. C. (2017). Auto-induction of *Pichia pastoris* AOX1 promoter for membrane protein expression. *Protein Exp Purif*, *137*, 7-12. https://doi.org/10.1016/j.pep.2017.06.006

Lee, M. C., Miller, E. A., Goldberg, J., Orci, L., & Schekman, R. (2004). Bi-directional protein transport between the ER and Golgi. *Annu Rev Cell Dev Biol*, *20*, 87-123. https://doi.org/10.1146/annurev.cellbio.20.010403.105307

Leisola, M., Jokela, J., Pastinen, O., Turunen, O., & Schoemaker, H. (2001). *Industrial use of enzymes*. Eolss Publishers, Oxford. http://cmsc.ac.in/bot23.pdf

Levskaya, A., Weiner, O. D., Lim, W. A., & Voigt, C. A. (2009). Spatiotemporal control of cell signalling using a light-switchable protein interaction. *Nature*, *461*(7266), 997-1001. https://doi.org/10.1038/nature08446

Liu, C., Kobashigawa, Y., Yamauchi, S., Toyota, Y., Teramoto, M., Ikeguchi, Y., Fukuda, N., Sato, T., Sato, Y., Kimura, H., & Morioka, H. (2019). Preparation of single-chain Fv antibodies in the cytoplasm of *Escherichia coli* by simplified and systematic chaperone optimization. *J Biochem*, *166*(6), 455-462. https://doi.org/10.1093/jb/mvz059

Liu, Y., & Huang, H. (2018). Expression of single-domain antibody in different systems. *Appl Microbiol Biotechnol*, *102*(2), 539-551. https://doi.org/10.1007/s00253-017-8644-3

Longtine, M. S., Fares, H., & Pringle, J. R. (1998). Role of the yeast Gin4p protein kinase in septin assembly and the relationship between septin assembly and septin function. *J Cell Biol*, *143*(3), 719-736. https://doi.org/10.1083/jcb.143.3.719

Loubradou, G., Brachmann, A., Feldbrügge, M., & Kahmann, R. (2001). A homologue of the transcriptional repressor Ssn6p antagonizes cAMP signalling in *Ustilago maydis*. *Mol Microbiol*, *40*(3), 719-730. http://www.ncbi.nlm.nih.gov/pubmed/11359577

Luo, M., Zhao, M., Cagliero, C., Jiang, H., Xie, Y., Zhu, J., Yang, H., Zhang, M., Zheng, Y., Yuan, Y., Du, Z., & Lu, H. (2019). A general platform for efficient extracellular expression and purification of Fab from *Escherichia coli*. *Appl Microbiol Biotechnol*, *103*(8), 3341-3353. https://doi.org/10.1007/s00253-019-09745-8

Luo, Y., Na, Z., & Slavoff, S. A. (2018). P-Bodies: Composition, Properties, and Functions. *Biochemistry*, *57*(17), 2424-2431. https://doi.org/10.1021/acs.biochem.7b01162

Mahdieh, N., & Rabbani, B. (2013). An overview of mutation detection methods in genetic disorders. *Iran J Pediatr*, *23*(4), 375-388. https://www.ncbi.nlm.nih.gov/pubmed/24427490

Mahlert, M., Leveleki, L., Hlubek, A., Sandrock, B., & Bolker, M. (2006). Rac1 and Cdc42 regulate hyphal growth and cytokinesis in the dimorphic fungus *Ustilago maydis*. *Mol Microbiol*, *59*(2), 567-578. https://doi.org/10.1111/j.1365-2958.2005.04952.x

Malhotra, V. (2013). Unconventional protein secretion: an evolving mechanism. *EMBO J*, *32*(12), 1660-1664. https://doi.org/10.1038/emboj.2013.104

Martinez, D., Berka, R. M., Henrissat, B., Saloheimo, M., Arvas, M., Baker, S. E., Chapman, J., Chertkov, O., Coutinho, P. M., Cullen, D., Danchin, E. G., Grigoriev, I. V., Harris, P., Jackson, M., Kubicek, C. P., Han, C. S., Ho, I., Larrondo, L. F., de Leon, A. L., Magnuson, J. K., Merino, S., Misra, M., Nelson, B., Putnam, N., Robbertse, B., Salamov, A. A., Schmoll, M., Terry, A., Thayer, N., Westerholm-Parvinen, A., Schoch, C. L., Yao, J., Barabote, R., Nelson, M. A., Detter, C., Bruce, D., Kuske, C. R., Xie, G., Richardson, P., Rokhsar, D. S., Lucas, S. M., Rubin, E. M., Dunn-Coleman, N., Ward, M., & Brettin, T. S. (2008). Genome sequencing and analysis of

the biomass-degrading fungus *Trichoderma reesei* (syn. *Hypocrea jecorina*). *Nat Biotechnol*, *26*(5), 553-560. https://doi.org/10.1038/nbt1403
Mattanovich, D., Branduardi, P., Dato, L., Gasser, B., Sauer, M., & Porro, D. (2012). Recombinant protein production in yeasts. *Methods Mol Biol*, *824*, 329-358. https://doi.org/10.1007/978-1-61779-433-9_17
Mellman, I., & Emr, S. D. (2013). A Nobel Prize for membrane traffic: vesicles find their journey's end. *J Cell Biol*, *203*(4), 559-561. https://doi.org/10.1083/jcb.201310134
Meyer, V., Wanka, F., van Gent, J., Arentshorst, M., van den Hondel, C. A. M. J. J., & Ram, A. F. J. (2011). Fungal gene expression on demand: an inducible, tunable, and metabolism-independent expression system for *Aspergillus niger*. *Appl Environ Microbiol*, *77*(9), 2975-2983. https://doi.org/10.1128/Aem.02740-10
Miller, G. L. (1959). Dinitrosalicylic Acid Reagent for Determination of Reducing Sugar. *Anal Chem*, *31*(3), 426-428. https://doi.org/10.1021/ac60147a030
Motta-Mena, L. B., Reade, A., Mallory, M. J., Glantz, S., Weiner, O. D., Lynch, K. W., & Gardner, K. H. (2014). An optogenetic gene expression system with rapid activation and deactivation kinetics. *Nat Chem Biol*, *10*(3), 196-202. https://doi.org/10.1038/nchembio.1430
Mueller, O., Kahmann, R., Aguilar, G., Trejo-Aguilar, B., Wu, A., & de Vries, R. P. (2008). The secretome of the maize pathogen *Ustilago maydis*. *Fungal Genet Biol*, *45 Suppl 1*, S63-70. https://doi.org/10.1016/j.fgb.2008.03.012
Mukherjee, J., Tremblay, J. M., Leysath, C. E., Ofori, K., Baldwin, K., Feng, X., Bedenice, D., Webb, R. P., Wright, P. M., Smith, L. A., Tzipori, S., & Shoemaker, C. B. (2012). A novel strategy for development of recombinant antitoxin therapeutics tested in a mouse botulism model. *PLoS One*, *7*(1), e29941. https://doi.org/10.1371/journal.pone.0029941
Müller, K., Siegel, D., Rodriguez Jahnke, F., Gerrer, K., Wend, S., Decker, E. L., Reski, R., Weber, W., & Zurbriggen, M. D. (2014). A red light-controlled synthetic gene expression switch for plant systems. *Mol Biosyst*, *10*(7), 1679-1688. https://doi.org/10.1039/c3mb70579j
Müller, K., & Weber, W. (2013). Optogenetic tools for mammalian systems. *Mol Biosyst*, *9*(4), 596-608. https://doi.org/10.1039/c3mb25590e
Müller, M. J. (2019). *Online analytics of pectic vompound degradation in small-scale using Ustilago maydis* RWTH Aachen]. http://publications.rwth-aachen.de/record/774743/files/774743.pdf
Müntjes, K., Philipp, M., Hüsemann, L., Heucken, N., Weidtkamp-Peters, S., Schipper, K., Zurbriggen, M. D., & Feldbrügge, M. (2020). Establishing polycistronic expression in the model microorganism *Ustilago maydis*. *Front Microbiol*, *11*, 1384. https://doi.org/10.3389/fmicb.2020.01384
Muyldermans, S. (2013). Nanobodies: natural single-domain antibodies. *Annu Rev Biochem*, *82*, 775-797. https://doi.org/10.1146/annurev-biochem-063011-092449
Nevalainen, H., & Peterson, R. (2014). Making recombinant proteins in filamentous fungi- are we expecting too much? *Front Microbiol*, *5*, 75. https://doi.org/10.3389/fmicb.2014.00075
Nicaud, J.-M., Mackman, N., & Holland, I. (1986). Current status of secretion of foreign proteins by microorganisms. *J Biotechnol*, *3*(5-6), 255-270. https://doi.org/10.1016/0168-1656(86)90008-8
Nickel, W. (2005). Unconventional secretory routes: direct protein export across the plasma membrane of mammalian cells. *Traffic*, *6*(8), 607-614. https://doi.org/10.1111/j.1600-0854.2005.00302.x
Nickel, W. (2010). Pathways of unconventional protein secretion. *Curr Opin Biotechnol*, *21*(5), 621-626. https://doi.org/10.1016/j.copbio.2010.06.004
Nickel, W., & Rabouille, C. (2009). Mechanisms of regulated unconventional protein secretion. *Nat Rev Mol Cell Biol*, *10*(2), 148-155. https://doi.org/10.1038/nrm2617

Niessing, D., Jansen, R. P., Pohlmann, T., & Feldbrügge, M. (2018). mRNA transport in fungal top models. *Wiley Interdiscip Rev RNA*, *9*(1). https://doi.org/10.1002/wrna.1453

Novick, P., Field, C., & Schekman, R. (1980). Identification of 23 complementation groups required for post-translational events in the yeast secretory pathway. *Cell*, *21*(1), 205-215. https://doi.org/10.1016/0092-8674(80)90128-2

Nowag, H., & Münz, C. (2015). Diverting autophagic membranes for exocytosis. *Autophagy*, *11*(2), 425-427. https://doi.org/10.1080/15548627.2015.1009793

O'Donnell, K. L., & McLaughlin, D. J. (1984). Ultrastructure of meiosis in *Ustilago maydis* *Mycologia*, *76*(3), 468-485 https://doi.org/10.1080/00275514.1984.12023868

O'Flaherty, R., Bergin, A., Flampouri, E., Mota, L. M., Obaidi, I., Quigley, A., Xie, Y., & Butler, M. (2020). Mammalian cell culture for production of recombinant proteins: A review of the critical steps in their biomanufacturing. *Biotechnol Adv*, *43*, 107552. https://doi.org/10.1016/j.biotechadv.2020.107552

Okmen, B., Kemmerich, B., Hilbig, D., Wemhoner, R., Aschenbroich, J., Perrar, A., Huesgen, P. F., Schipper, K., & Doehlemann, G. (2018). Dual function of a secreted fungalysin metalloprotease in *Ustilago maydis*. *New Phytol*. https://doi.org/10.1111/nph.15265

Olgeiser, L., Haag, C., Boerner, S., Ule, J., Busch, A., Koepke, J., König, J., Feldbrügge, M., & Zarnack, K. (2019). The key protein of endosomal mRNP transport Rrm4 binds translational landmark sites of cargo mRNAs. *EMBO Rep*, *20*(1). https://doi.org/10.15252/embr.201846588

Page, D. R., & Grossniklaus, U. (2002). The art and design of genetic screens: *Arabidopsis thaliana*. *Nat Rev Genet*, *3*(2), 124-136. https://doi.org/10.1038/nrg730

Pereira, R., Mohamed, E. T., Radi, M. S., Herrgård, M. J., Feist, A. M., Nielsen, J., & Chen, Y. (2020). Elucidating aromatic acid tolerance at low pH in *Saccharomyces cerevisiae* using adaptive laboratory evolution. *Proc Natl Acad Sci U S A*, *117*(45), 27954-27961. https://doi.org/10.1073/pnas.2013044117

Peterson, R., & Nevalainen, H. (2012). *Trichoderma reesei* RUT-C30--thirty years of strain improvement. *Microbiology*, *158*(Pt 1), 58-68. https://doi.org/10.1099/mic.0.054031-0

Petrus, M. L. C., Kiefer, L. A., Puri, P., Heemskerk, E., Seaman, M. S., Barouch, D. H., Arias, S., van Wezel, G. P., & Havenga, M. (2019). A microbial expression system for high-level production of scFv HIV-neutralizing antibody fragments in *Escherichia coli*. *Appl Microbiol Biotechnol*, *103*(21-22), 8875-8888. https://doi.org/10.1007/s00253-019-10145-1

Pfeifer, G. P., You, Y. H., & Besaratinia, A. (2005). Mutations induced by ultraviolet light. *Mutat Res*, *571*(1-2), 19-31. https://doi.org/10.1016/j.mrfmmm.2004.06.057

Pohlmann, T., Baumann, S., Haag, C., Albrecht, M., & Feldbrügge, M. (2015). A FYVE zinc finger domain protein specifically links mRNA transport to endosome trafficking. *Elife*, *4*. https://doi.org/10.7554/eLife.06041

Potelle, S., Klein, A., & Foulquier, F. (2015). Golgi post-translational modifications and associated diseases. *J Inherit Metab Dis*, *38*(4), 741-751. https://doi.org/10.1007/s10545-015-9851-7

Punt, P. J., van Biezen, N., Conesa, A., Albers, A., Mangnus, J., & van den Hondel, C. (2002). Filamentous fungi as cell factories for heterologous protein production. *Trends Biotechnol*, *20*(5), 200-206. https://doi.org/10.1016/S0167-7799(02)01933-9

Rabouille, C. (2017). Pathways of unconventional protein secretion. *Trends Cell Biol*, *27*(3), 230-240. https://doi.org/10.1016/j.tcb.2016.11.007

Rabouille, C., Malhotra, V., & Nickel, W. (2012). Diversity in unconventional protein secretion. *J Cell Sci*, *125*(Pt 22), 5251-5255. https://doi.org/10.1242/jcs.103630

Rahbarizadeh, F., Rasaee, M. J., Forouzandeh, M., & Allameh, A. A. (2006). Over expression of anti-MUC1 single-domain antibody fragments in the yeast *Pichia pastoris*. *Mol Immunol*, *43*(5), 426-435. https://doi.org/10.1016/j.molimm.2005.03.003

Rastogi, R. P., Richa, Kumar, A., Tyagi, M. B., & Sinha, R. P. (2010). Molecular mechanisms of ultraviolet radiation-induced DNA damage and repair. *J Nucleic Acids*, *2010*, 592980. https://doi.org/10.4061/2010/592980

Rayne, F., Debaisieux, S., Bonhoure, A., & Beaumelle, B. (2010). HIV-1 Tat is unconventionally secreted through the plasma membrane. *Cell Biol Int*, *34*(4), 409-413. https://doi.org/10.1042/CBI20090376

Reindl, M. (2020). *A novel core factor for unconventional secretion in Ustilago maydis* https://docserv.uni-duesseldorf.de/servlets/DerivateServlet/Derivate-57324/Dissertation-Michele-Reindl_2020_pdfA-1b.pdf

Reindl, M., Hänsch, S., Weidtkamp-Peters, S., & Schipper, K. (2019). A potential lock-type mechanism for unconventional secretion in fungi. *Int J Mol Sci*, *20*(3). https://doi.org/10.3390/ijms20030460

Reindl, M., Stock, J., Hussnaetter, K. P., Genc, A., Brachmann, A., & Schipper, K. (2020). A novel factor essential for unconventional secretion of chitinase Cts1. *Front Microbiol*, *11*, 1529. https://doi.org/10.3389/fmicb.2020.01529

Renicke, C., Schuster, D., Usherenko, S., Essen, L. O., & Taxis, C. (2013). A LOV2 domain-based optogenetic tool to control protein degradation and cellular function. *Chem Biol*, *20*(4), 619-626. https://doi.org/10.1016/j.chembiol.2013.03.005

Rezaie, F., Davami, F., Mansouri, K., Agha Amiri, S., Fazel, R., Mahdian, R., Davoudi, N., Enayati, S., Azizi, M., & Khalaj, V. (2017). Cytosolic expression of functional Fab fragments in Escherichia coli using a novel combination of dual SUMO expression cassette and EnBase((R)) cultivation mode. *J Appl Microbiol*, *123*(1), 134-144. https://doi.org/10.1111/jam.13483

Rivera, V. M., Wang, X., Wardwell, S., Courage, N. L., Volchuk, A., Keenan, T., Holt, D. A., Gilman, M., Orci, L., Cerasoli, F., Jr., Rothman, J. E., & Clackson, T. (2000). Regulation of protein secretion through controlled aggregation in the endoplasmic reticulum. *Science*, *287*(5454), 826-830. https://doi.org/10.1126/science.287.5454.826

Rothbauer, U., Zolghadr, K., Muyldermans, S., Schepers, A., Cardoso, M. C., & Leonhardt, H. (2008). A versatile nanotrap for biochemical and functional studies with fluorescent fusion proteins. *Mol Cell Proteomics*, *7*(2), 282-289. https://doi.org/10.1074/mcp.M700342-MCP200

Saccardo, P., Corchero, J. L., & Ferrer-Miralles, N. (2016). Tools to cope with difficult-to-express proteins. *Appl Microbiol Biotechnol*, *100*(10), 4347-4355. https://doi.org/10.1007/s00253-016-7514-8

Sagane, Y., Inui, K., Miyashita, S.-I., Miyata, K., Niwa, K., Watanabe, T., & Suzuki, T. (2012). Botulinum toxin complex: a delivery vehicle of botulinum neurotoxin traveling in the digestive tract. *Structure and Function of Food Engineering. InTech, Rijeka*, 137-150. http://dx.doi.org/10.5772/46023

Sandberg, T. E., Salazar, M. J., Weng, L. L., Palsson, B. O., & Feist, A. M. (2019). The emergence of adaptive laboratory evolution as an efficient tool for biological discovery and industrial biotechnology. *Metab Eng*, *56*, 1-16. https://doi.org/10.1016/j.ymben.2019.08.004

Sandomenico, A., Sivaccumar, J. P., & Ruvo, M. (2020). Evolution of *Escherichia coli* expression system in producing antibody recombinant fragments. *Int J Mol Sci*, *21*(17). https://doi.org/10.3390/ijms21176324

Sandrock, B., Bohmer, C., & Bolker, M. (2006). Dual function of the germinal centre kinase Don3 during mitosis and cytokinesis in *Ustilago maydis*. *Mol Microbiol*, *62*(3), 655-666. https://doi.org/10.1111/j.1365-2958.2006.05405.x

Sarkari, P. (2014). *Optimizing the expression of antibody formats in protease-deficient Ustilago maydis strains* https://d-nb.info/1062696735/34

Sarkari, P., Feldbrügge, M., & Schipper, K. (2016). The corn smut fungus *Ustilago maydis* as an alternative expression system for biopharmaceuticals. *Fungal Biology. Gene expression systems in fungi: advancements and applications*, *Springer Book Series.*, 183-200. https://doi.org/10.1007/978-3-319-27951-0_7

Sarkari, P., Reindl, M., Stock, J., Müller, O., Kahmann, R., Feldbrügge, M., & Schipper, K. (2014). Improved expression of single-chain antibodies in *Ustilago maydis*. *J Biotechnol*, *191*, 165-175. https://doi.org/10.1016/j.jbiotec.2014.06.028

Schimek, C., Egger, E., Tauer, C., Striedner, G., Brocard, C., Cserjan-Puschmann, M., & Hahn, R. (2020). Extraction of recombinant periplasmic proteins under industrially relevant process conditions: Selectivity and yield strongly depend on protein titer and methodology. *Biotechnol Prog*, *36*(5), e2999. https://doi.org/10.1002/btpr.2999

Schink, K. O., & Bölker, M. (2009). Coordination of cytokinesis and cell separation by endosomal targeting of a Cdc42-specific guanine nucleotide exchange factor in *Ustilago maydis*. *Mol Biol Cell*, *20*(3), 1081-1088. https://doi.org/10.1091/mbc.E08-03-0280

Schneeberger, K. (2014). Using next-generation sequencing to isolate mutant genes from forward genetic screens. *Nat Rev Genet*, *15*(10), 662-676. https://doi.org/10.1038/nrg3745

Schuler, D., Holl, C., Grün, N., Ulrich, J., Dillner, B., Klebl, F., Ammon, A., Voll, L. M., & Kämper, J. (2018). Galactose metabolism and toxicity in *Ustilago maydis*. *Fungal Genet Biol*, *114*, 42-52. https://doi.org/10.1016/j.fgb.2018.03.005

Schuster, M., Martin-Urdiroz, M., Higuchi, Y., Hacker, C., Kilaru, S., Gurr, S. J., & Steinberg, G. (2016). Co-delivery of cell-wall-forming enzymes in the same vesicle for coordinated fungal cell wall formation. *Nat Microbiol*, *1*(11), 16149. https://doi.org/10.1038/nmicrobiol.2016.149

Schuster, M., Schweizer, G., Reissmann, S., & Kahmann, R. (2016). Genome editing in Ustilago maydis using the CRISPR–Cas system. *Fungal Genet Biol*, *89*, 3-9. https://doi.org/10.1016/j.fgb.2015.09.001

Schwarz, C. K., Landsberg, C. D., Lenders, M. H., Smits, S. H., & Schmitt, L. (2012). Using an *E. coli* Type 1 secretion system to secrete the mammalian, intracellular protein IFABP in its active form. *J Biotechnol*, *159*(3), 155-161. https://doi.org/10.1016/j.jbiotec.2012.02.005

Schwarz, C. K., Lenders, M. H., Smits, S. H., & Schmitt, L. (2012). Secretion of slow-folding proteins by a Type 1 secretion system. *Bioengineered*, *3*(5), 289-292. https://doi.org/10.4161/bioe.20712

Shibai, A., Takahashi, Y., Ishizawa, Y., Motooka, D., Nakamura, S., Ying, B. W., & Tsuru, S. (2017). Mutation accumulation under UV radiation in *Escherichia coli*. *Sci Rep*, *7*(1), 14531. https://doi.org/10.1038/s41598-017-15008-1

Shimizu-Sato, S., Huq, E., Tepperman, J. M., & Quail, P. H. (2002). A light-switchable gene promoter system. *Nat Biotechnol*, *20*(10), 1041-1044. https://doi.org/10.1038/nbt734

Siegel, V., & Walter, P. (1988). Each of the activities of signal recognition particle (SRP) is contained within a distinct domain: analysis of biochemical mutants of SRP. *Cell*, *52*(1), 39-49. https://doi.org/10.1016/0092-8674(88)90529-6

Sinha, J., Plantz, B. A., Inan, M., & Meagher, M. M. (2005). Causes of proteolytic degradation of secreted recombinant proteins produced in methylotrophic yeast *Pichia pastoris*: case study with recombinant ovine interferon-tau. *Biotechnol Bioeng*, *89*(1), 102-112. https://doi.org/10.1002/bit.20318

Sommer, M. S., & Schleiff, E. (2014). Protein targeting and transport as a necessary consequence of increased cellular complexity. *Cold Spring Harb Perspect. Biol.*, *6*(8). https://doi.org/10.1101/cshperspect.a016055

Song, P., Zhang, K., Zhang, S., Huang, B. Q., Ji, X. J., Ren, L. J., Gao, S., Wen, J. P., & Huang, H. (2018). Enhancement of pneumocandin B0 production in *Glarea lozoyensis* by low-temperature adaptive laboratory evolution. *Front Microbiol*, *9*, 2788. https://doi.org/10.3389/fmicb.2018.02788

Spadiut, O., Capone, S., Krainer, F., Glieder, A., & Herwig, C. (2014). Microbials for the production of monoclonal antibodies and antibody fragments. *Trends Biotechnol*, *32*(1), 54-60. https://doi.org/10.1016/j.tibtech.2013.10.002

Steringer, J. P., Lange, S., Cujova, S., Sachl, R., Poojari, C., Lolicato, F., Beutel, O., Müller, H. M., Unger, S., Coskun, U., Honigmann, A., Vattulainen, I., Hof, M., Freund, C., &

Nickel, W. (2017). Key steps in unconventional secretion of fibroblast growth factor 2 reconstituted with purified components. *Elife*, *6*. https://doi.org/10.7554/eLife.28985

Steringer, J. P., Müller, H. M., & Nickel, W. (2015). Unconventional secretion of fibroblast growth factor 2--a novel type of protein translocation across membranes? *J Mol Biol*, *427*(6 Pt A), 1202-1210. https://doi.org/10.1016/j.jmb.2014.07.012

Steringer, J. P., & Nickel, W. (2018). A direct gateway into the extracellular space: Unconventional secretion of FGF2 through self-sustained plasma membrane pores. *Semin Cell Dev Biol*. https://doi.org/10.1016/j.semcdb.2018.02.010

Stock, J., Sarkari, P., Kreibich, S., Brefort, T., Feldbrügge, M., & Schipper, K. (2012). Applying unconventional secretion of the endochitinase Cts1 to export heterologous proteins in *Ustilago maydis*. *J Biotechnol*, *161*(2), 80-91. https://doi.org/10.1016/j.jbiotec.2012.03.004

Stock, J., Terfrüchte, M., & Schipper, K. (2016). A reporter system to study unconventional secretion of proteins avoiding *N*-Glycosylation in *Ustilago maydis*. *Unconventional Protein Secretion: Methods and Protocols. Springer Protocols.*, *1459*, 149-160. https://doi.org/10.1007/978-1-4939-3804-9_10

Stoffels, P., Müller, M. J., Stachurski, S., Terfrüchte, M., Schröder, S., Ihling, N., Wierckx, N., Feldbrügge, M., Schipper, K., & Büchs, J. (2020). Complementing the intrinsic repertoire of *Ustilago maydis* for degradation of the pectin backbone polygalacturonic acid. *J Biotechnol*, *307*, 148-163. https://doi.org/10.1016/j.jbiotec.2019.10.022

Studier, F. W. (2005). Protein production by auto-induction in high-density shaking cultures. *Protein Expr Purif*, *41*(1), 207-234. https://doi.org/10.1016/j.pep.2005.01.016

Sun, X., & Su, X. (2019). Harnessing the knowledge of protein secretion for enhanced protein production in filamentous fungi. *World J Microbiol Biotechnol*, *35*(4), 54. https://doi.org/10.1007/s11274-019-2630-0

Tagliabracci, V. S., Engel, J. L., Wen, J., Wiley, S. E., Worby, C. A., Kinch, L. N., Xiao, J., Grishin, N. V., & Dixon, J. E. (2012). Secreted kinase phosphorylates extracellular proteins that regulate biomineralization. *Science*, *336*(6085), 1150-1153. https://doi.org/10.1126/science.1217817

Tan, G., Opitz, L., Schlapbach, R., & Rehrauer, H. (2019). Long fragments achieve lower base quality in Illumina paired-end sequencing. *Sci Rep*, *9*(1), 2856. https://doi.org/10.1038/s41598-019-39076-7

Terfrüchte, M. (2016). *Expression of biopharmaceuticals in Ustilago maydis* https://docserv.uni-duesseldorf.de/servlets/DerivateServlet/Derivate-43489/Marius%20Terfr%C3%BCchte_Dissertation_PDF%20A-1b.pdf

Terfrüchte, M., Joehnk, B., Fajardo-Somera, R., Braus, G. H., Riquelme, M., Schipper, K., & Feldbrügge, M. (2014). Establishing a versatile Golden Gate cloning system for genetic engineering in fungi. *Fungal Genet Biol*, *62*, 1-10. https://doi.org/10.1016/j.fgb.2013.10.012

Terfrüchte, M., Reindl, M., Jankowski, S., Sarkari, P., Feldbrügge, M., & Schipper, K. (2017). Applying unconventional secretion in *Ustilago maydis* for the export of functional nanobodies. *Int J Mol Sci*, *18*(5). https://doi.org/10.3390/ijms18050937

Terfrüchte, M., Wewetzer, S., Sarkari, P., Stollewerk, D., Franz-Wachtel, M., Macek, B., Schlepütz, T., Feldbrügge, M., Büchs, J., & Schipper, K. (2018). Tackling destructive proteolysis of unconventionally secreted heterologous proteins in *Ustilago maydis*. *J Biotechnol*, *284*, 37-51. https://doi.org/10.1016/j.jbiotec.2018.07.035

Thomassen, Y. E., Verkleij, A. J., Boonstra, J., & Verrips, C. T. (2005). Specific production rate of VHH antibody fragments by *Saccharomyces cerevisiae* is correlated with growth rate, independent of nutrient limitation. *J Biotechnol*, *118*(3), 270-277. https://doi.org/10.1016/j.jbiotec.2005.05.010

Treangen, T. J., & Salzberg, S. L. (2011). Repetitive DNA and next-generation sequencing: computational challenges and solutions. *Nat Rev Genet*, *13*(1), 36-46. https://doi.org/10.1038/nrg3117

Tripathi, N. K., & Shrivastava, A. (2019). Recent developments in bioprocessing of recombinant proteins: expression hosts and process development. *Front Bioeng Biotechnol*, *7*, 420. https://doi.org/10.3389/fbioe.2019.00420

Tsukuda, T., Carleton, S., Fotheringham, S., & Holloman, W. K. (1988). Isolation and characterization of an autonomously replicating sequence from *Ustilago maydis*. *Mol Cell Biol*, *8*(9), 3703-3709. https://doi.org/10.1128/mcb.8.9.3703

Tull, D., Gottschalk, T. E., Svendsen, I., Kramhoft, B., Phillipson, B. A., Bisgard-Frantzen, H., Olsen, O., & Svensson, B. (2001). Extensive *N*-glycosylation reduces the thermal stability of a recombinant alkalophilic bacillus alpha-amylase produced in *Pichia pastoris*. *Protein Expr Purif*, *21*(1), 13-23. https://doi.org/10.1006/prep.2000.1348

van Rossum, T., Kengen, S. W., & van der Oost, J. (2013). Reporter-based screening and selection of enzymes. *FEBS J*, *280*(13), 2979-2996. https://doi.org/10.1111/febs.12281

Verduyn, C., Postma, E., Scheffers, W. A., & Van Dijken, J. P. (1992). Effect of benzoic acid on metabolic fluxes in yeasts: a continuous-culture study on the regulation of respiration and alcoholic fermentation. *Yeast*, *8*(7), 501-517. https://doi.org/10.1002/yea.320080703

Vijayakrishnapillai, L. M. K., Desmarais, J. S., Groeschen, M. N., & Perlin, M. H. (2018). Deletion of ptn1, a PTEN/TEP1 orthologue, in *Ustilago maydis* reduces pathogenicity and teliospore development. *J Fungi*, *5*(1). https://doi.org/10.3390/jof5010001

Viotti, C. (2016). ER to Golgi-dependent protein secretion: The conventional pathway. In A. Pompa & F. De Marchis (Eds.), *Unconventional Protein Secretion: Methods and Protocols* (pp. 3-29). Springer New York. https://doi.org/10.1007/978-1-4939-3804-9_1

Walsh, G. (2018). Biopharmaceutical benchmarks 2018. *Nat Biotechnol*, *36*(12), 1136-1145. https://doi.org/10.1038/nbt.4305

Walsh, G., & Jefferis, R. (2006). Post-translational modifications in the context of therapeutic proteins. *Nat Biotechnol*, *24*(10), 1241-1252. https://doi.org/10.1038/nbt1252

Wang, Q., Zhong, C., & Xiao, H. (2020). Genetic engineering of filamentous fungi for efficient protein expression and secretion. *Front Bioeng Biotechnol*, *8*. https://doi.org/ARTN 293

10.3389/fbioe.2020.00293

Ward, O. P. (2012). Production of recombinant proteins by filamentous fungi. *Biotechnol Adv*, *30*(5), 1119-1139. https://doi.org/10.1016/j.biotechadv.2011.09.012

Wedlich-Soldner, R., Straube, A., Friedrich, M. W., & Steinberg, G. (2002). A balance of KIF1A-like kinesin and dynein organizes early endosomes in the fungus *Ustilago maydis*. *EMBO J*, *21*(12), 2946-2957. https://doi.org/10.1093/emboj/cdf296

Weickert, M. J., Doherty, D. H., Best, E. A., & Olins, P. O. (1996). Optimization of heterologous protein production in *Escherichia coli*. *Curr Opin Biotechnol*, *7*(5), 494-499. https://doi.org/10.1016/s0958-1669(96)80051-6

Weinhandl, K., Winkler, M., Glieder, A., & Camattari, A. (2014). Carbon source dependent promoters in yeasts. *Microb Cell Fact*, *13*, 5. https://doi.org/10.1186/1475-2859-13-5

Weinzierl, G., Leveleki, L., Hassel, A., Kost, G., Wanner, G., & Bölker, M. (2002). Regulation of cell separation in the dimorphic fungus *Ustilago maydis*. *Mol Microbiol*, *45*(1), 219-231. https://doi.org/10.1046/j.1365-2958.2002.03010.x

Wibberg, D., Price-Carter, M., Rückert, C., Blom, J., & Möbius, P. (2020). Complete Genome Sequence of Ovine *Mycobacterium avium* subsp. *paratuberculosis* Strain JIII-386 (MAP-S/type III) and Its Comparison to MAP-S/type I, MAP-C, and *M. avium* Complex Genomes. *Microorganisms*, *9*(1). https://doi.org/10.3390/microorganisms9010070

Wierckx, N., Miebach, K., Ihling, N., Hussnaetter, K. P., Buchs, J., & Schipper, K. (2021). Perspectives for the application of Ustilaginaceae as biotech cell factories. *Essays Biochem*. https://doi.org/10.1042/EBC20200141

Woodley, J. M. (2020). Towards the sustainable production of bulk-chemicals using biotechnology. *N Biotechnol*, *59*, 59-64. https://doi.org/10.1016/j.nbt.2020.07.002

Xue, L., & Tao, W. A. (2013). Current technologies to identify protein kinase substrates in high throughput. *Front Biol*, *8*(2), 216-227. https://doi.org/10.1007/s11515-013-1257-z

Zahiri, A. R., Babu, M. R., & Saville, B. J. (2005). Differential gene expression during teliospore germination in *Ustilago maydis*. *Mol Genet Genomics*, *273*(5), 394-403. https://doi.org/10.1007/s00438-005-1142-9

Zander, S., Baumann, S., Weidtkamp-Peters, S., & Feldbrügge, M. (2016). Endosomal assembly and transport of heteromeric septin complexes promote septin cytoskeleton formation. *J Cell Sci*, *129*(14), 2778-2792. https://doi.org/10.1242/jcs.182824

Zarnack, K., Maurer, S., Kaffarnik, F., Ladendorf, O., Brachmann, A., Kämper, J., & Feldbrügge, M. (2006). Tetracycline-regulated gene expression in the pathogen *Ustilago maydis*. *Fungal Genet Biol*, *43*(11), 727-738. https://doi.org/10.1016/j.fgb.2006.05.006

Zehe, C., Engling, A., Wegehingel, S., Schäfer, T., & Nickel, W. (2006). Cell-surface heparan sulfate proteoglycans are essential components of the unconventional export machinery of FGF-2. *Proc Natl Acad Sci U S A*, *103*(42), 15479-15484. https://doi.org/10.1073/pnas.0605997103

Zhang, K., & Cui, B. (2015). Optogenetic control of intracellular signaling pathways. *Trends Biotechnol*, *33*(2), 92-100. https://doi.org/10.1016/j.tibtech.2014.11.007

Zhang, Y., Liu, R., & Wu, X. (2007). The proteolytic systems and heterologous proteins degradation in the methylotrophic yeast *Pichia pastoris*. *Ann Microbiol*, *57*(4), 553-560. https://doi.org/10.1007/BF03175354

Zuo, W., Depotter, J. R., & Doehlemann, G. (2020). Cas9HF1 enhanced specificity in *Ustilago maydis*. *Fungal Biol*, *124*(3-4), 228-234. https://doi.org/10.1016/j.funbio.2020.02.006

# Web references

Web reference: Agilent Side-directed mutagenesis kit manual.
Available from: https://www.agilent.com/cs/library/usermanuals/Public/200523.pdf; last accessed: 2021/01/25.

Web reference: EnsemblFungi *U. maydis* genome browser
Available from: https://fungi.ensembl.org/Ustilago_maydis/Info/Index; last accessed: 2021/01/25

Web reference: MycoCosm: *Ustilago maydis* 521
Avaiable from: https://mycocosm.jgi.doe.gov/Ustma2_2/Ustma2_2.home.html; last accessed 2021/06/01.

Web reference: NetNGlyc 1.0 Server.
Available from: http://www.cbs.dtu.dk/services/NetNGlyc/; last accessed 2021/06/01

Web reference: Pedant *U. maydis* genome browser
Available from: http://pedant.gsf.de/pedant3htmlview/pedant3view?Method=analysis&Db=p3_t237631_Ust_maydi_v2GB; last accessed: 2018/06/13; no longer accessible

Web reference: SMART (Simple Modular Architecture Research Tool).
Available from http://smart.embl-heidelberg.de/; last accessed 2021/06/01.

Web reference: *U. maydis* 521 (whole genome Shotgun sequencing project).
Available from: https://www.ncbi.nlm.nih.gov/nuccore/AACP00000000.2; last accessed: 2021/06/01.

Web reference: *Ustilago* community Institute for Microbiology, Heinrich Heine University Düsseldorf.

Available from: https://www.mikrobiologie.hhu.de/ustilago-community.html;
last accessed: 2021/06/01.
Web reference: WGS of *Ustilago maydis* mutant impaired in unconventional secretion.
Avaiable from: https://www.ncbi.nlm.nih.gov/bioproject/634537;
last accessed: 2021/06/01.

# Directory of publications and author contributions

The following chapter provides information on author contributions to individual studies and publications. Information of contributions to individual figures is described in chapter **Directory of figures**. All other chapters, including "**1 Introduction**", "**4 Outlook and further perspectives for inducible secretion in *Ustilago maydis***", "**7 Outlook and further perspectives for establishment and adaption of a genetic screen for hyper secretion candidates**" and "**8 Final evaluation of biotechnological potential of unconventional secretion *in Ustilago maydis***" were prepared for this dissertation and are not published elsewhere. Chapter "**6 Isolation *of Ustilago maydis* mutants with enhanced capacity for unconventional export of heterologous proteins**" has not been submitted, peer-reviewed or published yet.

---

**This thesis consists of the following published research articles:**

**Chapter 2** The germinal centre kinase Don3 is crucial for unconventional secretion of chitinase Cts1 in *Ustilago maydis*

Aschenbroich, J., **Hussnaetter, K. P.**, Stoffels, P., Langner, T., Zander, S., Sandrock, B., Bölker, M., Feldbrügge, M. & Schipper, K. (2019). The germinal centre kinase Don3 is crucial for unconventional secretion of chitinase Cts1 in *Ustilago maydis*. *Biochimica et Biophysica Acta (BBA)-Proteins and Proteomics*, *1867*(12), 140154.

**K.H.** planned, performed and evaluated all Don3 complementation experiments. This included design and strain generation as well as enzymatic assays for reporter activity. Results are depicted in Figure 2.6C and D as well as Figure S2.9B. Microscopy of respective strains was performed by **K.H.** in cooperation with J.A. Micrographs are shown in Figure S2.9A.

---

**Chapter 3** Controlling unconventional secretion for production of heterologous proteins in *Ustilago maydis* through transcriptional regulation and chemical inhibition of the kinase Don3

**Hussnaetter, K. P.**, Philipp, M., Müntjes, K., Feldbrügge, M., & Schipper, K. (2021). Controlling unconventional secretion for production of heterologous proteins in

*Ustilago maydis* through transcriptional regulation and chemical inhibition of the kinase Don3. *Journal of Fungi*, *7*(3), 179.
**K.H.** designed and performed all experiments in this publication. All experimental data was evaluated and visualized by **K.H.** Application of autoinduction cultivation, read-out via ELISA was performed and evaluated in cooperation with M.P, depicted in Figure 3.7. Literature research, and manuscript preparation was performed by K.S. with input and support of **K.H.**

---

**Chapter 5** A novel factor essential for unconventional secretion of chitinase Cts1

Reindl, M., Stock, J., **Hussnaetter, K. P.**, Genc, A., Brachmann, A., & Schipper, K. (2020). A novel factor essential for unconventional secretion of chitinase Cts1. *Frontiers in microbiology*, *11*, 1529.

**K.H.** performed and evaluated experiments for demonstration of suitability of extracellular reporter read-out including plate assays, membrane assays and mixed cultures experiments. Results are depicted in Figure 5.2B, E-G, and Figure 5.3A. Furthermore, **K.H.** performed interaction studies via Yeast-two hybrid assays in the course of another thesis (Hussnaetter, 2016), shown in Figure 5.5F.

---

**Manuscripts in this thesis that have not been published yet:**

**Chapter 6** Isolation of *Ustilago maydis mutants* with enhanced capacity for unconventional export of heterologous proteins

**Hussnaetter, K. P.**, Philipp, M., Stock, J., Busche, T., Wibberg, D., Kalinoswki, J., Brachmann, A., Feldbrügge, M. & Schipper, K. (2021). Isolation of mutants with enhanced capacity for unconventional export of heterologous proteins. *Manuscript*

High troughput isolation of UV-mutagenized candidate was performed by **K.H.** with advice by J.S. and support by M.P. Results are depicted in Figure 6.2 and Figure6.3. All further investigations on selected candidates, including generation of reproducible data, determination of all reporter activities, selection of hypersecretion candidates, genetic crossing, progeny isolation and enzymatic and mating assays, as well as isolation of genomic DNA was performed by **K.H.** All data evaluation and visualization was performed by **K.H.** Bioinformatic data evaluation was performed by D.W. and A.B. with minor input by **K.H.**

Visualization of bioinformatic evaluations are shown in Figure 6.8 and Figure S6.8. Literature research and manuscript preparation was performed by **K.H.** with advice by K.S.

---

**Further contributions in publications that are not part of this thesis:**

Perspectives for the application of Ustilaginaceae as biotech cell factories

Wierckx, N., Miebach, K., Ihling, N., **Hussnaetter, K. P.**, Büchs, J., & Schipper, K. (2021). *Essays in Biochemistry*.

K.H. designed lock-type secretion mechanism figure (adapted in Figure 1.3) and supported design of other figures.

Detailed information on the relevance of this publication is provided below.

# Perspectives for the application of Ustilaginaceae as biotech cell factories

Nick Wierckx[1], Katharina Miebach[2], Nina Ihling[2], **Kai P. Hussnaetter**[3], Jochen Büchs[2], Kerstin Schipper[3]*

[1]Institute of Bio- and Geosciences IBG-1: Biotechnology, Forschungszentrum Jülich and Bioeconomy Science Center (BioSC), Wilhelm-Johnen-Str., 52425 Jülich, Germany

[2]Aachener Verfahrenstechnik – Biochemical Engineering, RWTH Aachen University, Forckenbeckstr. 51, 52074 Aachen, Germany and Bioeconomy Science Center (BioSC), Wilhelm-Johnen-Str., 52425 Jülich, Germany

[3]Institute for Microbiology, Heinrich Heine University Düsseldorf, Universitätsstraße 1, 40225 Düsseldorf, Germany and Bioeconomy Science Center (BioSC), Wilhelm-Johnen-Str., 52425 Jülich, Germany

* Corresponding author: E-mail: kerstin.schipper@uni-duesseldorf.de (KS)

This review was published in Essays in Biochemistry, Special issue Microbial Cell Factories and can be found at doi.org/10.1042/EBC20200141

**Publication summary**

The family of Ustilaginaceae belongs to the phylum of basidiomycota and is mainly known for plant pathogenic fungi. Importantly, several members are natural producers of biotechnologically relevant products. Furthermore, the repertoire of carbohydrate active enzymes harbors potential towards degradation, utilization and upcycling of plant biomass. Extensive investigations and understanding of basic biology of *Ustilago maydis* resulted in a broad portfolio of molecular biological, genetic, synthetic and biochemical methods allowing applications in biotechnological strategies.

The review covers different tools and strategies in strain generation, cultivation, and monitoring, as well as examples for biotechnological products. Of special interest for studies in the course of this thesis is the application of unconventional secretion for secretion of heterologous proteins

# Directory of figures

● - Figures with own contributions in design or experimental data.

**6 Isolation of *Ustilago maydis mutants* with enhanced capacity for unconventional export of heterologous proteins**

# Acknowledgments

First, I would like to thank Michael for accompanying me in my scientific career since my bachelor thesis. Your support, enthusiasm and ideas motivated and certainly inspired me!

I would like to thank Kerstin especially for her commitment and organization during all my projects. I was able to learn an incredible amount under your supervision and got exactly the balancing act of assistance and independent work.

I would also like to thank Matias for accepting the second supervision of my thesis. In discussions you were always a good mentor and helped me to see and understand my work as a whole instead of viewing it with tunnel vision.

I would like to thank the Clib Competence Cluster Biotechnology and the European Regional Development Fund for the funding and scientific exchange during my doctoral thesis.

A big thank you goes to all old and new members of RabXpress. I am happy (almost) every day that I come to work, become desperate and celebrate with great folks like you! First, I want to thank Tina for incredible results, a great work ethic, and for always being there to help no matter how busy it got. Thanks to Magnus and Peter for great Ballerei, productive and unproductive nightshifts and friendship between chaos and science. ENDFIT! ENDFIT! An extra thank to Magnus for spellchecking the thesis! Also to Silke many thanks for settling in in our working group. I would like to thank Marius, Michele and Jörn for a nice working atmosphere, an open ear and a lot of experience! You made my start in RabXpress very pleasant. To all former members I would like to thank for the preliminary work. Slowly it becomes unrealistic, but I am still in for a RabXpress revival, Janpeter and Parveen. To all RabXpress students my thanks for you nice time. Marta, Laura, Dennis and of course especially Flippo and Püppi. Malte, Florian, Mara and Katharina I want to thank you for supporting my work as Hiwi or intern. I hope I did not confuse you too much. Special thanks also go to Kira, who always had an open ear for my problems between RabXpress and all her other tasks. Last but not least, again a big thank you to Kerstin for keeping the group together.

I would like to thank the Südfront for nice evenings and afternoons! All the lab stress was only half as bad when you folks were around! Greetings to Magnus, Natascha, Lea, Philipp, Anton and Kira! I salute you!

To I would like to thank Ute, Simone and Jessica for answering all my little "where's that?"- to big "what came first, the yeast or the negative result"-questions.

Vera, Lilli and Carl I would like to thank you for your scientific input in the context of my work and all possible further projects.

For nice get-togethers at the institute, I would like to thank Nina, Senthil, Sri, Woogie, Summia, Markus and Kristin. Even though the last party was a while ago, I still have great memories of cooking, barbecuing, celebrating and drinking together at lab parties.

I appreciate scientific collaborations with Sebastian Bauer, Sebastian Theisen and Andreas Biselli.

I would like to thank Elisabeth, Uli and Caro for the organization and for keeping my save of all bureaucratic burdens! That was really a big help for me!

To Anna, Max and Nic I would like to thank you for the escapades pretended to be scientific exchanges! To the iGEM team 2017, I would like to thank you for your enthusiasm! To the Driemtiem I would like to thank you for excellent taste in music and stylish evenings.

At this point again a special thanks to Püppi, for the Christmas party and every single day afterwards ❤.

Of course, I also want to thank my family and especially my parents for all the support since the beginning! I know how much I owe to you!